

Some pages of this thesis may have been removed for copyright restrictions.

If you have discovered material in AURA which is unlawful e.g. breaches copyright, (either yours or that of a third party) or any other law, including but not limited to those relating to patent, trademark, confidentiality, data protection, obscenity, defamation, libel, then please read our [Takedown Policy](#) and [contact the service](#) immediately

THE EFFECT OF FLOW REGIMES IN THE
DISTILLATION OF SYSTEMS CONTAINING
TWO LIQUID PHASES.

A THESIS SUBMITTED FOR THE DEGREE
OF DOCTOR OF PHILOSOPHY

BY
ZAFAR ALI [B.Sc, M.Sc.]

DEPARTMENT OF CHEMICAL ENGINEERING AND APPLIED CHEMISTRY
UNIVERSITY OF ASTON IN BIRMINGHAM
BIRMINGHAM.
NOVEMBER 1988.

This copy of the thesis has been supplied on condition that anyone who consults it is understood to recognise that its copyright rests with its author and no quotation from the thesis and no information derived from it may be published without the author's prior, written consent.

بِسْمِ اللَّهِ الرَّحْمَنِ الرَّحِيمِ

In the Name of God, the Compassionate, the Merciful

LIST OF PUBLICATIONS

1. A.I.Ch.E.J., 1987, 33(1), 161-163.
2. Institute of Chemical Engineers Research Meeting, April 1987, Nottingham.
3. Distillation and Absorption 1987, Brighton, I.Chem.E. Symp. Series, no 62, vol. 2, B541-B551.
4. Institute of Chemical Engineers Research Meeting, April 1988, London.

University of Aston in Birmingham
**THE EFFECT OF FLOW REGIMES IN THE DISTILLATION OF SYSTEMS
CONTAINING TWO LIQUID PHASES.**

Thesis submitted for the degree of Doctor of Philosophy
November 1988.

ABSTRACT

Single phase solutions containing three components have been observed to exhibit foaminess near a single to two liquid phase boundary. It was seen, in a sintered plate column under mass transfer conditions, that distillation systems where the liquid appeared as one phase in one part of a column and two phases in another part, exhibited foaminess when the liquid concentration was near the one phase to two phase boundary. Various ternary systems have been studied in a 50 plate, 30mm i.d. Oldershaw column and it was observed that severe foaming occurred in the middle section of the column near the one liquid phase to two liquid phase boundary and no foaming occurred at the end of the column where liquid was either one phase or two phase. This is known as Ross type foam.

Mass transfer experiments with Ross type ternary systems have been carried out in a perspex simulator with small and large hole diameter trays. It was observed that by removal of the more volatile component, Ross type foam did not build up on the tray. Severe entrainment of liquid was observed in all cases leading to a 'dry' tray, even with a low free area small diameter hole tray which was expected to produce a bubbly mixture. Entrainment was more severe for high gas superficial velocities and large hole diameters. This behaviour is quite different from the build up of foam observed when one liquid phase/two liquid phase Ross systems were contacted with air above a small sintered disc or with vapour in an Oldershaw distillation column. This observation explains why distillation columns processing mixtures which change from one liquid phase to two liquid phases (or vice versa) must be severely derated to avoid flooding.

Single liquid phase holdups at the spray to bubbly transition were measured using a perspex simulator similar to that of Porter & Wong (17), i.e. with no liquid cross flow. A light transmission technique was used to measure the transition from spray regime to bubbly regime. The effect of tray thickness and the ratio of hole diameter to tray thickness on the transition was evaluated using trays of the same hole diameter and free area but having thickness of 2.38 mm, 4 mm, and 6.35 mm. The liquid holdup at the transition was less with the thin metal trays. This result may be interpreted by the theory of Lockett (101), which predicts the transition liquid holdup in terms of the angle of the gas jet leaving the holes in the sieve plate. All the existing correlations have been compared and none were found to be satisfactory and these correlations have been modified in view of the experimental results obtained. A new correlation has been proposed which takes into account the effect of the hole diameter to tray thickness ratio on the transition and good agreement was obtained between the experimental results and the correlated values of the liquid holdup at the transition.

Results have been obtained for two immiscible liquids [kerosene and water] on trays to determine whether foaming can be eliminated by operating in the spray regime. Kerosene was added to a fixed volume of water or water was added to a fixed volume of kerosene. In both cases, there was a transition from spray to bubbly. In the water fixed system, the liquid holdup at the transition was slightly less than the pure kerosene system. Whilst for the kerosene fixed system, the transition occurred at much lower liquid holdups. Trends in the results were similar to those for single liquid phase. New correlations have been proposed for the two cases.

It has been found that Ross type foams, observed in a sintered plate column and in the Oldershaw column can be eliminated by either carrying out the separation in a packed column or by the addition of defoaming additives.

Key words: Ternary systems, Foaming, Antifoaming agents, Packed column, Single/Two liquid phases, Spray/Bubbly transition, Surface tension.

DECLARATION

I hereby declare that no portion of the Ph. D. thesis entitled "The Effect of Flow Regimes in the Distillation of Systems Containing Two Liquid Phases " has been previously submitted to this or any other institution in application for admission to another degree or qualification. Also the work presented in this thesis has been done by the candidate except where otherwise acknowledged.

.....

[Mr Zafar Ali - Student]

.....

[Dr Bruce Davies - Research Supervisor]

ACKNOWLEDGEMENTS

I wish to express my sincere gratitude to my supervisors, Prof. K. E. Porter and Dr B. Davies, for their enlightening supervision, constant encouragement and advice throughout the course of the studies.

Thanks are also to the head of department for providing research facilities in the Department of Chemical Engineering.

My sincere thanks to the technical staff of the department for their help during construction of the experimental equipment.

I wish also to thank the University of Aston for the scholarship during the research work.

Finally, I wish to express my sincere gratitude to my wife and my son, without whose encouragement and faith in him, this thesis would never have been written.

DEDICATION

Dedicated to the memory of my late father haji Mansabdar Khan, whose dream was for me to achieve a Ph.D. and my wife who made this dream a reality through her understanding and patience, particularly at difficult times.

CONTENTS

Contents

List of Publications	3
Abstract	4
List of Tables	13
List of Figures	14
Nomenclature	17
 Chapter 1 Introduction	 19
 Chapter 2 Literature Survey	 22
2.1 Introduction	22
2.2 Foams	23
2.2.1 Ross type foam	24
2.2.2 Mechanism of foam stabilisation	25
2.3 System derating factor	25
2.4 Marangoni effect	26
2.4.1 Causes of the Marangoni effect	27
2.4.2 Mass transfer induced by Marangoni effect	27
2.5 Dealing with foaming systems	28
2.5.1 Additives and anti-foaming agents	28
2.5.2 Action of anti-foaming agents	29
2.6 Hydrodynamic conditions for foam stability on trays	29
2.6.1 Foam and tray design	30
2.6.2 Tray behaviour with two immiscible liquid phases	30
2.7 Flow regimes and tray/plate hydraulics	30
2.7.1 Discrete bubbling	31
2.7.2 Cellular foam	32
2.7.3 Froth regime	33
2.7.4 Spray regime	34
2.8 Transition between different regimes	36
2.9 Spray to bubbly transition	36

2.9.1	Early observations	36
2.9.2	Measuring techniques	38
2.9.3	Mechanism and prediction of transition	39
2.10	Entrainment	46
2.10.1	Prediction of entrainment	46
2.10.2	Mechanism of entrainment	49
2.10.3	Measurement of entrainment	50
2.11	Efficiency	51
2.11.1	Tray efficiency	51
2.11.2	Effect of entrainment on plate efficiency	51
2.12	Concluding remarks	52
Chapter 3	Approach to the problem	55
3.1	Introduction	55
3.2	Experimental program	55
3.3	Choice of equipment	56
Chapter 4	Experimental equipment	57
4.1	Preliminary considerations	57
4.2	Oldershaw column	57
4.3	Air-water simulator	57
4.3.1	Liquid circuit	58
4.3.2	Air Circuit	58
4.3.3	Scrubber	59
4.3.4	Extraction of air	59
4.4	Sintered plate column	59
Chapter 5	Oldershaw Column Studies	65
5.1	Introduction	65
5.2	Ternary systems previously studied	66
5.3	Object of the Work	66
5.4	Sintered plate column	66
5.4.1	Systems to be studied	67
5.4.2	Observations	67
5.5	Oldershaw column experiments	67
5.5.1	Experimental procedure	68

5.5.2	Observations	68
5.6	Column modification	69
5.6.1	Reboiler	69
5.6.2	Sampling points	69
5.6.3	Temperature measurements	69
5.6.4	Operating procedure	70
5.7	GLC analysis	71
5.7.1	Calibration of the chromatograph	71
5.7.2	Results	72
5.8	Measurement of surface tension	72
5.8.1	Experimental procedure	73
5.8.2	Results	73
5.9	Conclusions	73
Chapter 6	The Transition from Spray to Bubbly Regime	84
6.1	Introduction	84
6.2	Object of the work	85
6.3	The determination of the spray to bubbly regime transition	85
6.4	Experimental program	86
6.5	Experimental procedure	87
6.5.1	Column operation	87
6.5.2	Experimental determination of the transition	87
6.6	Effect of operating conditions on the transition	88
6.6.1	Effect of plate thickness and ratio (d_H/X)	88
6.7	Comparison of experimental data	88
6.8	Correlation of experimental results	90
6.8.1	Proposed correlation for spray to bubbly transition	91
6.9	Modification of existing correlations	92
6.10	Conclusions	93
Chapter 7	Spray to Bubbly Transition with Two Immiscible Liquid Phases	116
7.1	Introduction	116
7.2	Object of the work	116
7.3	Experimental determination of the transition	117
7.4	Column modifications	117

7.5	Experimental procedure	117
7.6	Experimental results	118
7.7	Small column experiments	119
7.8	Experimental details	120
7.8.1	Sintered Plate	120
7.8.2	Orifice plate	120
7.9	Observations	120
7.9.1	Sintered plate	120
7.9.2	Orifice plate	121
7.10	Discussion	122
7.11	New proposed correlations for spray to bubbly transition for two liquid phases	123
7.12	Conclusions.	124
Chapter 8	Elimination of Foams	148
8.1	Introduction	148
8.2	Objective of the work	149
8.3	Methods of foam elimination	149
8.4	Packed column	149
8.4.1	Experimental procedure	149
8.4.2	Observations	150
8.5	Use of additives	150
8.5.1	Experimental procedure-Sintered plate column	151
8.5.1.1	Observations	151
8.5.2	Experimental procedure-Oldershaw column	151
8.5.2.1	Observations	152
8.6	Perspex simulator	152
8.6.1	Experimental procedure	153
8.6.2	Observations	154
8.7	Sintered disc column experiments	155
8.7.1	Experimental procedure	155
8.7.2	Observations	155
8.8	Discussion	155
8.9	Wind tunnel experiments	156
8.9.1	Experimental details	156
8.9.2	Measurement of droplet size	157
8.9.3	Discussion of results	157

8.10	Conclusions	157
Chapter 9	Conclusions	161
Chapter 10	Recommendations For Future Work	163
References		164
Appendices		170
Appendix 1	Physical property data	170
Appendix 2	Polynomial computer programme	171
Appendix 3	Liquid profile in Oldershaw column at various volume ratios of water/n-hexane	176
Appendix 4	Surface tension results	180
Appendix 5	Spray/bubbly transition results	183
Appendix 6	Computer programme to calculate h_{CL} from different spray/bubbly transition correlations	197
Appendix 7	Details of sieve trays used by previous researchers	204
Appendix 8	Computer programme to evaluate 'a' in Lockett's model	205
Appendix 9	Computer programme to correlate experimental results	212
Appendix 10	Variation of droplet diameter with time	220
Published Papers		221

LIST OF TABLES

Table:

2.1	System factors.	26
4.1	Details of sieve plates used in experiments.	60
5.1	Ross foaming systems.	66
5.2	Ternary systems used in sintered plate column.	67
5.3	Systems studied in the Oldershaw column.	68
5.4	Details of chromatograph apparatus.	71
5.5	Number of plates foamed with different ratios of water/n-hexane.	72
6.1	Operating conditions for the air-water simulator.	87
6.2	Values of constants in Lockett's model (101).	91
6.3	Modified correlations for spray to bubbly transition.	92
8.1	Additives used in sintered plate column.	150
8.2	Additives used in Oldershaw column.	151
8.3	Details of sieve plates used in air-water simulator.	153
8.4	Experimental conditions for air-water simulator.	154

LIST OF FIGURES

Figure:

2.1	Dispersion formed above sieve plates.	53
2.2	Flow regime diagram.	54
4.1	Oldershaw Column.	61
4.2	Air-water simulator.	62
4.3	Dimensions of the air-water simulator.	63
4.4	Line diagram of the air-water simulator.	64
5.1	Sintered plate column.	75
5.2	Foaming of Water - Kerosene - Acetone system.	76
5.3	n-Hexane - Water - Propan-1-ol system in 30 mm diameter Oldershaw column.	77
5.4	Distillation line predicted by UNIFAC for the system n-Hexane - Water - Propan-1-ol.	78
5.5	Experimental distillation lines at various ratios of water/n-hexane.	79
5.6	Variations in plates foamed in Oldershaw column with changes in ratios of water/n-hexane in initial charge.	80
5.7	Temperature profile across the column for the n-Hexane - Water - Propan-1-ol system.	81
5.8	Changes in composition with surface tension for n-Hexane - Water - Propan-1-ol system during titration.	82
5.9	Variation of surface tension with composition for n-Hexane - Water - Propan-1-ol system.	83
6.1	Diagram to show light transmitted through dispersion.	94
6.2	Calibration of light transmission technique.	95
6.3	Effects of gas superficial velocity on the transition. Air-Water system. Tray no. 3.	96
6.4	Effects of hole diameter on the transition. Air-Water system.	97
6.5	Effects of free area on the transition. Air-Water system.	98
6.6	Effects of liquid density on the transition. Air-Water system.	99
6.7	Effects of plate thickness and the ratio of (d_h/X) on the transition.	100

	Air-Water system.	
6.8	Transition results of Payne & Prince (21). Air - Water only.	101
6.8.1	Transition results of Prince, Jones & Panic (102). Distillation systems.	102
6.8.2	Transition results of Pinczewski & Fell (22). Air - Water only.	103
6.8.3	Transition results of Porter & Wong (17). Air - Water only.	104
6.8.4	Transition results of Porter & Wong (17). Non Air - Water.	105
6.8.5	Transition results of this study. Air - Water only.	106
6.8.6	Transition results of this study. Air - Kerosene only.	107
6.9	Performance of different correlations for single liquid phase.	108
	Tray no. 14.	
6.9.1	Performance of different correlations for single liquid phase.	109
	Tray no. 3	
6.10	Variation of jet angle with tray floor.	110
6.11	Comparison of experimental h_{cl}/d_h with Barber/Wijn	111
	correlation (103) & Lockett's model (101) when 'n' = 1. Tray no. 12.	
6.12	Performance of Lockett's model when 'n' = 1. Tray no. 12.	112
6.13	Proposed new correlation for spray/bubbly transition.	113
6.14	Performance of modified correlations. Tray no. 14.	114
6.14.1	Performance of modified correlations. Tray no. 3.	115
7.1	Effects of gas superficial velocity on the transition.	125
	Air-Water-Kerosene. Tray no. 3.	
7.2	Effects of hole diameter on the transition. Water fixed.	126
7.2.1	Effects of hole diameter on the transition. Kerosene fixed.	127
7.3	Effects of free area on the transition. Water fixed.	128
7.3.1	Effects of free area on the transition. Kerosene fixed.	129
7.4	Effects of liquid density on the transition. Tray no. 5.	130
7.4.1	Effects of liquid density on the transition. Tray no. 5.	131
7.5	Effects of plate thickness and the ratio (d_h/X) on the transition.	132
	Water fixed.	
7.5.1	Effects of plate thickness and the ratio (d_h/X) on the transition.	133
	Kerosene fixed.	
7.6	Variation of volume fraction of liquid with gas superficial velocity.	134
	Water fixed. Tray no. 8.	
7.7	Variation of ratio (water/kerosene) with gas velocity.	135
	Water fixed. Tray no. 8.	

7.8	Variation of mixture density with gas superficial velocity. Water fixed. Tray no. 8.	136
7.9	Variation of liquid density with ratio (water/kerosene). Water fixed. Tray no. 8.	137
7.10	Variation of density with volume fraction of liquids. Water fixed. Tray no. 8.	138
7.11	Variation of ratio (water/kerosene) with the volume fraction of liquids. Water fixed. Tray no. 8.	139
7.12	Variation of volume fraction of liquid with gas superficial velocity. Kerosene fixed . Tray no. 8.	140
7.13	Variation of ratio (water/kerosene) with gas velocity. Kerosene fixed . Tray no. 8.	141
7.14	Variation of mixture density with gas superficial velocity. Kerosene fixed . Tray no. 8.	142
7.15	Variation of liquid density with ratio (water/kerosene). Kerosene fixed . Tray no. 8.	143
7.16	Variation of density with volume fraction of liquids. Kerosene fixed. Tray no. 8.	144
7.17	Variation of ratio (water/kerosene) with the volume fraction of liquids. Kerosene fixed. Tray no. 8.	145
7.18	Proposed new correlation for spray to bubbly transition. Water fixed.	146
7.18.1	Proposed new correlation for spray to bubbly transition. Kerosene fixed.	147
8.1	Packed column.	158
8.2	Cumene - Water - Propan-1-ol system in perspex simulator.	159
8.3	Changes in droplet diameter with time in wind tunnel.	160

NOMENCLATURE

A	Air volume flow rate (cm^3/s)
a	Constant in equation 2.21
A_f	Free area of plate (=actual area/bubbling area)
C_t	Drag coefficient
d	Slot width (m)
d_h	Hole diameter (m) [inches in equation 2.9 & 2.10]
D	Jet diameter (m)
E	Entrainment rate (kg of liquid entrained/ kg of liquid)
E_M	Liquid entrainment rate (kg/s)
g	Acceleration due to gravity (m/s^2)
h_{cl}	Clear liquid height (m) [inches in equation 2.9 & 2.10]
h_w	Weir height (m)
K	Constant
L	Depth of the orifice at the transition
L_v	Liquid flow rate (m^3/h m of weir length)
M_G	Vapour flow rate (kg/s)
M_L	Liquid flow rate (kg/s)
P	Triangular pitch (m)
P_{dp}	Pressure drop (m water)
P_{res}	Residual pressure drop (m water)
P_t	Total pressure drop (m water)
Q_l	Liquid flow rate (m^3/s)
s	Tray spacing (mm)
u_h	Hole gas velocity (m/s) [ft/s in equation 2.10]
u_s	Gas superficial velocity (m/s) [ft/s in equation 2.9 & 2.10]
u_t	Terminal velocity (m/s) [ft/s in equation 2.8 & 2.10]
v_l	Volume of liquid entrained ($\text{ft}^3/\text{s ft}^2$)
w_g	Mass gas flow rate (lb/s ft^2)

x	Mole fraction of mvc in liquid
x^*	Liquid composition in equilibrium with the mean vapour composition leaving the tray
y	Mole fraction of mvc in vapour
y^*	Mole fraction of mvc in the vapour which is in equilibrium with the liquid
X	Tray thickness (m)
z	Maximum height of drop trajectory (ft)
ϵ	Gas volume fraction in the liquid phase
ρ_f	Froth density [$=\rho_l(1-\epsilon)$]
ρ_g	Gas density (kg/m^3)
ρ_l	Liquid density (kg/m^3)
σ_x^*	Surface tension of liquid having composition x^*
σ	Surface tension (dynes/cm)
σ_i	Interfacial tension (dynes/cm)
μ_g	Vapour viscosity (Ns/m^2)

CHAPTER 1

INTRODUCTION

Gas-liquid contacting is the basis of many production processes in which adequate interfacial area is required for good mass transfer, but where excessive foaming leads to instabilities, reduced capacity and efficiency. In many distillation systems, the choice of flow rates and operating conditions often lead to such behaviour, for example, in high pressure distillation of 'Butanes' a foaming factor is used to derate the column. Although the evidence that the system actually foams is rather limited.

In some systems, it is thought that the presence of two liquid phases may cause excessive foaming. Some qualitative data have been published by Ross & Nishioka (1-4) concerning the foaminess of systems which under conditions of mass transfer were thought to contain two liquid phases. Using a perforated plate, the authors (2) investigated the foaminess of liquid mixtures under mass transfer conditions in which a change from single liquid phase to two liquid phases was approached. With two liquid phases on the tray foaming was inhibited. This phenomena has not been reported for systems being separated in distillation columns although it is suspected that a similar phenomena could occur. For this reason the cause of foam in distillation column is not clearly understood. Though during the development of three phase distillation, large effort has been made to study the thermodynamics of phase equilibria (5) and the simulation of whole processes (6-14). The models proposed are for highly non-ideal mixtures for two liquid phases and the essential element of all such models is an algorithm for testing the stability of the liquid phase on each tray. In all such cases where two liquid phases could occur, very little information is available, the columns are often derated by as much as 50-100 %.

Thus, current design practice is based on inadequate and limited data and traditionally, most columns are designed on the assumption of a foaming system with a high foaming factor leading to oversized columns and inflated capital costs. Where foaming factors are not used, and presently, where raw materials for separation may be varied in source and quality, the column may be undersized leading to higher operating costs caused by the loss of production time.

For tray columns, the investigations of the AIChE Research Committee (15,16) showed that the efficiency depended on the nature of the dispersion formed on the sieve plate. Thus, the study of these dispersion has received considerable attention by several groups of research workers.

The capacity and separation efficiency of plate columns with liquid cross flow are always limited by hydrodynamic phenomena such as entrainment and foaming. Entrainment flooding occurs when the gas rate is very high so that excessive liquid is carried from one

plate to the other by the gas. Entrainment has been widely studied and a significant amount of data have been reported in the literature. However, less attention has been given to foaming. Therefore, it is of interest to find out: (i) if foaminess occurs when two liquid phases are present on distillation trays, (ii) how to predict when this behaviour occurs and (iii) to find ways of minimising its effect on column capacity.

In most industrial applications, the problem of foaming is usually solved by the introduction of a defoamer to depress the amount of foam being generated or the use of anti-foaming agent to prevent formation of the foam. This approach does not in general terms give satisfactory results as firstly it requires an amount of defoamer or anti-foaming agents to arrest the situation and secondly it requires extra separation equipment to remove the defoamer or anti-foaming agent. Both these factors may inhibit the economics of the operation and also the eventual contamination of the final product can be closely associated with the use of these chemicals. In most distillation and absorption processes, the provision of large interfacial areas for mass transfer is usually associated with the attainment of a high degree of separation. Hence, the operation of most columns is conducted in the foaming or frothing regime. Much as the provision of large interfacial area is recognised as the basis for a high degree of separation, the generation of unwanted foams poses a difficult problem to the process engineer, as this leads to complications in the separation process.

It is thought that the foaming associated with two liquid phases on a tray can be reduced or avoided by the proper choice of tray design to produce jetting rather than bubbling at the perforations i.e. by operating in or close to the spray regime. Foaming does not occur on trays operating in the spray regime because coalescence proceeds by drainage of the intervening liquid film. A foam will tend to form when a mechanism exists to maintain the liquid film and to prevent it rupturing prematurely during the drainage process.

Within industrial plate columns, sieve trays continue to enjoy considerable popularity as they are simple to manufacture and are not prone to mechanical problems of alternative trays, such as valve trays. Since their introduction to replace bubble cap trays several decades ago, the design of sieve trays has undergone continuous evolution. Research into sieve tray performance has not kept pace with changing tray design and much of the available literature on sieve trays refers to small hole diameter trays operating at low liquid and vapour loadings.

The importance of the tray operating regime was first recognised by Porter & Wong (17) in 1969 and since then, a number of methods have been developed for estimating whether a given tray will operate in the bubbly or the spray regime. The identification of the tray operating regime for a given loading has become an important step in tray design and the properties of the dispersion must clearly be related to the specific operating regime.

Recent investigations of the hydrodynamic behaviour of sieve plates have

indicated that the operating range of a plate can be divided into four regimes. These are:

- i. Discrete bubbling - Consists of a swarm of regular size bubbles rising through clear liquid. This regime exists only at only very low gas rates.
- ii. Cellular foam - Foams tend to result when bubble coalescence is hindered. It is composed of closely packed polyhedral bubbles and can form at low gas and liquid rates.
- iii. Froth regime - This regime is liquid continuous. Gas passes through the liquid as jets and bubbles of ill-defined and rapidly changing shapes and there is a range of bubble size present. It is encountered in high pressure distillation.
- iv. Spray regime - Consists of an array of droplets in a continuous gas phase and the liquid is projected up by the gas jets to form small drops. It is favoured by high gas momentum and low liquid depths. This regime is encountered in industry in vacuum distillation column and in atmospheric distillation columns with high gas loadings.

These regimes are supposedly encountered in the above order as the vapour rate is increased. However, of these four regimes only the froth and the spray regime are normally encountered on large plates operated at industrial loadings. Most of the correlations and models that have been proposed to predict the transition from spray to bubbly are based on the experimental results of Porter & Wong (17).

This work seeks to identify whether foaming occurs on sieve trays in the presence of two liquid phases with a view to recommending new procedures and techniques for the design of plate columns processing foaming mixtures.

The studies undertaken are reported under three broad classes: (i) Observing whether foam builds up in distillation columns processing Ross type ternary mixtures, (ii) If so, can the foaminess be controlled by equipment design. (iii) Finally, a Ross type mixture has been used to test the commercial design of sieve trays at different hydrodynamic conditions.

CHAPTER 2

LITERATURE SURVEY

2.1 Introduction

Some knowledge of how close the calculated conditions will approach the operating conditions is necessary in order to design distillation columns satisfactorily. Investigations by the A.I.Ch.E. Research Committee (15,16) showed that the efficiency of a distillation column depends on the type of dispersion formed above a plate. Therefore, when calculating the efficiency of a plate, there is a need to know the flow or dispersion regime present on the tray at the column operating conditions. The study of these dispersions is, therefore, an integral part of the plate efficiency and the column capacity.

If a liquid is present on a sieve tray and vapour is passing through it, a variety of different dispersions can form ranging from a continuous column of bubbles at low vapour rates and large liquid depths to a spray of fluidised drops at very high vapour flow rates and low liquid depths. Thus, the dispersion can have either liquid or vapour as the continuous medium with vapour or liquid as the dispersed phase. Even within the bubbly type of dispersion, i.e. dispersion with the liquid phase continuous, different dispersions have been noted. Therefore, depending on the operating conditions and the system used, it is possible for a froth, a foam, an emulsified flow, or a spray to be formed on or above the trays. Usually foams have stability of only a few seconds but in some systems, especially systems containing two liquid phases, the foam may cause a severe problem by tending to fill the interplate space and the capacity of the distillation column is greatly reduced. As a 'rule of thumb', the columns are derated from their original specifications by as much as 50% - usually by increasing the column cross section.

A vast amount of information has been gathered on the performance of sieve trays with reference to flow regimes over the past few decades and it has been summarised by Zuideweg (148). However, in recent years the operation of sieve trays in the spray regime has become increasingly widespread, both as a result of a deliberate design policy at the design stage or as a consequence of a demand for increasing throughput from already installed equipment. Indeed, it is likely that most trays having large diameter holes and operated under vacuum or atmospheric pressure will function in the spray regime. The detailed knowledge of the number and size of droplets comprising the dispersion and their motion on and above the tray are important considerations in understanding the tray mass transfer and hydrodynamics in this regime.

Early studies of sieve tray pressure drop characteristics led to the conclusions that four distinct types of tray action could exist: free draining, weeping, normal operation, and

oscillation. Research was carried out in favour of characteristics of sieve trays operating in the normal operation region. However, research into sieve tray performance has not kept pace with the tendency for industrial trays to operate in the spray regime and only a few researchers have studied this regime. In the period since the spray regime was first recognised, the work (17-31) which has been done has concentrated on (i) the measurement of the gas velocity at which the phase inversion [the transition from spray to bubbly regime operation] takes place (17,19-22), (ii) the determination of the droplet size distributions (25,28, 31) and (iii) the projection velocities at the formation level in the spray regime dispersions (25,28,31). No attention has been given to the fate of the droplets after formation [i.e. whether they coalesce or breakup] and such information is required if the nature of the spray regime is to be fully understood.

One further matter of concern is that the extent of entrainment from a spray regime dispersion is still poorly quantified. Based on the limited data available (24) it is generally agreed that entrainment is high in the spray regime. However, there has been no systematic research undertaken to measure entrainment at different tray spacings.

The literature survey has concentrated on information available for single liquid phase systems because very little work has been reported for systems containing two liquid phases. Throughout this literature review, foam formation/destruction and the explanation of foam stability is stressed in terms of interfacial area and surface tension. Possible methods of foam elimination such as the use of additives, packed columns and the spray regime are discussed and therefore, the transition from spray to bubbly regime and the available correlations are considered in detail.

2.2 Foams

A foam is formed when bubbles rise to the surface of a liquid and persist for a while without coalescence with one another or without rupture into vapour space. The formation of foam consists simply of formation, rise and aggregation of bubbles in a liquid in which a foam can exist. Calderbank & Rennie (32) described foams as being comprised of large cellular, relatively stable bubbles in close proximity and they observed that the bubble's size vary from 50 μm to several millimetres with foam densities ranging from 200 g/l to 500 g/l. The life of a foam varies from seconds to years, but in general is finite. The maintenance of a foam is therefore, a dynamic phenomena.

Foam properties depend primarily on the chemical composition and the properties of the absorbed film. They are influenced by numerous factors such as:

- i. Extent of absorption from solution at the liquid-gas surface.
- ii. The rheology of the absorbed layer.

- iii. Gaseous diffusion out of and into the bubbles.
- iv. Size distribution of the bubbles.
- v. Surface tension of the liquid.
- vi. External temperature and pressure.

Gravity effects favour the separation of a dispersed gas in a pure liquid causing the bubbles to rise to the liquid surface and the liquid contained in and between the bubble walls to drain downward to the main body of liquid. Interfacial tension favours the coalescence and ultimate disappearance of the bubbles. The bubble destruction is caused by the rupture of the lamellae.

The viscosity of the liquid in a film opposes the drainage of the film and its displacement by the approach of coalescing bubbles. Bikerman (33) pointed out that the life of a foam is proportional to surface viscosity and inversely proportional to interfacial tension. He also disagreed with the idea that the foam film drains to a critical thickness at which the bubble will spontaneously burst.

Non-aqueous foams have been investigated in recent years by many workers (34,35). They have highlighted bulk viscosity, interfacial viscosity and surface tension as being important factors in non-aqueous foam stability.

The foaming has been correlated with a maximum in the following stabilisation indices S . When mass transfer occurs:

$$S = \frac{\delta\sigma}{\delta x} (y^* - y) \quad \text{Hart \& Haselden (36)} \quad \dots 2.1$$

$$S = \delta x^* - \delta x \quad \text{Lowery \& Van Winkle (37)} \quad \dots 2.2$$

$$S = \frac{\delta\sigma}{\delta x} (x - x^*) \quad \text{Hovestreydt (38)} \quad \dots 2.3$$

Hart & Haselden (36) pointed out that the rate of foam drainage increases with liquid density. As a consequence, in binary distillation maximum foaming occurs at a composition which is shifted slightly towards the less dense component compared with the composition at which S is a maximum as given by equation (2.1).

2.2.1 Ross Type Foam

Ross & Nishioka (2) have argued that in a distillation system of two or more components, surface activity of one of the components is a result of a weak interaction with the others. Thus, a tendency towards the separation of the two liquid phases serves as an indication that surface activity and hence foaming, is likely to occur. They suggest that this

may explain why foaming is often a problem in extractive distillations in which liquid phase non-ideality, while increasing the relative volatility of the components to be separated, also leads to a tendency towards the separation of the two liquid phases.

They demonstrated that as the mixture composition approaches the Plait point, however, one of the phases acts to destroy the foam if the separated phase is present in small quantity and it has a lower surface tension than the other.

2.2.2 Mechanism of Foam Stabilisation

Foams cannot be formed from pure liquids and an explanation has been put forward in terms of thermodynamics theory (39). The theory has been advanced in terms of Gibbs function (34) and Helmholtz function of foam (40). The latter gives a complete explanation of foam stability.

Helmholtz function of foam is:

$$df = -PdV - SdT - \sigma dA + \mu_1 dn_1 + \mu_2 dn_2 \quad \dots 2.4$$

Integration give:

$$df = \sigma A - \int PdV \quad \dots 2.5$$

Equation (2.4) applied to a foam shows that a decrease of free energy results from a loss of area and from the expansion of gas, both of which are caused by the coalescence of bubbles. Hence, a foam composed of gas in a pure liquid is thermodynamically unstable.

For dilute solutions of low viscosity, foam stability and foaminess are directly proportional to the work required to transfer excess solute from the film surface into the bulk liquid.

2.3 System Derating Factor

Correlations for estimating the active and downcomer areas involve only the vapour and liquid densities. The effect of all other properties on tray sizing calculation is introduced through the system factor which derates the tray load-handling capacity.

Derating factors for the various systems are listed in table 2.1. The foaming factors systems listed in table 2.1 are not necessarily for foaming due to two liquid phases.

Table 2.1 System factors (41)

Foaming system	Derating factor
Non foaming	
Regular	1.0
Slight foaming	
Depropanisers	0.9
H ₂ S stripper	0.9
Moderate foaming	
De-ethanisers	0.85
Amine strippers	0.85
Crude towers	0.85
Furfural refining	0.80
Heavy foaming	
Amine absorbers	0.75
Glycol contactors	0.65
Methylethyl ketone	0.60
Stable foam	
Alcohol synthesis absorbers	0.35
Caustic regenerators	0.30

2.4 Marangoni Effect

A spontaneous agitation of the interface between two immiscible liquids has been observed when a solute is passing from one phase to the other. The effect appears to depend upon the direction of transfer of the solute and is apparently associated with local variations in interfacial concentration and interfacial tension and is often referred to as the Marangoni effect (42).

If the interfacial tension is sensitive to the interfacial composition with respect to consolute point, the Marangoni effect can occur giving a pronounced interfacial instability and enhancement of the mass transfer rate.

2.4.1 Causes of the Marangoni Effect

The commonest mechanism influencing film stability is the Marangoni effect, which can arise in several ways.

The current theory concerning the cause of foaming in distillation columns indicates that the foaming is caused by the Marangoni flow induced by differences in composition between thin films of liquid. Liquid films or lamellae, because of their extended surface, evaporate faster than the bulk liquid phase. If the loss of the volatile constituent causes the surface tension of the residual solution to increase, then the liquid lamellae of great surface tension pumps more liquid into itself from the bulk liquid of smaller surface tension, and so maintains its stability.

2.4.2 Mass Transfer Induced by Marangoni Effect

Most of the previous work on foaming in distillation system has involved the investigation of the Marangoni effect. It has been observed that more foam is seen in the column when the liquid surface tension is lower at the top of the column than at the bottom [positive system] than when the surface tension gradient is reversed [negative system].

Zuiderweg and Harmens (43) categorised the distillation and adsorption systems into three types:

- i. Positive (σ^+) - Surface tension increases as the liquid proceeds down the column.
- ii. Negative (σ^-) - Surface tension falls as the liquid proceeds down the column.
- iii. Neutral (σ^0) - Surface tension is virtually unchanged from tray to tray. This can arise either because the components have similar surface tensions or because the composition change due to similar relative volatilities is small and thus the change in surface tension is negligible.

Thus, σ^- and σ^0 systems do not foam to any significant extent. Sawistowski and co-workers (18,44) pointed out that the Marangoni effect also operates during the break down of ligaments to form drops in the spray regime. Ligaments are stabilised in σ^+ systems whilst ligament break down is assisted in σ^- systems. Thus, smaller and more numerous drops are expected in σ^- systems operating in the spray regime. The authors found higher stage efficiencies for negative systems as against positive systems for plates operating in spray regime.

2.5 Dealing With Foaming Systems

One aim of the present work is to find alternative ways of coping with foaming problems on sieve trays. Traditional methods of foam elimination are:

- i. Chemical methods.
- ii. Physical methods.

The use of Chemical method is discussed in detail in section 2.5.1, whilst the use of Physical methods is discussed briefly. Physical methods involve:

- i. Mechanical methods - Use of mechanical barriers to break foam.
- ii. Thermal methods - Contacting foam with hot surface will destroy foam.
- iii. Electrical methods - Use of electric field to disintegrate or weaken foam or decomposition of the desired component into others.
- iv. Acoustic vibrations - Use of high frequency impulses to break foam.

2.5.1 Additives and Antifoaming Agents

It is known, however, that the addition of small quantities of specific agents to foaming systems can reduce the stability of any foams subsequently formed. These agents can be divided into two groups.

- i. **Foam breakers.**

These are added to existing foams and they are generally considered to act in the form of small droplets which spread on the foam lamellae so that the spreading liquid film carries with it a layer of underlying liquid which comprises the foam lamellae. This means that the lamellae is thinned and the foam breaks.

- ii. **Foam Preventatives**

These generally adsorb at the air-water interface in preference to the film stabilising surfactants. These molecules which have a strong affinity for the air-water interface do not have the capacity for stabilising foam and foam prevention is achieved. Van der Meer (45) and Van der Meer & Zuiderweg (46) suggested that foam preventatives can cause a large reduction in the overall surface tension such that surface tension gradients along the film are practically eliminated.

The major requirements for foam breakers and preventatives are cost efficiency, ease of handling, specific action, absence of any adverse effect on the final product and

environmental safety. Theoretical explanations concerning foaming breakdown mechanisms have been given by Ross (30,34) and Bikerman (33).

Glausser (47) found that the use of a silicone antifoam agent [3 ppm] in natural gas absorber reduced foaming and the gas capacity could be increased by 50 % and the liquid capacity by 135 %. The effective use of antifoam additives in many different processes has been described by Bolles (48), Sabia (49) and Goldmann (50). An exhaustive compilation on industrial antifoaming agents in tray columns is given by Kerner (51).

2.5.2 Action of Antifoaming Agents

Generally defoamers are more surface active than the foaming liquid. The insoluble defoamers function largely by spreading on the surface of the foam or by entering the foam. Thus the film formed by the spread of the defoamer on the surface of a foaming liquid does not support the foam and a foam is not formed.

Robinson & Wood (52) indicated that the entry of a defoamer droplet into the foam surface is associated with film collapse. Bubble rupture does not occur instantly after the entry of the defoamer droplet into the foam surface as according to Ross (34) the film is thinned by gravitational drainage until the defoamer film bridges the surface. At this point the foam becomes highly vulnerable to rupture.

The work of Roberts, Axeberg & Osterlund (53) based on cinematic microphotography indicates that emulsified drops of defoamer locate in the body of the foam lamellae and cause the foam to rupture.

When the defoamer phase becomes saturated with the foaming phase, the surface tension of the defoamer and interfacial tension are affected, decreasing the value of the spreading coefficient.

2.6 Hydrodynamic conditions for foam stability on trays

The effect of plate characteristics on foaming and defoaming have been studied by Rennie & Smith (54) and Rennie & Evans (55). They observed that the formation of foam on a sieve tray is facilitated by closely spaced holes [resulting in large free areas], small diameter holes, low liquid flow rates and high Reynolds number. They found that the foam tends to break down when the Reynolds number is greater than 2,100.

Goederen (26) and Pozin, Mukhlenov & Tarat (56) found that foaming is favoured by low gas velocities. Hofhuis & Zuiderweg (57) have proposed that foaming occurs in the emulsion regime at high gas to liquid ratios.

2.6.1 Foam and Tray Design

Foaming does not occur on a tray operating in the spray regime. This is due to the limited number of bubbles separated by liquid films and also to the large gas inertia which mechanically disrupts any foam which tends to form.

When foaming occurs on industrial trays, the liquid is likely to have a significant horizontal velocity. Excessive foaming usually increases entrainment and downcomer backup and eventually leads to premature flooding. Calderbank & Rennie (32) studied foaming in a small diameter column (0.1 m) where the liquid was introduced near the tray floor and was pumped upwards by the gas to leave the column over the weir. However, this arrangement is unsatisfactory because it fails to reproduce the situation on large diameter trays where the liquid which flows to the top of the foam has to drain down again against the gas flow.

It has been suggested by Andrew (20) that unstable foam in which relative bubble movement occurs are more characteristic of the foam found in practice.

2.6.2 Tray Behaviour with Two Immiscible Liquid Phases

The only work existing on the tray behaviour in presence of two liquid phases is that of Ashton, Arrowsmith & Yu (152). The authors investigated three phase distillation hydraulics using water, kerosene and air in a glass column of 38 mm diameter and 200 mm high using a plate with a single orifice of 1 mm diameter. Six flow regimes were identified in terms of liquid depth, the ratio of water to kerosene depth and gas velocity through the orifice. These are: entraining regime, shallow water regime, shallow kerosene regime, kerosene drop regime, foam circulation regime and the transient regime.

The authors concluded that liquid-liquid mixing pattern is time and process dependent.

2.7 Flow Regimes and Tray/Plate Hydraulics

Two phase flow patterns on perforated plates can effectively be described and characterised by considering the different types of flow behaviour of the dispersion existing on the plate. Traditionally, the operating range of sieve plates is characterised by an upper boundary-the flooding limit and a lower boundary-the weeping limit. Visual observations have shown that within this range, different flow regimes exist in which either the vapour/gas or the liquid is the dominant dispersed phase.

Four two phase flow pattern regimes can be identified on the plate. Different authors describe these regimes by different names, but basically the general characteristics and properties of the regimes are the same.

With increasing superficial gas velocity for a fixed liquid loading on the plate, Muller & Prince (58) described the regimes as bubbles, cellular foam, frothing and spray regimes. These regimes are discussed in detail below and illustrated in figure 2.1. A good representation of all flow regimes is given in the form of a flow diagram [figure 2.2] due to Hofhuis & Zuiderweg (57).

2.7.1 Discrete Bubbling [Region of independent bubble rise]

At very low gas velocities of approximately 0.5 ft/s, separate bubbles of gas rise in the column through clear liquid. The main feature of this regime is that the gas flow passes through the two phase dispersion as discrete bubbles. A bubble is a globule of gas or vapour surrounded by a thin liquid film. The dispersion has a discrete surface although this surface is some times very mobile.

A large number of small diameter holes help the formation of the bubble regime and the bubble regime is visually observed in high pressure distillation.

The holdup is found to be proportional to the gas velocity until the limit of spherical packing is reached when the voidage fraction is 0.5. At this point bubbles start to coalesce and the next dispersion regime is formed. However, due to the small number of holes, the lower free areas required for this type of operation and the large amount of weeping which occurs at such low gas velocities, this region is not encountered in the normal operation of distillation sieve trays where generally there is the need for high throughputs with consequent high gas loadings. This method of gas contacting is mainly found in bubble columns.

The bubble formation phenomena and the methods of evaluating bubble volume, frequency of formation, influence of various factors on bubble size, effect of orifice characteristics and submergence have been extensively covered by Clift, Grace & Weber (59) and Kumar & Kuloor (60).

Calderbank & Moo-Young (61) and later Abdell-aal & Plank (62) studied the efficiency and mass transfer characteristics of bubbly gas-liquid dispersions. In more recent work Pinczewski (63) proposed a new model describing the effect of the gas momentum on the modified Raleigh equation for bubble growth. The agreement was good between the model and available experimental data. Bubble velocity (64), flow (65-67), size (68) and formation at special environment (69,70) were all studied extensively either individually or in a swarm.

However even though efforts were made to relate their findings to the operation of sieve trays in the bubbly regime any further development has been prevented by limitation in practical applications.

2.7.2 Cellular Foam

As the gas velocity is increased further, the flow regime changes to the cellular foam regime. The bubbles in the close packed condition deform into a polyhedra or cellular foam. The stability of the cellular foam is a function of the physical properties of the two contacting phases as well as the geometrical characteristics of the contacting device. The operating conditions which are favourable to the formation of cellular foam on sieve trays are given in section 2.6.

Calderbank & co-workers (32,61,71,72) were probably the first to investigate the existence of cellular foams in a series of articles dealing with vapour liquid dispersions on sieve plates. The authors, using various gas liquid systems in a perspex column, observed the bubble volume through the walls. The cellular foam regime was described as a region of rising bubbles of approximately 1.5 cm in diameter, existing at low air superficial velocities of approximately 0.31 m/s and low liquid flow rates of 2.8 l/min and containing a low liquid content. From the calculations made by Davies (73) it can be concluded that the cellular foam consists essentially of uniform size bubbles. Davies (73) calculated the formation bubble size from bubble frequency measurements and these sizes are in close approximation to those observed in cellular foams. It is probably correct to conclude that the characteristics of a cellular foam are that bubbles are of uniform size.

This view was reinforced by Wong (74) and Porter, Davies & Wong (75). However, Sargent & McMillan (76) argued that Calderbank used conditions in his research which are not generally found in industrial distillation columns and also they considered that cellular foam was only found with dilute aqueous systems. However, Goederen (26) reported that cellular foam occurred with air-toluene and air-ethanol systems.

A typical analysis of the structure of the cellular foam may be represented by the structure of dodecahedral bubbles having two components: films formed by the faces of the bubbles and intersections of these forces called plateau border. A description of 'dynamic foam' was given by Hartland & Barber (77) and subsequently a model was derived by Steiner, Hunkeler & Hartland (78) in which liquid in the film flows towards the plateau borders by a pressure difference between the two sites and then drains back to the bottom by the action of gravity. The cycle is repeated when the liquid is carried upward again by the action of the foam bubbles. The maximum height that the bubbles can reach before rupture caused by drainage defines the height of the foamy dispersion.

However, like the bubbly regime, the foam regime is seldom encountered and undesirable in the operation of the sieve trays. Their understandings although necessary, remain to be the starting point for the more practical research on the froth and spray regime.

2.7.3 Froth Regime

This is the last bubbly dispersion to be formed before the onset of the spray regime. In certain situations, in large columns with large holes and pure liquids, it is possible for this regime to appear immediately after the independent bubble rise regime. One of the major differences, however, between the foam and froth is that in the froth there is marked circulation of bubbles whereas with a foam there is no circulation.

Ho, Muller & Prince (27) concluded that froth is formed when the liquid on the sieve plate is deep and circulation of the gas and liquid becomes very intense. This leads to the break-up of the large bubbles to produce a wide range of smaller size bubbles of 1.3 to 1.7 cm diameter. Thus the two main characteristics of the froth are:

- i. Circulation of liquids.
- ii. Small bubbles of a wide range of sizes.

Whilst it is generally accepted that bubbles of uniform size are predominant in a cellular foam, there is a considerable disagreement as to the size of the bubbles present in the froth. Calderbank (79) originally suggested that bubbly dispersion consists mainly of formation size bubbles and are of constant size through out the dispersion, even at the column walls. This means that there are no wall effects. This idea has been questioned (73,75,76,80) by many workers who consider that there will be a wall effect on the bubble size. Wong (74) took photographs using a high speed cine camera from vertically above the plate and found considerable variation in the size of bubbles ranging from 1.4 cm to 2.5 cm at the same vapour and liquid flow rates.

Rennie & Smith (54) argued that the froth must consist of small bubbles, as large bubbles would be broken up due to vigorous circulation of liquid and vapour. Garner & Porter (80) calculated that, if the froth consists of 0.4 cm diameter bubbles and the mass transfer coefficient is calculated from the molecular diffusivity, the efficiency of a sieve plate should be greater than 99%. Efficiencies of this value are seldom found in practice so it must be concluded that either the value of molecular diffusivity used was too high or, more reasonably, large bubbles were found in the bulk of the froth.

Calderbank & Rennie (32) argued with this and put forward the theory that, although much of the froth consists of small bubbles, a large proportion of the vapour leaks through the froth in the form of very large bubbles reducing the effective mass transfer coefficient. Davies (73) found that wall side bubbles are considerably smaller than the bubbles present in the bulk of the froth. This view was simplified by Porter, Davies & Wong (74) who concluded that the froth consists of bubbles of a variety of sizes.

Garner & Porter (80) suggested that three zones can be distinguished at different levels above the floor of the sieve trays in the froth regime:

- i. A clear liquid layer remains on the tray floor through which the high velocity

bubbles are rising from the holes.

- ii. Mass of the froth which contains various size circulating bubbles on the top of first region.
- iii. At the surface, a spray of liquid droplets formed from the bubbles bursting or the jetting of the gas through the liquid.

In the first zone, kinetic energy from the rising gas is partly converted into pressure energy, resulting in a high degree of turbulence and mixing in the clear liquid. This intense mixing is effective in promoting mass transfer between the two phases. The momentum of the rising gas also causes the bubbles to rise into the second zone with a velocity higher than their terminal rising velocity. As the bubbles get larger, some burst into small bubbles while some rise very close to each other with entrained liquid. Finally, the large bubbles reach the surface and burst, causing droplets of liquid to be thrown above as fine sprays. Garner & Porter's (80) description of the spray caused by bubbles bursting and gas jetting was among the few earliest observations which later led to the identification and study of the spray regime.

Burgess & Calderbank (81), using a conductivity probe, carried out an extensive study on the distribution of bubble size and velocity distribution. The bubble distribution curves were presented as a function of the gas velocity. From this the froth properties such as flow, gas-liquid interfacial area and local liquid contents were derived.

More recently Lockett & Uddin (82) and Lockett, Kirkpatrick & Uddin (83) using a 'two dimensional' column and cine study, reported a region of formation and a region of bulk froth. The authors showed that the large bubbles reported by Porter, Davies & Wong (75) to be pulsating jets similar to those described by Muller & Prince (58) in their single hole studies. In the bulk froth region, the pulsating jet gave rise to large bubbles of elongated shapes and also small bubbles were reported to circulate among the liquid in this region.

2.7.4 Spray Regime

It is generally accepted that the spray regime is associated with low liquid holdup (15,75) and consists of liquid drops dispersed in a continuous gas stream. For present purposes it is sufficient to assume that the drops form beneath the surface of the liquid and generally form the liquid surrounding the orifice, although it is not strictly true. Most of the spray visible on sieve trays is of this type, i.e. 'formation spray', produced solely by the jetting of the gas through the liquid phase. Smaller drops are formed from bubbles bursting at the surface of the bubbly dispersion.

The existence of the spray regime has only been recognised since 1965 (26) and

therefore, only limited investigations have been carried out (84) to characterise the nature of the dispersion formed on a tray operating in this regime.

It was not until the International Distillation Symposium in 1969 that systematic studies on the spray regime began to appear and these were mainly concerned with the investigation of the phase inversion point, i.e. the spray to bubbly transition.

Andrew (20) described the dispersion as being like a 'fluidised bed of droplets' and similar descriptions were proposed by Ho, Muller & Prince (27) and Porter & Wong (17). The latter authors used this description as the basis of a model from which the gas velocity at the onset of the spray regime could be predicted. The model also assumed the existence of a coalescence zone.

A different description of the spray regime was proposed by Fane & Sawistowski (18). By visual observations and the determination of vertical density profiles, the authors proposed a mechanism for the formation of a gas continuous dispersion. Liquid entering the tray was considered to be atomised near the tray floor with each droplet undergoing an independent trajectory in to the gas space. Vertical dispersion density profiles showed a maximum at a height which was interpreted to be the level to which the majority (by volume) of the droplets rose.

In later work, Pinczewski, Benke & Fell (24) and Pinczewski & Fell (28) investigated the nature of the dispersion produced on typical industrial sieve trays operating in the spray regime. Droplet sizes, measured at the formation level by a combination of both photographic and electronic techniques, were found to decrease with increasing gas rate and vertical density dispersion density profiles were found to have a local maximum at about 100 mm above the tray floor. The shape of these profiles were similar to those previously reported by Fane & Sawistowski (18) except that the height of the dispersion was found to be greater on industrial scale trays used by Pinczewski & Fell (22) than those by Fane & Sawistowski (18).

By measurement of dispersion density profiles, Pinczewski & Fell (29) and later Raper, Hai, Pinczewski & Fell (85) showed that a zone of low liquid density existed immediately above each orifice up to about a height of some 100 mm above tray floor. Beyond this level, the influence of the jet was no longer felt and the dispersion became longitudinally homogeneous. Pinczewski & Fell (29) therefore proposed that the dispersion was made up of two zones. In the lower or formation zone, droplets were atomised from the clear liquid pool on the tray floor. These droplets underwent their trajectories in the propagation zone and left the dispersion by jumping the exit weir.

Further work by Fane & Sawistowski (30) and Jeronimo & Sawistowski (86) was concerned with the correlation of experimental droplet size and dispersion density parameters (sauter mean and height of local maximum) with tray geometry and tray loading.

It is noteworthy that the droplet size distributions measured by Fane, Lindsey & Sawistowski (30) within their small scale dispersions exhibited bimodal behaviour whereas Pinczewski's (25) droplet size distributions were all unimodal.

2.8 Transition Between Different Regimes

As stated in Section 2.7, there are significant differences in the hydrodynamic and mass transfer characteristics of the four operating regimes. Design quantities, models and operating parameters are specific for each regime. Before these equations, models or correlations can be applied, it is necessary to be able to predict the specific regime for a given set of operating conditions. Over the range of increasing gas velocity, the transitions from one regime to another are in the following order: bubble flow to foam; foam to froth; direct transition from bubble flow to foam and finally transition from froth to spray.

2.9 Spray to Bubbly Transition

Due to the constant demand for high throughput, the bubbly and foam regimes are relatively insignificant and thus little attention has been given to the transition between these regimes. The transition from spray to bubbly regime has received considerable attention because of an increasing tendency to use the spray regime as a deliberate design policy and also a means of uprating existing columns (87,88). The following section is subsequently devoted to a survey of the investigations carried out in the study of the spray-bubbly transition.

2.9.1 Early Observations

Spell & Bakowski (89) found, when investigating the flow of air from long narrow slots [0.4 cm by 0.5 cm] submerged in water, that there were two modes of bubble formation. In the first mode, which they call the shallow mechanism, it was found that the development of bubbles was inhibited by the presence of the liquid above the slot. They found that a new bubble was formed before the previous bubble had completely left the orifice. This continuous procession of incompletely formed bubbles led to the formation of a channel from one slot to the surface of the liquid. They also observed that the onset of the shallow mechanism was accompanied by the presence of a large number of drops. A second mode, the deep mechanism, was found to occur at liquid depths greater than 5.08 cm. In this mechanism, the surface had no influence on the bubble formation and the bubbles were observed to leave the slots separately.

Spell (84) continued his investigations and found using high speed cine

photography and a stroboscope, that the height of the liquid at which the transition from the shallow to the deep pool mechanism occurred, could be correlated by:

$$\frac{L}{A} = K [\sigma d (\rho_l)]^{-0.5} \quad \dots 2.6$$

In this model the transition is primarily dependent on the surface tension effects and not the gravitational or inertial forces. Payne & Prince (90), by using a cine study of the transition showed that the jet breaks close to the orifice. The work of Pinczewski, Yeo & Fell (91) also supports this conclusion. The authors used a small probe, inserted through the orifice so that it protruded 6 mm above the plate, to determine the jet to bubble transition. Since at the transition, the depths of the liquid were considerably greater than the height of the probe, it was concluded that jet breakage must occur near the orifice rather than close to the liquid surface [as suggested by Spell (84)].

Kutateladze & Styrikovick (92) also used jet theory to develop a relationship for the transition from spray to bubbling which can be reduced to:

$$u_s = \frac{2.5 \sigma^{3/4}}{d (\rho_g)^{0.5} g \sqrt{(\rho_l - \rho_g)}} \quad \dots 2.7$$

However, this equation is in disagreement with the experimental observations, as it implies that, for any given gas velocity, the transition from the spray to bubbly regime is independent of liquid holdup and strongly dependent on surface tension.

Goederen (26), using a variety of gas liquid systems, found a bubbling regime for high liquid holdups of the order of 2 cm and low gas superficial velocities of about 0.1 m/s, whereas, at low liquid holdups [0.5 cm] and high velocities of 2 m/s, he found that the spray regime became apparent. He noted that, at a superficial gas velocity of 0.5 m/s, the liquid tended to become the dispersed phase and that many droplets were present at a height of 20 cm or more above the plate. Even so, he did not notice any great effect of liquid depth on the transition.

Akselrod & Yusova (93) measured the amount of entrainment present in a column by counting and sizing the number of drops. They noted that above a superficial vapour velocity of 0.4-0.6 m/s, there was an abrupt change in the size and number of drops. They called this regime 'fountain condition' and it is probably due to the onset of spraying.

Mukhenov (94) found that the break-down of foam to a suspended layer of mobile drops began at a superficial vapour velocity of 1 m/s but, for the transition to be complete,

the vapour velocity had to be of the order of 4 m/s indicating that froth could exist with spray over it.

In later studies Fane & Sawistowski (95) showed that the liquid holdup becomes practically independent of the type of system, weir height and vapour velocity once spray conditions have become fully developed.

These observations all indicate little effect of liquid height. Although it is very difficult to obtain information on the actual vapour hole velocity, they also show that the hole velocity is a more important variable than the superficial velocity. However, all the experimenters found the same basic relationship, i.e. increasing the vapour flow rate and decreasing the liquid depth on the sieve plate induced the amount of spray present to increase. This, as will be shown, is due mainly to the effect of the bubbling to spray transition and the increasing dominance of the gas momentum.

2.9.2 Measuring Techniques

Some techniques for measuring the onset of the froth-spray transition were based on the differences in the proposed mechanisms between the froth and spray regimes whilst others methods used more basic techniques such as visual observation. Spell & Bakowski (89) reported the transition as a result of visual observations and no further methods were attempted to locate the transition.

Pinczewski & Fell (22) used windows and photographic observations as an aid to cross check more elaborate methods such as an electrical probe. The authors used an electrical probe at the orifice of a small-scale single hole sieve tray and the pulse rate obtained was compared with the bubbling frequency obtained from photographic measurements. The electrical probe has been used by several workers (96,97) to measure the transition.

Porter & Wong (17) used a perspex column, containing a single plate and having no liquid cross flow. This arrangement enabled photographs to be taken from underneath. The authors used visual observations and a subsequent light transmission technique to identify the transition. An explanation of the technique is given in section 6.3. Burgess & Robinson (81) also used the light transmission technique to study the froth-spray transition in a 1.2 m [4 ft.] column with liquid cross flow. Pinczewski & Fell (22) suggested that the surface of the froth for a cross flow tray was much less distinct than Porter & Wong (17) indicated and constructed a probe which measured the bridging frequency of the tray holes by the liquid. Bubbling at the holes would correspond to a high bridging frequency as bubbles issued whilst a sharp decrease was obtained when the gas changed to that of a continuous jet. This method was shown to be adequate concerning bubbling to jetting transition on individual holes but its value remained in question without a satisfactory proof

in the direct correspondence between bubbling-jetting to that of the froth-spray transitions.

Muller & Prince (55) first pointed out the variation of residual pressure drop with liquid holdup could be employed as a measure of the transition from jetting to bubbling in a tray hole. A maximum was reached in the residual pressure drop when the liquid fraction was increased. Payne & Prince (90) utilised this approach in first locating the bubbling to jetting transition in single holes and subsequently related it to that of the spray to bubbly transition and later showed that the transition measured by the residual pressure technique is identical to that measured by the light transmission technique.

Some workers (98-100) have shown that that a decrease in entrainment occurs as the operating regime changes from the spray to bubbly. The entrainment has shown to go through a minimum at the transition point.

2.9.3 Mechanism and Prediction of Transition

The most extensive work on the spray to bubbly transition has been carried out by Porter & Wong (17) for a number of gas-liquid systems. The authors investigated the transition from spray to bubbling for a wide range of physical properties of liquid and vapour on a 0.45 m [17.75 inches] square sieve plate. Their experimental results were performed without liquid cross flow to eliminate any effect that the liquid momentum may have at the transition point. They correlated their results by a simple model which brought together two factors: The rate at which the gas or liquid slowed down after emerging from the orifice in the plate and the settling characteristics of the system represented by the terminal velocity above a sieve plate as the gas slowed down from the hole to superficial velocity. In developing the model, they measured the transition by the changes observed as light was transmitted through a bed of droplets comprising the gas liquid mixture.

The liquid droplets that make up the spray bed are distributed in the various sizes in the space above the tray. Theoretically droplets of a similar size are expected to form a plane above the tray whose height was determined by their terminal velocity u_t . Droplets with their terminal velocity below u_t will rise above the plane and then descend or get entrained in the gas stream. Drops of corresponding size and hence of similar terminal velocity to u_t will form a hypothetical plane. These are designated as 'large drops'. It was found that for drops larger than 5.0 mm diameter the terminal velocity becomes independent of size. Coalescence between rising and descending drops forms even larger drops that concentrate below the plane. The formation of larger drops increases with increase in the liquid flow rate (and thus liquid holdup). At the transition, multiple coalescence takes place transforming the plane into the surface of a bubbly 'dispersion'.

They correlated the liquid holdup at the transition in terms of the dimensionless ratio of the foam height to hole diameter and the fractional slowing of the gas at the large

droplet terminal velocity, $(u_h - u_t)/((u_h - u_s))$. The large drop terminal velocity was in turn related to the physical properties of the gas and liquid by the equation:

$$u = 1.04 \left(\frac{\rho_l}{\rho_g} \right)^{0.5} \quad \dots 2.8$$

Other physical properties were found to be relatively unimportant.

From the experimental findings of the authors the following correlation was proposed for values of $0 < [(u_h - u_t)/(u_h - u_s)] < 0.8$:

$$\frac{h_d}{d_h \rho_f} = 4.0 + 9.0 \left[\frac{1 - A_f C_{tg}^{0.5} (\rho_l / \rho_g)^{0.5} 1/h_s}{(1 - A_f)} \right] \quad \dots 2.9$$

or

$$\frac{h_d}{d_h \rho_f} = 4.0 + 9.0 \left[\frac{(u_h - u_t)}{(u_h - u_s)} \right] \quad \dots 2.10$$

Burgess & Robinson (19) extended the study of Porter & Wong (17) to real situations where liquid flows across the plate and over a weir. They used a 1.2 m diameter column in their study. Their results compared favourably with those of Porter & Wong (17) for plates with 1.27 cm hole diameter. However, with plates having a 4.76 cm holes considerably greater foam height was found and they noticed that the transition occurred at different holdup values at different parts of the plate. The authors pointed out that the lack of correlation of the 4.76 cm diameter hole tray may be caused by depletion of the liquid layer near the tray floor of the plate by entrainment.

Pinczewski & Fell (22) measured the transition in an air-water simulator for large hole diameter sieve trays [0.635-19.05 cm diameter holes] at commercial gas and liquid loadings. The measured transition were reasonably correlated by Spell's (84) equation for gas issuing from a submerged orifice. They proposed a correlation based on the Raleigh instability analysis for a column of air surrounded by a liquid to predict the boundary between 'deep mechanism (bubbling)' and 'shallow mechanism (jetting)' for single vertical rectangular slots submerged in water. They concluded that the analysis is equally valid for a submerged orifice on a sieve tray and proposed the following correlation:

$$h_{cl} = K d^{1/2} \frac{(\rho_l - \rho_g)^{1/2} u_h}{\sigma^{1/2}} \quad \dots 2.11$$

Experimental results show that there is a linear dependence of the liquid holdup at the transition on hole velocity as suggested by the above equation. However, Payne & Prince (90) have argued that Raleigh's jet break down mechanism of capillary instability is inappropriate to froth-spray transition on sieve trays.

In their work Pinczewski & Fell (22) found that the existing correlations of Ho, Muller & Prince (27), Kutateladze & Styrikovick (92) and Andrew (20) failed to predict the observed dependence of the gas velocity at the transition on the fractional free area of the tray, the hole diameter and the liquid holdup.

Jeronimo & Sawistowski (86) proposed a number of correlations for hole velocity and liquid holdup on sieve plates at the transition from froth regime to spray regime as a function of physical properties and plate geometry. Their final correlation is:

$$h_{cl} = 1.059 u_s d_h A_f^{0.209} \left(\frac{\rho_g}{\Delta \rho} \right) \sigma^{-1/2} \quad \dots 2.12$$

where:

$$u_s = \frac{0.655(g\Delta\rho\sigma^2/d_h\rho_g^3)^{1/6}}{A_f(1 + 0.000104 L_v^{-0.59} A_f^{-1.79})}$$

The above equation correlates the experimental data with an average error of 8% although the correlation is based only on air-water data. The authors have introduced system physical properties by basing their analysis on Kutateladze & Styrikovick (92) correlation for deep pool bubbling.

The above correlation indicates a strong dependence of the transition on surface tension. This is in variance with experimental measurements which show little or no effect of surface tension on the transition. Lockett (99) reported that above equation severely underpredicts the transition for the data of Prince, Jones & Panic (102), Payne & Prince (21) and Hofhuis & Zuiderweg (57).

A different approach was adopted by Payne & Prince (90). They showed, by cine studies, that the transition between jetting and bubbling at a single submerged orifice

occurred gradually through a range of depths and/or gas velocities. The authors recommended a correlation for the transition as:

$$\frac{\rho_g}{(\rho_l - \rho_g)} \cdot \frac{u_h^2}{gd_h} = \frac{h_{cl}}{d_h} + 14.6 \left[\frac{\sigma}{(\rho_l - \rho_g)gd_h} \right]^{1/2} - 2.2 \quad \dots 2.13$$

The transition range is here characterised by using the change in residual pressure drop with depth. The authors proposed a mechanism according to which the transition depends on the gas jet inertia and the acting gravitational force by the surrounding liquid. The ratio of the opposing force was represented by a modified Froude number. At low Froude numbers, the effect of the surface tension became significant and another group, the Bond number was proposed. Where:

$$Fr^* = \left[\frac{\rho_g}{(\rho_l - \rho_g)} \frac{u_h^2}{gd_h} \right]^{1/2} \quad \text{and} \quad B = \frac{(\rho_l - \rho_g)gd_h}{\sigma}$$

Muller & Prince (27) found that the transition from jetting to bubbling could be characterised by the pressure fluctuations in the chamber below the orifice or by the variation of residual pressure drop with liquid depth. Both the residual pressure drop and the amplitude of the pressure fluctuations reached a maxima at the transition.

The residual pressure drop criterion has been used as the basis by Payne & Prince (40). It is calculated from the mean pressures which can be simply and accurately measured. It is defined as the total pressure drop across a plate less the dry plate pressure drop and liquid depth. They assumed that the pressure drop resulting from gas flow through the orifice during bubbling and jetting is independent of liquid head effects and is equal to the dry plate pressure drop.

$$P_{res} = P_t - P_{\phi} - h_{cl} \quad \dots 2.14$$

As the liquid depth is increased, interaction between the gas and liquid increases resulting in increased momentum transfer and an increasing residual pressure drop. This interaction causes bulk motion of the liquid near the orifice, as the liquid pulses back and forth and atomisation of the liquid around the periphery of the jet. This atomisation

increases with increasing depth and so the residual pressure drop rises to the transition. When the system is in the jetting/bubbling regime entrainment is less than in the jetting regime, so the transition from the jetting to bubbling is accompanied by a reduction in entrainment. There is thus a decrease in momentum transfer and consequently in residual pressure drop, when the system enters the bubbling regime. A new modified Froude number was proposed and its relationship with liquid holdup was suggested.

$$\frac{h_d}{d_h \epsilon} = 1.5 Fr^* \quad \dots 2.15$$

where

$$Fr^* = \left(\frac{\rho_g u_h^2}{\epsilon \rho_l g d_h} \right)^2$$

Prince, Jones & Panic (102) studied the transition under distillation conditions using water-dilute acetic acid, ethanol-water at two concentrations [64% and 36%] and pure alcohol. They identified the transition by residual pressure drop measurements and dispersion height by the light transmission technique and found that both the light transmission and the residual pressure drop technique give the same liquid holdup at the same point. It was concluded that during mass transfer and without mass transfer, the bubbly-spray transition occurred under identical conditions to the change from bubbling to jetting at the same hole size. Low liquid holdups will also lead to spray rather than to froth and these conditions will be brought about by the use of low weir heights, by operating at low liquid loadings, or at low liquid to vapour ratios [i.e. low reflux ratios].

The authors found that their results could be correlated quite easily by Payne & Prince (21) correlation, although they found that by using all the data, the coefficient was 1.6 instead of 1.5.

Hofhuis & Zuiderweg (57) identified four separate flow regimes and perhaps the most significant implication of their findings is the suggestion that the transition from spray to bubbly and vice-versa occurs over a range of liquid flow rates for a fixed gas flow rate. This implies that the bubbly and spray regimes may not be representative of most operating system as hitherto understood. The authors proposed the following correlation for the spray to bubbling transition:

$$\frac{h_{cl}}{d_h} = \frac{1.1}{A_f} \frac{u_s}{\sqrt{gh_d}} \sqrt{\frac{\rho_g}{\rho_l}} \quad \text{..... 2.16}$$

Following discrepancies between this and other models, it was pointed out by Lockett (101) that the relationship between h_{cl}/d_h and u_s , as proposed in this correlation, is misleading particularly at high gas velocities where tray oscillation occurs and becomes significant to the tray behaviour.

Barber & Wijn (103) used Ruff's analysis for bubbling to jetting transition at orifice of hole diameters greater than 5 mm. Ruff (104) showed that:

$$\frac{\lambda_h}{\sqrt{gd_h}} = 0.61 [\Delta\rho/\rho]^{1.8} \quad \text{..... 2.17}$$

where λ_h is the load factor in the hole $[= u_h(\rho_g/\Delta\rho)^{1/2}]$.

When the velocity through the hole is higher than the 'critical' velocity (u_h) given by equation 2.17, a vapour jet develops at the opening of the hole and persists until the velocity is reduced below the critical velocity.

The vapour velocity at the top of the liquid layer is greater than that given by above equation. Assuming constant jet expansion angle and the height of clear liquid is proportional to the liquid holdup, h_{cl} , the above equation was used to derive a relationship for the liquid holdup at which the froth-spray transition is complete.

$$\frac{h_{cl}}{d_h} = A \left(\frac{\lambda_h}{\sqrt{gd_h}} \right)^{0.4} \left(\frac{\rho_g}{\Delta\rho} \right)^{0.05} - B \quad \text{..... 2.18}$$

The authors used all the available data for hole diameters greater than 5 mm and a correction factor was introduced for the effect of the pitch of the perforation. The closer together the holes are placed, the greater will be interaction between them. This will affect the relationship between the total liquid holdup and the height of the jet. By regression analysis they derived the following correlation:

$$\frac{h_{cl}}{d_h} = \left[1.35 \left(\frac{\lambda_h}{\sqrt{gd_h}} \right)^{0.4} - 0.59 \right] \left(\frac{P}{d_h} \right)^{0.33} \quad \text{..... 2.19}$$

where the density ratio has been incorporated in the constant 1.35.

Originally Ruff (104) considered the forces acting on a bubble and in his analysis neglected the inertia effect. Payne & Prince (90) have shown that the transition also depends on the inertia of gas flow and therefore, the effect of inertia cannot be neglected. Lockett (101) also argued that the constant jet angle is only to be expected if the liquid surrounding the jet is stationary and that in general the cone angle is expected to decrease as liquid height increases. Similarly Chen, Kwan & Wong (105) considered the ideal situation of the growth of a bubble in a gas-liquid mixture. The point of bubbling to spray transition was taken as the situation when the diameter of the growing bubble was equal to the dispersion height. The results obtained in the new model agreed excellently with that by Barber & Wijn (103).

Porter & Wong's (17) model was modified by Wong & Kwan (106) to remove the restriction of the free area. They measured local gas velocities above sieve plates in an empty column and found that the variation in velocity above a sieve plate depends only on hole size, gas velocity and is virtually independent of the free area.

Their final correlation is:

$$\frac{h_{cl}}{d_h \rho_f} = 2.06 + 30.5 \frac{u_g \rho_g^{0.5}}{A_{fg}^{0.5} (\rho_l - \rho_g)^{0.5}} \quad \dots 2.20$$

A 'modified jet penetration model' was proposed by Lockett (101). The model was derived by assuming a stable liquid bridge is present where the kinetic energy of the gas across the jet equals the potential energy of the liquid/gas dispersion above the bridge. The model generalises a number of existing correlations with suitable assigned indices.

$$\frac{h_{cl}}{d_h} = \frac{[(4+n)/n]}{(4/n)^{4/(4+n)}} \cdot \frac{\rho_g^{n/(4+n)}}{\rho_l} \cdot \frac{u_h^{2n/(4+n)}}{a^{4/(4+n)}} \cdot \frac{(1-\epsilon)^{4/(4+n)}}{(gd_h)^{n/(4+n)}} - \frac{(1-\epsilon)}{a} \quad \dots 2.21$$

However, despite detailed analysis Lockett (101) proceeded to correlate the data from various sources by an empirical equation which is not dimensionless.

$$\frac{h_{cl}}{d_h} = 2.78 \left(\frac{\rho_g}{\rho_l} \right)^{0.5} u_h \quad \dots 2.22$$

2.10 Entrainment

It is important to estimate the rate of entrainment, both as a check on the approach to flooding and also to estimate the reduction in tray efficiency. Reliable methods for predicting entrainment allow designers to minimise overdesign and enables operators to identify excessive entrainment problems when they occur.

2.10.1 Prediction of Entrainment

Most published entrainment prediction methods were developed in the late 1950's and early 1960's and were derived before the major effect on flow regime was appreciated.

Eld (107) developed an equation based on the gain in the energy of the drops and equating this gain to the loss of energy in the gas as it emerges from the dispersion.

$$\frac{w_g}{2} (u_h - u_g)^2 = z v_l (\rho_l - \rho_g) g \quad \dots 2.23$$

Hunt (108) correlated entrainment as a function of surface tension, gas superficial velocity and plate spacing. The correlation makes no allowance of the hole diameter and free area, factors that have an important impact on the behaviour of the dispersion on the tray and thus, the nature of the entrainment (109,110). As most of the data were in the froth regime and noting that no allowance for free area and hole diameter have been made, it is unlikely that this correlation can be used for the spray region. Attempts to apply it to the spray regime (110,24) were unsuccessful and in one instance (111), it was reported to severely underpredict the measured entrainment.

$$E = 0.073 \left(\frac{u_g}{s} \right)^{3.2} \quad \dots 2.24$$

where $s' = s - 2.5z_c$

Fair (112) correlated entrainment, based on published data, as a function of liquid and vapour flow rates and liquid and vapour densities. The correlation requires knowledge of the percentage approach to flood; this parameter is also used to account for free area effects. As stated by the author, this correlation is intended to provide a simple design tool. Attempts to apply the correlation to predict spray regime entrainment data can give reasonable agreement (24,111), but also can produce a large scatter (24,111,113) and overprediction of the entrainment rates for high free area trays (24).

Friend, Lemieux & Schreiner (114) graphically plotted entrainment as a function of gas hole velocity, expressed in the dimensionless form of u_h/u_t , where u_t is defined by:

$$u_t = \frac{2gd_p(\rho_l - \rho_g)^{0.5}}{3K\rho_g} \quad \dots 2.25$$

They compared the prediction with those of Hunt (108) and found that there was more entrainment than that predicted by Hunt (108).

Yoshida, Nishibe & Nagai (87) found an effect due to hole size and for the spray regime-entrainment could be predicted by:

$$E = \frac{d_h e^{1.75F}}{s^{1.95} A_f^{1.3}} \quad \dots 2.26$$

where $F = \text{hole factor} = u_g (\rho_g)^{0.5}$

It was also found that entrainment was independent of the liquid flow rate and weir height and this appears to be one of the basic properties of the spray.

Bain & Van Winkle (115) found that entrainment increased with decreasing weir height and increasing vapour flow and increasing liquid flow. The authors developed an empirical correlation based on their extensive air-water test data, which included both froth and spray regime data. They (115) and others (111) noted a large scatter when comparing predicted to experimental results. The correlation applies only to air-water system. At a later stage, Van Winkle (116) provided some guide lines for extending the correlation to other systems, but gave no basis for this.

Stichlmair (113) was perhaps the first to present an entrainment correlation based on the flow regime concept. In his graphical correlation, which applies to sieve, bubble - cap and valve trays, a distinct portion of the graph covers each regime. The only sieve tray data used in the spray regime portion of the correlation are air-water data. The correlation adequately predicts the effect of free area on entrainment, but the correlation is only applicable to small hole diameters [smaller than 9.5 mm].

In the froth regime, the disengaging space [$T_g - H_f$] is introduced. The correlation indicates the rapid rise in entrainment in the spray regime, although it fails to reflect any influence of the hole diameter in this regime.

Kister, Pinczewski & Fell (109) derived a correlation for entrainment in the spray regime. Their correlation covered a wide range of tray geometries and operating conditions (25,95,114,115,117-119). The data consisted primarily of fully developed spray regime data but, some data from partially developed spray region was also used to test the region.

At a later stage (110), a large number of data points were obtained in the partially developed spray region. The correlation gave a good fit to most of the data points. Kister, Pinczewski & Fell's (109) correlation parameters could be expressed in terms of dimensionless groups. The dimensionless version of the correlation suggested that the rate of entrainment was a function of gas and liquid densities, surface tension and gas viscosity. The agreement was encouraging (109) but not good (109,120).

$$\frac{E_m}{M_G} = K_1 \left[\frac{u_s}{(Q/L_v)^{0.25}} \cdot \frac{1}{(1 + K_2 h_w (d_h T_s)^{0.5})} \right]^{4.68} \left(\frac{\mu_G}{\sigma} \right)^{1.17} \quad \dots 2.27$$

In the spray regime $K_2 = 0$, $K_1 = 13.1$ for air-water and $K_1 = 30.6$ for hydrocarbons. In the mixed froth regime, $K_2 = 2.62$ and for air-water $K_1 = 20.5$.

The clear liquid height, h_{cl} , is obtained from a correlation which is strictly only applicable at the froth to spray transition (86). The above equations adequately correlate the available air-water data but the correlation has not been extensively tested for hydrocarbon systems.

Zuiderweg (121) developed an entrainment correlation for a hydrocarbon system in the spray regime based on FRI data.

$$\frac{E_M}{M_G} = 1 \times 10^{-8} \Phi^{-2} \left(\frac{h_{cl}}{T_s} \right)^3 \left(\frac{M_G}{M_l} \right)^3 \left(\frac{\rho_l}{\rho_g} \right)^2 \left\{ 1 + 265 \left[\frac{u_s}{(g \cdot h_{cl})^{0.5}} \left(\frac{\rho_g}{\rho_l} \right)^{0.5} \right]^{1.7} \right\}^3 \quad \dots 2.28$$

The correlation is based on dry tray entrainment where an estimate of the wet tray entrainment is required in practice.

Based on Hofhuis & Zuiderweg's (57) correlation for the clear liquid holdup in the spray regime, the influence of h_w on h_{cl} in the spray regime has not been confirmed. As neither d_h or s were involved, d_h was held constant at 12.7 mm, the equation must be considered specific for hole size.

More recently Kister & Hass (122) have modified and extended previous correlations and proposed a new correlation to predict sieve tray entrainment in the spray regime for the air-water system.

$$E = 4.742 (10\sqrt{\sigma})^{1.64} X (10/\sqrt{\sigma}) \quad \dots 2.29$$

where

$$X = 15,140 \left(\frac{\rho_g u_s^3}{\rho_l L_g} \right) \left(\frac{u_s^2}{g d_h} \right)^{0.5} \left[\frac{(\rho_l - \rho_g) g d_h^2}{g_c \sigma} \right]^{0.25} \left(\frac{h_d}{\sqrt{d_h s}} \right)^4$$

This correlation applies to fully developed spray regime. The reliability diminishes as the minimum in the entrainment curve is approached. It does not apply when the liquid flow exceeds the rate at which entrainment is at minimum.

2.10.2 Mechanism of Entrainment

The two methods of entrainment formation proposed hitherto are:

- i. Some formation of bubble collapse.
- ii. Friction between gas and liquid.

It is probable that, in the froth regime, method 1 produces most of the entrainment, whereas method 2 operates in the spray regime.

Using high speed photography, Newitt (123) studied the formation of droplets due to bubbles of air passing through water collapsing at the air-water interface. He observed that a well defined crater was left in the liquid after the bubble burst and this was filled with rapidly moving liquid which produced a jet from which it was possible that one or more drops could detach. These secondary drops are much larger than those produced by the bursting of the bubble and these large drops were considered to be the major source of entrainment.

Davies (124) showed that the disintegration of the jet of liquid produced by the inrush of fluid into the crater is described by Raleigh (125) providing that the jet would disintegrate due to the effect of surface tension forces. He also proceeded to calculate the height of the jet.

Various other mechanisms of bubble collapse have been proposed by Lane (126) and by Dombrowski & Fraser (127), but these are not so effective as the description given by Newitt (123). It has been suggested by Lane (126) that bubbles produced one or two large droplets when they burst and that, in turn depending on the Weber number of the drop, these would disintegrate. This was supported by Teller & Rodd (128) who suggested that the liquid attempts to cover the vapour flume, or rapidly moving bubble, at the surface by a momentary liquid seal. The drops formed by the liquid seal are large and tend to disintegrate, as described by Lane (126).

Nielson, Tek & York (129), studied the second method of drop formation by high speed flash photography. They suggested that the shearing action of a vapour jet produces

liquid sheets, ligaments and eventually drops, as described by Raleigh (125). The breakup of ligaments to form drops has also been described by Goedde & Yuen (130) who used a photographic technique.

In the spray regime, entrainment increases with hole vapour velocity and hole diameter and decreases with increased liquid weir load and increased fractional perforated area. Similar behaviour is found in the mixed froth regime where entrainment generation by vapour jets is still the predominant mechanism. In the froth regime and in the emulsion regime, entrainment primarily depends on the approach of the upper surface of the froth to the tray above. Those factors which increase froth height also increase entrainment and so the latter increases with vapour velocity, liquid load and weir height. In all regimes, a reduction of tray spacing increases entrainment. Surface tension is also important, with a high surface tension tending to stabilise drops and so lower entrainment. In the froth regime and emulsion regime, foaming raises the dispersion height and increases entrainment.

2.10.3 Measurement of Entrainment

i. Free entrainment.

Measured by sampling drops between the top of the froth/spray and the tray above. This is easy to measure under laboratory conditions by using a coated slide, but it is usually larger than the entrainment captured by the upper tray, although not always.

ii. Dry tray entrainment.

Measured by installing a special 'dry' tray above the operating tray and collecting the liquid which accumulates on it. Probably the most common technique but it suffers because it has to be assumed that no re-entrainment occurs from dry tray. Also the amount of liquid present on the tray probably influences the amount of entrainment it collects from the tray below.

iii. Wet tray entrainment.

Measured by introducing a non volatile tracer into the liquid on a tray and by sampling the liquid leaving the tray above for tracer. This is preferred because it is a direct method and can be used under actual operating conditions. It is accurate providing the tracer does not change the surface tension.

iv. Efficiency entrainment.

Estimated from the reduction in tray efficiency caused by entrainment. It is open to very large errors because of the difficulty of measuring with sufficient accuracy and then relating it to entrainment. Consequently, this method is unsuitable for use in industrial columns.

2.11 Efficiency

Many different approaches have been used to define the separation efficiency of the trays. There are two main definitions of the efficiency of a distillation column.

- i. The single plate efficiency.
- ii. The overall column efficiency.

The single plate efficiency has more fundamental significance and is more frequently used in theoretical analysis and this will be discussed below.

2.11.1 Tray Efficiency

The definition of efficiency proposed by Murphree (131) in 1925 is still almost universally accepted inspite of its limitations with respect to accuracy in numerical computation. Other tray efficiency models are Hausen (132) who related the vapour and liquid compositions in an equilibrium flash of feeds instead of an actual existing liquid would be in equilibrium with vapour, and Standart (133) who modified the Hausen efficiency to take account of any changes in total phase flow rates which might occur across the stage, but this is difficult to use in counter current situations. From this point of view the Standart efficiency is considered to be the most satisfactory definition (134). However, the apparent complications of its determination have not resulted in its wide spread use, and in a later paper Hartman, Griger & Standart (135) have reverted to the use of the Murphree efficiency. Experimental determinations of the Hausen efficiency have been presented by Hartman, Griger & Standart (136).

Holland (137) and Holland & McMohan (138) have proposed a vaporisation efficiency, which is defined as the ratio of the actual composition to the theoretical composition of the vapour leaving the real plate. The main attraction of its approach has been its usefulness in computation. It can be related to the Murphree efficiency (138,139) so it can be calculated if the latter can be calculated. This method is known to be superior to Murphree's efficiency from the calculation point of view but it lacks correspondence to the fundamental mass and heat transfer phenomena. It has been criticised (140,141) because it does not bear direct relationship between the ease or difficulty of separation.

2.11.2 Effect of Entrainment on Plate Efficiency

When the efficiency of a plate is calculated from theoretical or semi-theoretical equations, one of the first assumption made is that the amount of entrainment is negligible. Entrainment results in the recycle of liquid through the column. This causes:

- i. A reduction in the driving force for mass transfer between liquid and vapour.
- ii. An increase in the liquid to vapour ratio on each tray.
- iii. An increase in the liquid and point efficiency.

The net result is usually a reduction in tray efficiency.

The work of Colburn (142), although applied at the time solely to bubble cap plates, applies equally well to sieve trays and has emerged as the classic treatment of the effect of entrainment on mass transfer.

2.12 Concluding Remarks

From the literature review, it is evident that single phase solutions containing three components exhibit foaminess under a range of operating conditions and also near the single to two liquid phase boundary. Therefore, in the design of gas-liquid contacting equipment extra capacity is always provided for foaming systems.

Much of the literature on foaminess near to the phase boundary has been devoted to the explanation of composition changes and hence surface tension effects. The cause of foaming has been traced to Marangoni effects caused by changes in compositions and hence surface tension effects.

Attempts have been made to explain the stability of foams in terms of the thermodynamic theory. A complete explanation has not been put forward yet.

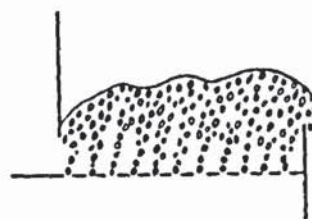
The modes of formation of foam and ways of preventing or destroying them have been examined. It is clear that an alternative method of coping with the problem of foaming in process units is desirable. The ability of foams to form depends basically on the stability of the thin films separating the bubbles and hence, on the physical properties of the liquids used.

Antifoaming agents are often used in systems where severe foaming may occur. Various additives and their mechanism of action have been studied extensively in the literature. Possibly the spray regime can be used to break foam and therefore, the spray to bubbly transition has been examined for single liquid phase systems. Several correlations and models exist in the literature to predict the spray to bubbly transition, based mainly on the experimental results of Porter & Wong (17). Unfortunately, these correlations and models do not agree with each other. Thus, there is still a lack of experimental data for the spray to bubbly transition for a single liquid phase. These correlations and models were derived for single liquid phases and no work has been carried out to attempt to define the flow regimes for systems with two liquid phases.

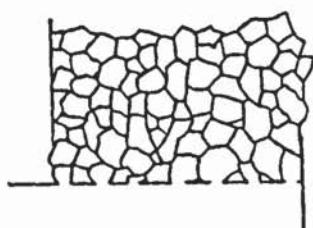
Thus, in any further work it would be useful to be able to map any potential regions of foaming on the phase diagram of the system. Further work is required on foaming caused by two liquid phases and to obtain data for two liquid phases on a distillation tray and to be able to predict the transition from spray to bubbly regime for two liquid phase system.



a. Spray



b. Discrete bubbling



c. Cellular foam



d. froth

Figure 2.1 Dispersions formed above sieve plate.

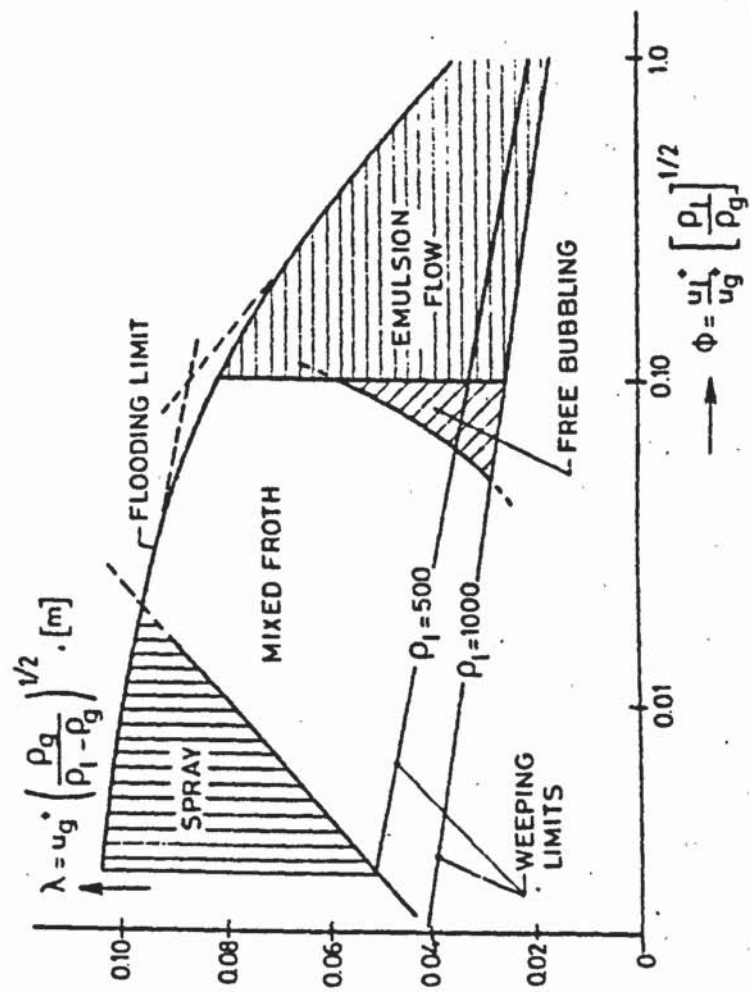


Figure 2.2. Flow regime diagram.

CHAPTER 3

APPROACH TO THE PROBLEM

3.1 Introduction

From the survey of the previous work, it appears that the presence of two liquid phases may cause excessive foaming. When this occurs distillation columns are derated by using foaming factors in the design methods. By simple stripping experiments (2) it was shown that as the solution changed from single liquid phase to two liquid phases the foam height increased, remained stable for a long period of time and then within the two liquid phase region foam was inhibited. Therefore, it was concluded that the maximum foam height occurred at the point of transition. It was suspected that the same phenomena may occur in a distillation column where single and two liquid phases exist. No work has been located in the open literature which has reported observations of foaming in the distillation columns with two liquid phases and also no experimental data are available in the literature about foaminess caused by the presence of two liquid phases.

It is known that foaming may sometimes be overcome by operating in the spray regime; thus there is interest in determining the conditions which determine spray or bubbly operation on a tray in the presence of two liquid phases. It is apparent from previous work that numerous attempts have been made to study the different types of dispersion above a sieve plate for a single liquid phase. To date, no information is available in the literature concerning the type of dispersion formed above a sieve plate by two immiscible liquids. The spray to bubbly transition has been studied experimentally by only few workers (17,21,22) and the most comprehensive study so far has been that of Porter & Wong (17). All the correlations and models available in literature to predict the transition from spray to bubbly regime are based on the experimental results of Porter & Wong (17). These correlations and models disagree with each other because perspex trays of different thickness have been used yet the effect of tray thickness is not included in the modelling. Thus, additional data for the spray to bubbly transition for single liquid phase would be advantageous and the whole question of flow regimes on a tray operating with two immiscible liquids needs examining.

3.2 Experimental Program

The objective of this work is to find out ways of minimising the effect of foaming on the column capacity. The experimental program is as follows:

- i. The Ross experiments would be repeated in a sintered plate column.
- ii. An Oldershaw column would be used to test the behaviour of various ternary systems where single and two liquid phases could occur.

- iii. Spray to bubbly transition experiments would be carried out for:
 - (a). Single liquid phase experiments with sieve trays of various free areas, hole diameters, plate thicknesses and different ratio of hole diameter to tray thickness.
 - (b). The spray to bubbly transition experiments would be repeated for two immiscible liquid phases to obtain data for the behaviour of two liquid phases on the tray and to observe the different flow regimes.
- iv. The effect of Ross type systems on a sieve plate of small and large hole diameter would be observed.
- v. Foam control would be investigated by the addition of another non-volatile component.
- vi. A packed column would be used to observe whether foam can build up in a packed bed.
- vii. The concentration profile across the column would be sampled in order to relate the behaviour of tray column to the physical properties of the dispersion.

3.3 Choice of Equipment.

The foaming behaviour of ternary mixtures in distillation columns would be studied using a glass Oldershaw column, thus allowing accurate observations to be made of the behaviour of the tray dispersion. The column will be operated at total reflux.

The gas-liquid or gas-liquid-liquid systems with negligible mass transfer would be studied in a perspex box apparatus with no downcomers or liquid crossflow. This approach has the following advantages:

- i. Gas flow rate and liquid holdup can be controlled easily and independently.
- ii. There are no heat losses and subsequent insulation problems;
- iii. Equilibrium is almost instantly reached.
- iv. There are no concentration changes across the plate.
- v. It is easier to use large sieve plate units for gas-liquid and gas liquid-liquid systems than for distillation.

The transition from the spray to bubbly regime will be studied using a light transmission technique. The liquid holdup at the transition will be measured using a manometer connected to the centre of the plate.

CHAPTER 4

EXPERIMENTAL APPARATUS

4.1 Preliminary Considerations

A perspex column simulator similar to that used by Porter & Wong (17) with no downcomers or liquid cross flow was constructed. The advantages of such an apparatus being: simplicity of construction, elimination of effects of liquid flow rates and weir height and independent control of gas and liquid flow rates. The details of the sieve plates used in the experiments are given in table 4.1.

A 50 plate, 30 mm diameter Oldershaw column was used to observe the foaminess near the single liquid phase to two liquid phase boundary of various ternary systems. The elimination of this foam by the use of additives, for the same systems under investigation, was also studied in the Oldershaw column.

4.2 Oldershaw Column

A 30 mm internal diameter, 50 plate Oldershaw column having a reboiler capacity of 2 litres was used for the visual observation of foaming near to the one liquid phase to two liquid phase boundary for different Ross type systems

The reboiler is heated by an isomantle and the boil up rate was controlled by the isomantle heat output. The column was operated at total reflux and atmospheric pressure. The assembled column is shown in figure 4.1.

4.3 Air-Water Simulator

The air-water simulator was constructed of perspex to facilitate observations through the column wall and to eliminate corrosion effects. The column was constructed with 6.35 mm and 9.35 mm thick perspex walls. The 6.35 mm sides were cemented to 9.35 mm side edges and then fitted firmly with screws. The column measured 45.09 cm square internally and was 76.2 cm high and flanged at the top and the bottom. The top flange was fixed to a 9.35 mm thick perspex plate which in turn was secured to the main gas circuit above. A hole, matching the dimensions of the gas ducting, was cut in the centre of this top plate to provide a gas outlet from the column.

The gas reservoir [or gas box], of the same internal cross section as the column, consisted of two 6.35 mm thick and two 9.35 mm thick perspex walls which were cemented to a base plate of 9.35 mm thick perspex. A liquid outlet of 12.7 mm internal

diameter was inserted centrally. Four perspex sheets were fitted inside the gas box base to allow complete drainage of the liquid collected in the gas box. The sheets were raised 12.7 mm at the walls of the gas box. A perspex tube, 6.35 cm external diameter, was inserted centrally in each of the four vertical walls. These acted as gas inlets and provided an evenly distributed gas flow to the apparatus. A flange, matching the one at the base of the column, was cemented to the top of the gas reservoir.

A perspex sieve plate without downcomer was bolted between the column and the gas reservoir flanges. The sieve plates could be changed as the gas reservoir could easily be removed and reassembled. The assembled column is shown in figure 4.2, and the dimensions of the main column are shown in figure 4.3.

A simplified flow diagram is given in figure 4.4. The gas circuit above the main column consisted of 29.85 cm diameter perspex tubing. An entrainment separator made of knitted wire mesh was provided in the gas ducting outlet above the column to prevent entrained liquid accumulating in the gas ducting. The perspex tubing was connected to the inlet of the scrubbing system.

4.3.1 Liquid Circuit

Four calibrated QVF glass tubes were used for storing the liquid. These tubes were 50.8 mm internal diameter and 69.9 cm high and were situated at a higher level than the sieve plates so that the liquid could enter by gravity onto the plate. These reservoirs have independent feed lines to the plates. A manometer was connected near the centre of the plate to measure the liquid holdup.

The liquid was injected onto the tray through the centre of the sieve plate. A T-piece was inserted in the flexible liquid line. One arm of this led to the liquid reservoir whilst the other arm led to a manometer so that when the liquid injection was momentarily stopped, the manometer reading gave a measure of the liquid holdup at the centre of the sieve plate.

The actual amount of liquid introduced onto the sieve plate could be calculated from the fall in level of the liquid in the storage tube. At the end of experiment, the liquid was dumped into the gas reservoir below from which the liquid was discharged into a phase separator.

4.3.2 Air Circuit

Air was supplied by means of a blower. The air flowrate was varied by a butterfly valve and measured by a U tube manometer connected to Dall tube. An entrainment separator made of knitted mesh was situated in the gas outlet duct above the column to prevent entrained liquid being carried out with the air.

4.3.3 Scrubber

A scrubber, constructed of perspex, was used to remove volatiles carried with the air. The scrubbing column measured 102 cm high and 60 cm square internally and was flanged at both ends. A mesh was fitted at the base of the column to support the packings.

A gas box 54 cm high and having the same internal dimensions as the column was fitted to the base of the column. A 29.83 cm perspex tube having the same diameter as the gas outlet from the simulator was inserted centrally in one side of the gas box.

A distributor plate was bolted between the top of the column and a water feed box, 30.5 cm high and having the same internal dimensions as the column. Water was fed onto the top of the distributor plate through six nozzles housed in the water box and the water was supplied through three flanged 24 K rotameters having independent controls.

A hole matching the dimensions of the gas exhaust fan line was cut in the centre of the water box line. A 13.24 cm perspex tube was fitted in this hole for connection to the exhaust line.

4.3.4 Extraction of Air

The air leaving the scrubber was ducted to an extraction fan which vented the exhaust air to the atmosphere outside the building.

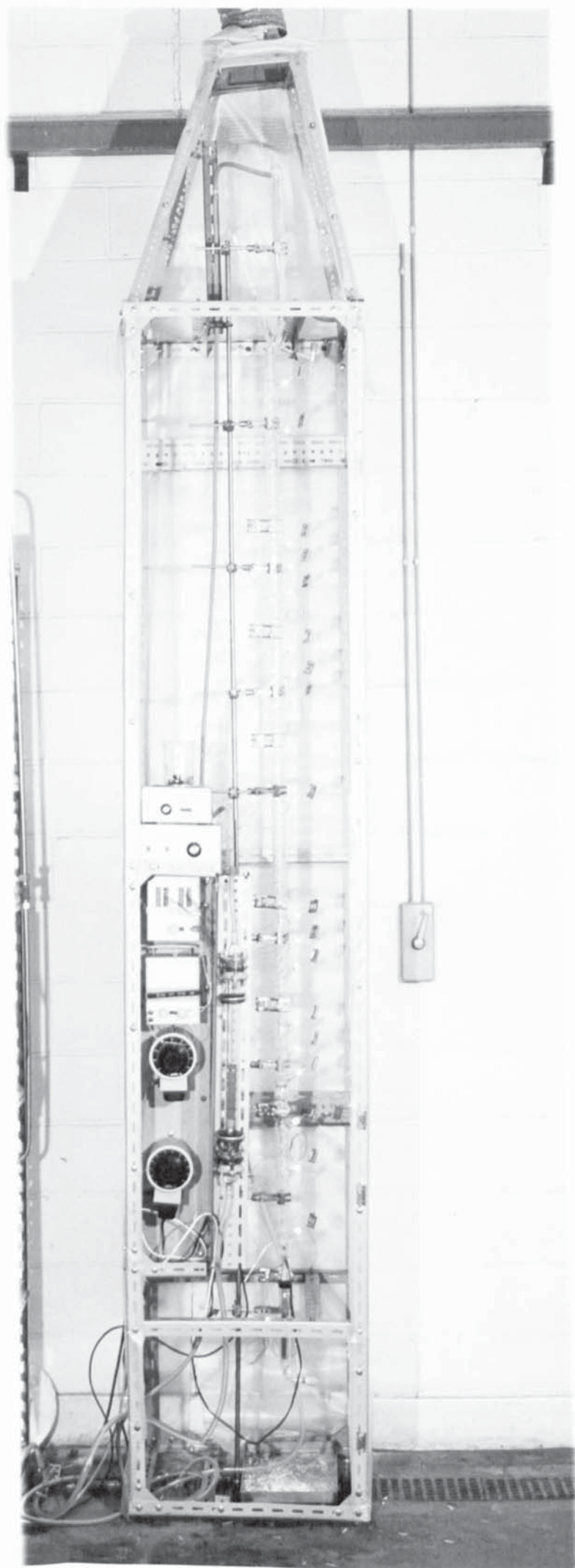
4.4 Sintered Plate Column

A 5.1 cm i.d. column was used for qualitative observations of Ross foaming for systems which changed from single liquid phase to two liquid phases when air was blown through the column. A further description of the column is given in section 5.4.

Table 4.1. Details of sieve plates used in experiments

Tray no.	Hole size d_h (mm)	Plate thickness X (mm)	No of holes	Triangular pitch P (mm)	% Free area	Ratio (d_h/X)	Tray material
1	3.18	6.35	1415	12.70	5.50	0.50	perspex
2	4.76	6.35	607	19.05	5.32	0.75	perspex
3	6.35	6.35	313	25.40	4.87	1.0	perspex
4	3.18	2.38	2613	9.50	10.18	1.33	metal
5	4.76	2.38	1267	14.4	11.10	2.0	metal
6	6.35	2.38	635	19.1	9.89	2.67	metal
7	12.7	2.38	149	38.1	9.29	5.34	metal
8	3.18	4.0	1415	12.7	5.50	0.82	perspex
9	4.76	4.0	1267	14.4	11.10	1.19	perspex
10	6.35	4.0	635	19.1	9.89	1.59	perspex
11	12.7	4.0	149	38.1	9.29	3.18	perspex
12	4.76	6.35	1267	14.4	11.10	0.75	perspex
13	6.35	6.35	607	19.66	9.46	1.0	perspex
14	12.7	6.35	149	38.1	9.29	3.81	perspex

Figure 4.1. Oldershaw Column.



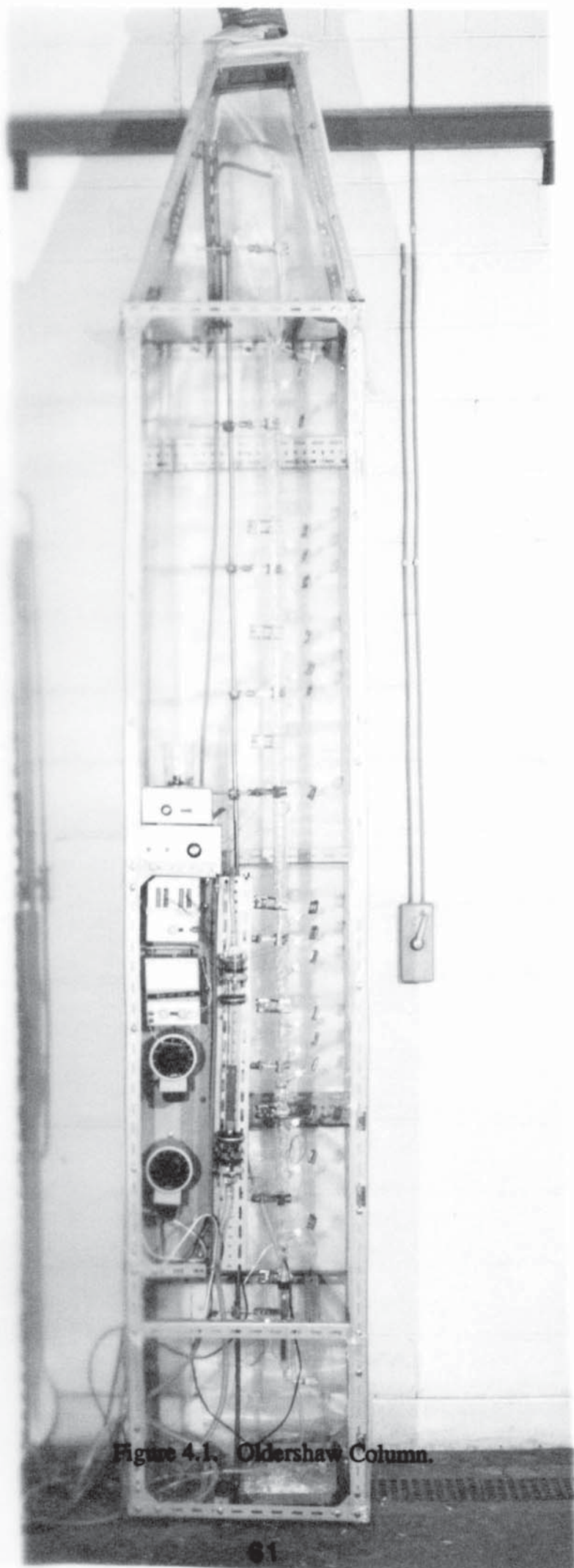


Figure 4.1. Oldershaw Column.

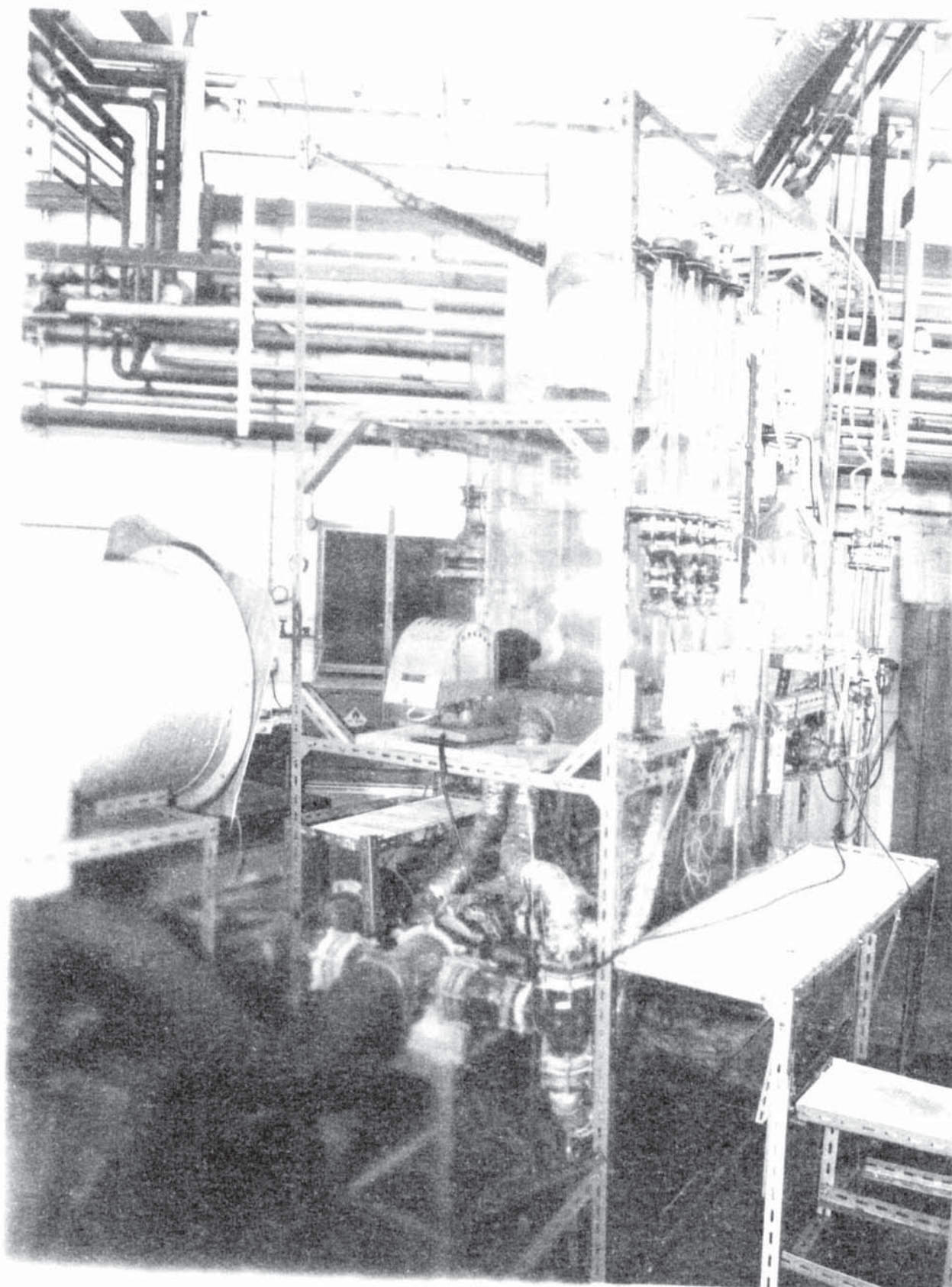


Figure 4.2. Air - Water Simulator

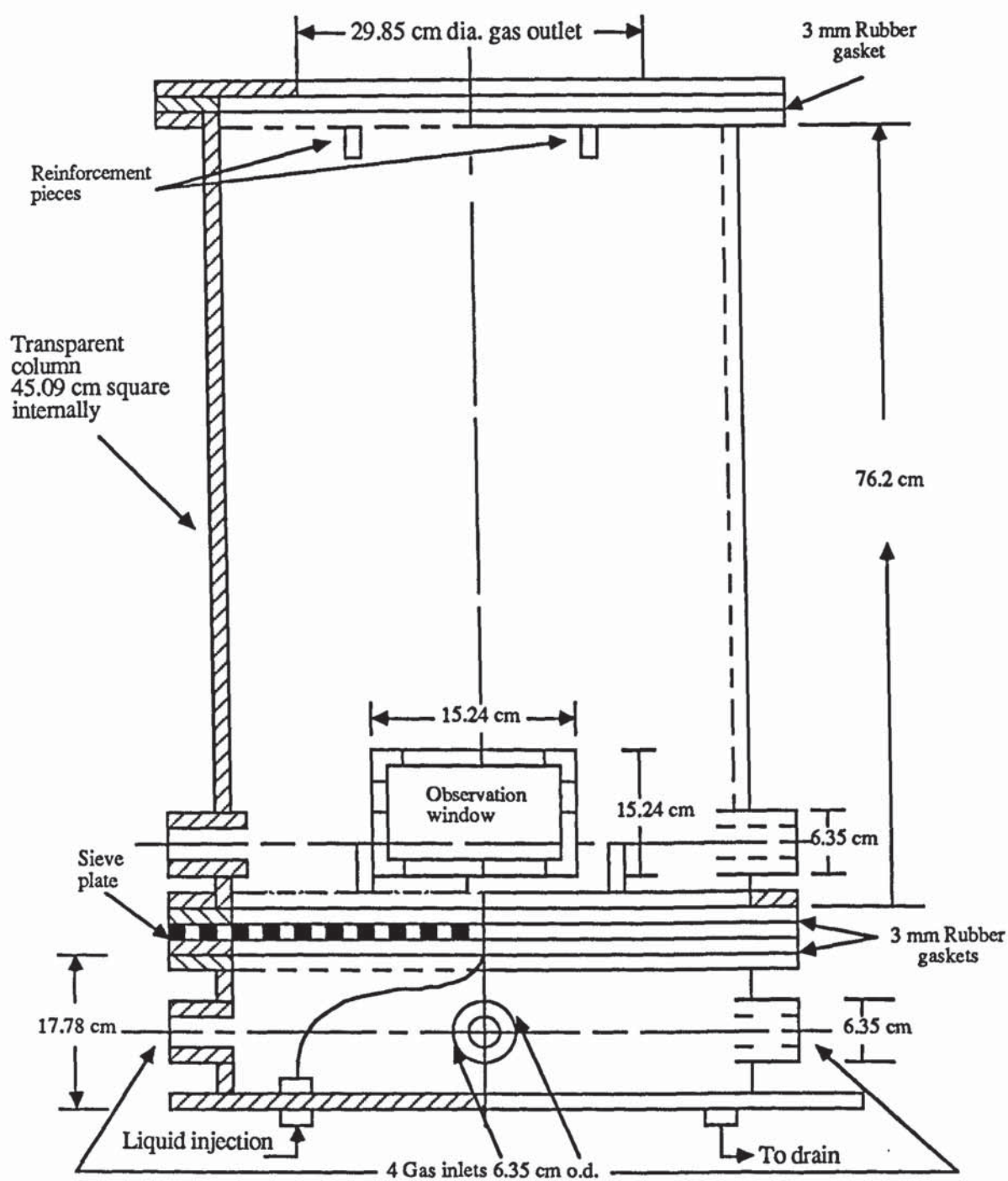


Figure 4.3. Dimensions of air-water simulator.

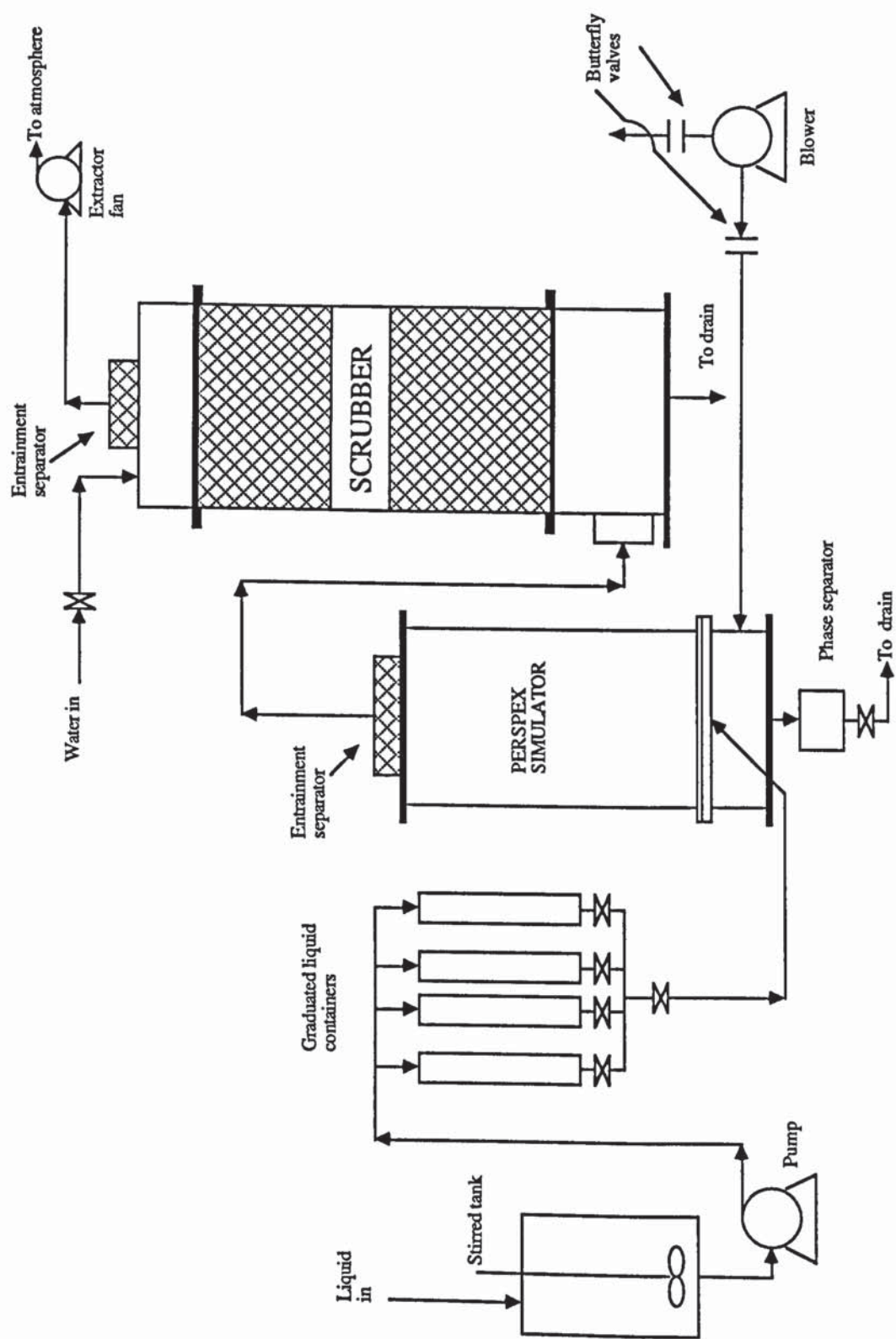


Figure 4.4 Line Diagram of the Air-Water Simulator

CHAPTER 5

OLDERSHAW COLUMN STUDIES

5.1 Introduction

Foaming may considerably reduce the capacity of vapour-liquid contacting devices. The foaming tendency of a system is often demonstrated by bubbling air or nitrogen through the liquid or by a pilot run in small scale equipment. However, the results obtained do not always hold for large-scale operation, since large-scale tray design and operation may change the flow regime on the trays, which will influence the degree of foaming.

For systems with a foaming tendency, the capacity correlations have to be corrected by using a foaming factor. Foaming is characterised by some stabilisation mechanism which prevents bubbles from coalescing in the dispersion and from breaking up when they reach the interface. The foaming factor will depend on the degree of stabilisation. It also depends on the flow regime where the vigorous action of the dispersion on the tray will promote bubble break-down or even prevents bubble formation. Foaming will be a minimum in the relatively calm bubble regime.

Systems in which two liquid phases are present on a tray are amongst those which are derated because of suspected foaming. One of the reason for such behaviour in a ternary system is the phase split which occurs in some systems near the single liquid phase to two liquid phase boundary.

The foam height of a foaming system, compared with that for a non-foaming system may provide the capacity correction or foaming factor. It should be realised that this method usually yields conservative values, since the operating velocities in the test apparatus are nearly always lower, due to smaller diameter holes, than the operating velocities in commercial trays.

Persistent foaming, as encountered on vapour-liquid contacting trays, may be due to surface-active 'impurities' in the liquid which reduce the surface tension. These surface active solutes counteract liquid drainage of the bubble wall when these reach the gas-liquid interface since during drainage the surface tension gradients develop which induce back flow of the liquid. Ross & Nishioka (2) commented that foaming is caused by changes in the composition of liquid. Therefore, surface active component will create local changes in concentration and thus cause changes in surface tension. They point out that the foaming tendency [in the absence of mass transfer] should be related to changes in surface tension with the concentration of the active component in the liquid.

The phenomena of foaming, caused by two liquid phases, has not been observed

in actual distillation columns, although it is suspected that foaming may occur in distillation columns separating mixtures in which one and two liquid phases may occur.

5.2 Ternary Systems Previously Studied

The systems listed in table 5.1 have been used by Ross and Nishioka (2) to demonstrate foaming/defoaming behaviour in a single perforated plate column in foam stabilisation experiments.

Table 5.1. Ross foaming systems

i.	Benzene	Ethanol	Water
ii.	n-Hexane	Ethanol	Water
iii.	Ethylene glycol	Butanol	Water

Solutions were foamed in a 70 cm high, 3 cm diameter column. Temperatures were controlled by means of oil circulating from a thermostatically controlled heater. The cooling of the oil due to heat losses as it passed through the jacketed column was counteracted by heating tapes wound in a wide spiral around the outside of the apparatus. Temperatures of the foamed solution were read directly by a thermocouple placed inside the sample space of the foam meter.

5.3 Object of the Work

- i. To repeat Ross & Nishioka (2) experiment in a single sintered plate column.
- ii. To test different ternary systems for foaming/defoaming behaviour in an Oldershaw column.
- iii. To map the concentration profile on a phase diagram from the samples taken from the Oldershaw column.

5.4 Sintered Plate Column

A 5.1 cm internal diameter and 17.8 cm long plain glass column, with a side feed point and one flanged end, was used to repeat the Ross type experiments. A 12.7 cm long flanged gas box with a side arm for the air inlet was attached below the column. The sintered plate was cemented between the column flange and the gas reservoir flange using

aquaria silicon rubber sealant. The air feed to this column was measured using a 10 K rotameter. A measured quantity of liquid was poured onto the sintered plate from above. The column is shown in figure 5.1. The physical properties of the systems used are listed in appendix 1.

5.4.1 Systems to be Studied

The systems listed in table 5.2 were used to study the change from a single liquid phase to two liquid phases when air was blown through the liquid. The change from single liquid phase to two liquid phases was caused by preferential evaporation of the volatile component in the liquid phase on the sintered plate.

Table 5.2. Ternary systems used in sintered plate column

i.	Kerosene	Acetone	Water
ii.	n-Hexane	Propan-1-ol	Water
iii.	Cumene	Propan-1-ol	Water

5.4.2 Observations

The foam height increased as the transition from one liquid phase to two liquid phase was approached. The maximum foam height occurred at the point of transition and then reduced when two liquid phases were formed. However, there was a significant time delay [about 1-3 minutes] before the foam started to decay and this depended on the volatility of the volatile component present in the liquid phase.

Figure 5.2 show the changes of the foam height of the kerosene-acetone-water system as the dispersion changed from one to two liquid phases.

These observations supported the work of Ross & Nishioka (2). In addition observations showed that stable foam remained for few minutes, which was not reported by Ross & Nishioka (2).

5.5 Oldershaw Column experiments

A 50 plate, 30 mm internal diameter Oldershaw column was used to observe the distillation of the systems which would contain one and two liquid phases. With such a large number of trays it was hoped to be able to observe both cases of the transition [single liquid phase to foam and foam to two liquid phases] simultaneously.

The systems studied in the Oldershaw column are listed in table 5.3.

Table 5.3. Systems studied in the Oldershaw column

i.	n-Hexane	Propan-1-ol	Water
ii.	Cyclohexane	Propan-1-ol	Water
iii.	n-Hexane	Ethanol	Water
iv.	Methyl ethyl ketone	Methanol	Water

5.5.1 Experimental Procedure

A feed of approximately 1.5 litres of a single liquid phase mixture was charged to the reboiler which was heated by an isomantle. Heat losses from the Oldershaw column were minimised by blowing hot air up and through an annular gap between the column and an external 12.2 cm diameter glass tube. The temperature of the hot air was maintained at approximately the temperature of the reboiler. It was important to minimise heat losses in order to prevent condensation of the vapour which might have influenced foam formation. Also it was important to maintain the hot air at the appropriate temperature so that no unnecessary vaporisation of liquid occurred at the column walls or within the column. The power supply to the air blower and the isomantle were switched on and the boil up rate set to a maximum. After about 15 minutes, the foam usually started to build up in the column and once the foam height had stabilised, the heat input to the reboiler was adjusted to stabilise both the height of the foam and the position of the foam to the middle of the column.

5.5.2 Observations

In all these systems, it was observed that the plates in the top and bottom sections of the column [approximately 15 plates in each section] did not exhibit foaming, whilst the plates in the middle section [approximately 20 plates] did exhibit significant foaming which completely filled the interplate space [figure 5.3]. It is worth noting that the boil up rate was such that the liquid back up in the downcomers was approximately half the tray spacing i.e. the column was not flooding due to an excessive boil up rate.

For the system 1 to 3 a single liquid phase was present on the plates at the bottom of the column and two liquid phases were observed on the plates at the top of the column. For system 4 the single liquid phase was present on the plates in the top section of the column whilst two liquid phases were observed on the trays in the bottom section of the column.

It was observed that the number of foaming plates in the middle of the column depended on the composition of the original mixture charged to the reboiler. In system 1, if

the mixture was n-hexane rich, more plates foamed than if the mixture was water rich.

A typical distillation line predicted from the UNIFAC method for one of the systems [n-hexane - water - propan-1-ol] is shown in figure 5.4 where the concentration profile passes through the one liquid phase to two liquid phase boundary. It is to be expected that the composition of the most volatile component [n-hexane] increases up the column. As the single liquid phase to two liquid phase boundary is approached, a phase split occurs and two liquid phases are formed and it is at this point that the experimental observations have shown that foaming commences.

5.6 Column Modification

The original 50 plate column was 'cut' into seven sections, comprising of 4, five plate sections and 3, ten plate sections. The sampling points were then placed on the first, third and fifth plate of each of the five plate sections. For the ten plate sections the sampling points for section A were (i) first and fifth plate, for section B (ii) fifth plate, and for section C (iii) second and tenth plate. The individual sections were joined together with a clip. The space between the top plate of one section and the bottom plate of the adjacent section was 100 mm. On the column wall a side arm was fixed through which a hypodermic tube was placed onto the tray in order to facilitate the removal of a sample. The column was erected as shown in figure 4.1.

5.6.1 Reboiler

A 1.5 litre capacity vessel was mounted immediately at the bottom of the column. The vessel had two side arms in which two 300 watt red hot immersion heaters were placed. The current to the heaters was controlled by a variable voltmeter.

5.6.2 Sampling Points

Sampling devices were prepared to fit in the sampling openings on the columns. These devices were each made of a glass tube with a threaded end which was closed by using a cap with a small gasket. A stainless steel hypodermic tube with some PTFE tubing on both ends was inserted through the gasket and into the downcomer of that sampling plate. The external end of the tube was fitted with a Hoffman's clip which was used to regulate the flow of liquid from the sampling plate.

5.6.3 Temperature Measurement

Thermocouples of type Ni/Cr were used to measure the temperature of the dispersion of a particular plate. The thermocouples were connected to a Comark selector

unit 1694 F. The temperature was read directly from the Comark electronic thermometer type 1601 which was connected to the selector unit.

5.6.4 Operating Procedure

The following procedure was used for each experiment:

- i. The required solution of the ternary system was prepared and charged into the reboiler.
- ii. The top condenser water supply was switched on.
- iii. The power supply was switched on to the heaters and to the Comark electronic thermometer.
- iv. Movement of rising vapour was noticed from the column and also from the temperature readings.
- v. The column was left to operate for another 30-45 minutes to reach steady state. During this period the heat input to the heaters was varied to stabilise the foam towards the middle of the column. The foam stability was checked through the side openings. The temperature readings were noted every five minutes in order to assess the stability of the distillation.
- vi. Sampling was commenced only when steady state operation had been achieved.
- vii. Samples were removed by a 5 ml syringe. Sampling was always started at the bottom of the column. Each time the liquid was withdrawn from the column, the first few drops were discarded because they did not represent the liquid in the downcomer of that particular plate. However, only 1 ml of liquid samples on the plate were withdrawn from the sampling points in order to minimise the disturbance to the equilibria on the plate. Care was taken in collecting a sample from the reboiler and this was achieved by slowly operating the valve until it was slightly open. The condenser sample was obtained using a reflux divider.
- viii. Once the sampling procedure was finished, the power supply to the reboiler heaters was switched off. The water supply to the condenser was left on for a further 15 minutes. After cooling the reboiler contents were discharged through the bottom valve.
- ix. The samples were quickly cooled by placing them in ice. After completion of the experiment, the samples were refrigerated until they were required for analysis.

5.7 Gas Liquid Chromatographic Analysis

A gas liquid chromatograph [GLC] was used for the analysis of solutions consisting of any combination of the three experimental liquids. The theory of GLC shows that each component of a given solution produces a peak height area that is proportional to its concentration. In addition, the resolution of the peaks as well as the elution time for its component are highly dependent upon:

- i. The temperature of the GLC column.
- ii. The rate of flow of the gas which carries the components through the column.
- iii. The nature of the components. Preliminary investigations were carried out to determine the optimum working conditions of the GLC apparatus with respect to operating temperature and flow rate of the chosen carrier gas.

Table 5.4. Details of chromatography apparatus

Type unit	Perkin - Elmer Sigma 2B
Type of column	Porpak Q
Range and attenuation	16 x 10
Type of gas carrier	Helium
Katharometer temperature	250° C
Injector temperature	250° C

Using a carrier gas flowrate of 30 ml/min acceptable resolution and elution times were obtained for the system. Temperature programming was used as follows: 75° C for 7 minutes and then increase to 200° C at the rate of 32° C/min and hold for 30 seconds. The temperature was again increased at the rate of 32° C/min to 220° C and held for 15 minutes.

Since the samples collected were not totally miscible over the whole composition range, a solvent [acetone] was added in order to create a homogeneous solution before injection of a sample into the GLC column.

5.7.1 Calibration of Chromatograph

The GLC apparatus was calibrated using a set of standard samples.

- i. In each case a number of standard solutions in the 2-98 mass percent concentration range were made up accurately by weighing out the necessary amount of each pure liquid into stoppered bottles.
- ii. A 5 µl sample of each standard solution was injected onto the GLC column

while the apparatus was set to operate at the appropriate conditions.

- iii. The peak heights corresponding to each component were measured. From these determinations the ratio of the average height areas corresponding to the mass ratio of the component in each standard solution were calculated.
- vi. The calibration data thus obtained were correlated using the least square method [programme is listed in appendix 2].

The temperature and concentration profiles along the Oldershaw column are listed in appendix 3.

5.7.2 Results

It is seen from figure 5.5 that foam builds up in the column [i.e. when phase split occurs] before single/two liquid phase boundary is reached. Defoaming occurs once the concentration moves into the two liquid phase region. It was also noticed that there is only small change in concentration across the foam [table 5.5]. It is also seen from table 5.5 that as the ratio of water/n-hexane increases the number of plate that foam decreases and a graph of number of foaming plates versus the water/n-hexane ratio is shown in figure 5.6.

In all the distillation lines, the reboiler is denoted as plate 1 and the reflux is plate 52. Figure 5.7 shows the temperature profile across the column of each run.

Table 5.5. No. of plates foamed with different ratios of water/n-hexane

Ratio of water/n-hexane	Foam starts	Foam finishes	No. of plates foamed	% water change
0.25	37	14	23	7.489
0.5	36	17	19	4.016
1.0	32	17	15	3.145
2.0	21	14	7	0.305

5.8 Measurement of Surface Tension.

The surface tension of the ternary system, n-hexane - water - propan-1-ol, was measured at different concentrations of propan-1-ol in the mixture and at different ratios of water/n-hexane in the original mixture at room temperature of 20° C.

5.8.1 Experimental Procedure

A mixture was made up of water and n-hexane and titrated with propan-1-ol so that a single phase solution was just reached. From the small sample, the surface tension was determined using a torsion balance. To this mixture a fixed volume of propan-1-ol was again added and the surface tension was determined again.

This procedure was repeated for various ratios of water and n-hexane with different concentrations of propan-1-ol and the results are tabulated in appendix 4.

5.8.2 Results

Figure 5.8 shows that all the lines are curved and converging towards 100% propan-1-ol.

Figure 5.9 shows the changes in surface tension at different concentrations. There is a maximum with decreasing surface tension on both sides of the maximum. Also figure 5.9 shows that the surface tension of a single phase mixture decreases to a low value near the single/two liquid phase boundary. There is an increase in surface tension as the concentration of propan-1-ol is increased in the mixture. The maximum change occurs when the concentration of propan-1-ol is in the range of 70-85%. After this point further increase in propan-1-ol concentration results in decrease in surface tension.

The changes in surface tension are higher when the ratio of water/n-hexane is higher. In all the cases the rate of decrease of surface tension is lower than the initial rate of increase.

In section 5.7.2, it was stated that there is only a small change in concentration of the components in the foam. This suggests that the observed foam, in the Oldershaw column, could be result of entrainment. The surface tension results obtained, in section 5.8.1, show that surface tension is minimum near the single/two liquid phase boundary. This means that there is very little mass transfer occurring in the foam and this suggests that the diffusion coefficient is very low. In either case this results in low efficiencies of the plates when the foam is present in the column.

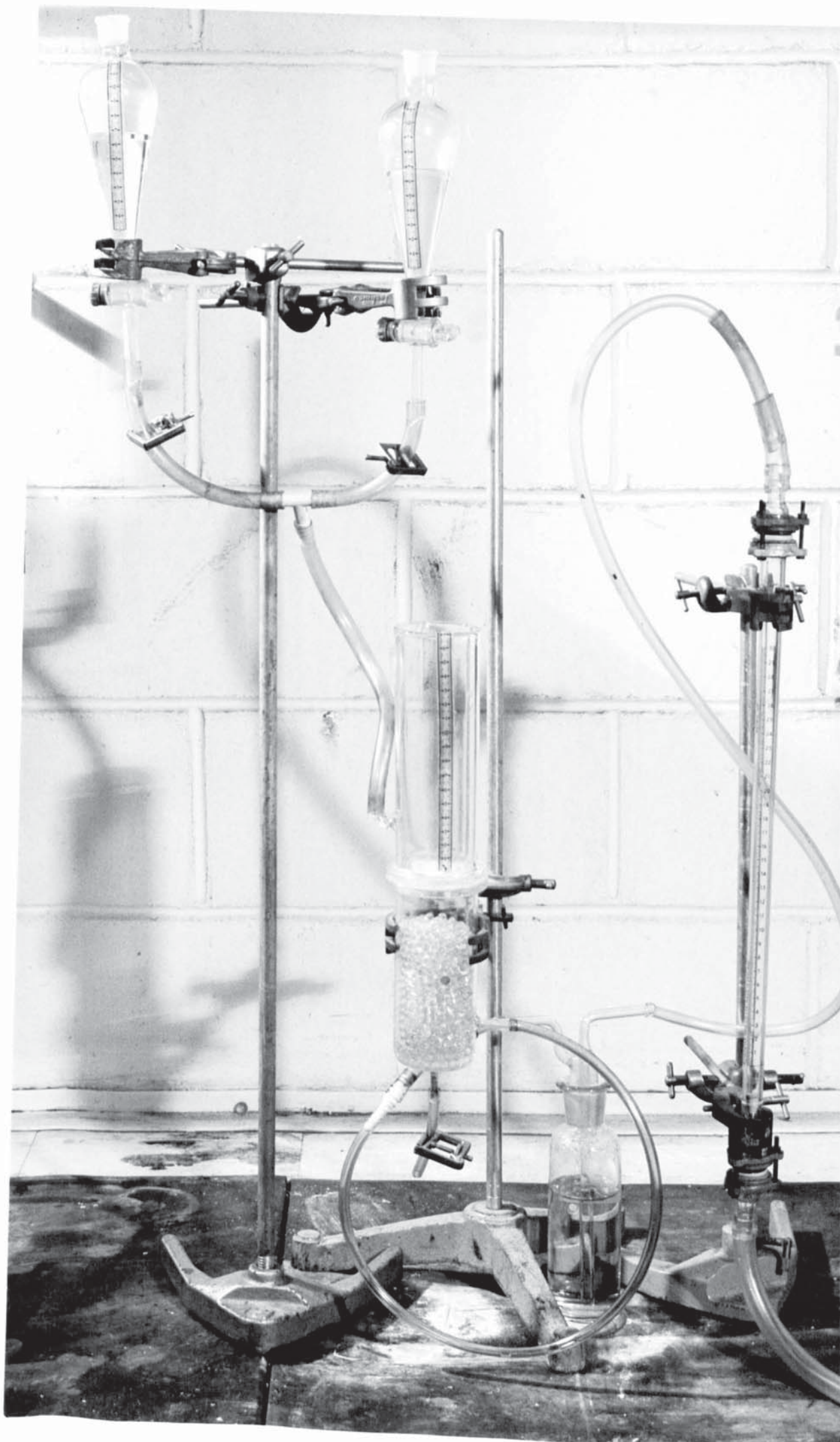
5.9 Conclusions

- i It was observed on the sintered plate that foaming does occur as a liquid passes from the single to two liquid phases and that foam which is formed remains stable for a long period of time.
- ii. Similar foams were noted for real distillation systems in an Oldershaw Column. The foaming region depended on the boil up rate and the initial composition of the charge to the reboiler. Also foaming occurred when the

top section was single liquid phase and the bottom section was two liquid phases and vice-versa.

- iii. Measurement of composition across the column show that there is small change of composition across the foam.
- iv. Measurement of surface tension show that surface tension is minimum near the two phase boundary. As propan-1-ol was added to the mixture, the surface tension increased to a maximum value. This maximum value occurred at concentrations of approximately 75% propan-1-ol. Further addition of propan-1-ol resulted in a decrease in the surface tension.
- v. Because foaming increased with vapour rate, one way of reducing or minimising the foam is to derate the column by increasing the column diameter.

Figure 5.1. Sintered Plate Column.



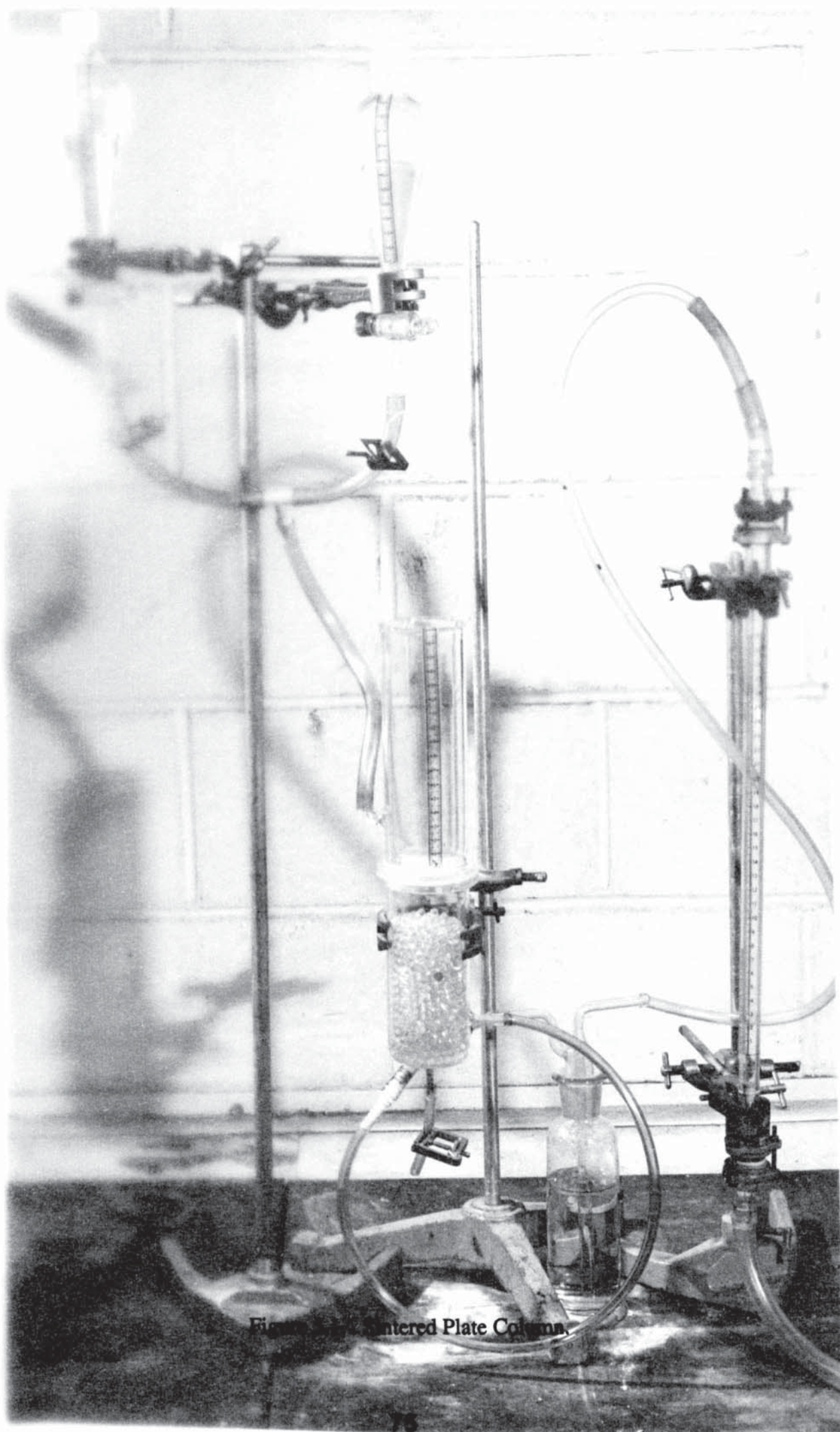
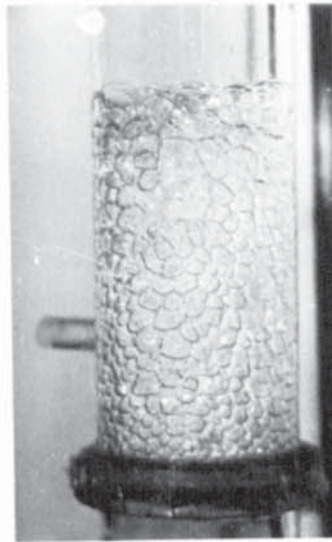


Figure 1. Counterplate Column.

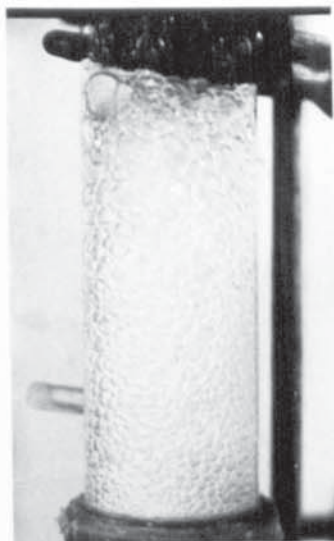
Figure 5.2. water - kerosene - acetone system.



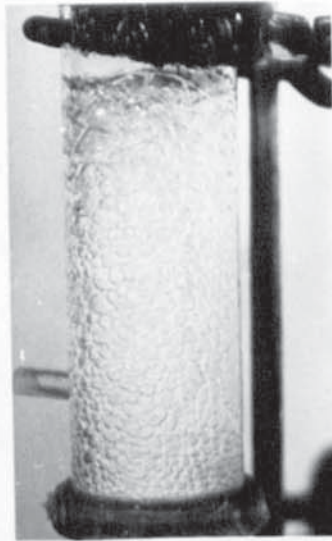
a. Foam height at start up of experiment.



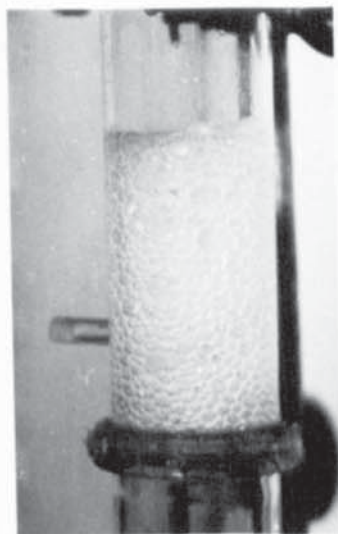
b. Foam expanding.



c. Foam expanded to its maximum height.



d. Foam expanded to its maximum height.

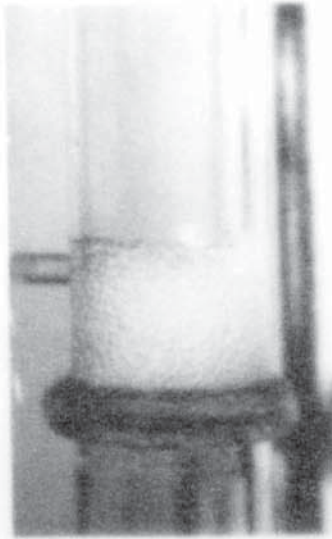


e. Foam decaying.

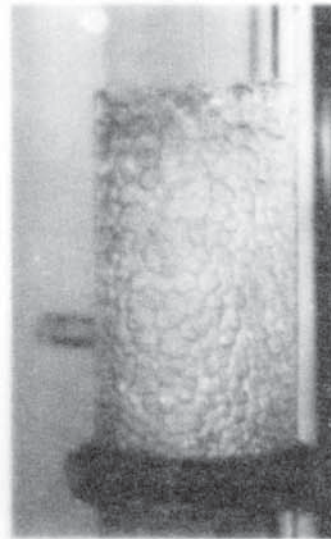


f. Foam completely destroyed. Two liquid phases are present on plate

Foaming of water - kerosene - acetone system.



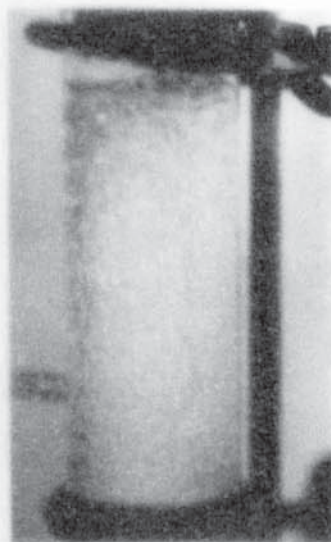
a. Foam height at start up of experiment.



b. Foam expanding.



c. Foam expanded to its maximum height.



d. Foam expanded to its maximum height.



Figure 5.2. water - kerosene - acetone system. Two liquid

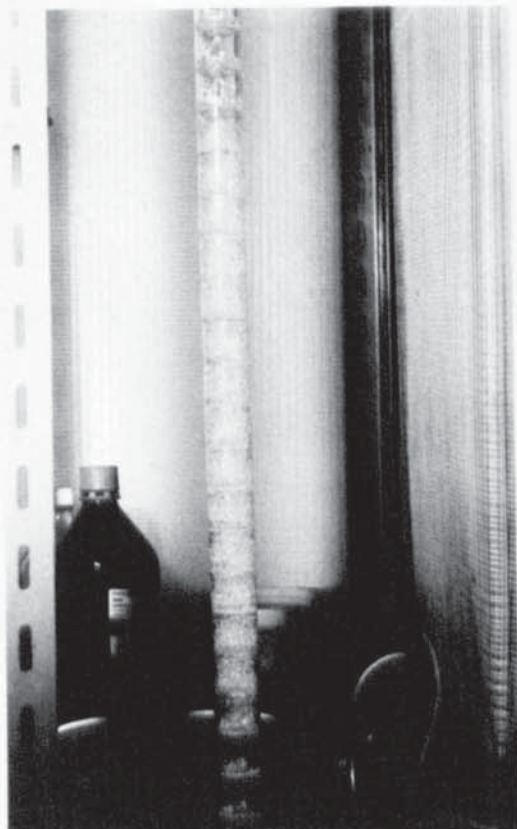
phases are present on plate

Foaming of water - kerosene - acetone system.

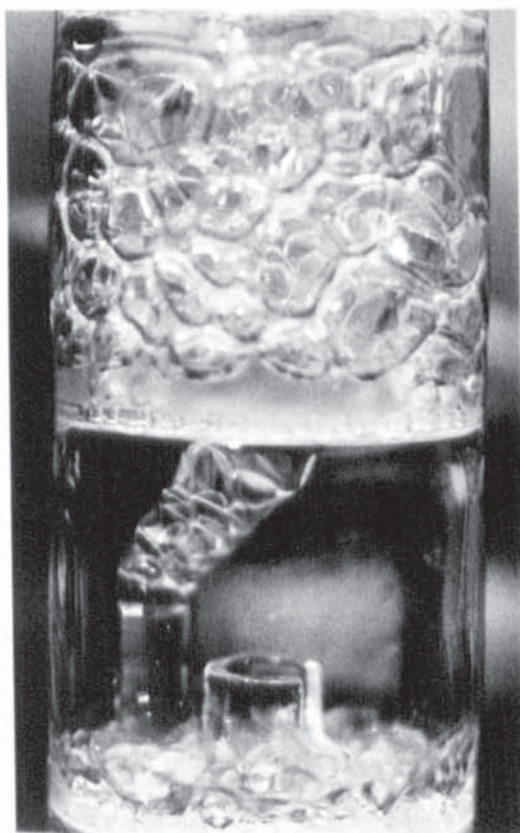
Figure 5.3. n-hexane - water - propan-1-ol system in 30 mm diameter Oldershaw column.



a. Single liquid phase, bottom column section.



b. Whole column.

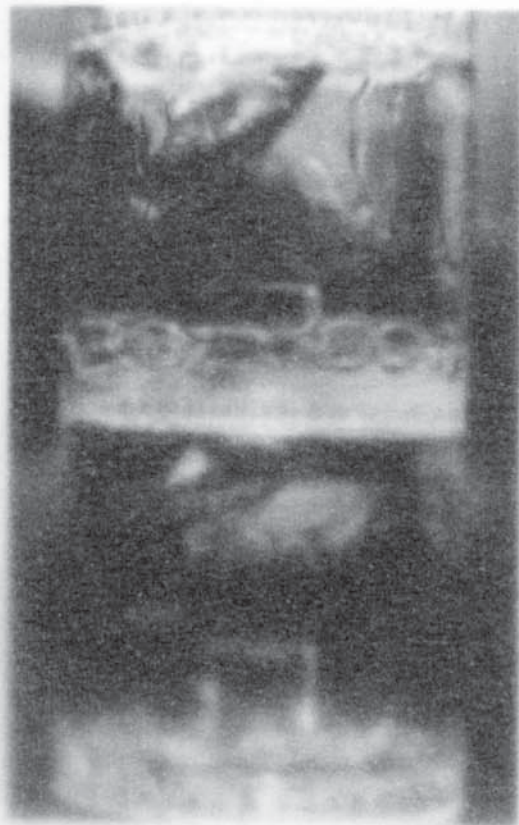


c. Single liquid phase to two liquid phase transition,
bottom column section.



d. Two liquid phases, top column sections.

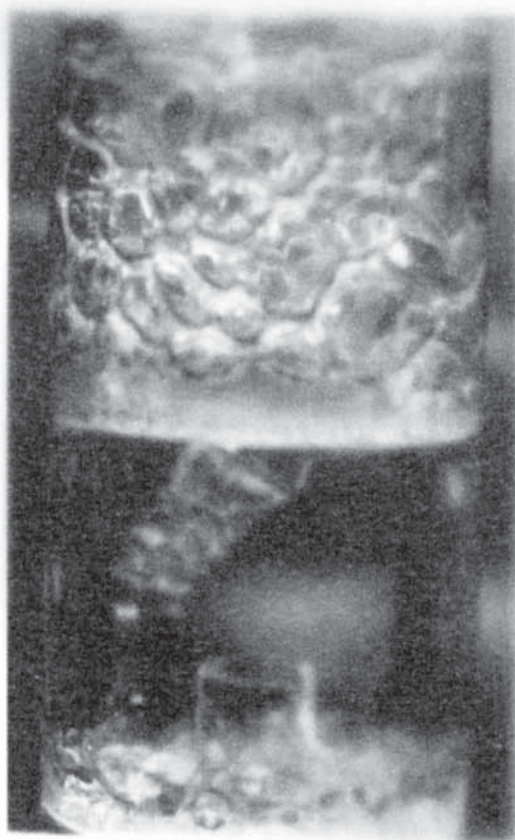
n-Hexane - Water - Propan-1-ol system in 30 mm diameter Oldershaw column.



a. Single liquid phase, bottom column section.



b. Whole column.



c. Single liquid phase to two liquid phase transition.



d. Two liquid phases, top column sections.

Figure 5.3. n-hexane - water - propan-1-ol system in 30 mm diameter Oldershaw column.

n-Hexane - Water - Propan-1-ol system in 30 mm diameter Oldershaw column.

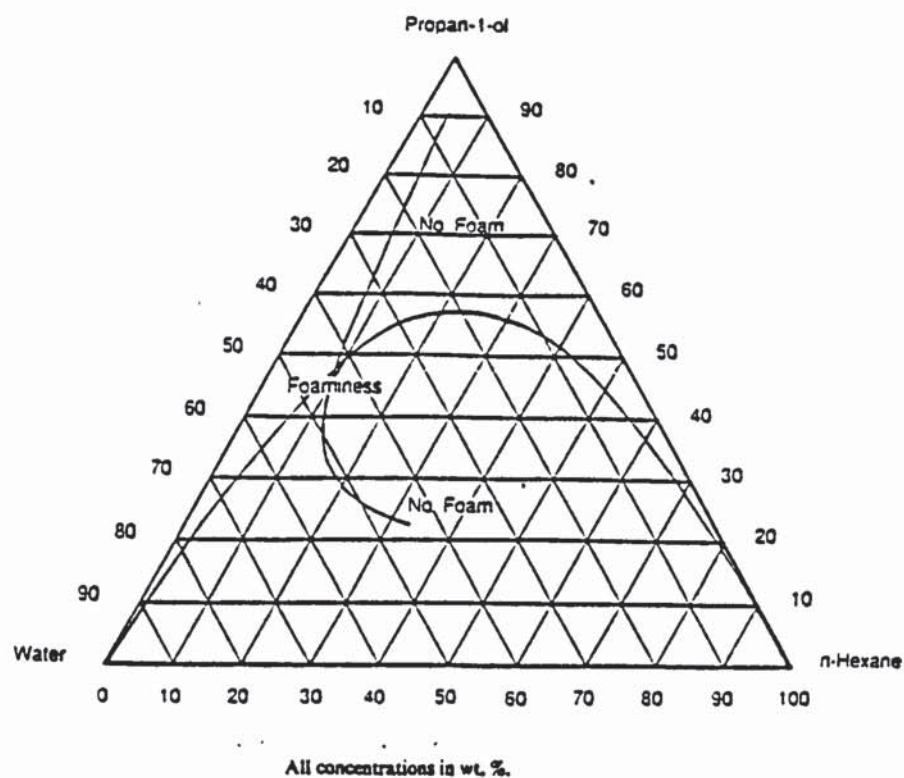


Figure 5.4. Distillation line predicted by UNIFAC for ternary system n-hexane - water - propan-1-ol, liquid-liquid boundary data is at 38°C.

Sym. Run Volume ratio
no. (water/n-hexane)

△ A 2.0
▽ B 1.0
× C 0.5
+ D 0.2

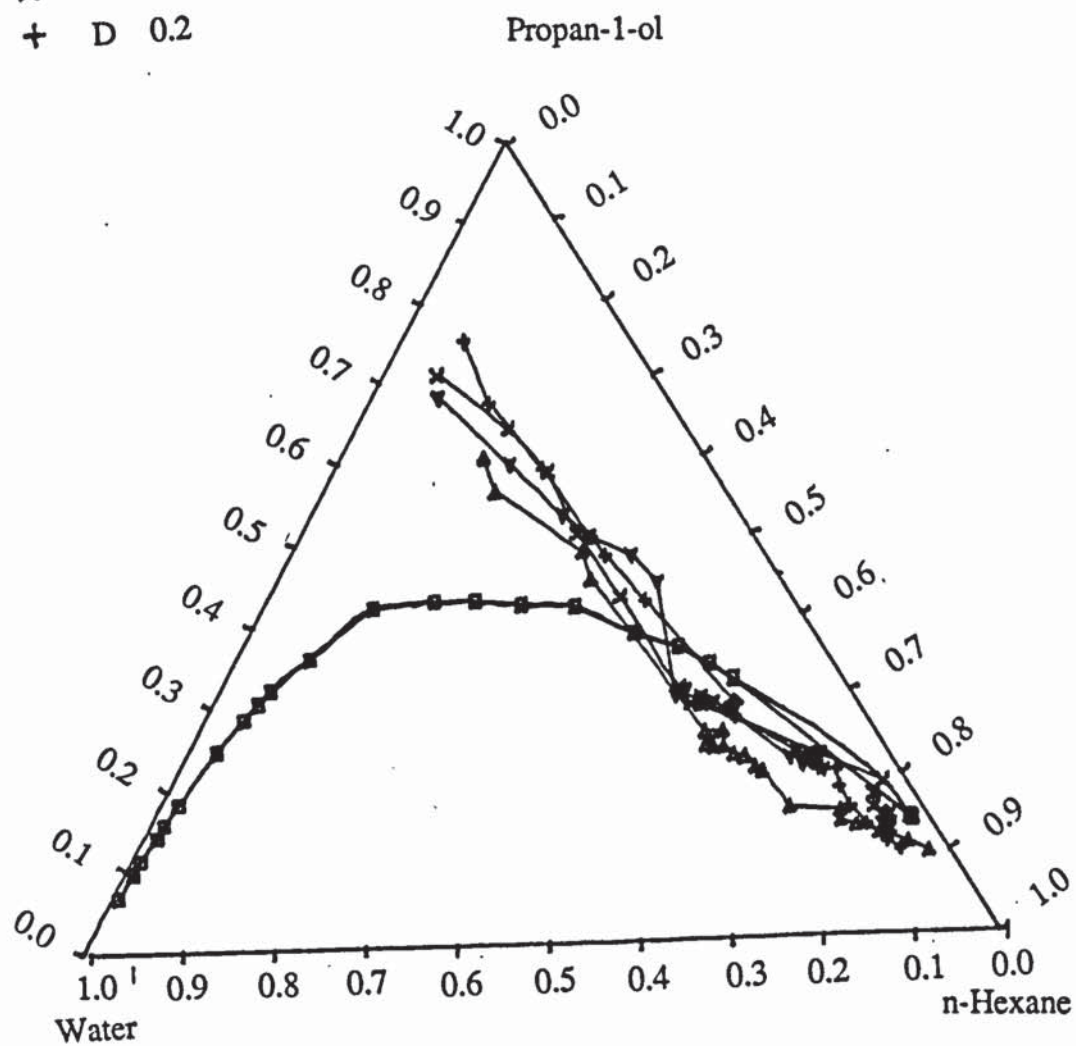


Figure 5.5. Experimental distillation lines at various volume ratios of water/n-hexane.

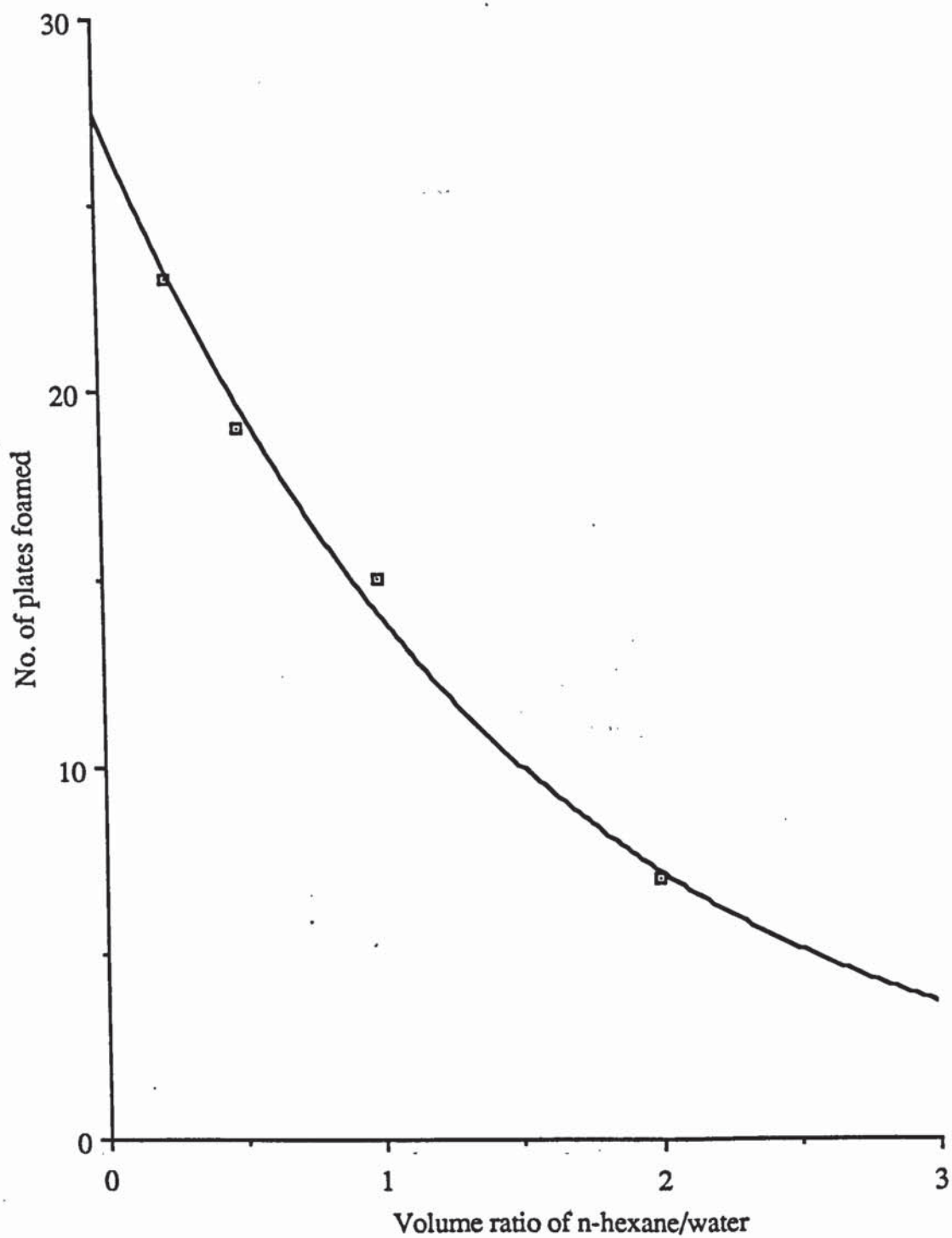


Figure 5.6. Variation in plates foamed in Oldershaw column with changes in volume ratios of water/n-hexane in the initial charge.

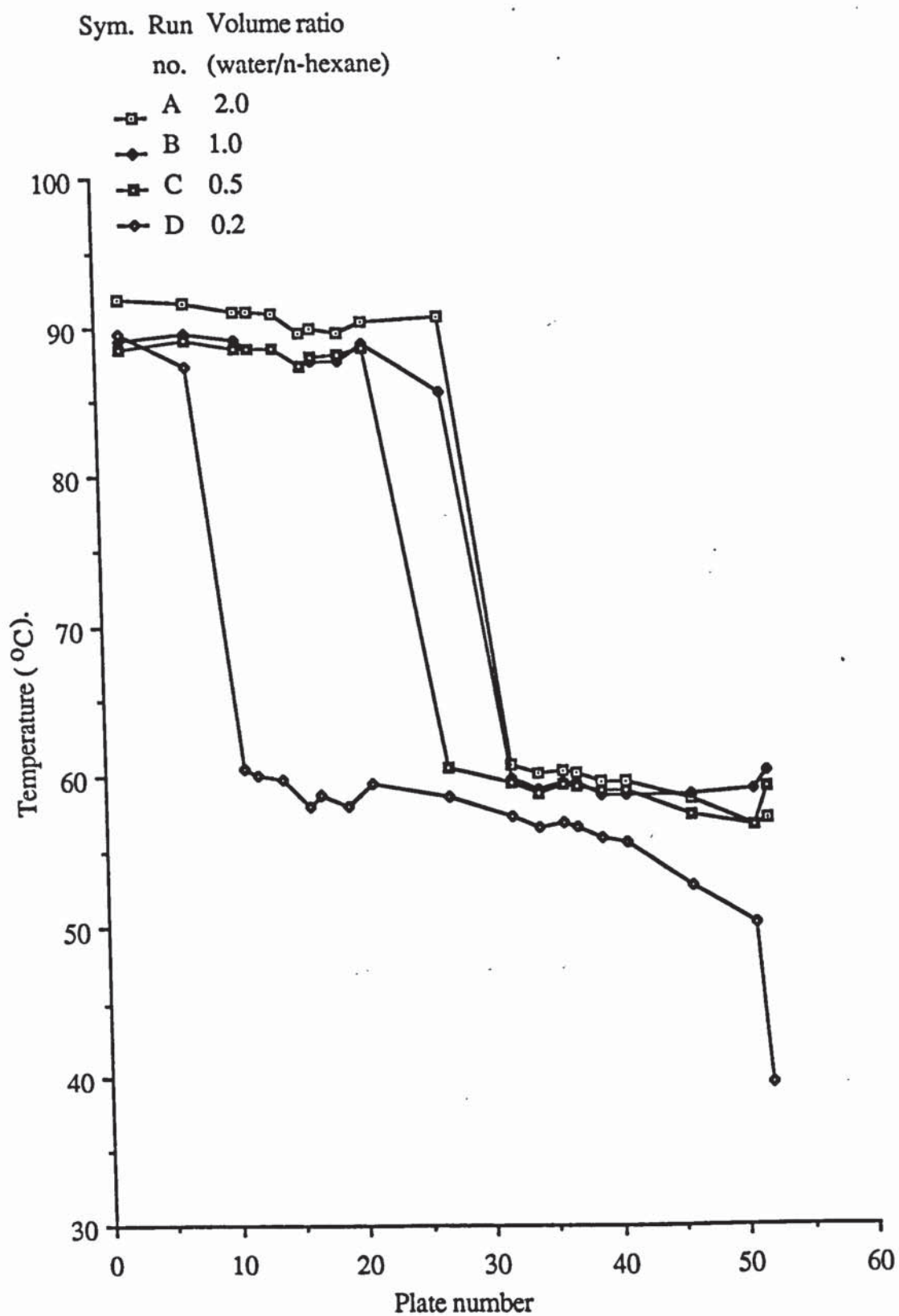


Figure 5.7. Temperature profile across the Oldershaw column for the n-hexane - water - propan-1-ol system.

Sym.	Titration run no.	Volume ratio n-hexane/water
Δ	1	0.20
∇	2	0.25
+	3	0.50
\times	4	1.0
\square	5	1.50
\diamond	6	2.0

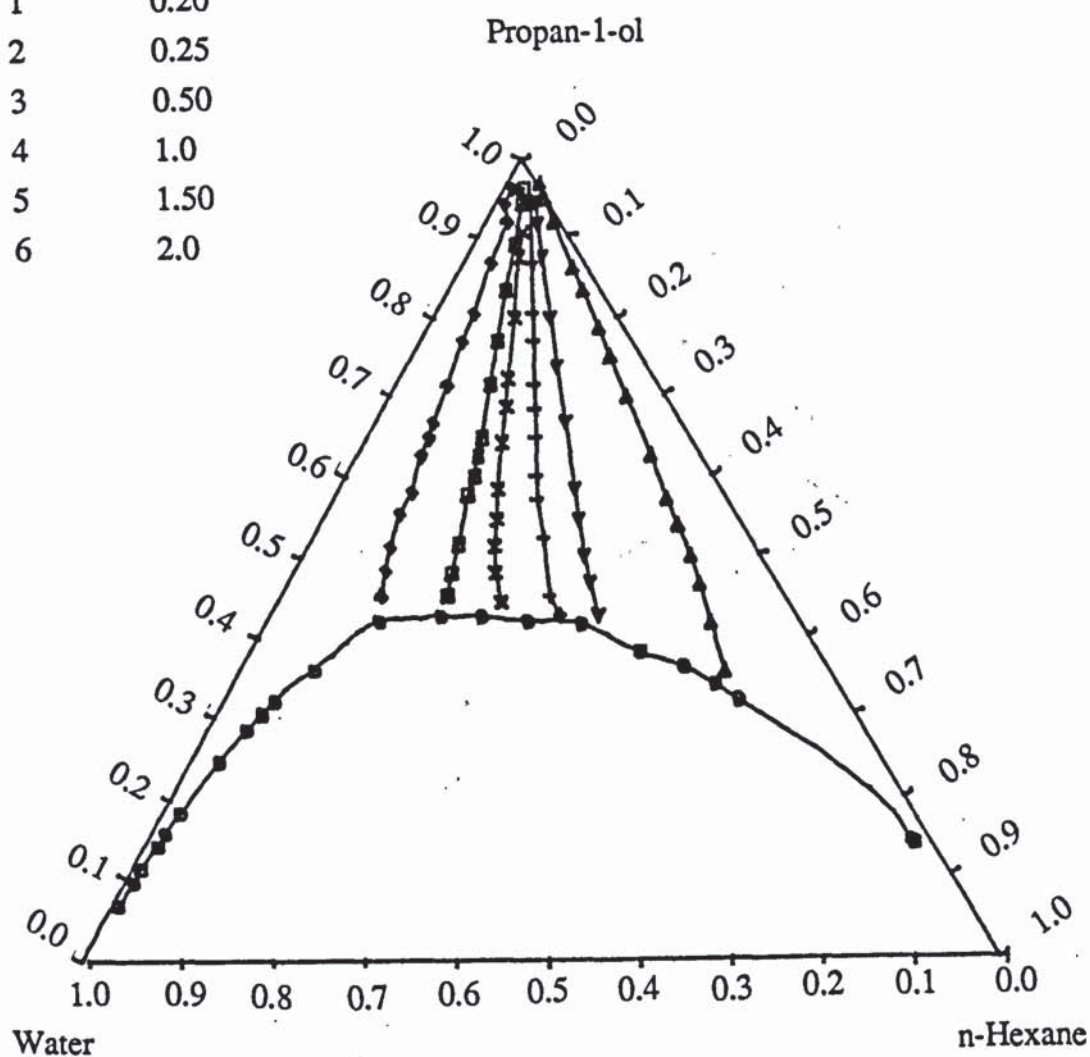


Figure 5.8. Changes in composition with surface tension for the n-hexane - water - propan-1-ol system during titration at 20° C.

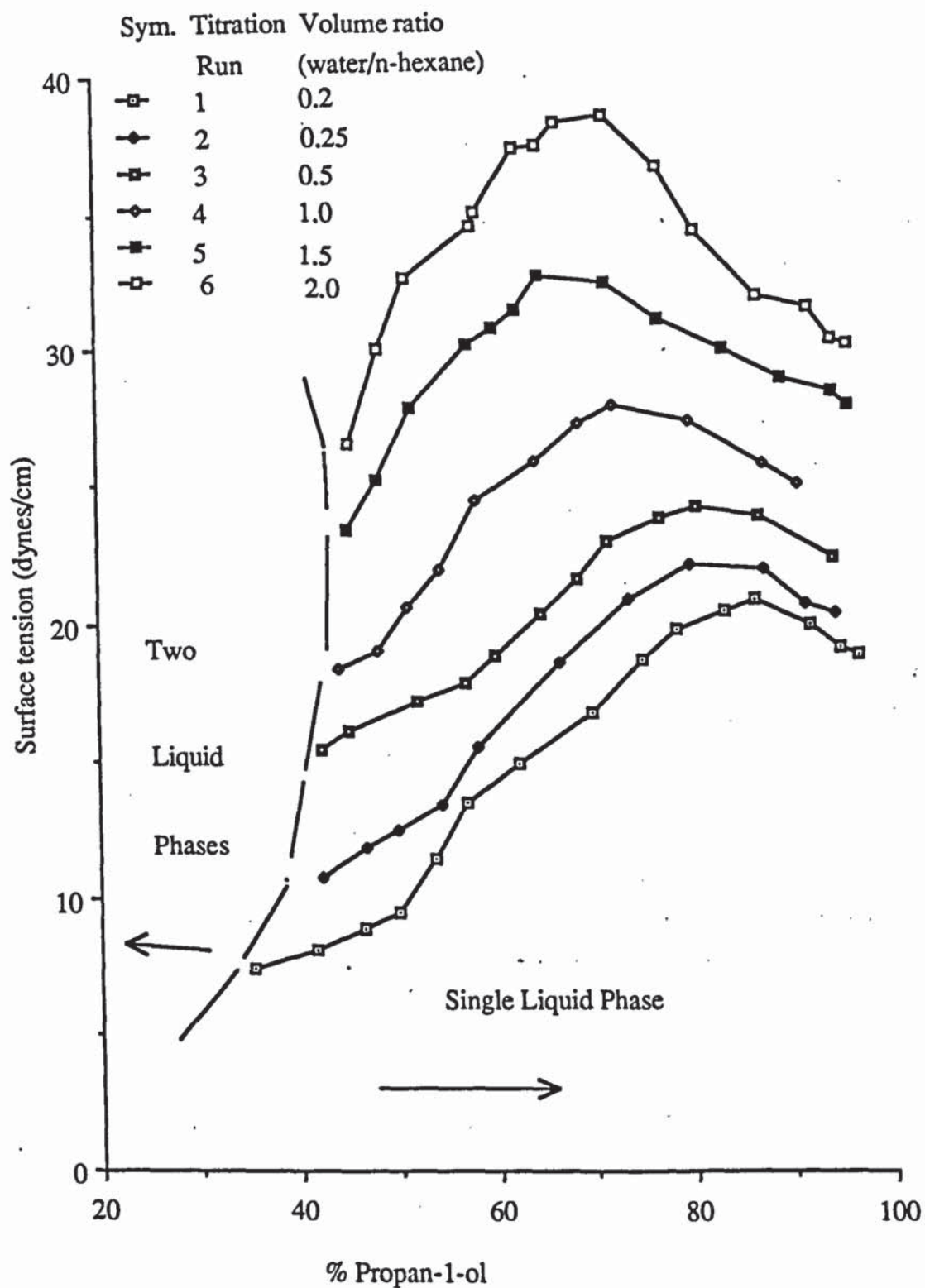


Figure 5.9. Variation of surface tension with composition for n-hexane - water - propan-1-ol system at 20° C.

CHAPTER 6

THE TRANSITION FROM SPRAY TO BUBBLY REGIME

6.1 Introduction

In recent years the problem of phase inversion on sieve trays, i.e. the transition from liquid-continuous bubbly to gas-continuous spray, has received considerable attention following the realisation that the spray regime represents a stable regime of operation at high column throughputs. It has already been shown that there is a fundamental difference in the dependence of the plate performance in the two regimes of operation on process parameters, tray geometry and system properties.

Initially spray was observed by some workers (16,143), but only Goederen (26) and Shakov, Noskov & Romankov (144) noted the existence of the spray regime at different operating conditions. Previous qualitative observations of the transition from spray to bubbly have been reported by Eduljee (146) and Foss, Gerster & Pigford (147) who noted that the vapour or gas tended to replace the liquid as the continuous phase at the highest gas velocities.

The importance of the tray operating regime was first recognised by Wong & Porter (146) and later by Fane & Sawistowski (18). Porter & Wong (17) carried out the most extensive work on the spray to bubbly transition using a light transmission technique to determine the transition. At the distillation symposium in 1969 several papers discussed the structure of the spray regime (17,27,95). Andrew (20), on the basis of some experimental observations, described the dispersion as being like a 'fluidised bed of droplets'. Similar descriptions were proposed by Porter & Wong (17) and Ho, Muller & Prince (27). The former authors used the description as the basis of a model in which the existence of a coalescence zone was assumed and by which the gas velocity could be predicted at which the onset of spray first started. Since then, a number of methods have been developed for estimating whether a given tray will operate in the bubbly regime or spray regime.

Based on the methods discussed in section 2.9.3, it would appear that the most important parameters for the transition from the spray to bubbly regime for a single liquid phase are: the vapour velocity through the holes, hole diameter and liquid holdup. Since the vapour velocity is high at the transition, inertia effects predominate and it has been shown that the surface tension is not important except perhaps for very small holes (22). Also it would appear that small hole diameter trays operate mostly in the froth regime but large diameter trays may operate in either the froth or spray regime. It can be assumed that this transition is independent of the foaming tendency of the liquid. The identification of the tray operating regime for a given loading thus becomes an important step in tray design and the properties of the dispersion must clearly be related to a specific operating regime.

Generally there is disagreement in the published correlations which seek to predict the liquid holdup at the transition. Lockett (101) has attempted to explain this difference in terms of the cone angle at which the jet issues from the hole. From his work it can be concluded that the angle of the jet will be less for thinner plates than for thicker plates. No published work has been found relating the tray thickness to the spray-bubbly transition. Therefore, the effect of tray thickness and the ratio of hole diameter to tray thickness should be included in any subsequent study of the spray to bubbly transition.

6.2 Object of the Work

The study of the spray to bubbly transition will be considered for systems containing a single liquid phase and two liquid phases. Chapter 6 will deal briefly with the single liquid phase systems and chapter 7 with the two liquid phase systems.

For single liquid phase, the object of this part of the research program is as follows:

- i. To study the transition from the spray to bubbly regime in terms of the following variables: hole diameter, free area, gas hole and superficial velocity and density.
- ii. To study the effect of plate thickness and the ratio of the hole diameter to plate thickness on the transition.
- iii. To compare the experimental results with the existing correlations and to include the effect of plate thickness in any new correlation for the transition.

6.3 The Determination of the Spray to Bubbly Regime Transition

Spray is formed at lower liquid holdups on a sieve plate than the froth at any given gas velocity. If the gas flow rate is kept constant and the liquid is gradually introduced onto the sieve plate, spray will be formed. As the liquid holdup is increased, the spray will change over to a bubbly dispersion with the formation of an interface. This interface prevents most of the formation spray rising above it. Any droplets seen above the interface are largely the result of bursting bubbles.

If a photocell is situated above the formation height of the interface, then prior to the formation of the interface, the light will be transmitted through a thick spray of suspended drops and the intensity of the light received by the photocell will be low. After the formation of the interface, the light transmitted through the fixed spray above the bubbly surface and the light received by the photocell will be greater, as shown diagrammatically in figure 6.1. The transition from spray to bubbly should therefore be accompanied by an increase in light transmitted through the column [i.e a drop in the voltage across the

photocell] provided the photocell is situated above the level at which the interface forms.

This phenomena is clearly shown in figure 6.2 where the amount of light received by the photocell, measured in terms of voltage, at a fixed height above the sieve plate is plotted against the liquid holdup on the tray. The gas flow rate was fixed and the amount of liquid on the plate was gradually increased. At first the intensity of the light dropped sharply from the value when the column was empty. This was because the spray grew more dense as the liquid holdup was increased and, as more liquid was available for dispersion.

Following this, there is an approximately constant region of low light transmission. This corresponds to the true spray region in which entrainment was independent of liquid holdup. When the formation of the continuous interface was complete, the light transmitted increased rapidly as more of the liquid drops were trapped by the interface. This is accompanied by a decrease in voltage.

This increase in light intensity [decrease in voltage] can be taken as a convenient reference point for the transition from spray to bubbling and as shown in figure 6.2 to be almost independent of the location of the photocell unit above the interface. Thus, there is no need to specify the height of the photocell unit at which the transition has to be determined. Thus, the liquid holdup required to effect the transition may be given by the vertical line in figure 6.2.

The position of the photocell is limited by the location of the froth interface on the one extreme and by the height of the falling liquid film on the column wall on the other. Below this limit, the formation of the froth prevents any light from being transmitted and above this limit, liquid drops on the column wall interfere with the passage of light.

The light transmission method is simple in principle and operation. Careful alignment of the light source and the photocell, while desirable, is not vital as the transition from the spray to bubbly regime is detected by changes in intensity of the light received by the photocell and thus absolute quantities are not necessary.

6.4 Experimental Program

The variables studied which influence the transition from the spray to bubbly regime are:

- i. Liquid density.
- ii. Liquid holdup [or clear liquid height] on the sieve plate.
- iii. Diameter of sieve holes.
- iv. Sieve plate free area and bubbling area of the sieve holes.
- v. Plate thickness.
- vi. Ratio of hole diameter to plate thickness.

The range of experimental variables are listed in table 6.1. Because of the material

of construction used in the apparatus, it was necessary to operate at approximately atmospheric pressure.

Table 6.1. Operating limits for the air-water simulator

Variable	Min.	Max.
Gas superficial velocity u_g (m/s)	0.45	2.2
Hole gas velocity u_h (m/s)	8.18	34.91
F - factor	0.49	2.17
Liquid density (kg/m ³)	768.0	1000.0
Surface tension (dynes/cm)	32.0	74.0

6.5 Experimental Procedure

The air-water simulator used in this part of the experimental work has already been described in section 4.3 in detail. The experimental procedure is described below.

6.5.1 Column Operation

The air blower and the extraction fan were started allowing air to flow through the sieve plate and also to be vented outside the building. The gas flow rate was adjusted such that weeping would not occur and the liquid was allowed to flow from the liquid storage vessels onto the sieve plate. Initially spray was observed but as the liquid holdup on the plate was increased, a bubbly dispersion was formed. The transition was determined by the light transmission technique.

6.5.2 Experimental Determination of the Transition

With the gas flow rate set, liquid was introduced slowly onto the sieve plate. The voltage indicated by the voltmeter represented the light transmitted and was recorded for the known liquid holdups on the sieve plate. This procedure was carried out well past the transition and the transition point was later determined graphically.

The spray to bubbly transition results can be found in appendix 5. A detailed discussion and interpretation of the results are given below, but it is now proposed to indicate some of the significant trends in the results. In all the graphs [figures 6.3-6.7], the column was operating in the spray regime for data below the solid line and in the bubbly regime above the line.

6.6 Effect of Operating Conditions on the Transition

The method of the investigations was to change one parameter at a time while keeping the others constant. Approximately 200 experiments were carried out and the effect of each parameter is now discussed separately:

For a particular sieve plate size hole, the liquid holdup at the transition from the spray to bubbling, increased as both the column and hole velocities are increased. The rate of increase decreased somewhat at the higher gas velocities [figure 6.3].

It was seen that at the same hole gas velocity a larger liquid holdup is required to effect the transition for larger holes [figure 6.4].

The effect of free area is illustrated in figure 6.5 for 6.35 mm hole size sieve plate. The liquid holdup at the transition was consistently higher for a lower free area plate.

As the liquid density was increased the liquid holdup was seen to decrease [figure 6.6]. Only water (1000 kg/m^3) and kerosene [768 kg/m^3] were used, covering the density limits used by Porter and Wong(17). Although the range is limited, the results do show that a 23.2% change in liquid density affects the liquid holdup at the transition.

Changes in the surface tension of the liquid caused no significant effect on the liquid holdup at the transition. Whilst the liquid holdup for kerosene was substantially greater than that of water at the same conditions, the difference is due to liquid density rather than surface tension effects.

6.6.1 Effect of Plate thickness and Ratio d_h/X

The effect of the plate thickness and the ratio of the hole diameter to the plate thickness [i.e. d_h/X] was investigated using plates 5, 9 and 12 [i.e. plates of the same free area and hole diameter, but with different thicknesses of 2.38 mm, 4.0 mm and 6.35 mm]. It was found that the transition [figure 6.7] was affected by both of these parameters. The liquid holdup at the transition was observed to increase with the plate thickness i.e. for the same gas and liquid loadings and thicker plates would tend to operate in the spray regime whilst thinner plates would tend to favour the bubbly regime.

It was also found that the liquid holdup would tend to increase with a decrease in the ratio d_h/X , so plates with a higher ratio would tend to favour the bubbly regime while plates with lower ratio tend to favour the spray regime.

6.7 Comparison of Experimental Data

The published experimental spray to bubbly transition data are shown in figures 6.8-6.8.6. All the previous correlations have been compared for high and low free area trays [figures 6.9 & 6.9.1] and it is seen that for high free area trays, none of the

correlations are satisfactory whilst for low free area trays some of the correlations are satisfactory. The computer programme used in calculating clear liquid holdup is listed in appendix 6 and the details of the sieve trays used by previous workers are listed in appendix 7.

The following conclusions may be drawn from these graphs:

- i. The ratio $[h_{cl}/d_h]$ at the spray to bubbly transition is proportional to u_h and independent of d_h , although there is some suggestion that for larger holes the linearity between $[h_{cl}/d_h]$ and u_h breaks down [figures 6.8, 6.8.1 & 6.8.3, 6.8.5, 6.8.6]. However, the results of Pinczewski & Fell (22) [figure 6.8.2], Payne & Prince (21) [figures 6.8] and Prince, Jones & Panic (102) [figure 6.8.1] show conflicting results. Taking the data as a whole, it is reasonable to conclude that $[h_{cl}/d_h]$ is proportional to u_h .
- ii. Porter & Wong (17) and later Hofhuis & Zuiderweg (57) showed that the surface tension and viscosity have little or no effect on the transition. Therefore, the correlations of Pinczewski & Fell (22) and Jeronimo & Sawistowski (86) will no longer be considered .
- iii. Extensive results on various gas-water systems, other than air, by Porter and Wong (17) [figure 6.8.4] showed that $[h_{cl}/d_h]$ is proportional to $[\rho_g/\rho_l]^{0.5}$.
- iv. The Payne and Prince (21) correlation is in doubt because there is no evidence to confirm that $[h_{cl}/d_h]$ depends on $[d_h^{0.5}]$ as suggested by their correlation.
- v. The correlation of Barber & Wijn (103) correctly predicted only a small dependence of $[h_{cl}/d_h]$ on d_h and $(1-\epsilon)$ and incorrectly predicted the variation of $[h_{cl}/d_h]$ on u_h .
- vi. The correlation of Hofhuis and Zuiderweg (57) also predicted a small dependence of $[h_{cl}/d_h]$ on d_h and $(1-\epsilon)$ incorrectly.
- vii. The model of Porter & Wong (17) overpredicted the transition for high free area trays [figure 6.9] because the original equation was applicable only to trays of 5% free area. For low free area trays, the agreement with experimental results was excellent [figure 6.9.1]

6.8 Correlation of Experimental Results

From the previous published data and from the experimental results of this study, it would appear that the most important parameters relating to the transition from the spray to bubbly regime are:

- i. Gas density
- ii. Liquid density
- iii. Free area of plate
- iv. Gas hole velocity
- v. Hole diameter

The results obtained in this study confirm the previous experimental data most of which is based on the data of Porter & Wong (17). However there are some fundamental differences between this work and previous correlations. These are due to differences in the type and size of the equipment, different techniques of determining the transition and also to the different tray thickness and therefore different ratios of hole diameter to plate thickness used by the respective researchers.

Lockett (101) has attempted to explain the differences by suggesting a model [equation 2.21] which considers the angle of the gas jet leaving the hole. This model has been compared with the correlations of Barber & Wijn (103), Hofhuis & Zuiderweg (57) and Payne & Prince (21) by substituting values of n equal to 1, 2, or 4 respectively. The computer programme used are listed in appendix 8. The values of 'a' were calculated from the experimentally determined values of h_{cl}/d_h . These values are given in table 6.2. The angle of the gas jet with the tray floor was calculated from the equation (101):

$$D = \frac{1}{2} \left\{ \left[a(X/d_h) + 1 \right]^{1/n} - d_h \right\} \quad \dots 6.1$$

It is seen from figure 6.10 that as the value of 'n' increased the angle of jet decreased linearly and the value of 'a' increased sharply [figure 6.10]. The experimental results obtained in this study confirm that the angle of jet should decrease as 'n' increases [i.e. the angle is larger with the tray floor for thinner plates than for thicker plates].

From figure 6.11 it can be seen that the model predicted the transition point better than the original correlation when the parameter 'a' was obtained by using the experimental values of h_{cl}/d_h in Lockett's model. However, when 'a' was obtained using predicted values of h_{cl}/d_h from the various correlations, the model showed that the liquid holdup at the transition was almost the same [figure 6.12].

From the results obtained in this study it is seen that the liquid holdup at the

transition is less for thinner plates than for thicker trays of the same free area and hole diameter [figure 6.7]. Therefore, it appears that the angle of the jet is less for the thinner plates than for thicker plates.

Table 6.2. Values of constants in Lockett's model (101)

'n'	'a'	Jet angle
1	0.70	70.5
2	2.0	64.5
4	8.33	53.0

6.8.1 Proposed Correlation for Spray to Bubbly Transition

From the previous work and this study, it appears that $[h_{cl}/d_h]$ is proportional to u_h and $[\rho_g/\rho_l]^{0.5}$. Also from this study it appears that $[d_h/X]$ has an effect on the transition.

The following correlation which takes into account the effect of the ratio of the hole diameter to plate thickness, has been proposed for the transition from spray to bubbly regime on sieve trays.

$$\frac{h_{cl}}{d_h} = 2.73 u_h \left(\frac{\rho_g}{\rho_l} \right)^{0.5} \left(\frac{d_h}{X} \right)^{-0.17} \quad \dots 6.2$$

It can be seen from figure 6.13 that this correlation satisfactorily predicted all the transition data in literature. The data of Fane & Sawistowski (95) have been ignored because the authors did not report the tray thickness. The data of Burgess & Robinson (19) have been omitted because Payne & Prince (21) have cast doubts on the reliability of the results.

The proposed correlation has been obtained by regression analysis. The computer programme is listed in appendix 9.

6.9 Modification of Existing Correlations

The effect of the ratio of the plate thickness to hole diameter on the transition from spray to bubbling has not been reported in any previously published data. Thus the existing correlations and models have been modified in the light of the experimental results obtained in this study and the modified form of these correlations are listed in table 6.3. However, it can be seen that the correlations of Hofhuis & Zuiderweg (57) still overpredict the transition and the correlation of Barber & Wijn (103) generally underpredicts the transition. The correlations of Wong & Kwan (106), Payne & Prince (21) and Porter & Wong (17) show an improvement in the prediction of the transition. Equation 6.2, though empirical, shows consistent results in the prediction of the transition [figures 6.14 & 6.14.1].

The modified form of the correlations are shown in table 6.3 and the computer programme used to obtain constants is listed in appendix 9.

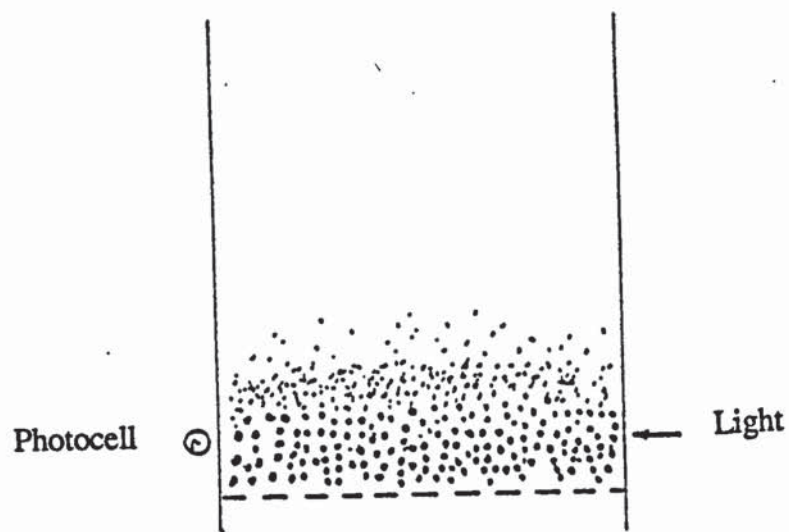
Table 6.3. Modified correlations for the spray/bubbly transition

Porter/Wong	$\frac{h_d}{d_h \rho_f} = 0.14 + 13.5 \left[\frac{(u_h - u_l)}{(u_h - u_s)} \right] \left(\frac{d_h}{X} \right)^{-0.17}$
Payne/Prince	$\frac{h_d}{d_h} = 2.37 \left(\frac{\rho_g}{\epsilon \rho_l} \cdot \frac{u_h^2}{g d_h} \right) \left(\frac{d_h}{X} \right)^{-0.17}$
Hofhuis/Zuiderweg	$\frac{h_d}{d_h} = \frac{6.09}{A_f} \frac{u_s}{\sqrt{g h_d}} \left(\frac{\rho_g}{\rho_l} \right)^{0.5} \left(\frac{d_h}{X} \right)^{-0.17}$
Barber/Wijn	$\frac{h_{cl}}{d_h} = \left[1.92 \left(\frac{\lambda_h}{\sqrt{g d_h}} \right)^{0.4} \left(\frac{d_h}{X} \right)^{-0.17} - 0.33 \right] \left(\frac{P}{d_h} \right)^{0.33}$
Wong/Kwan	$\frac{h_{cl}}{d_h} = 0.06 + 32.15 \frac{u_s \rho_g^{0.5}}{A_f^{0.5} (\rho_l - \rho_g)^{0.5}} \left(\frac{d_h}{X} \right)^{-0.17}$

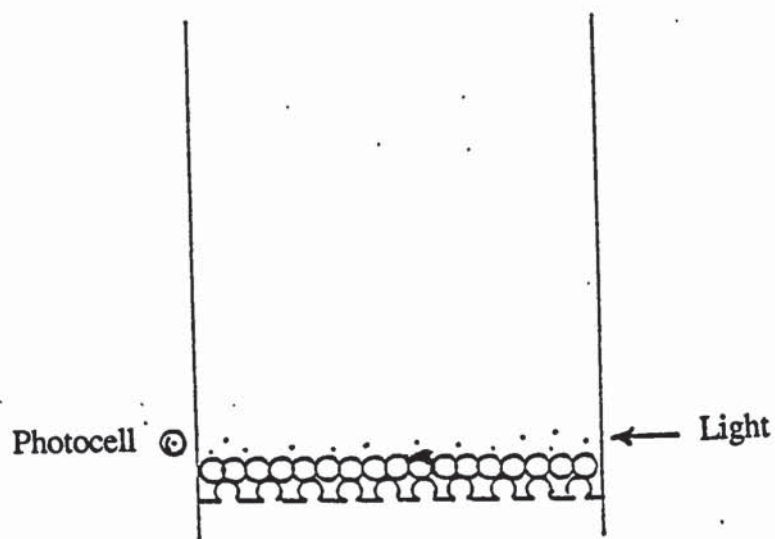
6.10 CONCLUSIONS

The following conclusions may be drawn from the experimental work in this chapter:

- i. Additional data have been determined for the transition from spray to bubbly regime for a single liquid phase. The data show good agreement with the data obtained by Porter & Wong (7).
- ii. Existing correlations have been compared and no correlation has been found which satisfactorily predicts the transition.
- iii. Generally the correlation of Hofhuis & Zuiderweg (57) overpredicts the transition for most of the trays.
- iv. The model of Porter and Wong (17) overpredicts the transition for high free area trays. This is because the original model was based only on data from a 5% free area tray.
- v. The correlation of Barber and Wijn (103) underpredicts the transition for small hole diameter trays [3.2 mm and 4.8 mm].
- vi. The effect of plate thickness and the ratio of hole diameter to plate thickness on the transition had not been investigated previously and this research program has now evaluated the effect of these parameters.
- vii. Existing correlations have been modified to include the effect of the ratio of hole diameter to plate thickness on the transition.
- viii. An empirical correlation has been proposed and compared with the existing and modified correlations. A comparison of the results has been obtained.
- ix. The parameters in Lockett's (101) model have been evaluated. The model shows an improvement in predicting the liquid holdup at the transition when the parameter 'a' is evaluated from the experimental results.



a . Formation spray resists light transmission.



b . Little resistance to light transmission by fine spray above bubbly interface.

Figure 6.1. Diagram to show light transmitted through dispersion.

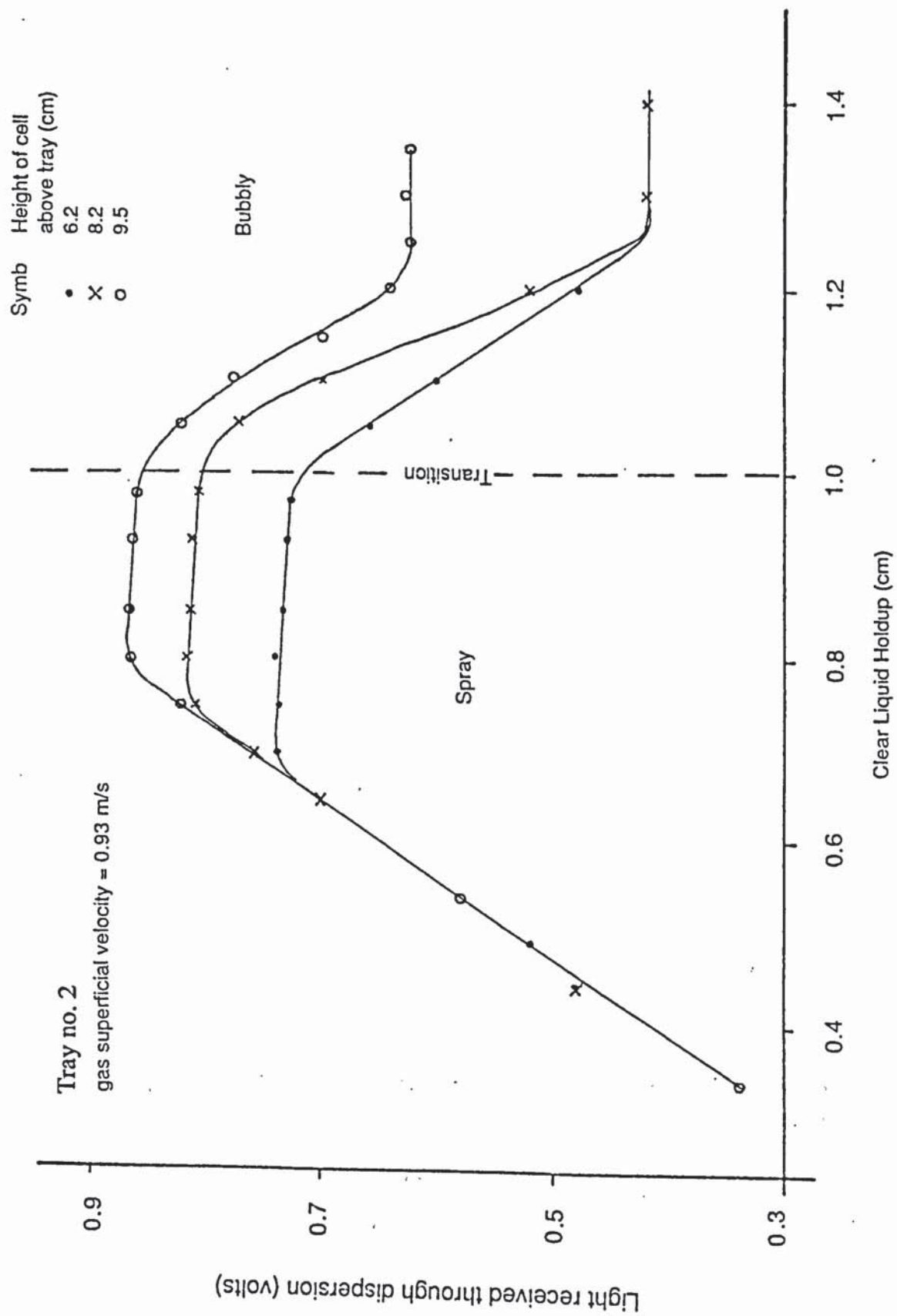


Figure 6.2. Calibration of light beam technique

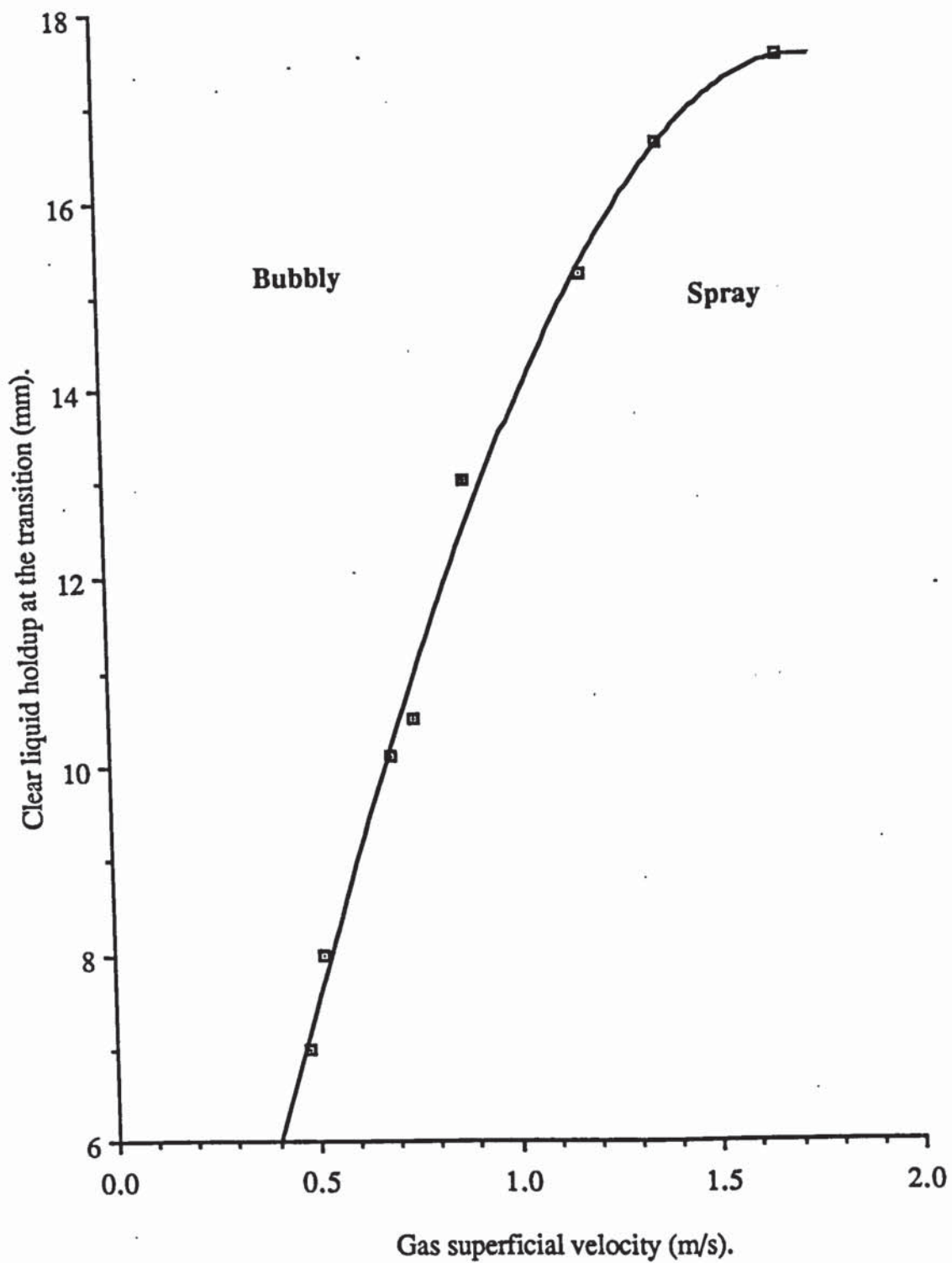


Figure 6.3. Effect of gas superficial velocity on transition. Air-Water system. Tray no. 3.

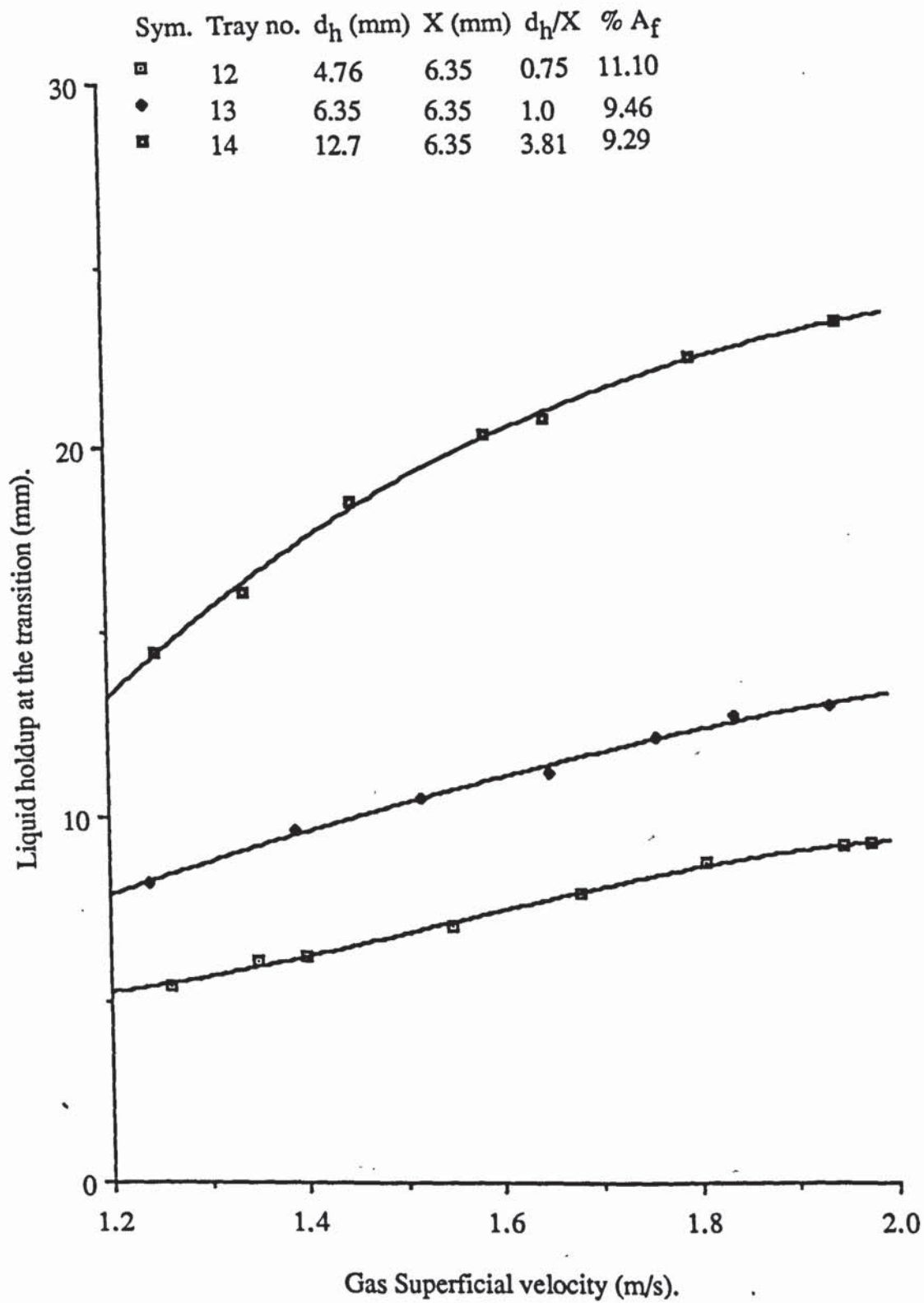


Figure 6.4. Effect of hole diameter on transition. Air-Water system.

Sym.	Tray no.	d_h (mm)	X (mm)	d_h/X	% A_f
□	3	6.35	6.35	1.0	4.87
•	13	6.35	6.35	1.0	9.46

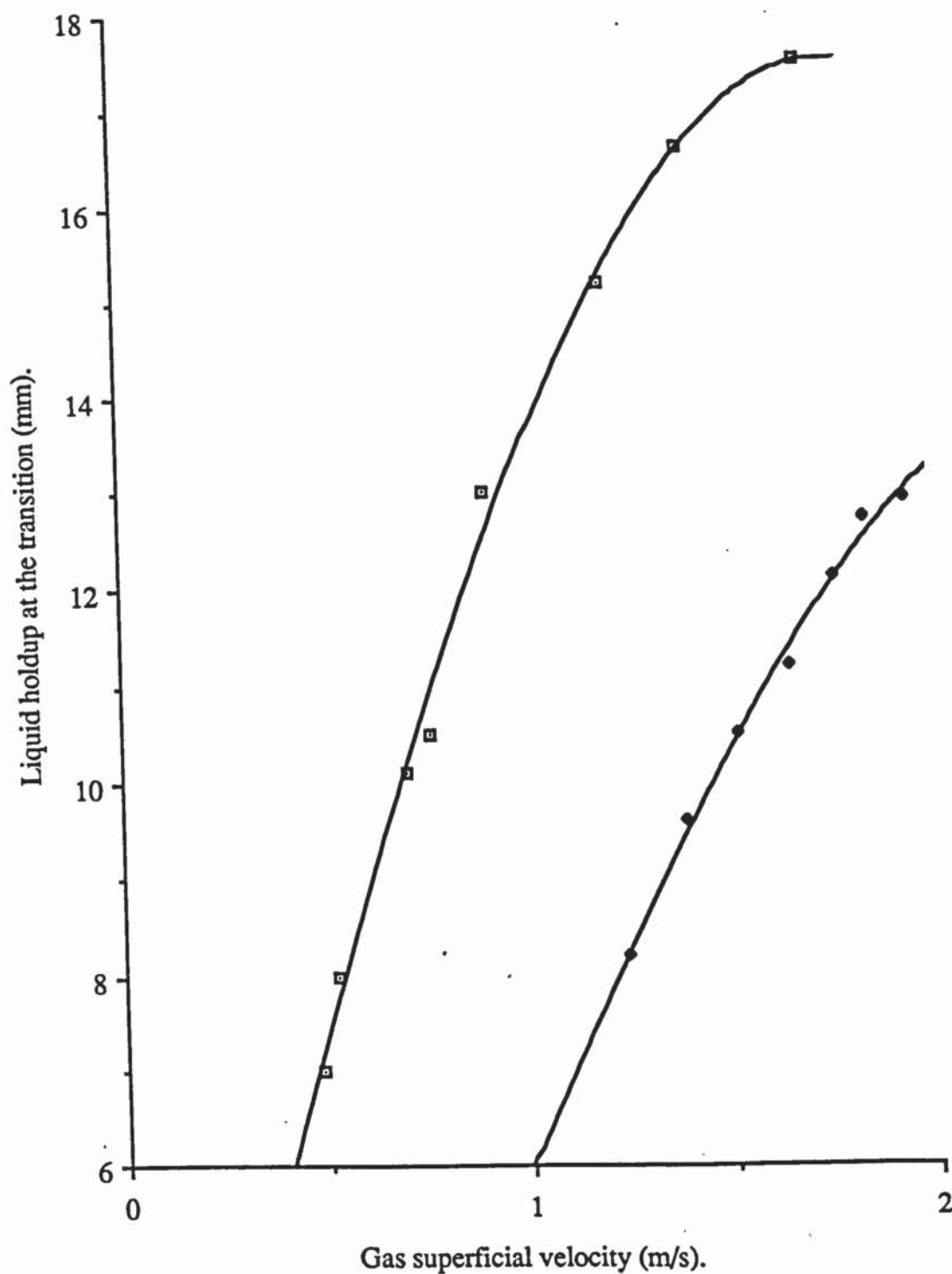


Figure 6.5. Effect of free area on transition. Air-Water system.

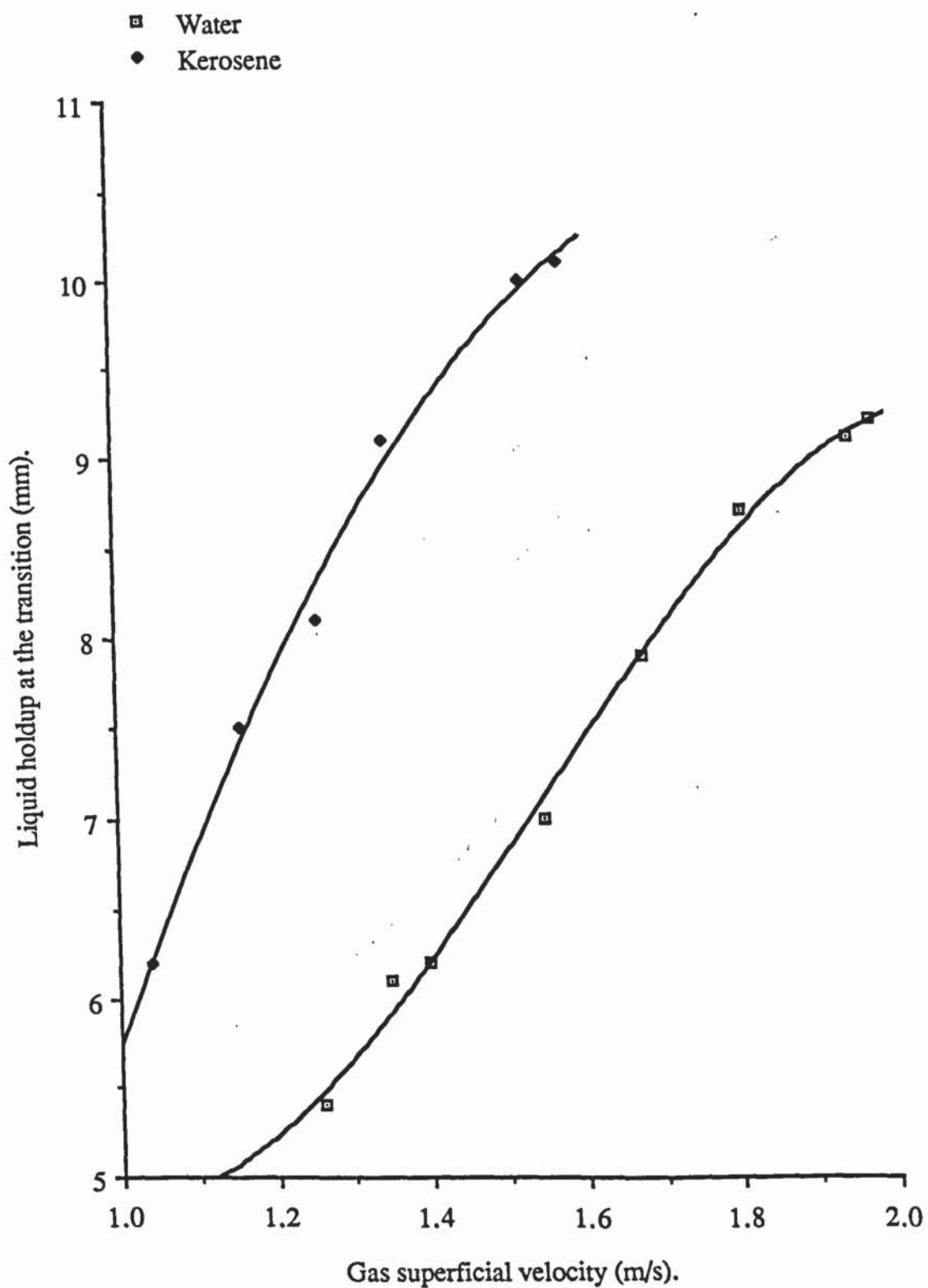


Figure 6.6. Effect of liquid density on transition. Air-Water system. Tray no. 12.

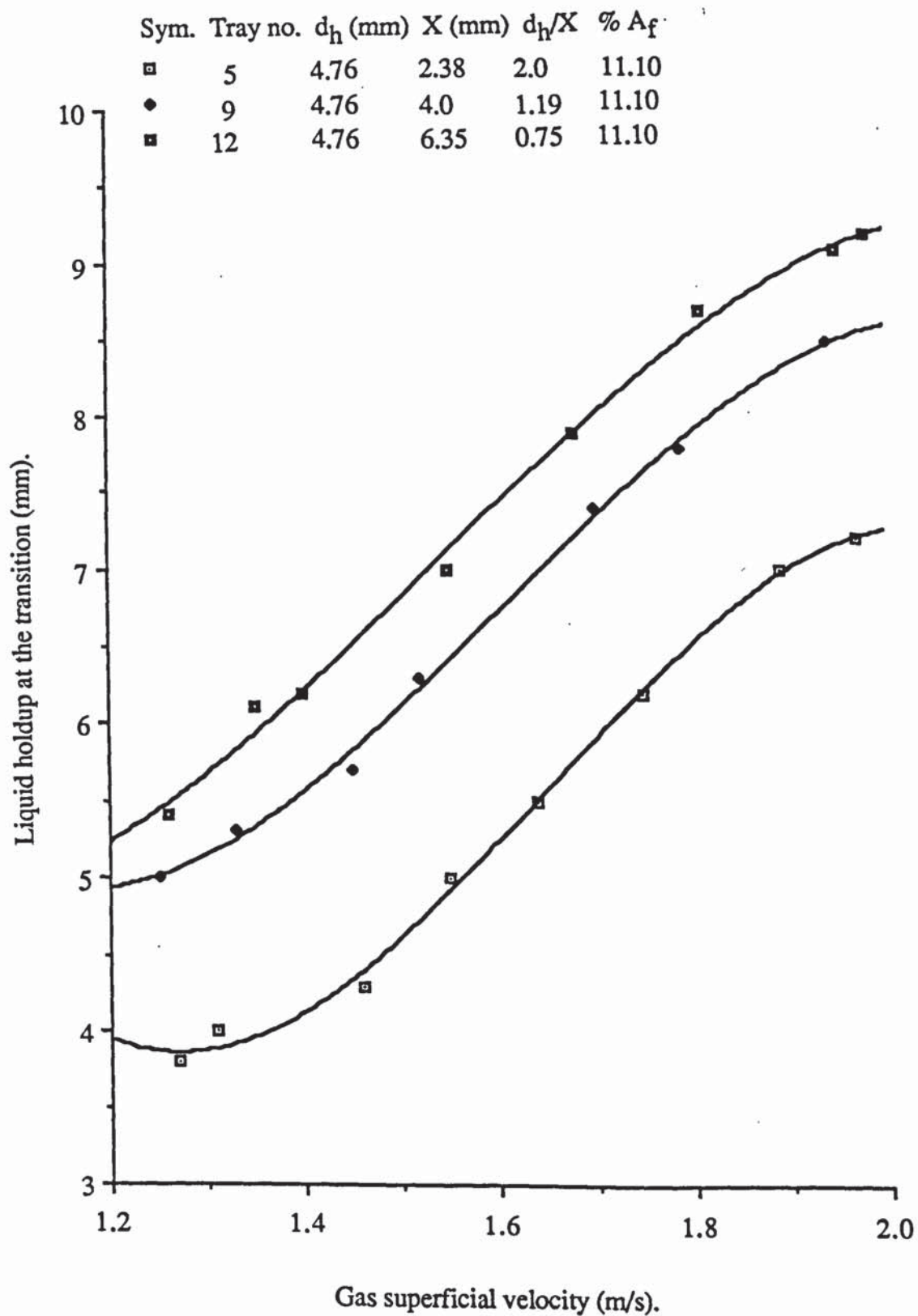


Figure 6.7. Effect of plate thickness and ratio (d_h/X) on the transition. Air-Water system.

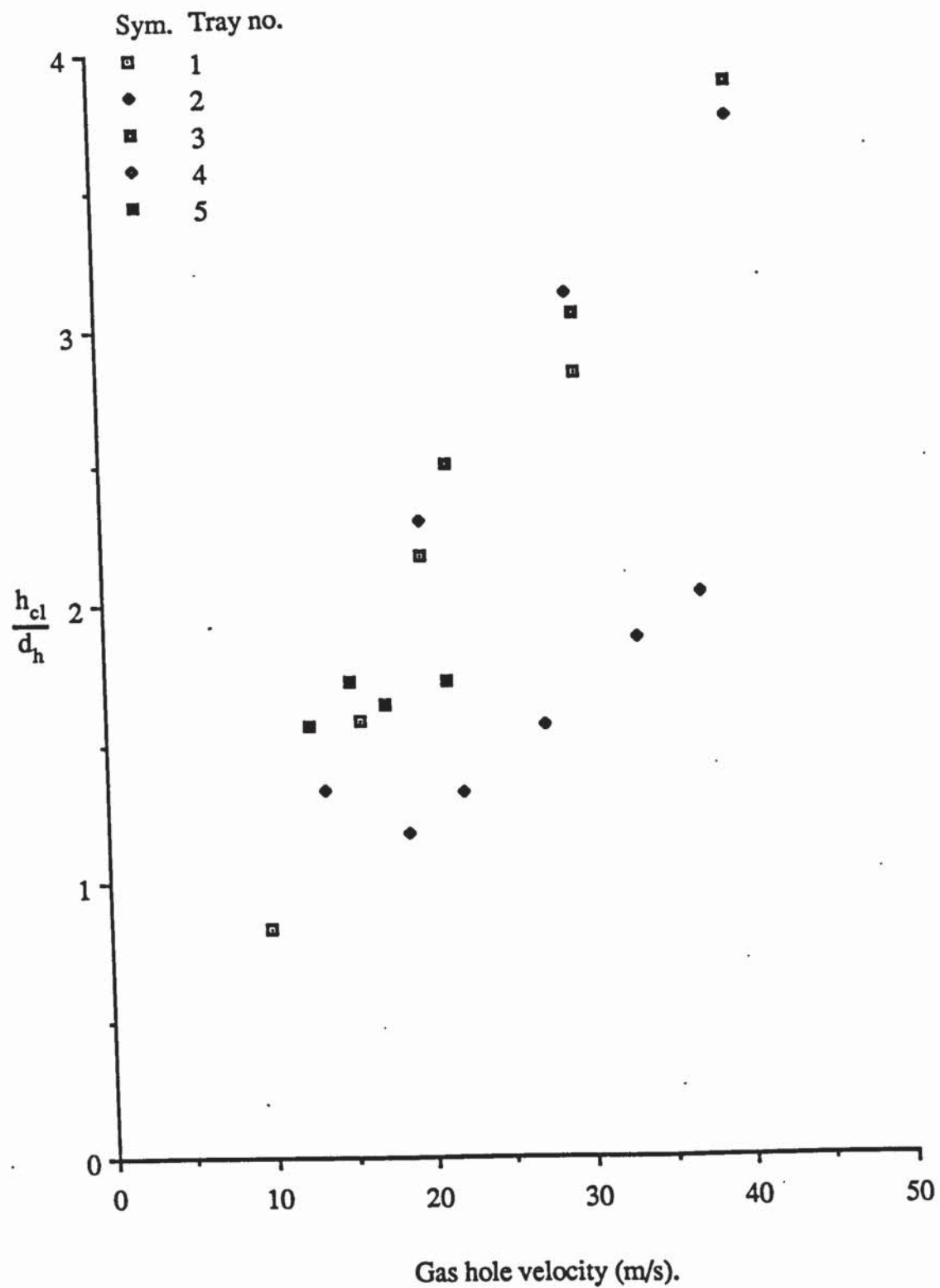


Figure 6.8. Transition results of Payne & Prince (21). Air-Water only.

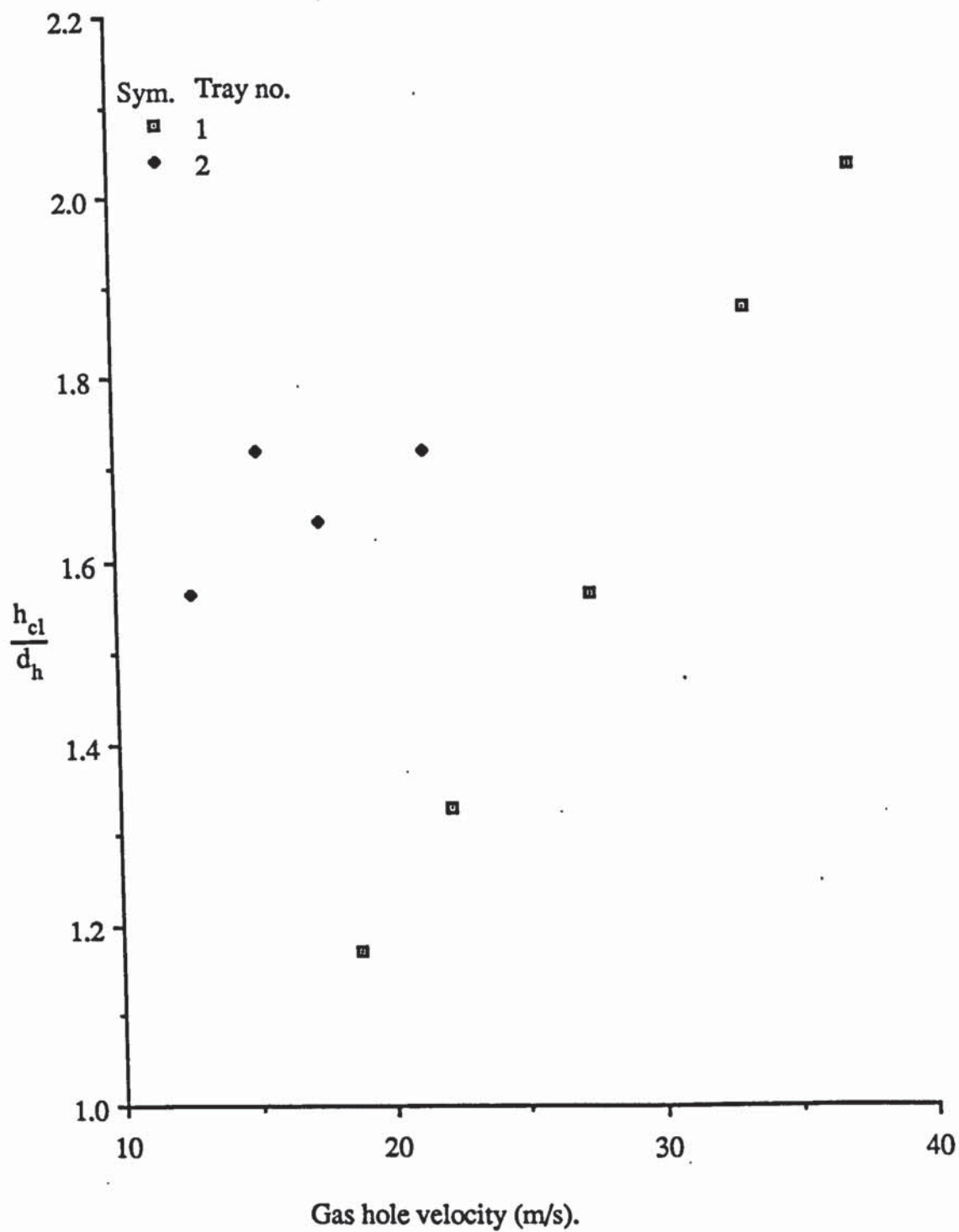


Figure 6.8.1. Transition results of Prince, Jones & Panic (102). Distillation systems.

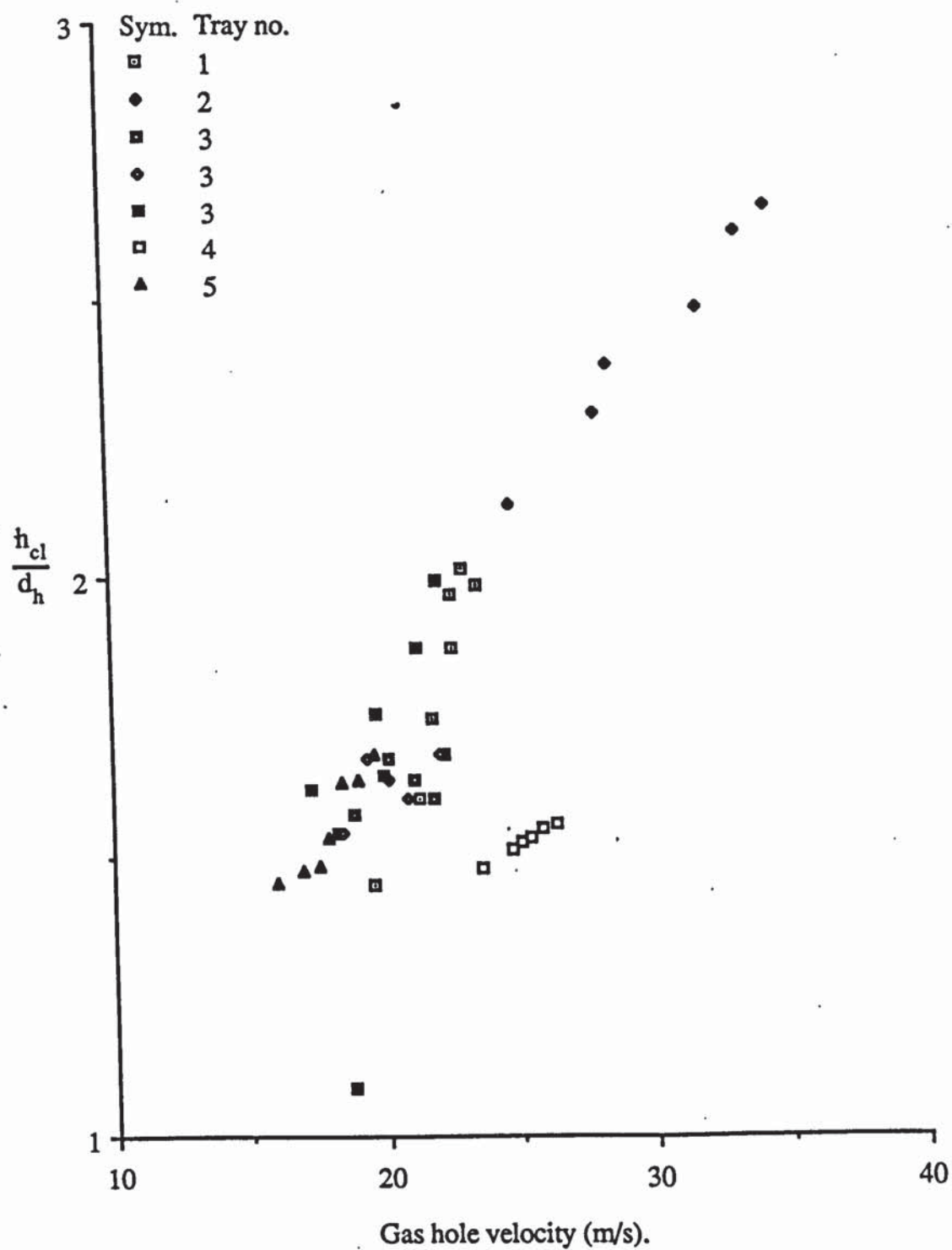


Figure 6.8.2. Transition results of Pinczewski & Fell (22). Air-Water only.

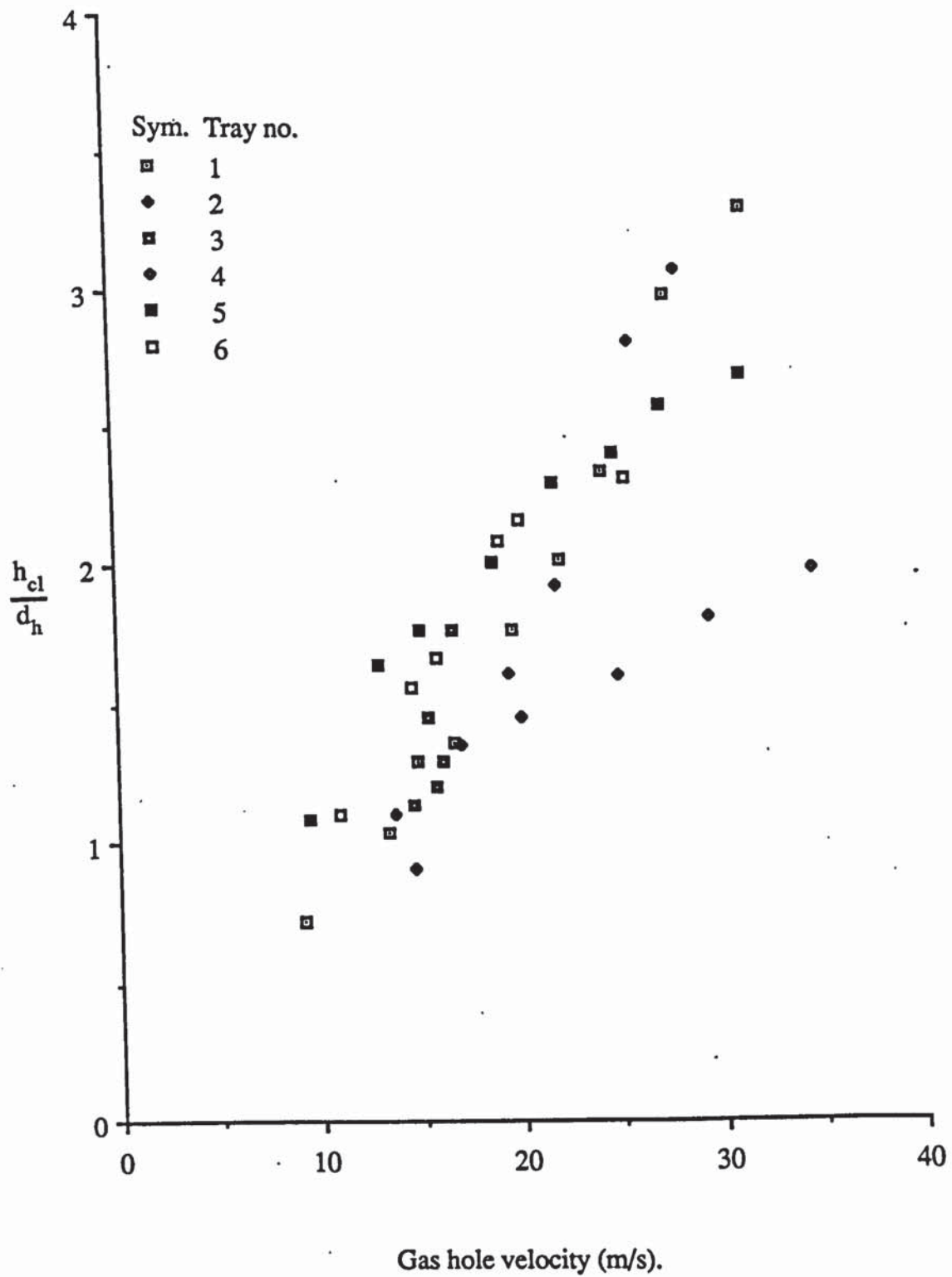


Figure 6.8.3. Transition results of Porter & Wong (17). Air-Water only.

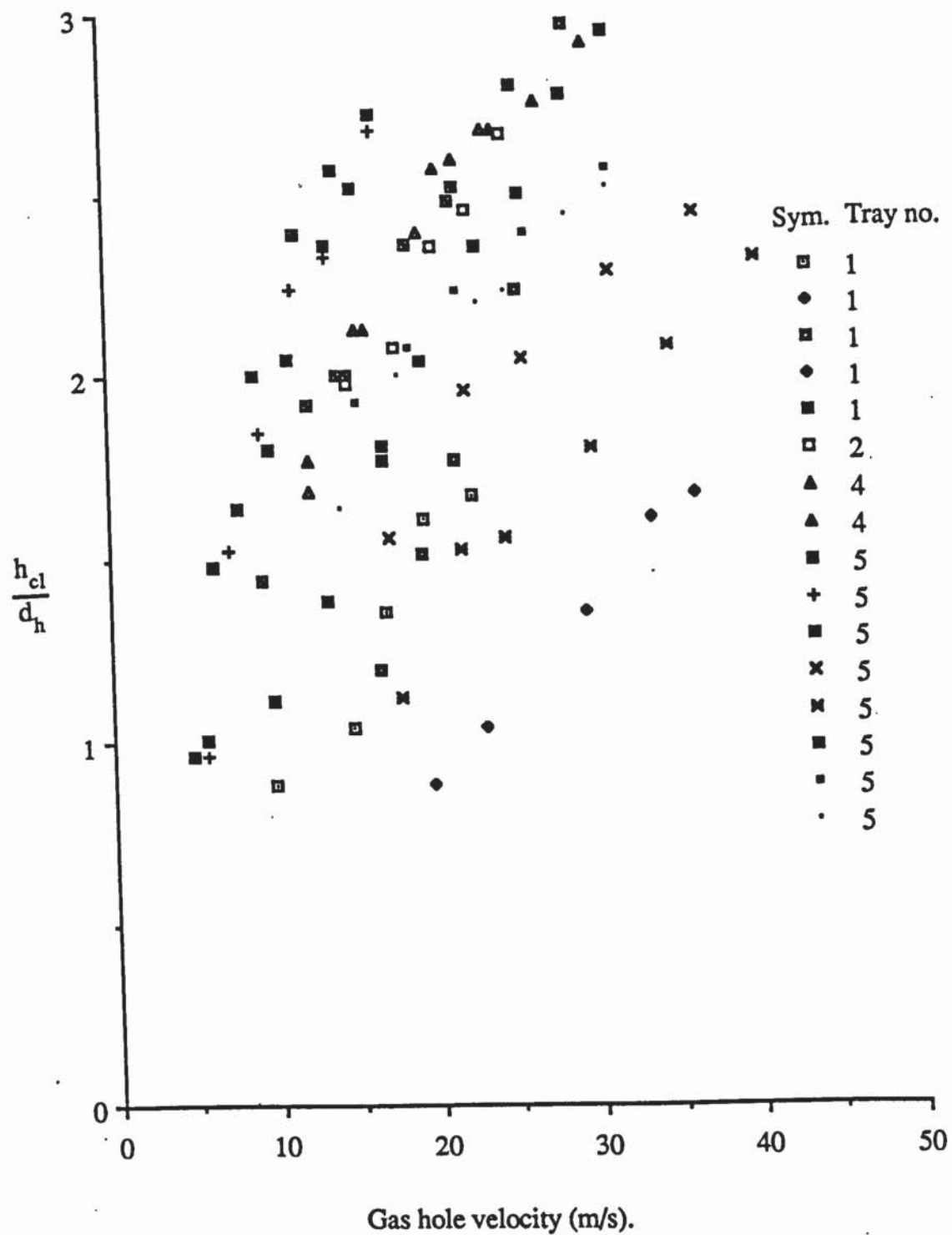


Figure 6.8.4. Transition results of Porter & Wong (17). Non air-water.

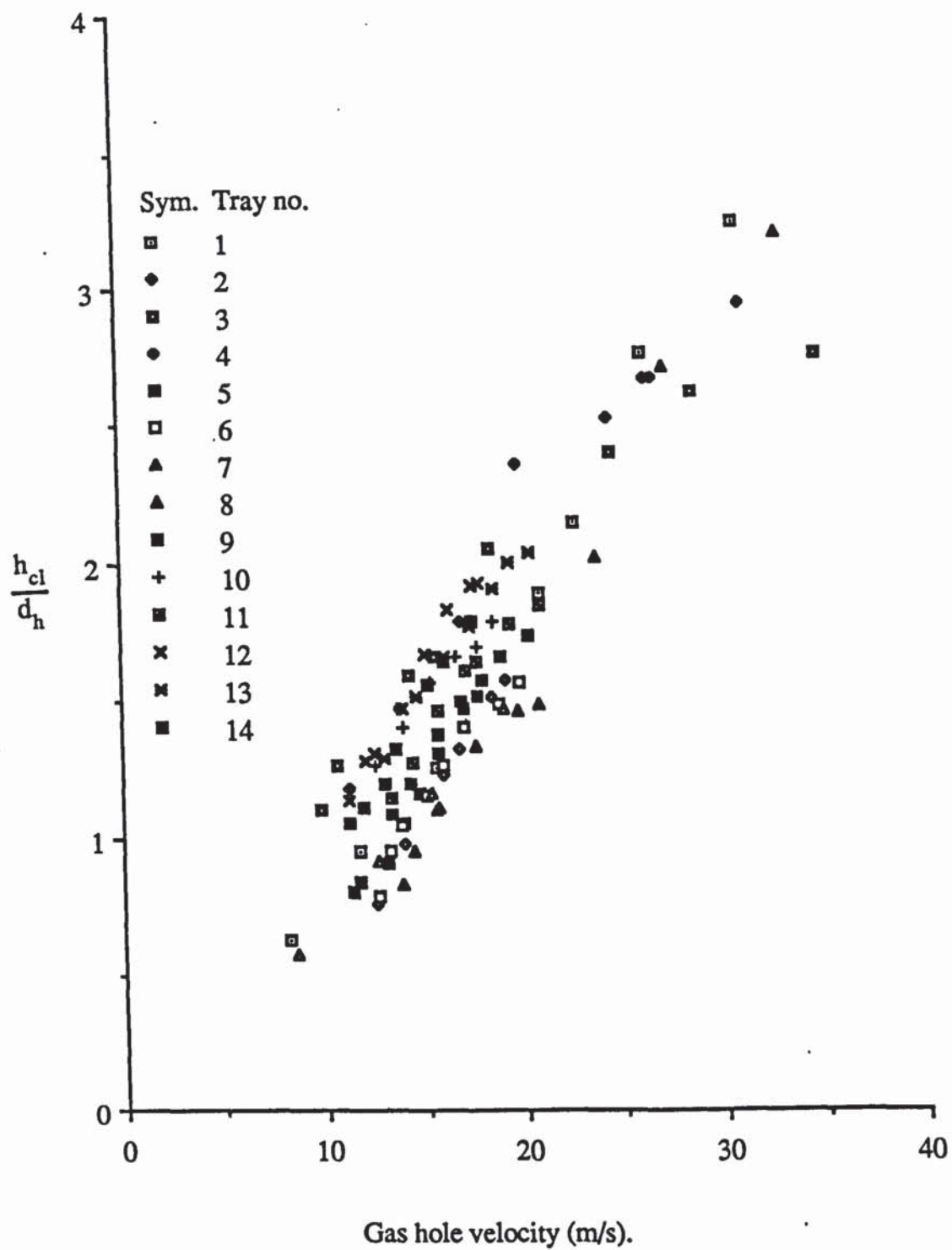


Figure 6.8.5. Transition results of this study. Air-water only.

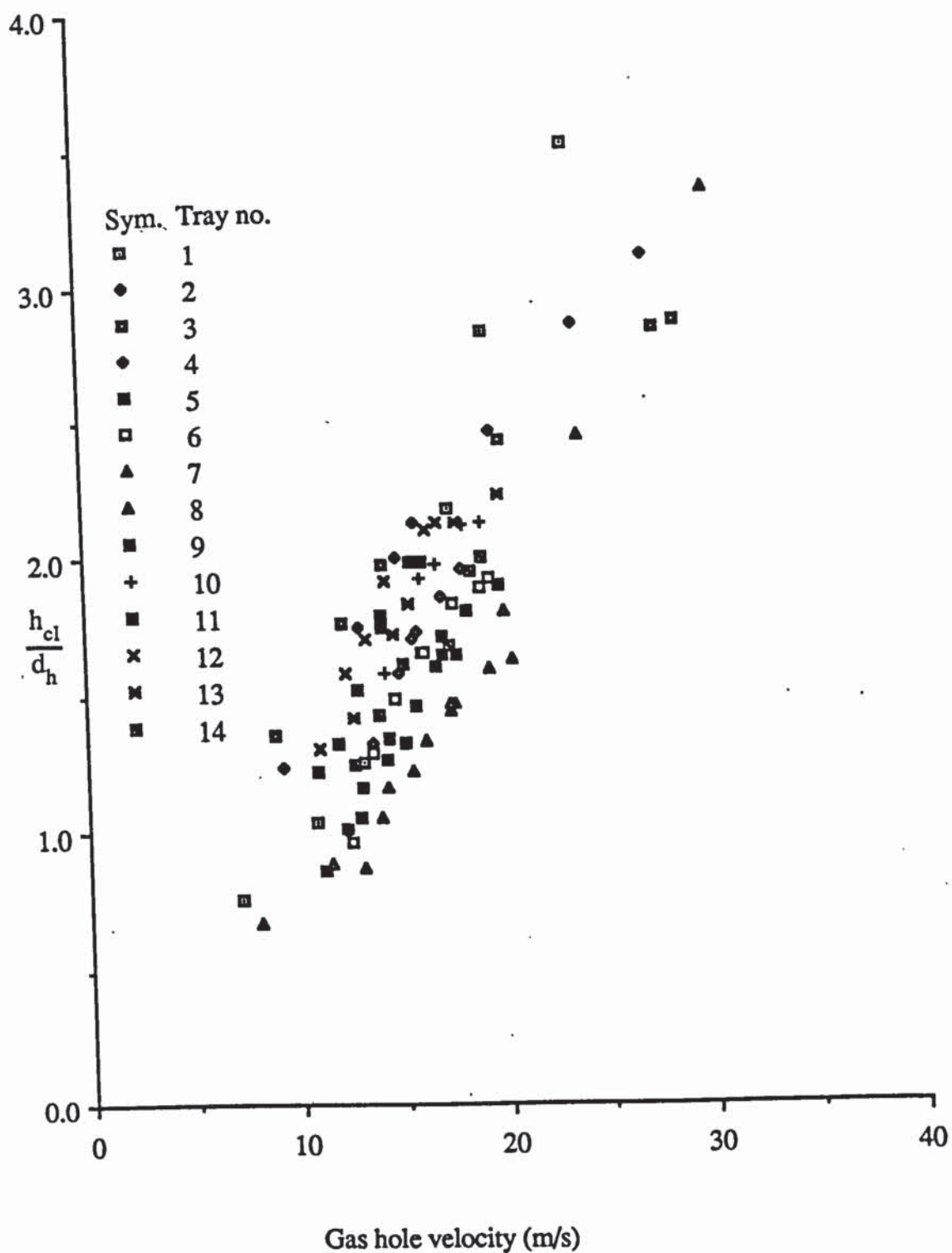


Figure 6.8.6. Transition results of this study. Air-Kerosene only.

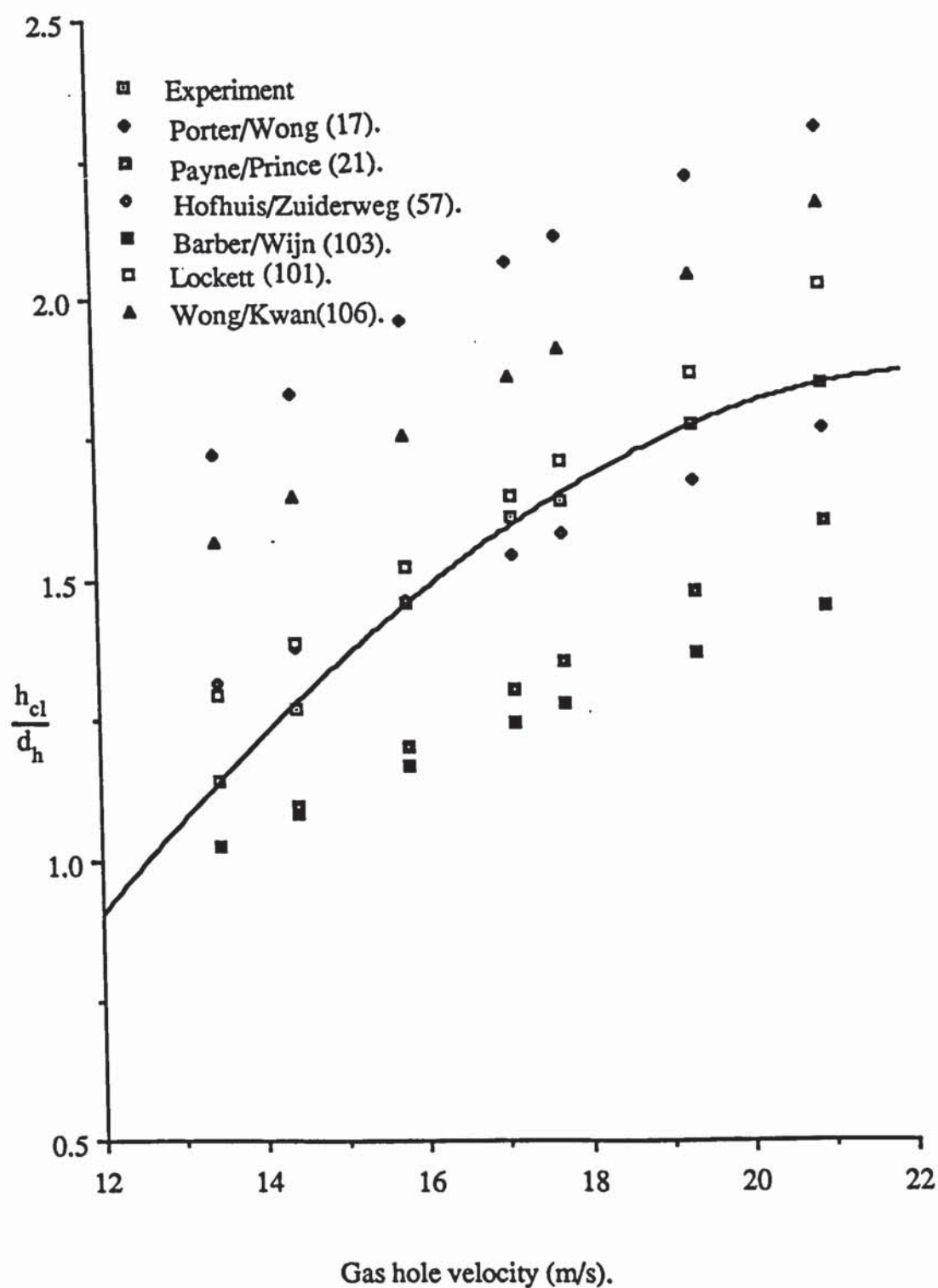


Figure 6.9. Performance of different correlations for single liquid phase. Tray no. 14.

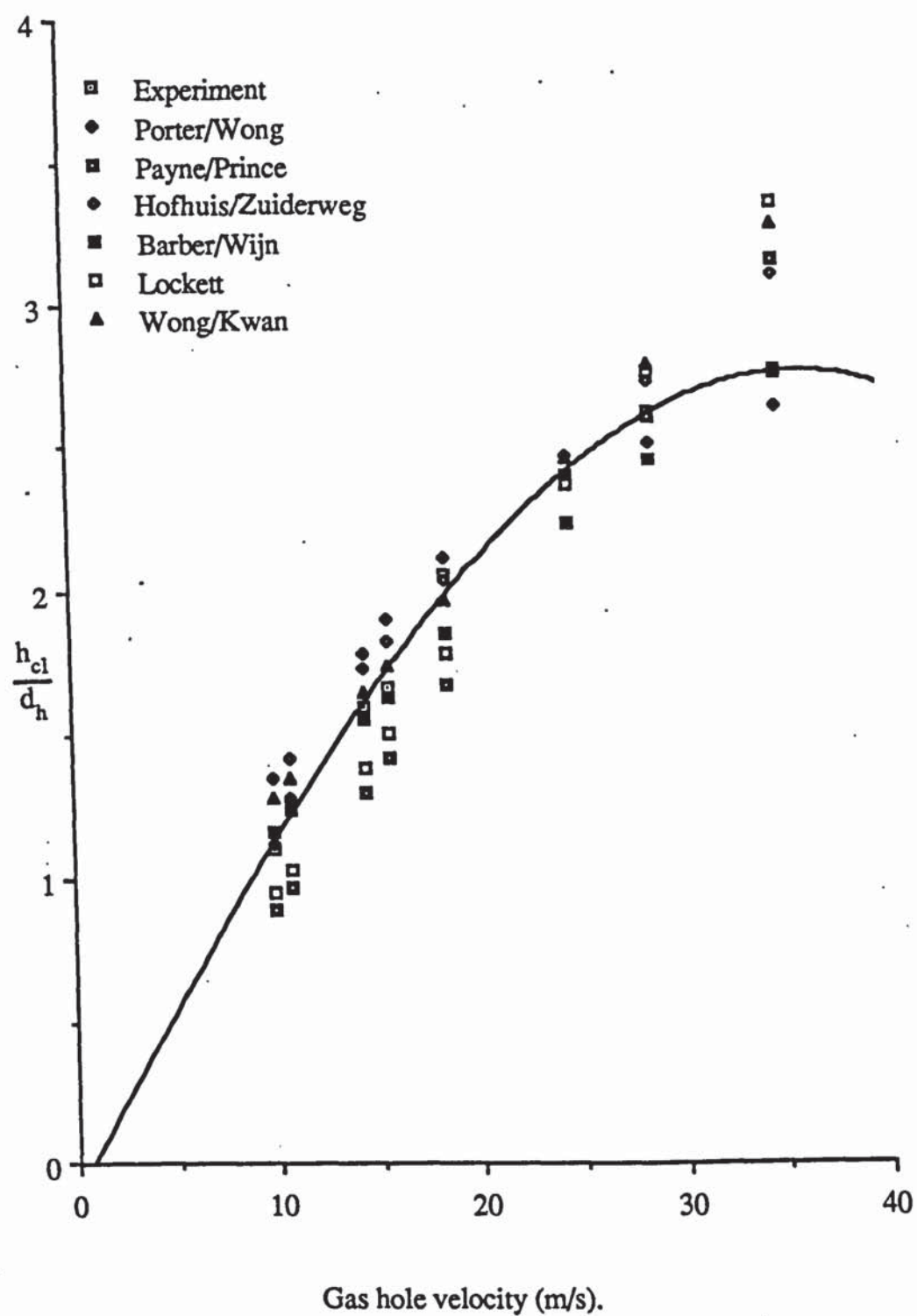


Figure 6.9.1. Performance of different correlations for single liquid phase. Tray no. 3.

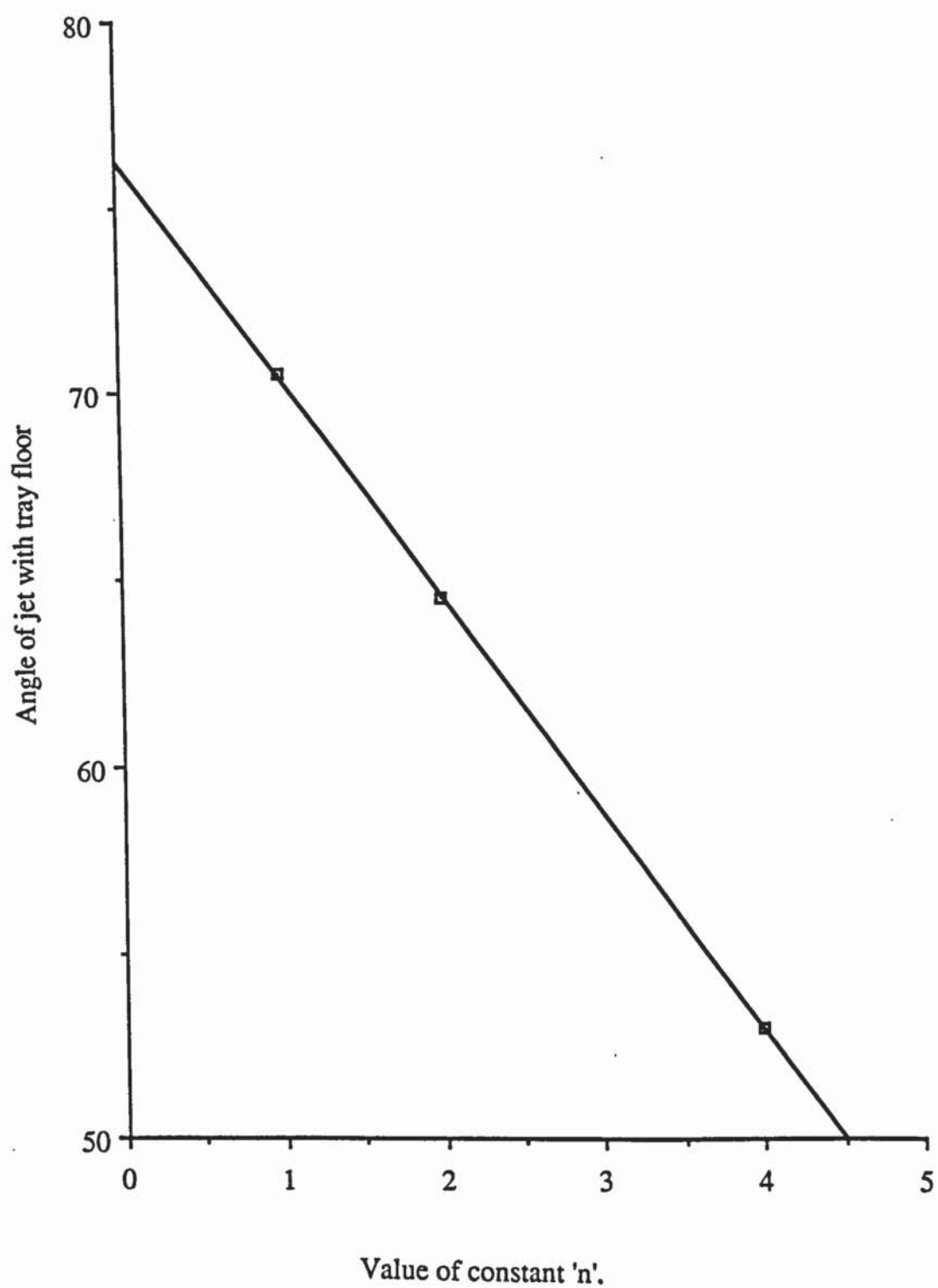


Figure 6.10. Variation of jet angle with tray floor.

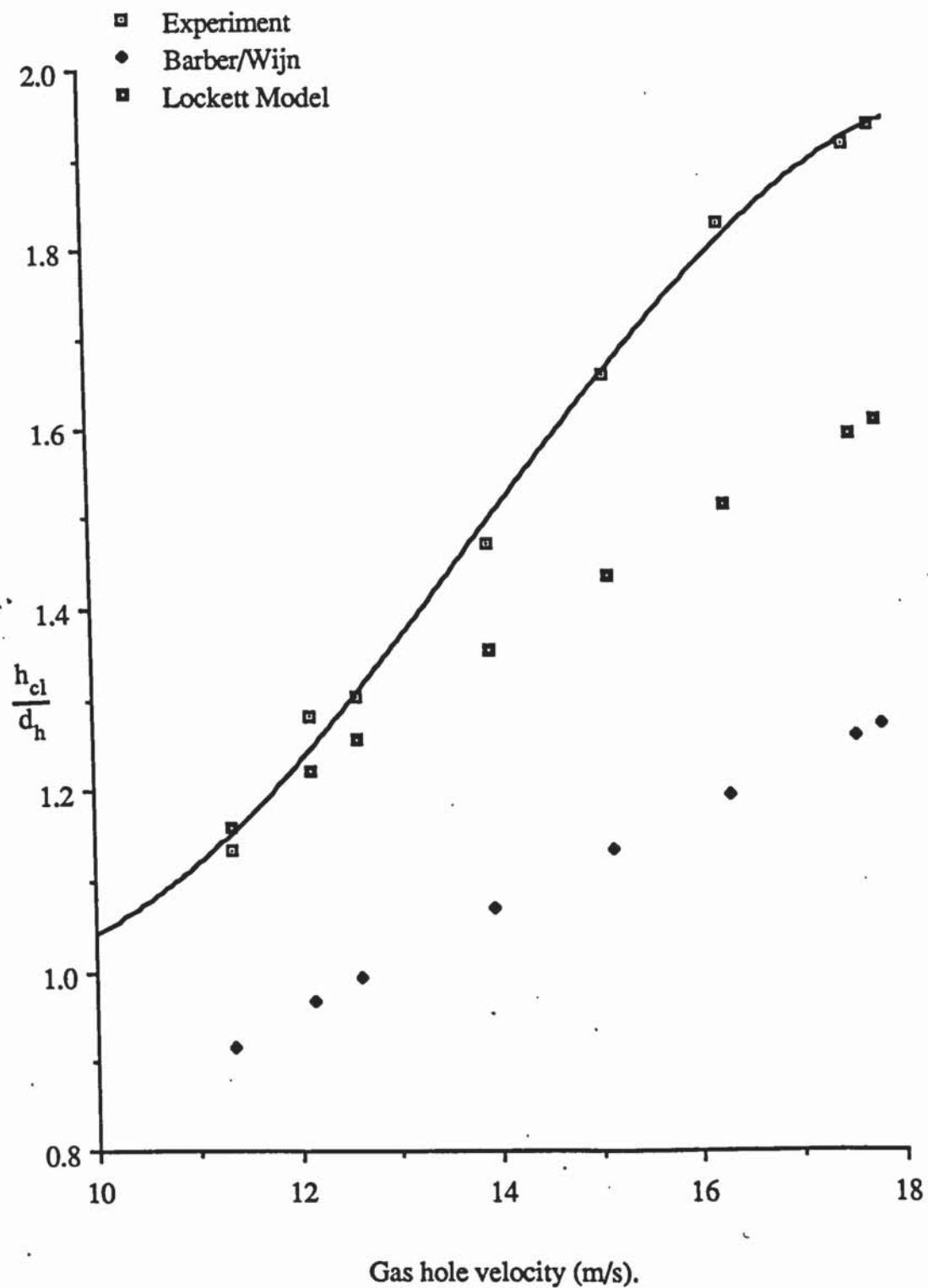


Figure 6.11. Comparison of experimental h_{cl}/d_h with Barber/Wijn correlation (103) and Lockett's model (101) when 'n'=1. Tray no. 12.

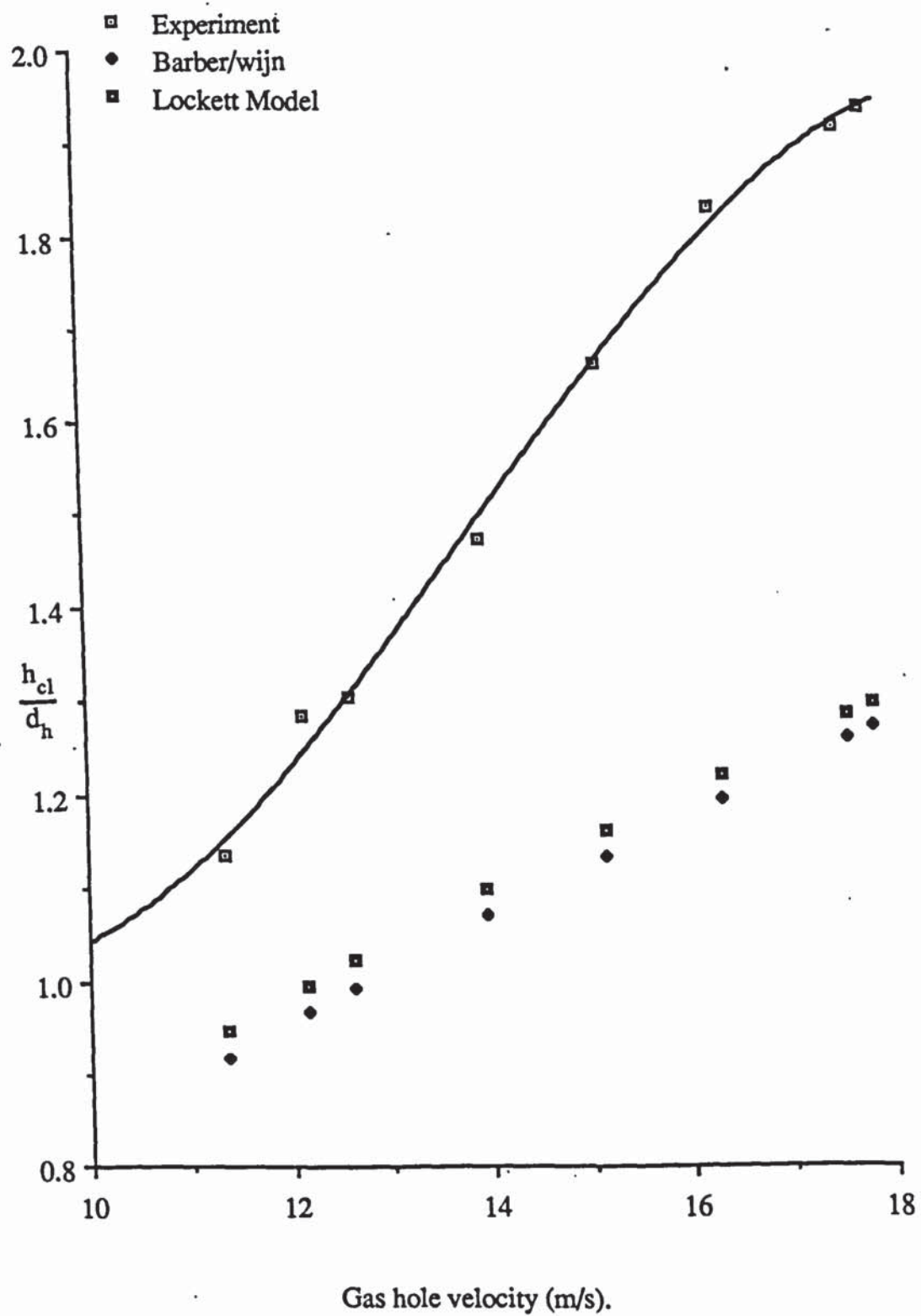


Figure 6.12. Performance of Lockett's model when 'n'=1. Tray no 12.

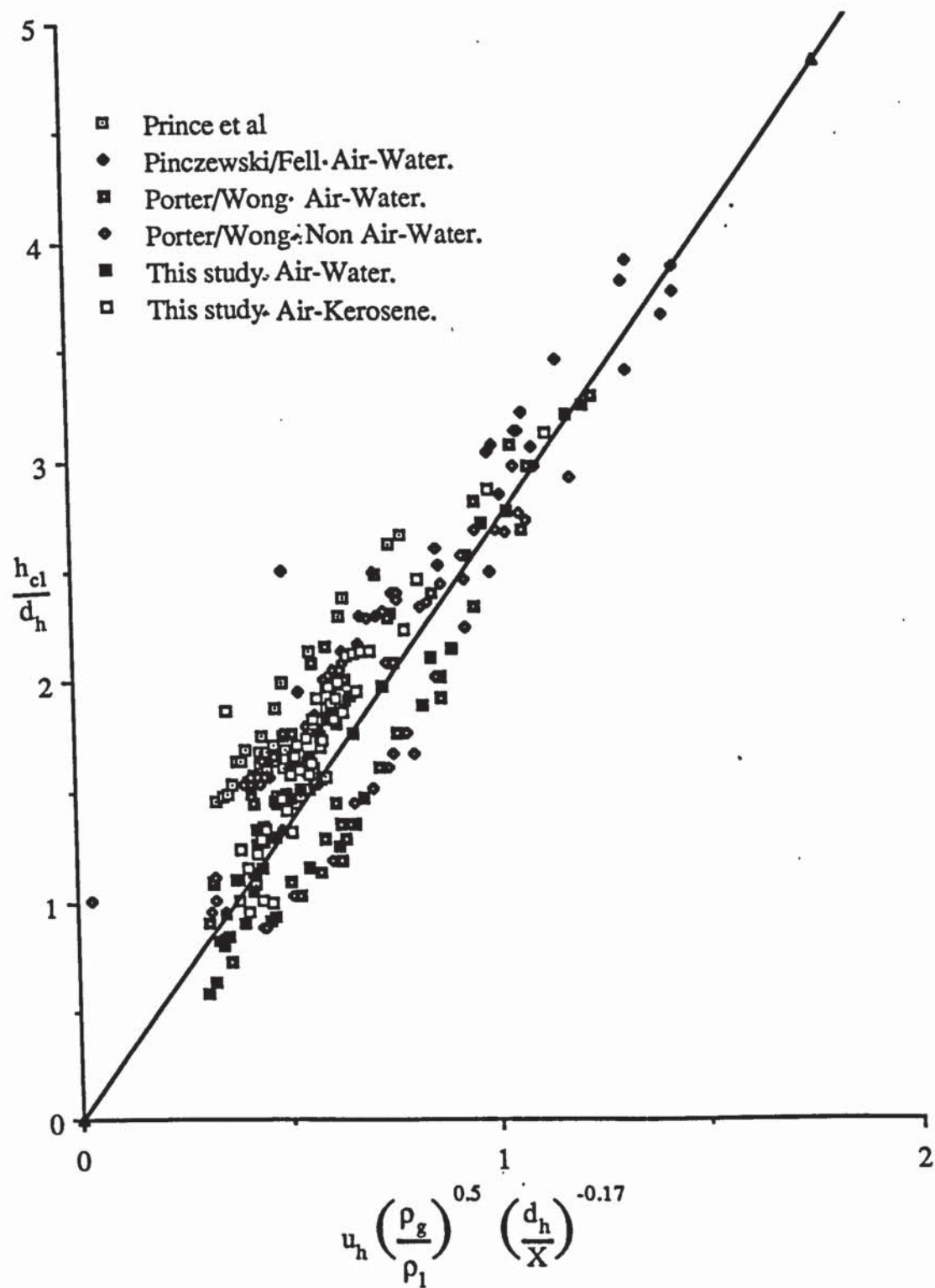


Figure 6.13. Proposed new correlation for spray to bubbly transition.

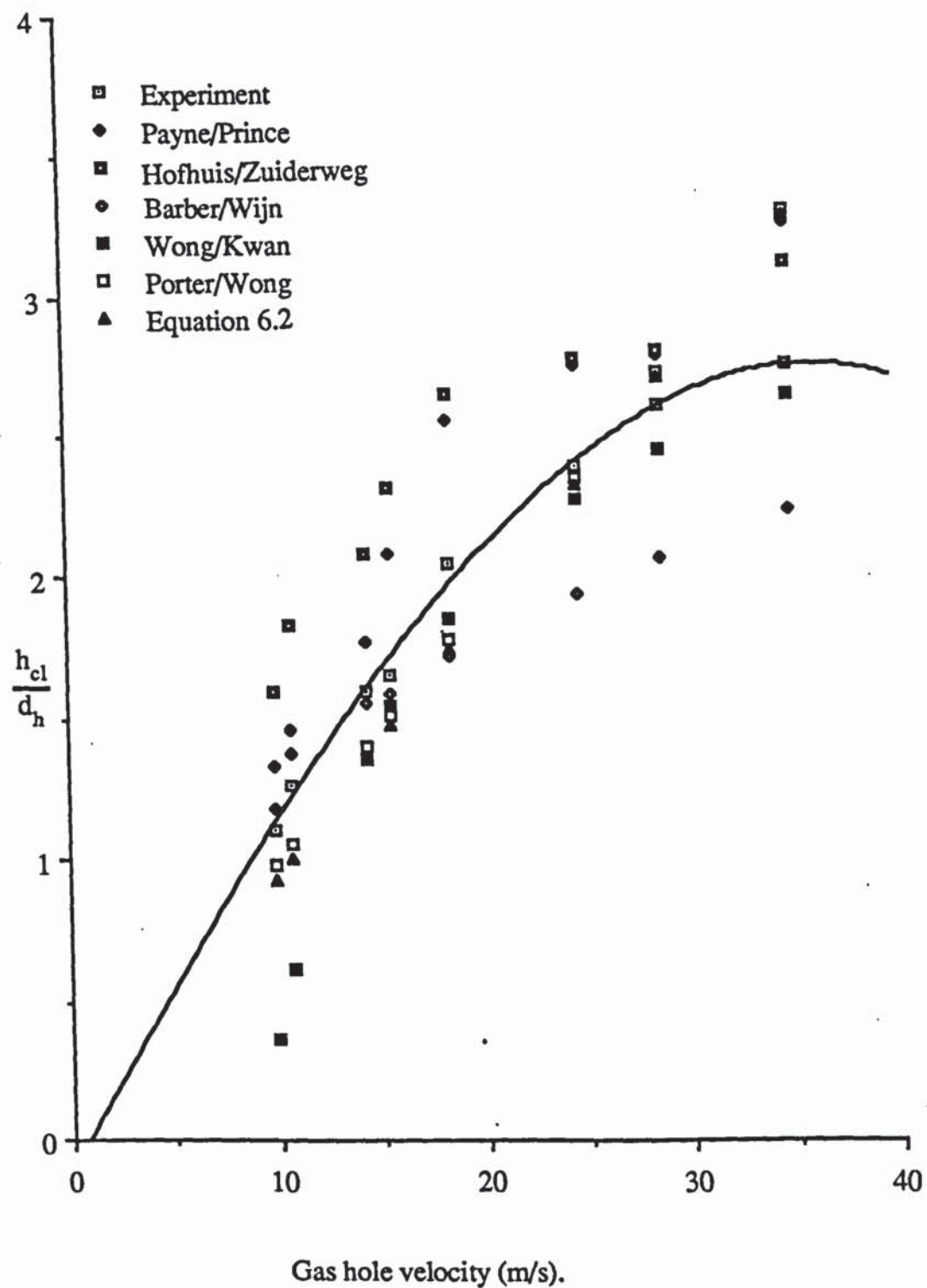


Figure 6.14. Performance of modified correlations. Tray no. 14.

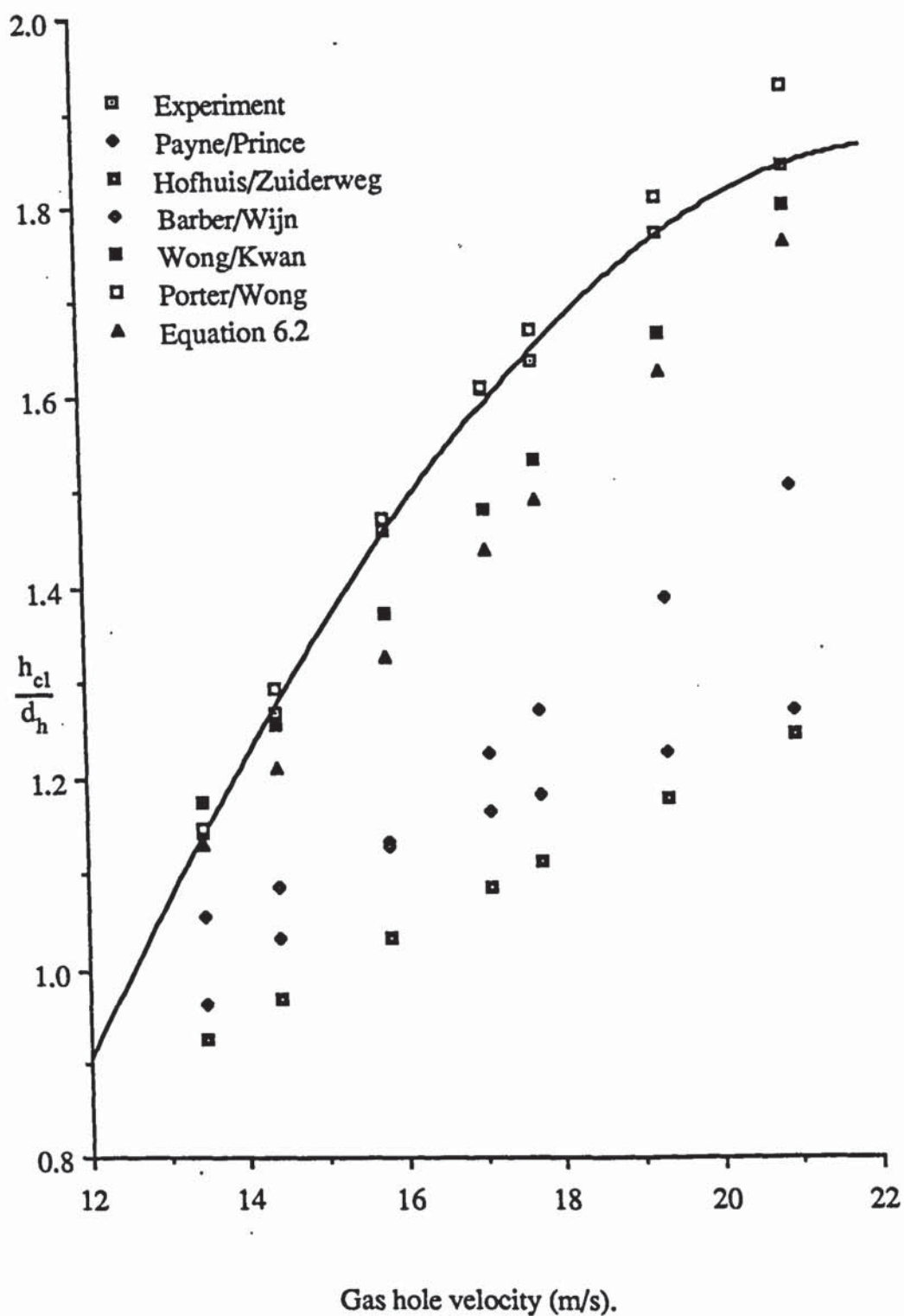


Figure 6.14.1. Performance of modified correlations. Tray no. 3.

CHAPTER 7

SPRAY TO BUBBLY TRANSITION WITH TWO IMMISCIBLE LIQUID PHASES

7.1 Introduction

Distillation of systems containing two immiscible liquid phases or partially immiscible liquid phases co-existing has been used industrially for many years and recently such separations are receiving more attention.

The study of the thermodynamics of the phase equilibria in three phase distillation has received some limited attention. However, virtually no published work is available concerning the study of plate and column hydrodynamics of such three phase systems. Shinskey (149) pointed out that the hydraulic behaviour of three phase system needs to be considered in tray design. A study of particular interest is by Bortolini, Brambilla & Nencetti (150) who performed some preliminary experiments on the fluid mechanics and mass transfer mechanism of two liquid phases on a tray. The poor understanding of the hydraulics of two liquid phases systems on distillation trays have been reported by the above authors.

Recently Ashton, Arrowsmith & Yu (151) have investigated the hydraulics of three phase systems in distillation columns. In particular, the motion of gas bubbling through the interface between two immiscible liquids was studied in a single orifice column under various conditions and six different flow regimes were identified.

The identification of the tray operating regime for a given gas and liquid loading has become an important step in any tray design procedure and the properties of the dispersion must be clearly related to the specific operating regime. It is thought that foaming associated with the presence of two liquid phases may be avoided by operating the tray in or close to the spray regime, since this regime represents a stable mode of operation at high column throughputs. Virtually no information is available concerning the behaviour of the dispersion when two liquid phases are present and therefore, there is a need to determine the dispersion behaviour on a tray in the presence of two liquid phases.

In this chapter the behaviour of a two liquid phase dispersion on a tray will be investigated and the transition between any regime will be determined and quantified.

7.2 Object of the Work

The object of this part of the research is as follows:

- i. To study the regimes and the transitions between the regimes on a tray containing two liquid phases.

- ii. To correlate the results for any regimes which are found for trays operating with two liquid phases.

7.3 Experimental Determination of the Transition

- i. General observations of a possible spray to bubbly transition using the light transmission technique.
- ii. Add a given volume of kerosene [kerosene fixed] onto the tray so that the tray was operating in the spray regime. Then add water slowly until the transition point noted.
- iii. Add a given volume of water [water fixed] onto the tray so that the tray was operating in the spray regime. Then add kerosene slowly until the transition point was achieved.

7.4 Column Modifications

In the initial experimental work, it was difficult to observe the behaviour of the liquid dispersion on the tray because of the formation of an emulsion on the inside surface of the perspex wall. Two 'port' holes were added on the opposite sides of the perspex walls so that the light beam would pass through an area of perspex which was relatively free from any liquid emulsion film.

In addition, a windscreen wiper was fitted to one of the adjacent walls to clean the wall and a small window [15.24 cm square] was inserted into the opposite wall for photographic and video recording studies.

7.5 Experimental Procedure

A similar experimental procedure was used to that outlined in section 6.3, except that one liquid was added first so that the tray was operating in the spray regime. Sufficient quantity of the second liquid was added until the transition point was reached. After the experiment was finished, the liquid was dumped into a phase separator. Kerosene was separated and returned to the liquid reservoirs and the water was then discarded.

The details of the sieve plates used in this part of the experimental program are given in table 4.1 and the experimental results obtained are listed in appendix 5.

7.6 Experimental Results

Preliminary experiments indicated that the tray dispersion behaviour did change in broadly the same way as the single liquid phase. Thus for example, it was possible to observe a bubbly regime and a spray regime and there was a definable transition between these operating regimes. Therefore, as one long term objective of this research program was to prevent the formation of foam associated with two liquid phases by operating in the spray regime, the remaining experimental work in this section was concentrated on the determination of the spray-bubbly transition.

The liquid holdup at the transition increased with increasing gas velocity [figure 7.1]. The rate of increase of liquid holdup at the transition decreased at higher gas velocities. The rate of increase was less for the kerosene fixed system than for the water fixed system.

The liquid holdup at the transition increased with increasing tray hole diameter [figures 7.2 & 7.2.1] and thus for a given gas superficial velocity small hole diameter trays favoured a bubbly dispersion whilst larger hole diameter trays favoured the spray regime. The liquid holdup increased with decreasing free areas [figures 7.3 & 7.3.1]. Hence plates with low free areas would tend to operate at or near to the spray regime. Also the liquid holdup at the transition decreased with increasing liquid density [figures 7.4 & 7.4.1]. However, it is seen that in each case the two liquid phase transition curve was lower than the corresponding pure liquid transition curves indicating that the dispersion would tend to move into the bubbly regime more quickly than the pure liquid.

The effect of plate thickness and ratio of hole diameter to tray thickness is shown in figures 7.5 & 7.5.1 for the water fixed system and the kerosene fixed system respectively. It can be seen that the liquid holdup at the transition tended to increase with increasing plate thickness and decrease with an increasing hole diameter to tray thickness ratio.

In all the transition curves [figures 7.1-7.5.1] the column is operating in the spray regime for the data below the solid line and in the bubbly regime for the data above the solid line.

In addition the following points can be noted for the two systems:

Water fixed system:

- i. As the gas superficial velocity increased, the volume fraction of the organic phase [VFK] increased and similarly the volume fraction of the aqueous phase [VFW] decreased [figure 7.6].
- ii. As the gas superficial velocity increased the ratio of the aqueous phase to the organic phase decreased [figure 7.7].
- iii. As the gas superficial velocity increased the density of the mixture decreased [figure 7.8].

- iv. As the ratio of aqueous phase to organic phase increased the density of the mixture increased [figure. 7.9].
- v. There was a linear increase in the density of the mixture with the VFW and similarly there was a linear decrease in density with the VFK [figure 7.10].
- vi. As VFK increased the ratio of aqueous phase to organic phase decreased and similarly as VFW increased ratio increased [figure 7.11].

Kerosene fixed system:

- i. As the gas superficial velocity increased the VFK decreased and similarly VFW increased [figure 7.12].
- ii. As the gas superficial velocity increased the ratio of aqueous phase to organic phase increased [figure 7.13].
- iii. As the gas superficial velocity increased the density of the mixture increased [figure 7.14].
- iv. As the ratio of aqueous phase to organic phase increased, the density of mixture increased [figure 7.15].
- v. The density increased linearly with VFW and also decreased linearly with VFK or an increase in VFW resulted in an increase in density and an increase in VFK resulted in a decrease in density [figure 7.16].
- vi. As VFW increased the ratio of water phase to organic phase increased and similarly as VFK decreased, the ratio decreased [figure 7.17].

In all cases [figures 7.1-7.5.1], it is seen that the spray to bubbly transition curves obtained for the kerosene fixed system were always lower than the water fixed transition curves. Therefore, for the kerosene fixed system the tray dispersion behaviour moved into the bubbly regime much more quickly than when the same tray is operating in the spray regime for the water fixed system at the same gas velocity. Consequently, the liquid holdup at the spray to bubbly transition for a system containing two liquid phases may be dependent upon the manner in which the two liquid phases are created. Thus in order to understand the differences between the water fixed and kerosene fixed systems behaviour at the spray to bubbly transition, a further series of experiments was carried out in the small column previously described in section 5.4.

7.7 Small Column Experiments

Ashton, Arrowsmith & Yu (151) found that the operating regimes on an orifice plate depended on the liquid depth of each phase [ratio of heavy phase to light phase] and the gas hole velocity. It was decided to repeat these experiments in order to relate the

observations to the results obtained in the perspex simulator.

The experiments were carried out in a small glass column [section 5.4] using either a sintered plate or an orifice plate with 1, 2 and 3 mm diameter holes.

7.8 Experimental Details.

7.8.1 Sintered Plate

An air flow rate of 12 litres/min was passed through a sintered plate on which 5 cm³ of water were added from a calibrated liquid reservoir. 15 cm³ of kerosene were then added and observations made on the behaviour of the dispersion of the two liquids on the plate. The procedure was repeated for the kerosene fixed system using 5 cm³ of kerosene and 15 cm³ of water.

7.8.2 Orifice Plates

An air flow rate of about 1 litre/min was passed through the orifice plate on which a given volume of water and kerosene was added. Observations were made of the behaviour of the bubbles with different water and kerosene depths. The liquid depth was changed by the addition of water or kerosene. The liquid depths were also varied with gas velocity and all the experiments were repeated for 2 mm and 3 mm diameter orifice plates.

7.9 Observations

7.9.1 Sintered plate

Water fixed.

At high gas flow rates the plate operated in the froth regime. As kerosene was added a cellular foam developed on top of the froth. The water that was entrained could be seen to fall back in the form of droplets between the cellular foam matrix. The total height of the dispersion was greater than that of the kerosene fixed system.

Kerosene fixed.

As kerosene was added slowly, a cellular foam was formed immediately. The height of the foam was much greater than the foam height produced by the same volume of water. When water was added onto the plate, the water fell onto the tray floor and formed a froth. Any water that was entrained subsequently fell back in the form of droplets through the foam matrix onto the tray floor.

7.9.2 Orifice Plate

At low gas hole velocities [below 0.01m/s] it was observed that as the air bubble rose through the water layer, some water was entrained with it. As the bubble with a water film surface rose into the kerosene, some water detached from the bubble and fell back onto the liquid-liquid interface. The water drop stayed at the interface there until it collapsed into the aqueous phase. The bubble rose upto the liquid air interface and remained until some more bubbles arrived and accumulated at the interface with subsequent rupture of the bubbles.

The following stages were observed for a drop arriving and coalescing at a plane liquid interface:

- i. The approach of the drop to the interface and subsequent deformation of the drop and interface profile.
- ii. The damping oscillations caused by the impact of the drop at the interface.
- iii. The formation and drainage of a continuous film between the drop and its bulk interface.
- iv. Rupture of the film.
- v. The drop contents are deposited onto the interface.

When the water layer is small [less than 0.5 cm] all the water is consumed by entrainment, a kerosene film surrounds the bubbles and kerosene is in contact with the tray floor. Once all the water has been consumed, the bubbles are formed in the kerosene phase at the orifice. Once the bubble collapses at the surface the water droplets fall back onto the tray floor where they are removed very quickly by entrainment after the clean water surface has been formed.

When the depth of kerosene is very small, the bubble reaches the top of the liquid surface without entrainment. When the bubble frequency is large, the bubbles form a continuous channel and there is no entrainment into the kerosene layer. If the volume ratio of kerosene to water is greater than 1.0, with an increase in gas flow rate kerosene is broken into droplets and forms a well mixed dispersion of kerosene in water. A drop-drop coalescence mechanism could then exist and possible steps are:

- i. A binary collision of the drops.
- ii. Drainage of the continuous phase film between the drops at a critical thickness.
- iii. Rupture of the film continuous phase film.
- iv. Consolidation of new drops.

Drop size increases with increasing concentration of the dispersed phase, probably as a result of more frequent drop collision. Thus, drop-drop coalescence studies necessitate

consideration of collision theory and coalescence processes. These are beyond the scope of this thesis. However, with these simple experiments it appears that when the dynamic balance between droplet breakup and coalescence in the perspex simulator and orifice plate column, is disturbed by an increase in coalescence, phase inversion may occur. In addition, it appears that at high dispersion concentrations the process of drop coalescence and breakup results in the entrainment of the continuous phase by the dispersed phase.

Close to the inversion point, drops of the continuous phase were observed contained within drops of the dispersed phase. It appears that the continuous process of drop coalescence and breakup results in the entrainment of the continuous phase by the dispersed phase.

7.10 Discussion

The type of dispersion formed on a sieve plate where two immiscible liquids are present, depended on the volume fraction of the two liquids and their physical properties. Because of the presence of immiscible liquids, coalescence phenomena will be an important mechanism in the behaviour of the dispersion on a sieve plate. A fundamental understanding of this process will be useful since, through its effect on drop size stability and distribution, drop-drop coalescence will exert an influence upon the behaviour of the dispersion and therefore the operating characteristics of a column. Furthermore, drop coalescence followed by breakup affects the mass transfer characteristics of the separation process.

There are two distinct modes of coalescence; drop-interface coalescence and drop-drop coalescence. In both cases the basic mechanism involved is the approach of a drop to an interface, trapping a film of continuous phase between the drop and the interface. This film drains away and ruptures at some critical thickness; subsequently, fusion of the drop with the home phase occurs. Hence, it was concluded that any direct collision will change the hydrodynamics of the coalescing drop. Also, the surface force ($\sigma_i/d_{\text{bubble}}$) arising from the interfacial tension (σ_i) which resists drop formation is smaller for a continuous water phase. This will affect tray behaviour in both the perspex simulator and the orifice plate column.

The approach of the spray/bubbly transition in the perspex simulator from two different directions [i.e. water fixed and kerosene fixed] and the different behaviour of the two cases may give some insight into the foaming behaviour of systems containing two liquid phases. For the kerosene fixed system; the low density, low surface tension organic layer on the tray will affect the surface behaviour of the bubbles as water is introduced onto the tray; which causes the surface of the air bubbles to be reinforced by a water film forming

around the air bubble. Small pockets of water may be created; as water is entrained from the tray floor by the rising gas bubbles, subsequently this falls through the liquid dispersion as the bubbles collapse at or near the surface. Such pockets of water will be associated with a larger surface tension and hence, the pockets will contract forcing the bubbles apart and creating a bubbly dispersion. Therefore, distillation columns where two liquid phases are present, are often derated due to the suspected presence of foaming.

7.11 New proposed correlations for Spray to Bubbly transition for two liquid phases.

Although several correlations and models exist in the literature to predict the transition from spray to bubbly regime for a single liquid phase, none of these can be applied satisfactorily to a two liquid phase system. Also the transition from spray to bubbly regime for a system containing two liquid phases depends on the manner in which the two liquid phases were created and based on this work, different correlations are required for the water fixed and the kerosene fixed systems. It has been found experimentally that the following parameters have an effect on the transition from spray to bubbly regime:

- i Gas density.
- ii. Liquid density
- iii. Free area of plate.
- iv. Gas hole velocity.
- v. hole diameter.
- vi. Ratio of hole diameter to tray thickness.

The following correlations are proposed for the two systems using the experimental data obtained in this study:

Water fixed system:

$$\frac{h_{cl}}{d_h} = 2.64 u_h \left(\frac{\rho_g}{\rho_l} \right)^{0.5} \left(\frac{d_h}{X} \right)^{-0.17}$$

Kerosene fixed system:

$$\frac{h_{cl}}{d_h} = 1.86 u_h \left(\frac{\rho_g}{\rho_l} \right)^{0.5} \left(\frac{d_h}{X} \right)^{-0.17}$$

It can be seen from figures 7.18 & 7.18.1 that both of these correlations, although empirical correlate the experimental data well. The computer programme used to evaluate the coefficients is listed in appendix 9.

7.12 Conclusions

The following conclusions may be drawn from the experimental work:

- i. Systems containing two liquid phases, as represented by the water-kerosene-air system, do exhibit both bubbly and spray regimes. Therefore there is considerable interest in further examining the transition between these regimes.
- ii. The mechanism of the dispersion formed on an orifice plate has been studied. It was found that the type of dispersion depends on the volume fraction of the two liquids and the gas velocity.
- iii. The transition was approached from two different directions. The tray was loaded with a fixed amount of water and kerosene was added until the spray-bubbly transition was reached or vice versa. The behaviour of the system in the water fixed experiment was different from those in the kerosene fixed system. The kerosene fixed system would form a bubbly regime at lower liquid holdups.
- iv. The liquid holdup at the transition for both kerosene fixed and water fixed was found to be a function of gas hole velocity, hole diameter, ratio of hole diameter to tray thickness, free area of the tray and the volume fraction of water and kerosene on the tray.
- v. Based on the results obtained in this study, correlations have been proposed for the kerosene fixed system and water fixed system to predict the transition from spray regime to bubbly regime.

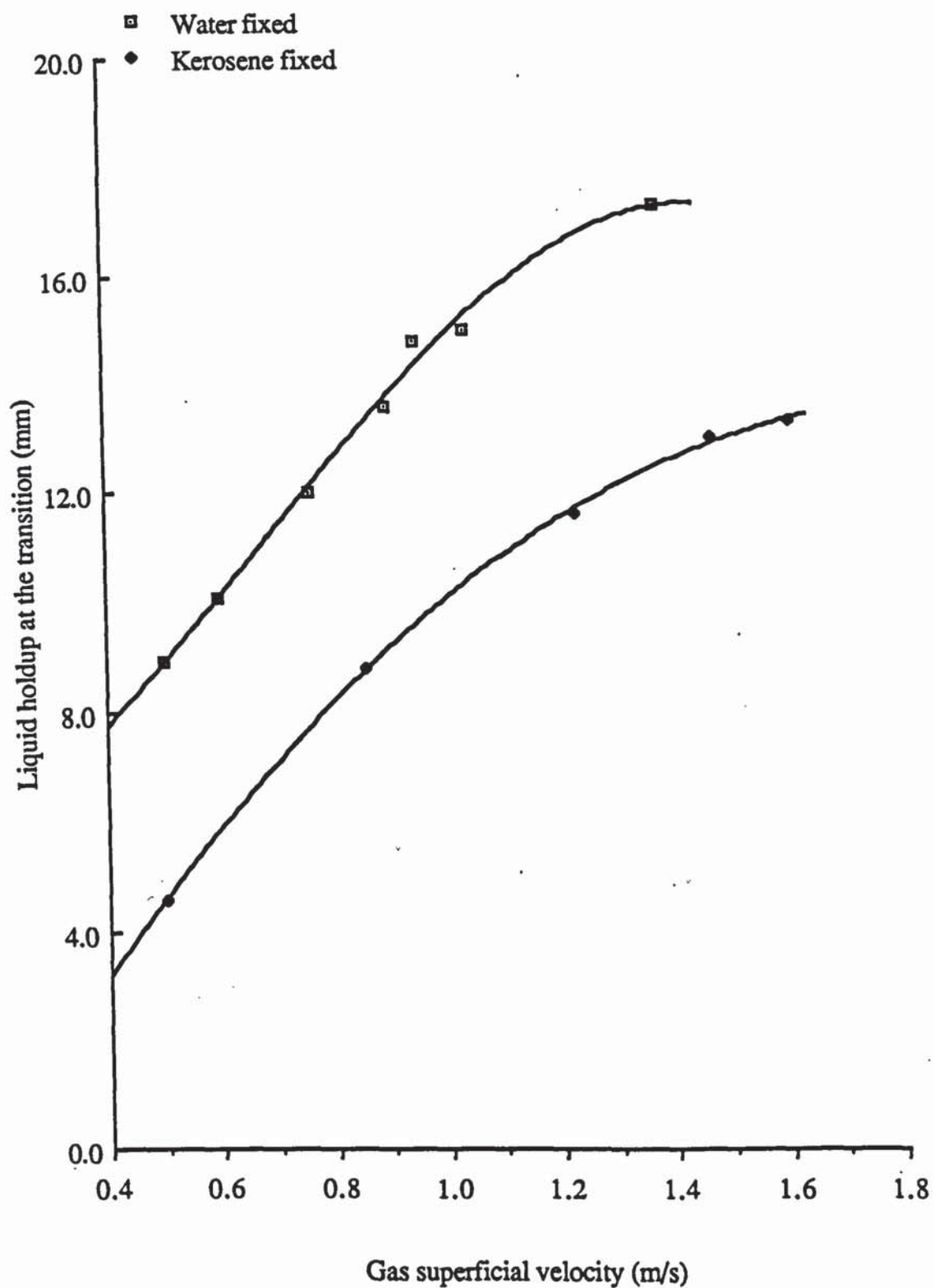


Figure 7.1. Effect of gas superficial velocity on transition. Air-Water-Kerosene. Tray no. 3.

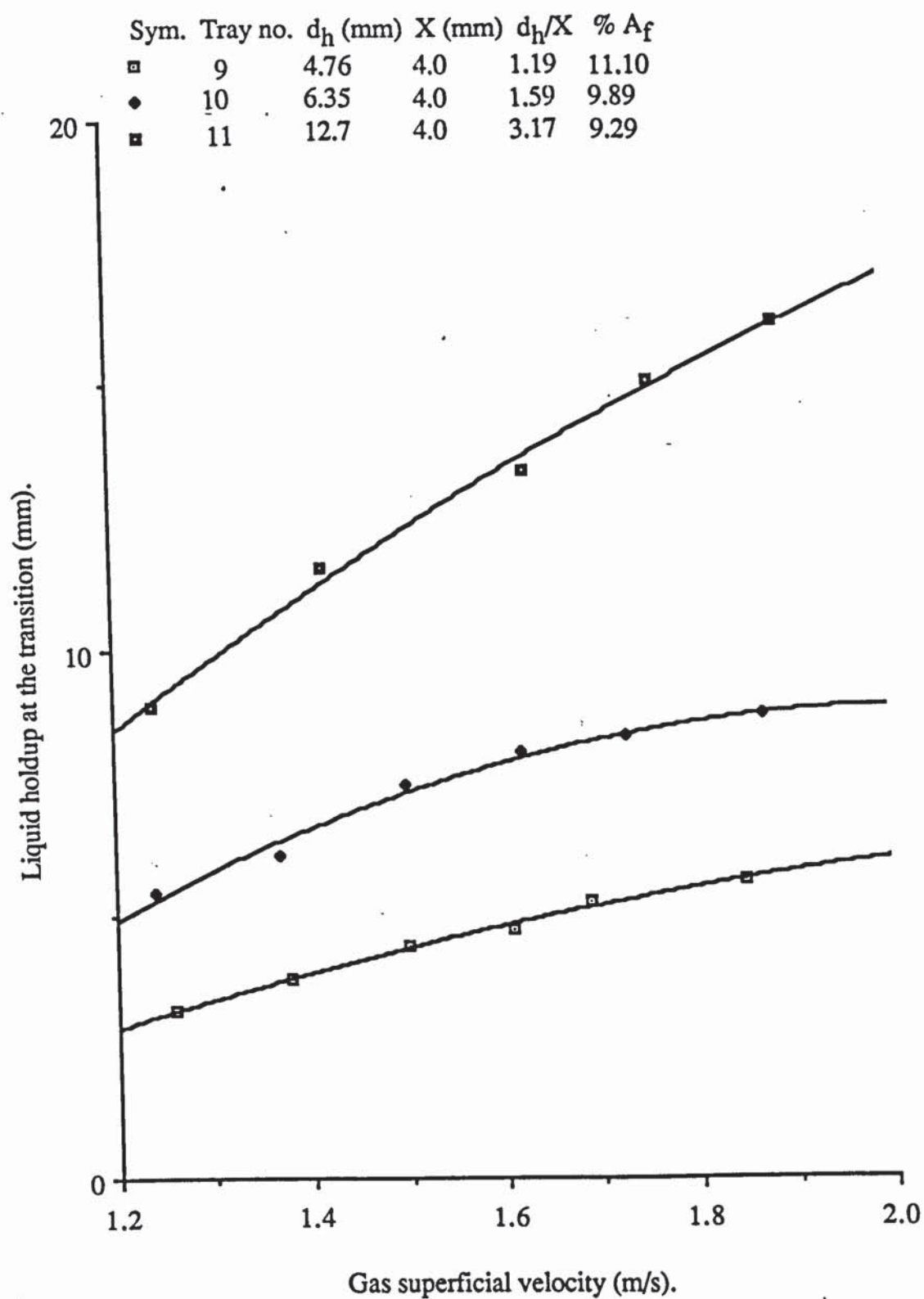


Figure 7.2. Effect of hole diameter on transition. Water fixed system.

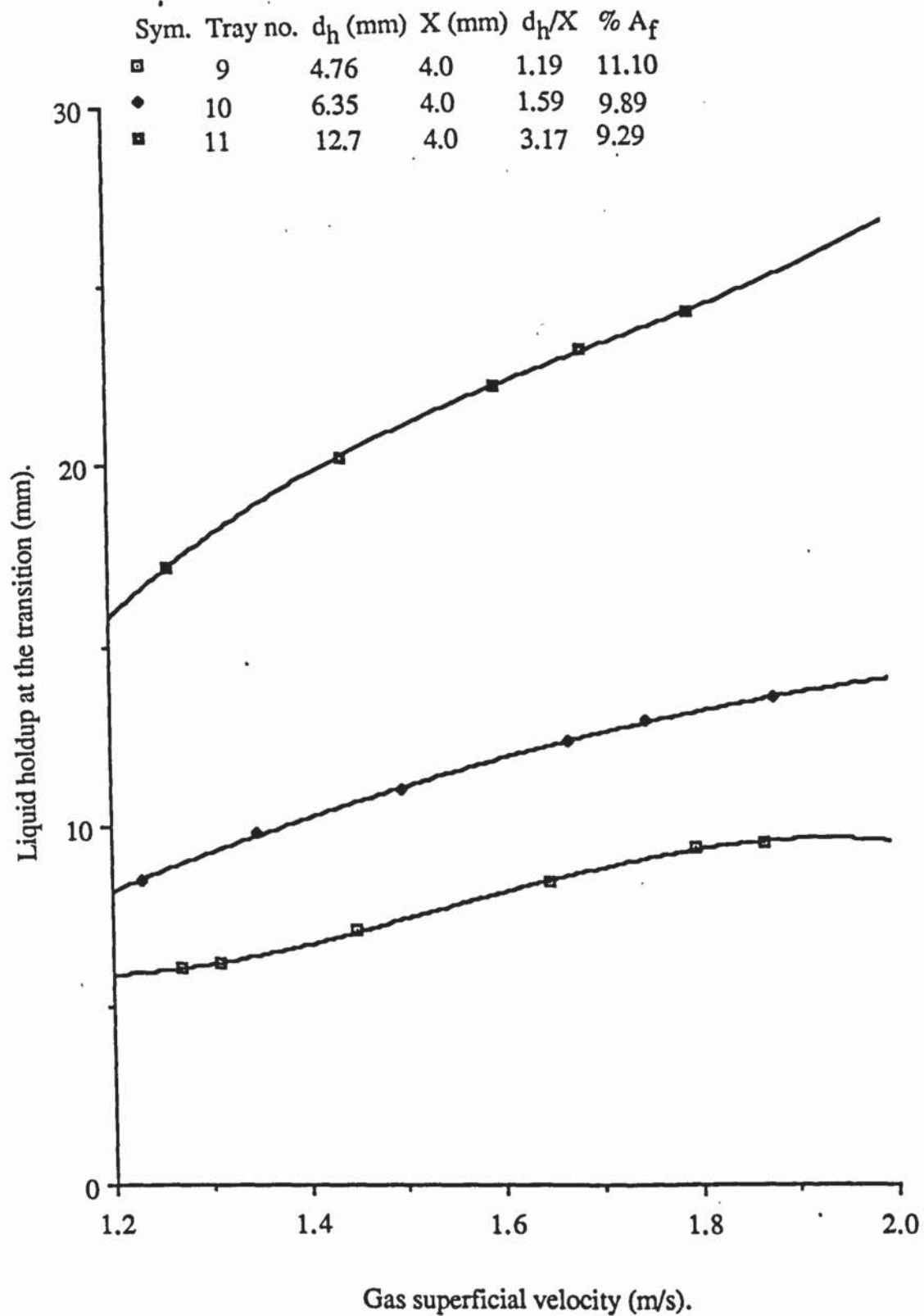


Figure 7.2.1. Effect of hole diameter on transition. Kerosene fixed.

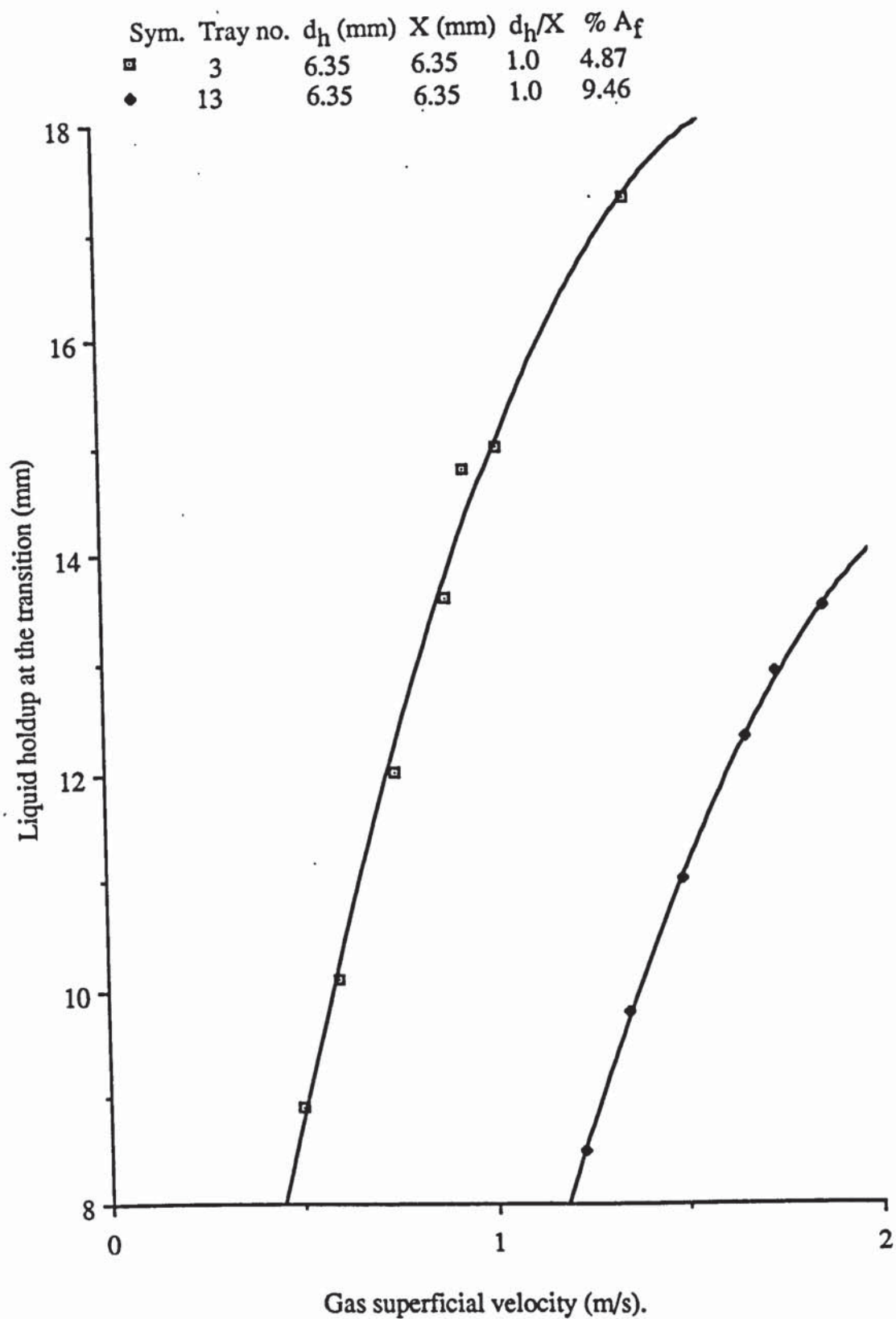


Figure 7.3. Effect of free area on transition. Water fixed.

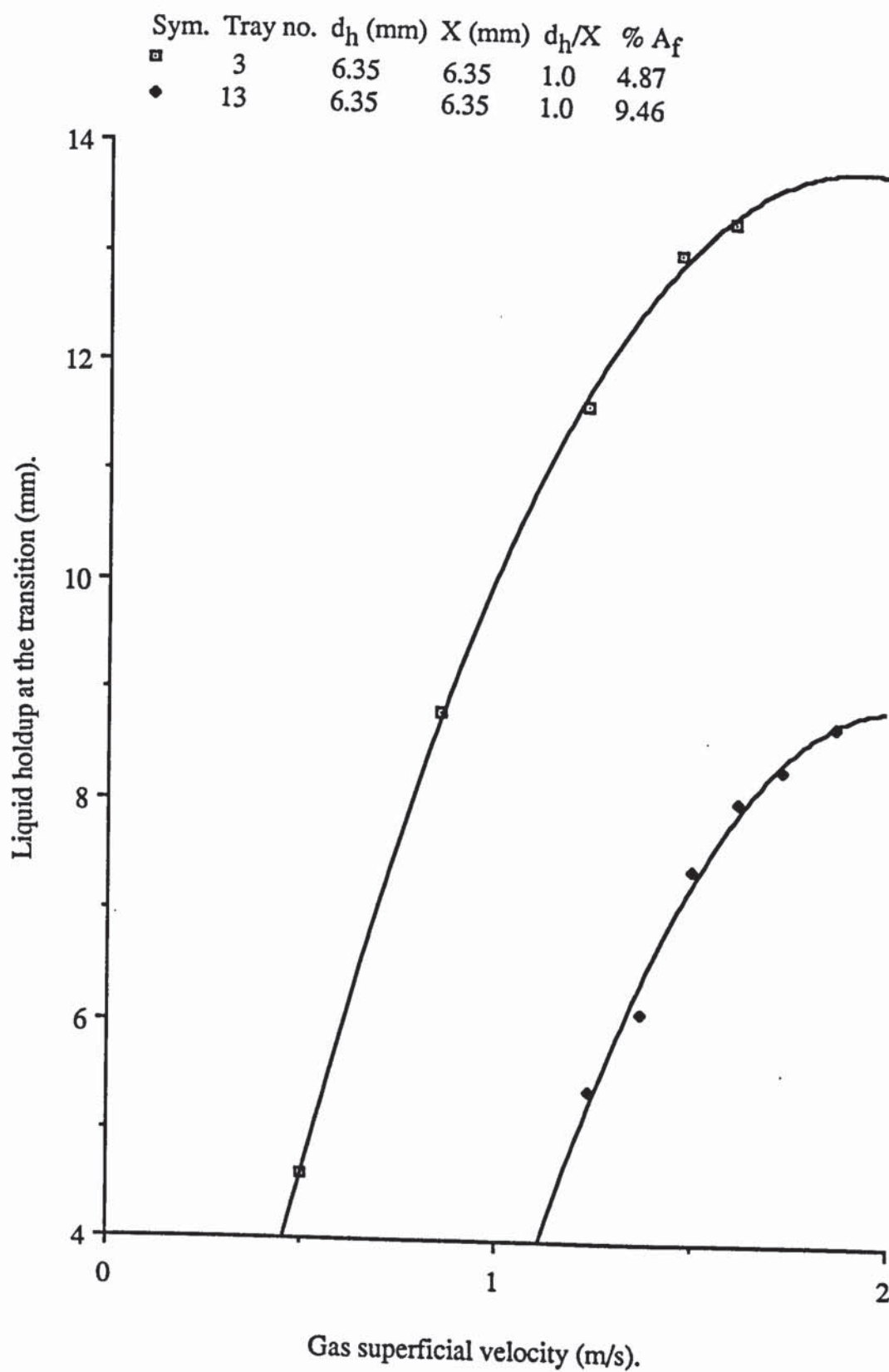


Figure 7.3.1. Effect of free area on transition. Kerosene fixed.

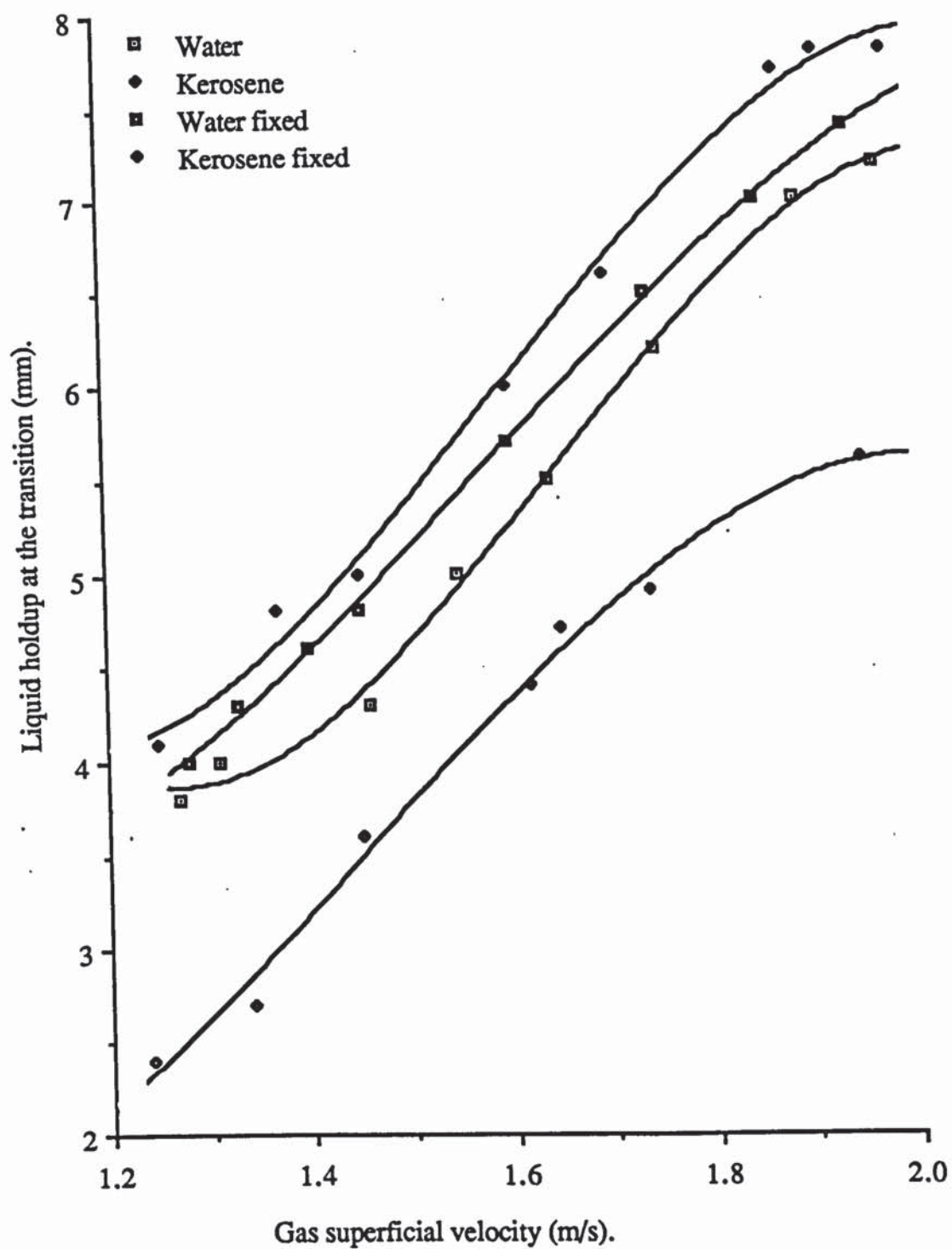


Figure 7.4. Effect of liquid density on transition. Tray no. 5.

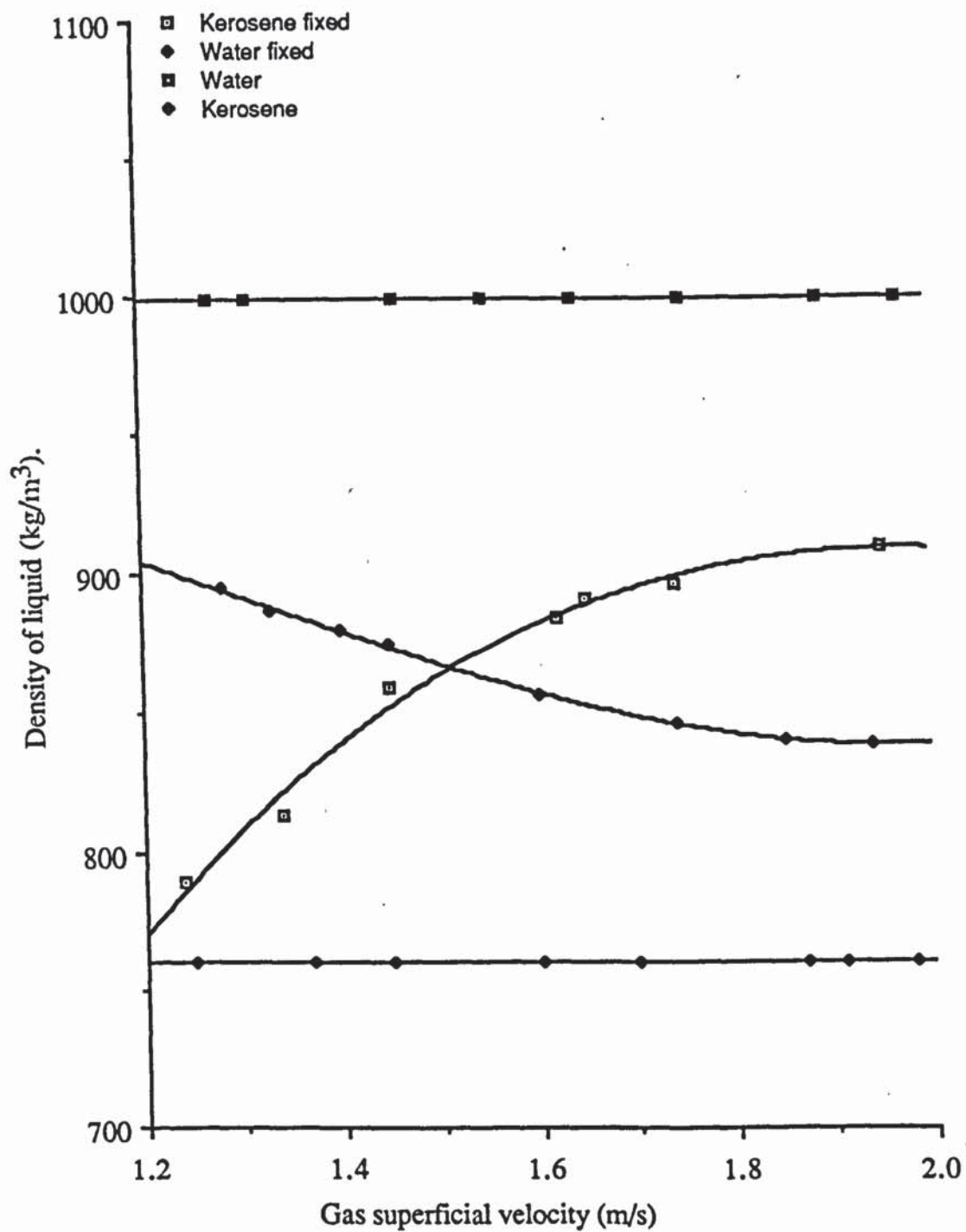


Figure 7.4.1. Effect of liquid density on transition. Tray no. 5.

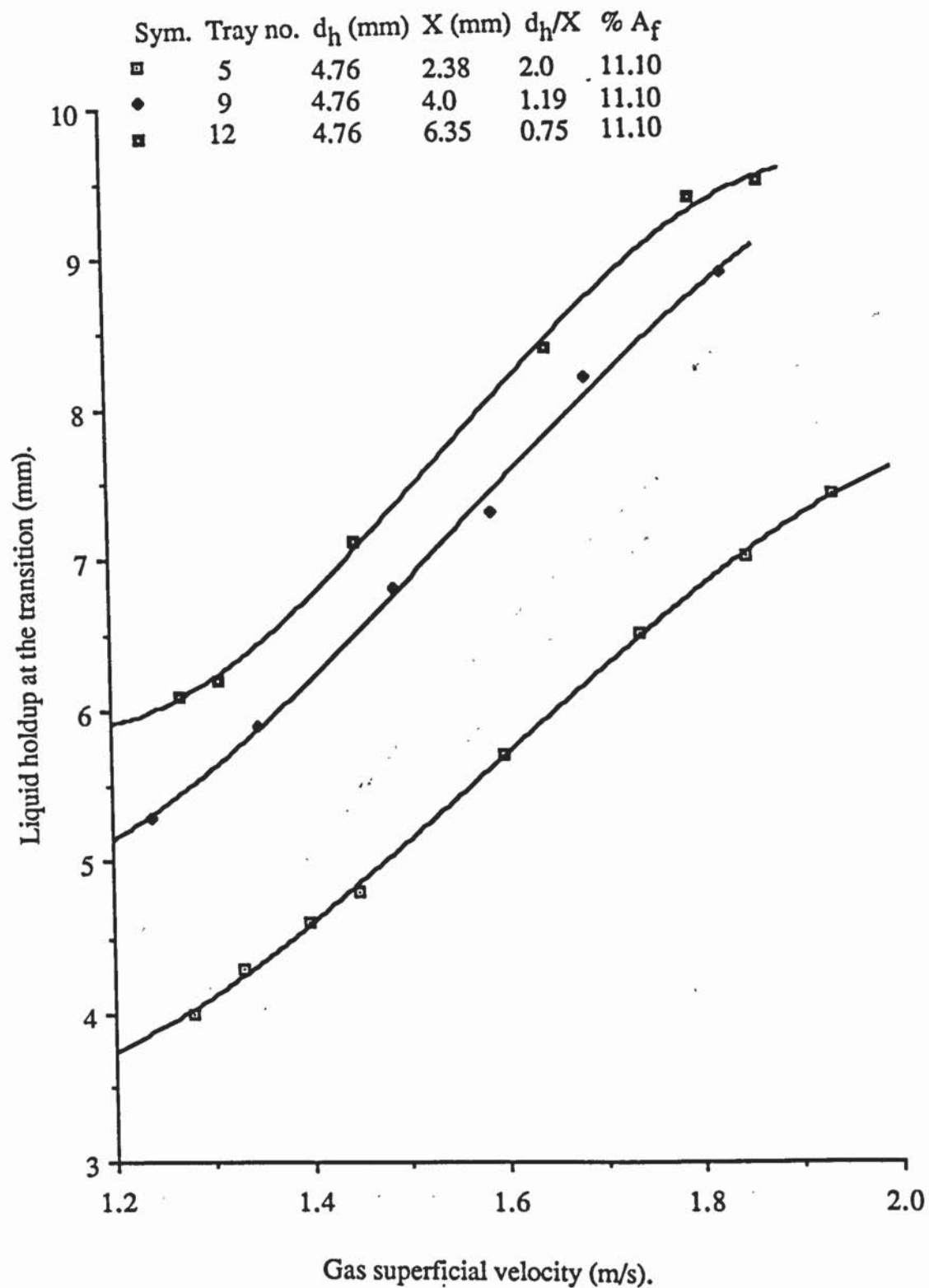


Figure 7.5. Effect of plate thickness & ratio (d_h/X) on transition. Water fixed.

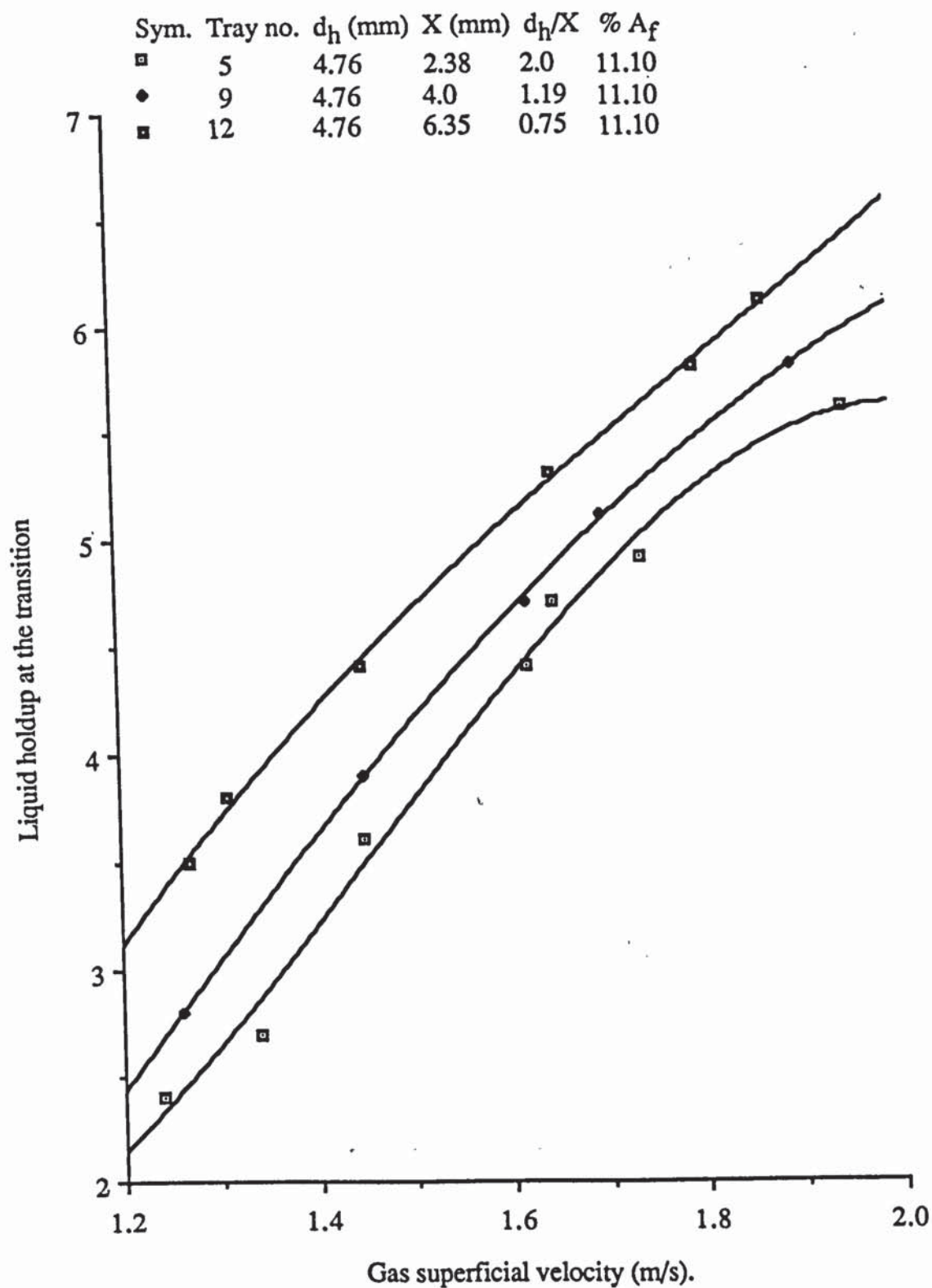


Figure 7.5.1. Effect of plate thickness & ratio (d_h/X) on transition. Kerosene fixed.

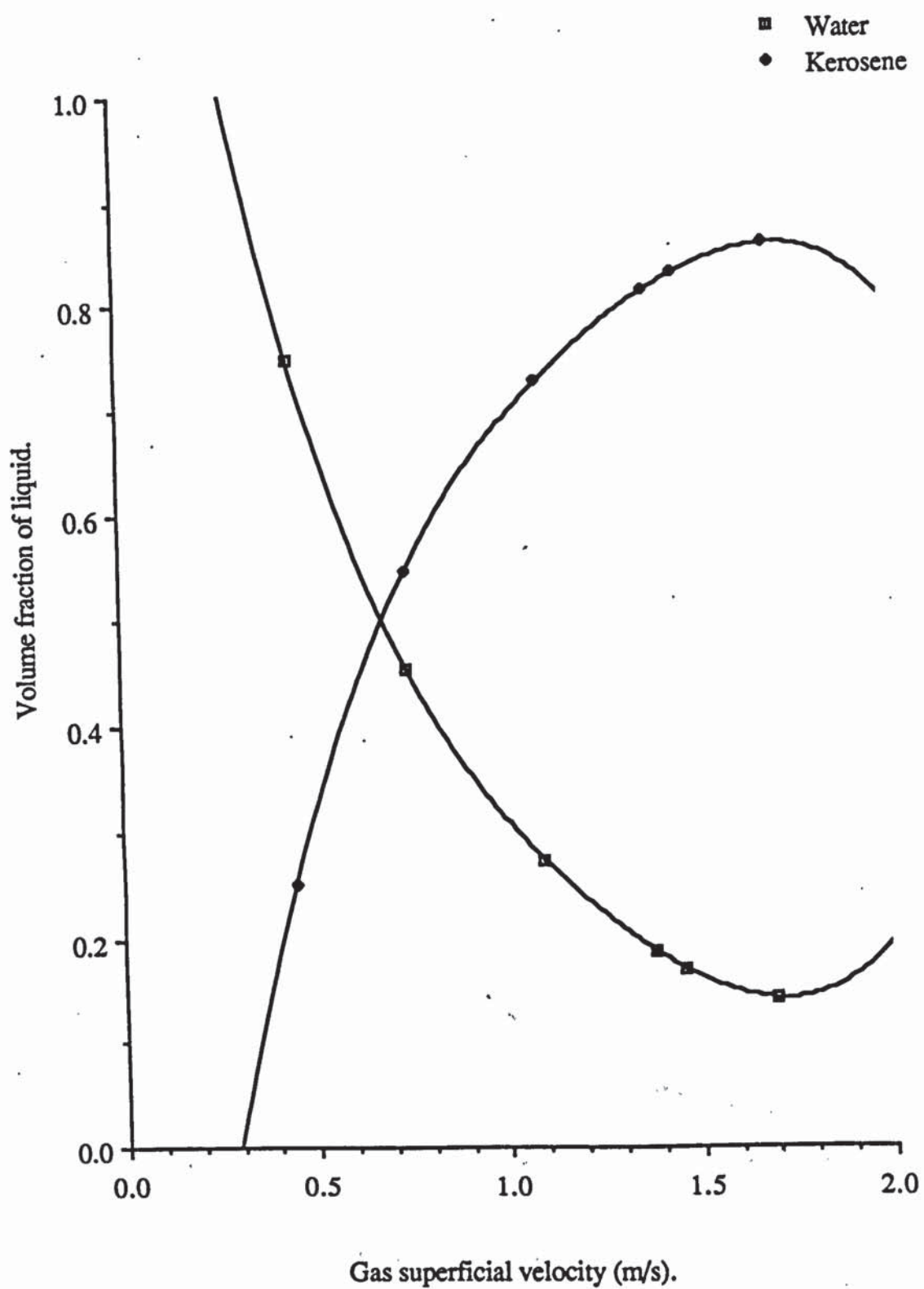


Figure 7.6. Variation of vol. fraction of liquid with gas velocity. Water fixed. Tray no. 8.

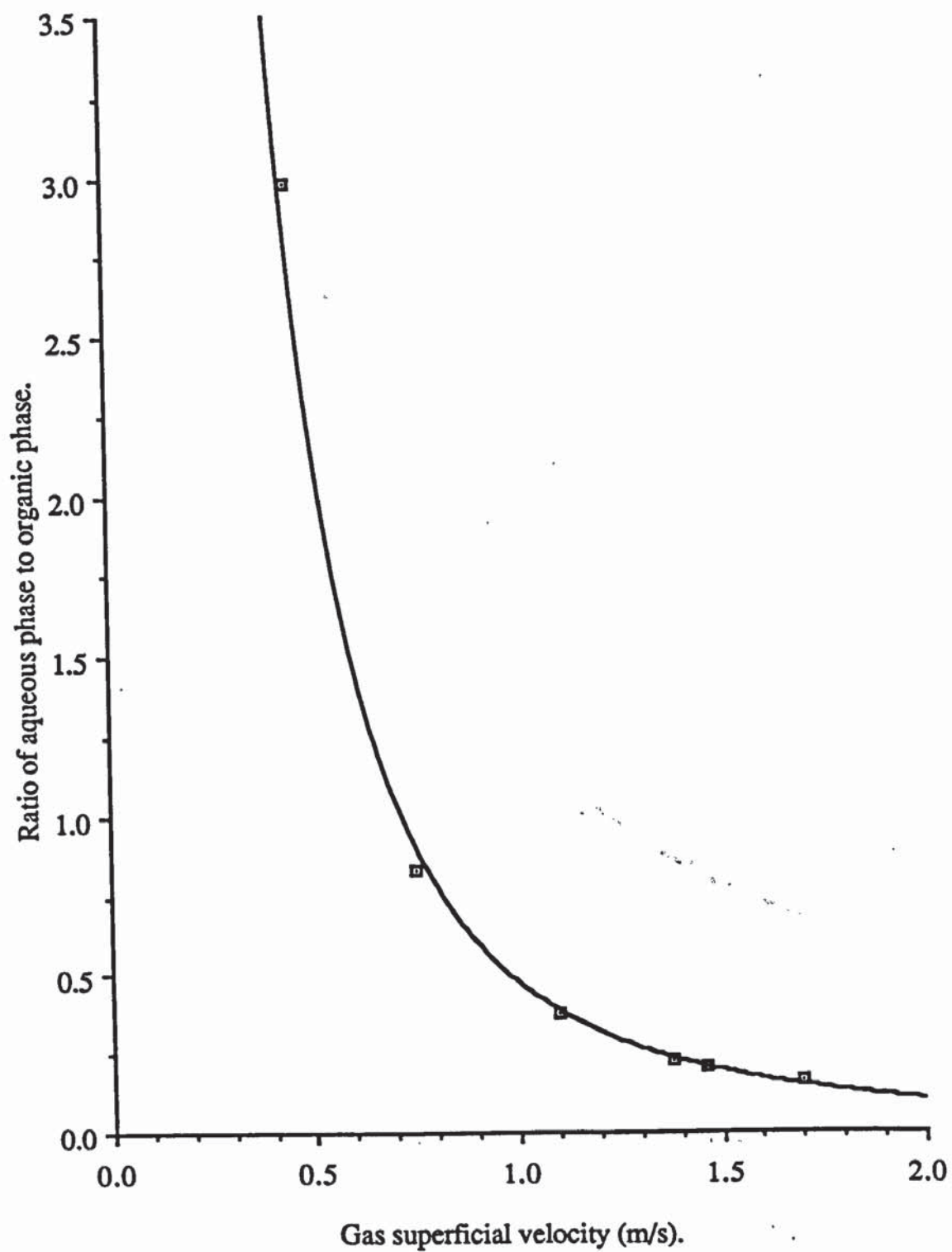


Figure 7.7. Variation of ratio (water/kerosene) with gas velocity. Water fixed. Tray no. 8.

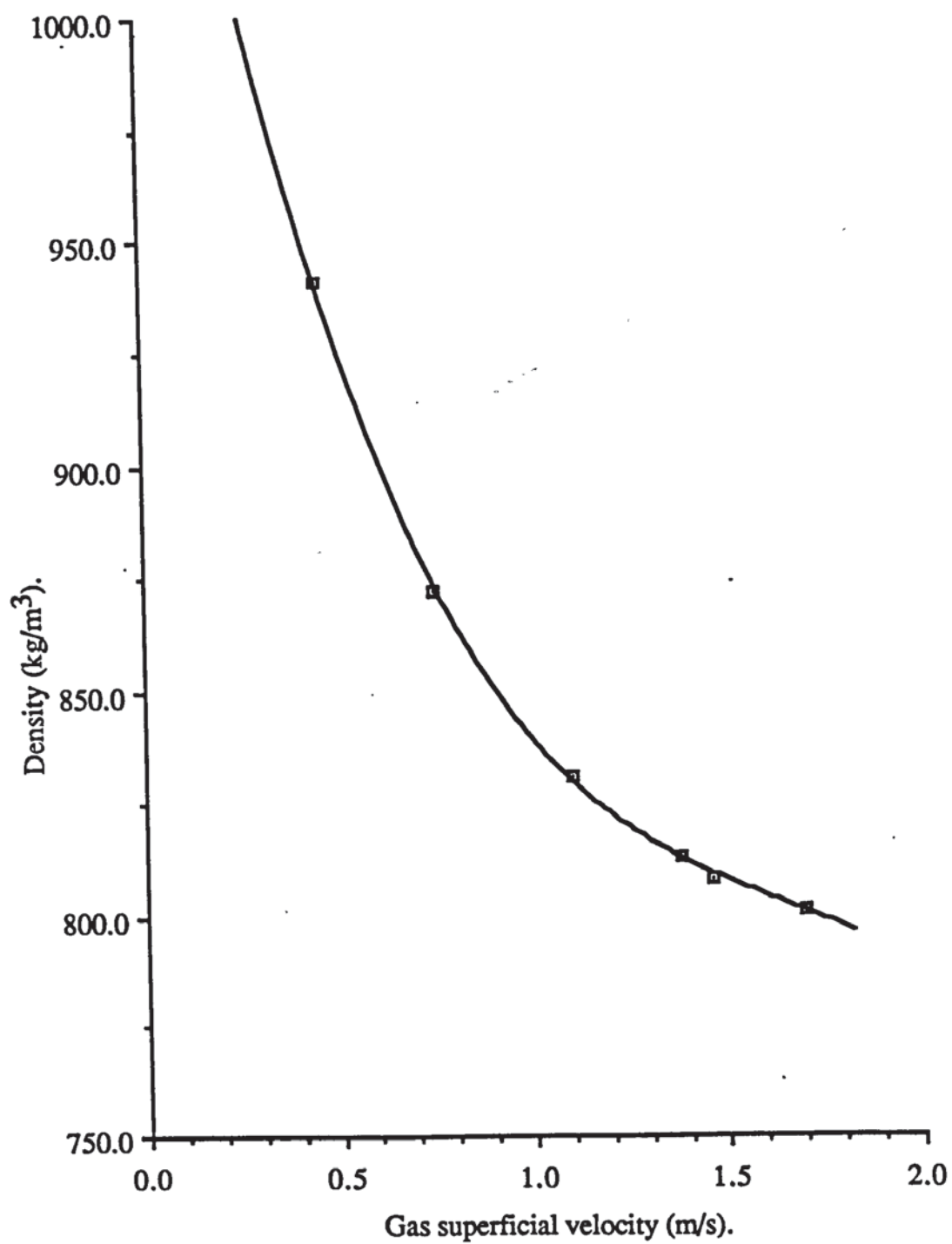


Figure 7.8. Variation of mixture density with gas velocity. Water fixed. Tray no. 8.

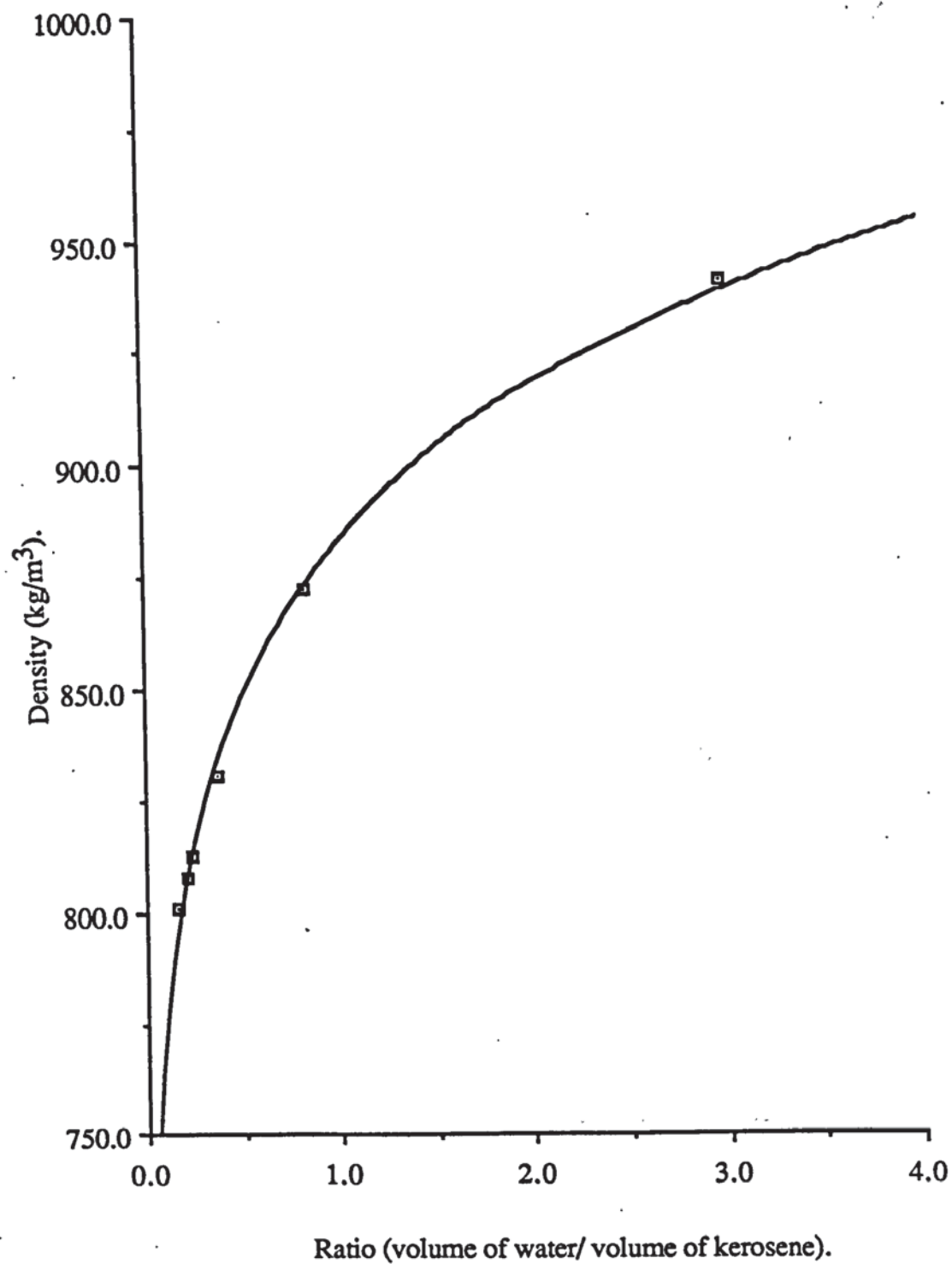


Figure 7.9. Variation of liquid density with ratio (water/kerosene). Water fixed. Tray no. 8.

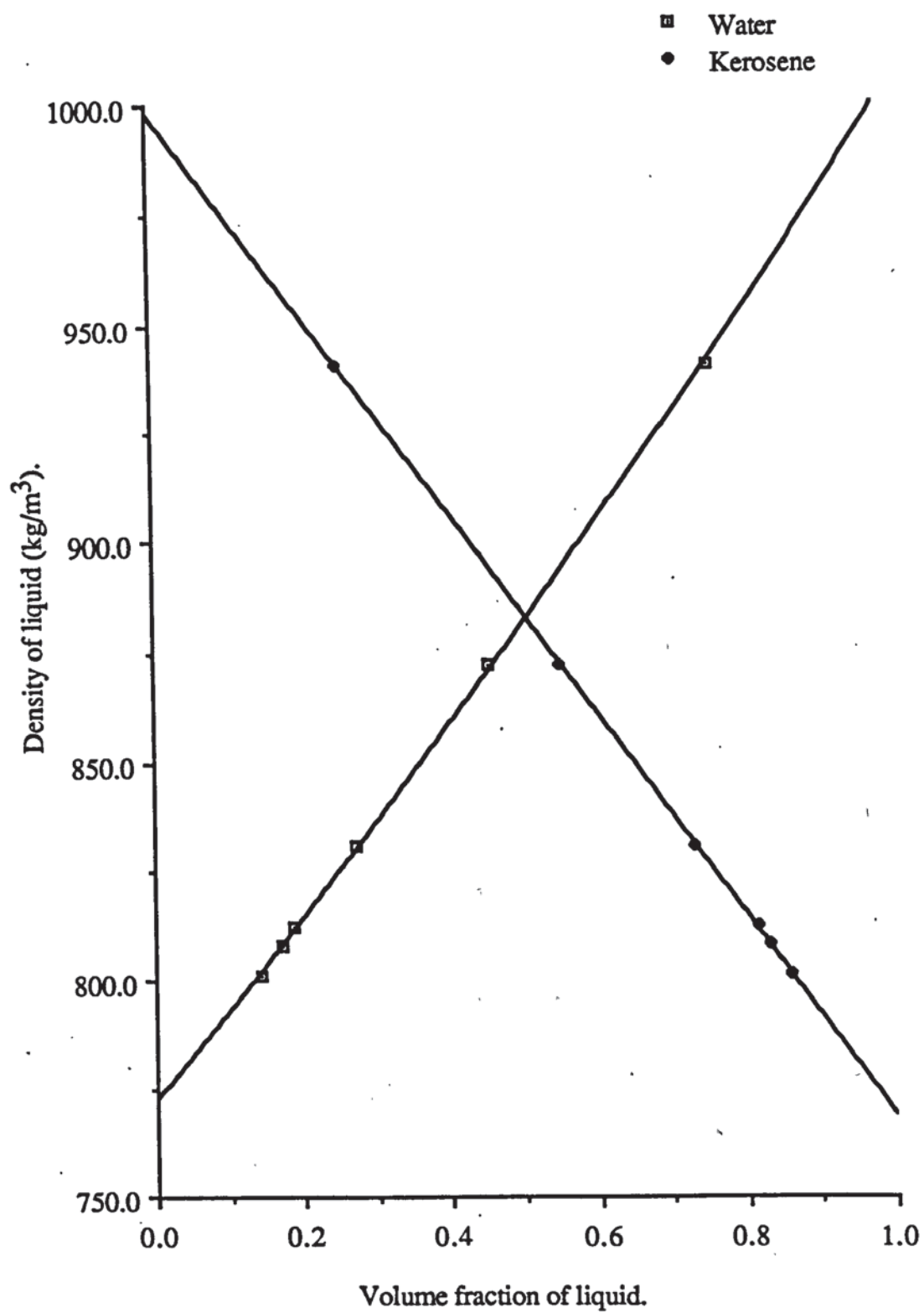


Figure 7.10. Variation of liquid density with vol. fraction of liquid. Water fixed. Tray no.8.

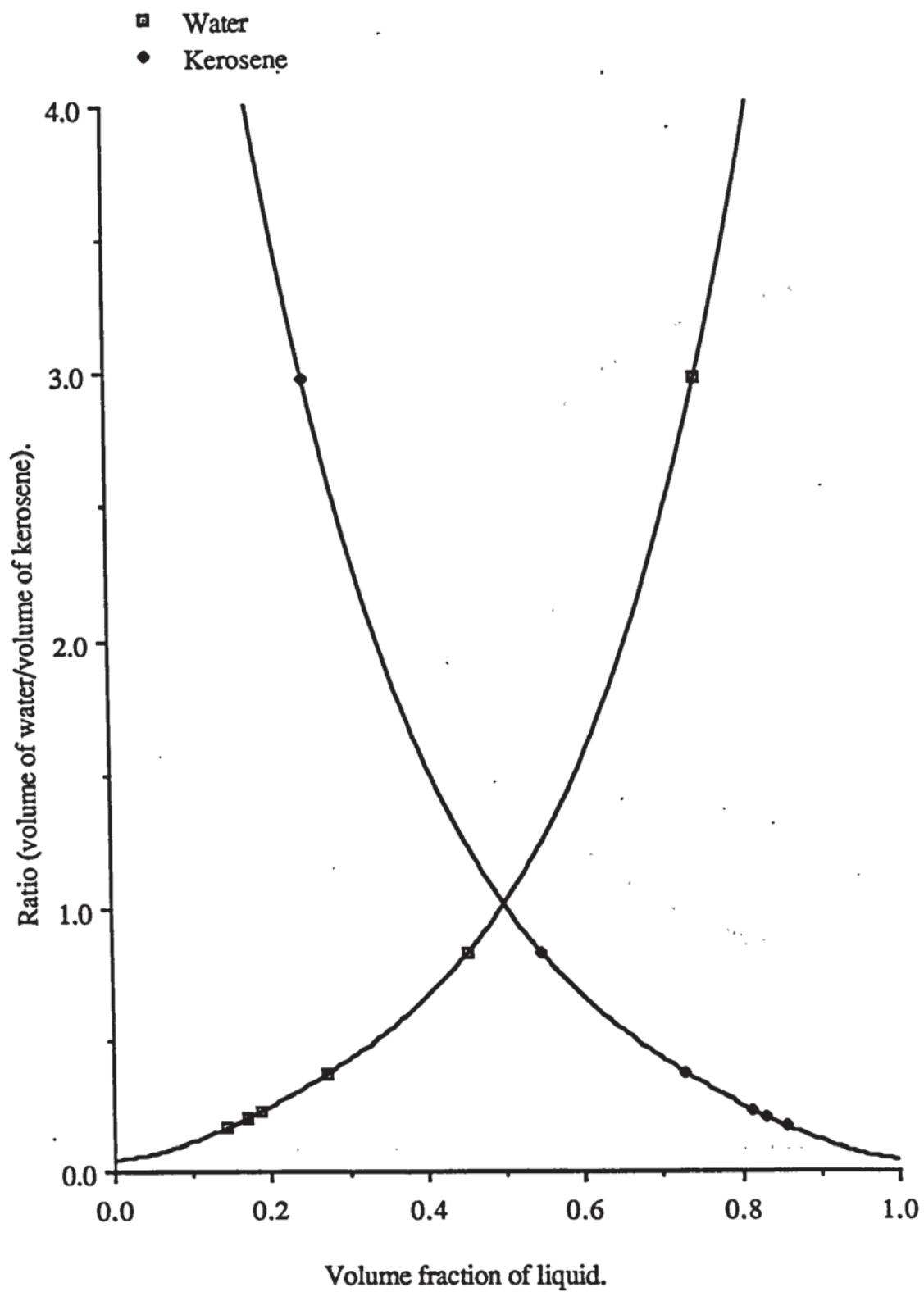


Figure 7.11. Variation of ratio (water/kerosene) with volume fraction of liquid.
Water fixed. Tray no. 8.

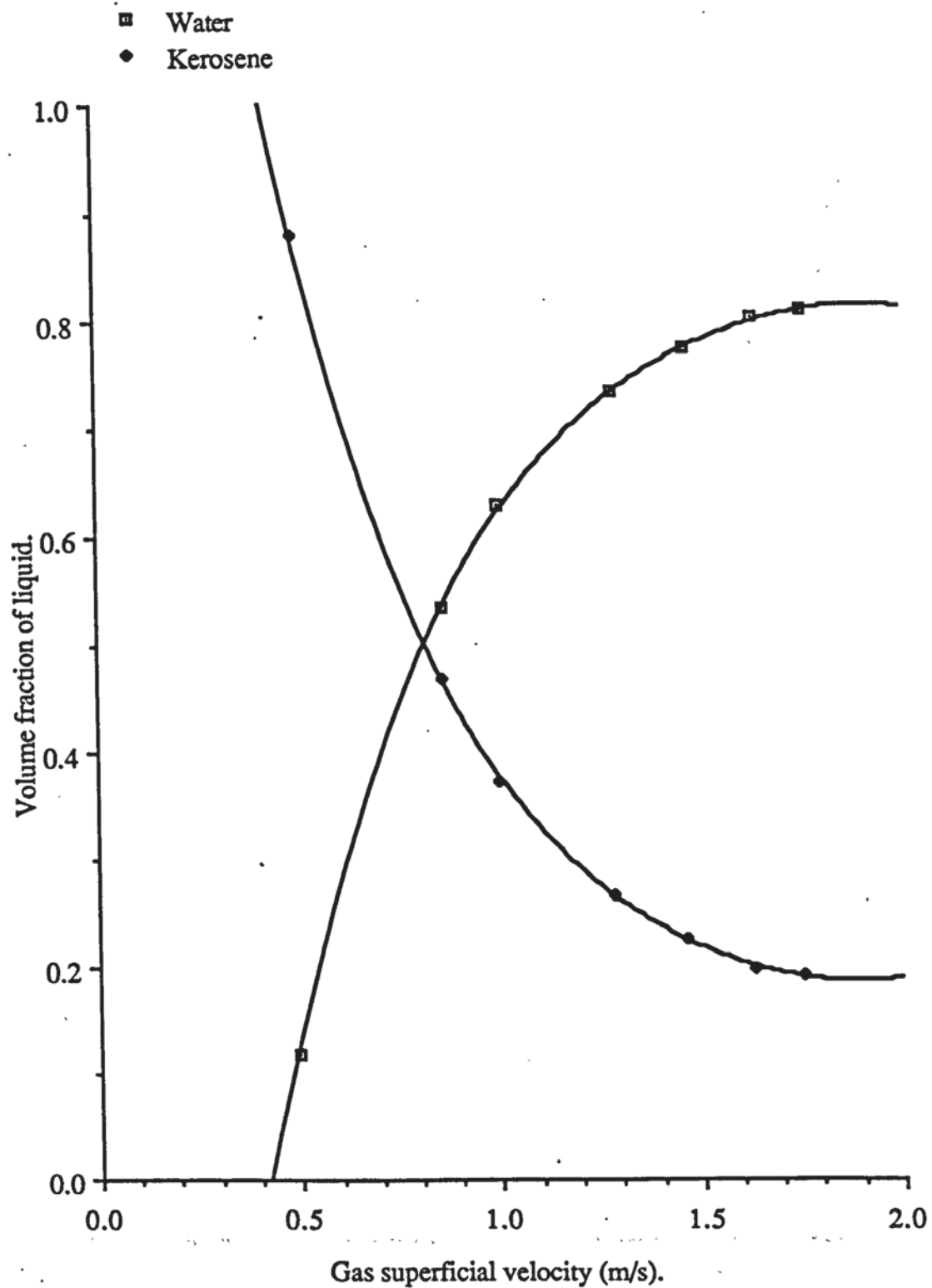


Figure 7.12. Variation of volume fraction of liquid with gas velocity. Kerosene fixed.
Tray no. 8.

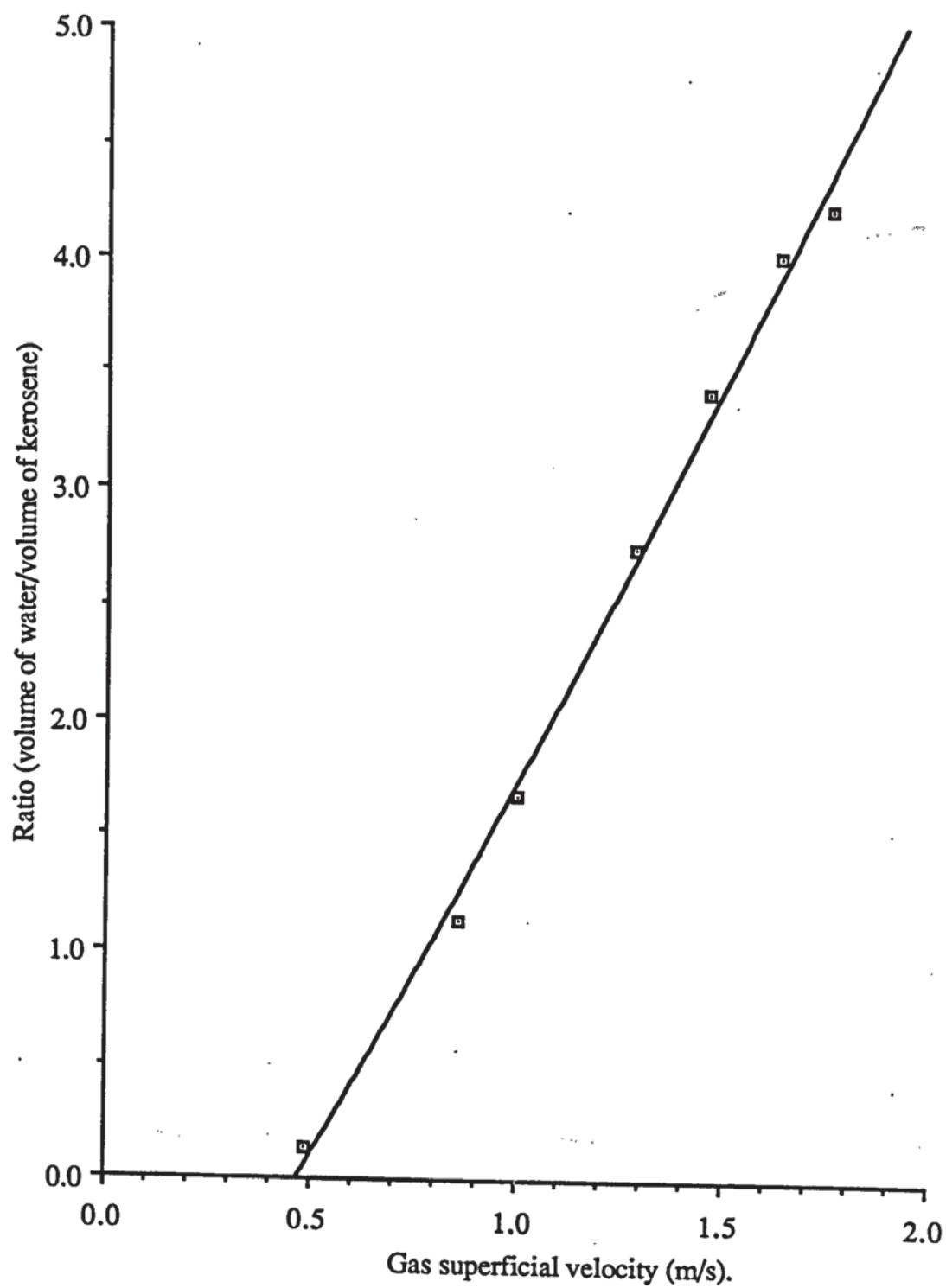


Figure 7.13. Variation of volume fraction of liquid with gas superficial velocity.
Kerosene fixed. Tray no. 8.

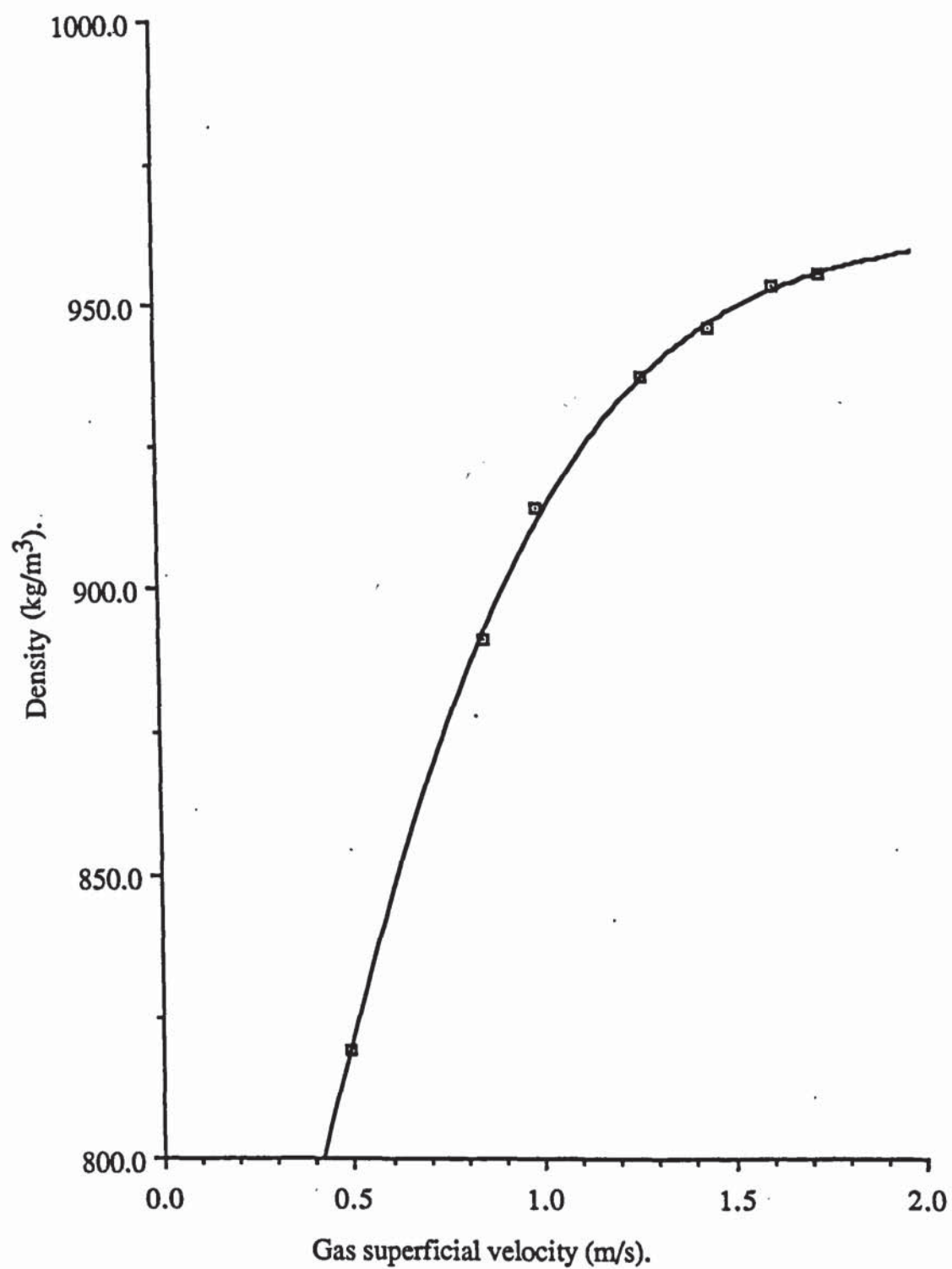


Figure 7.14. Variation of mixture density with gas superficial velocity. Kerosene fixed.
Tray no. 8.

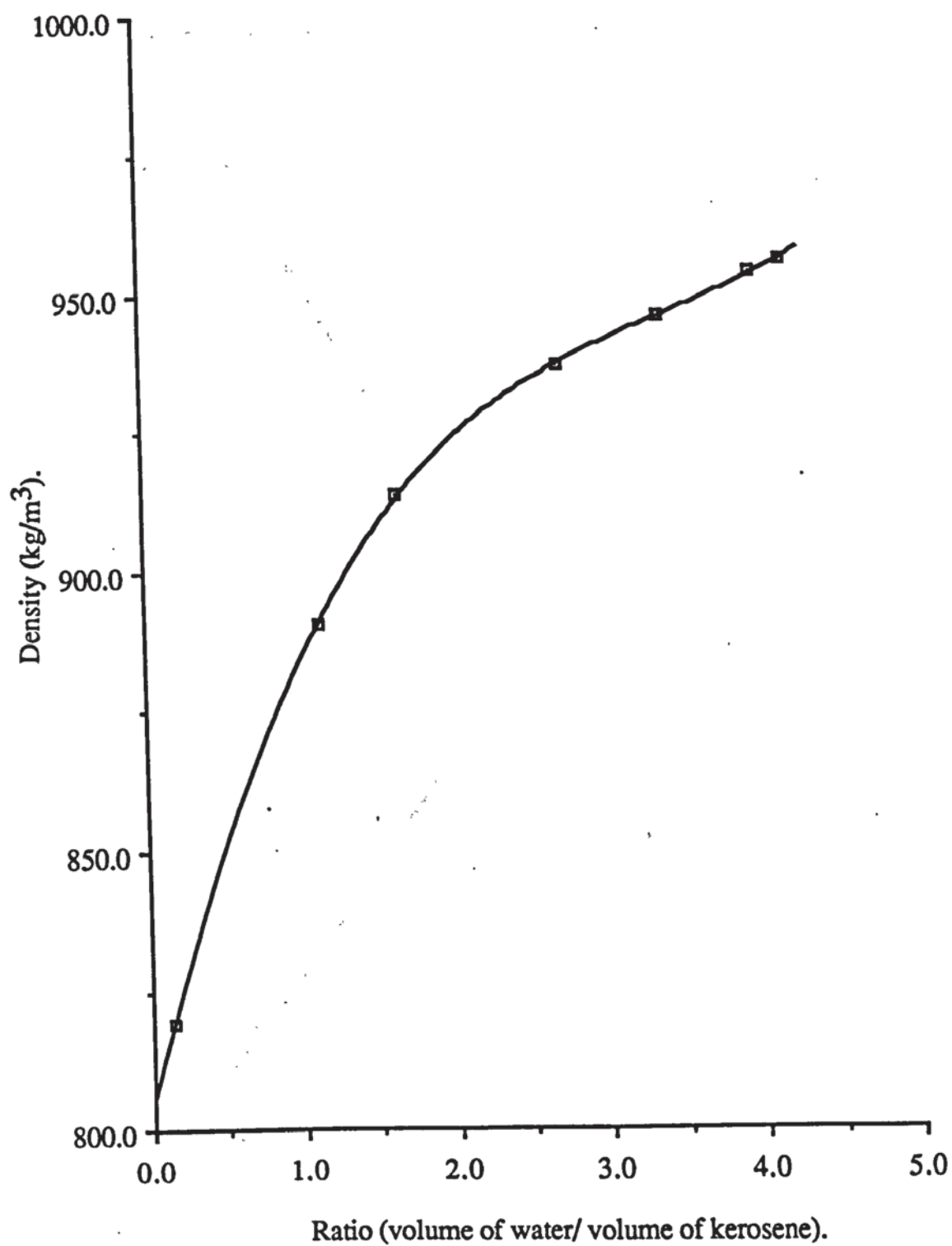


Figure 7.15. Variation of liquid density with ratio (water/kerosene).
Kerosene fixed. Tray no. 8.

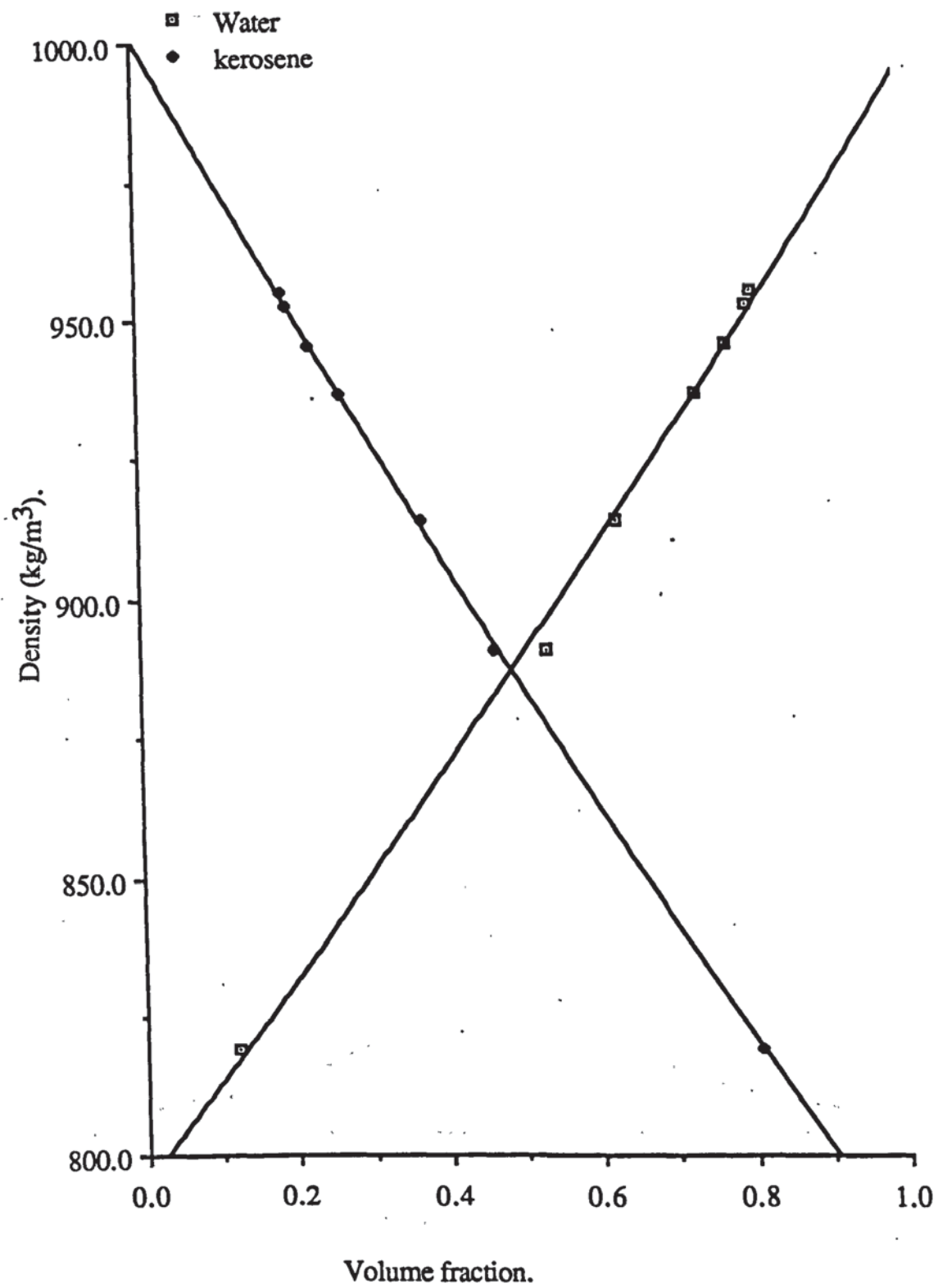


Figure 7.16. Variation of liquid density with volume fraction of liquid.
Kerosene fixed. Tray no. 8.

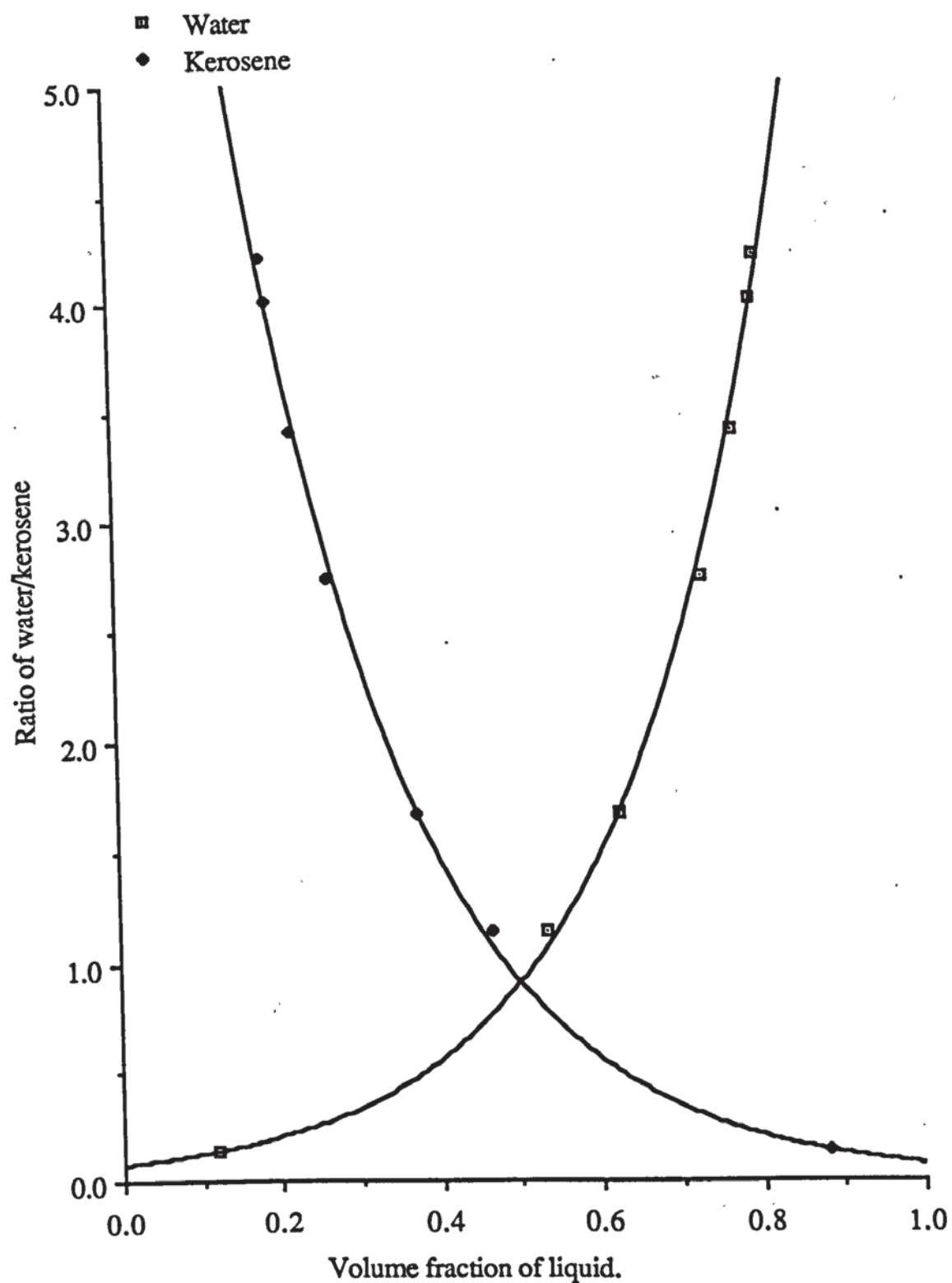


Figure 7.17. Variation of ratio (water/kerosene) with volume fraction of liquid.
Kerosene fixed. Tray no. 8.

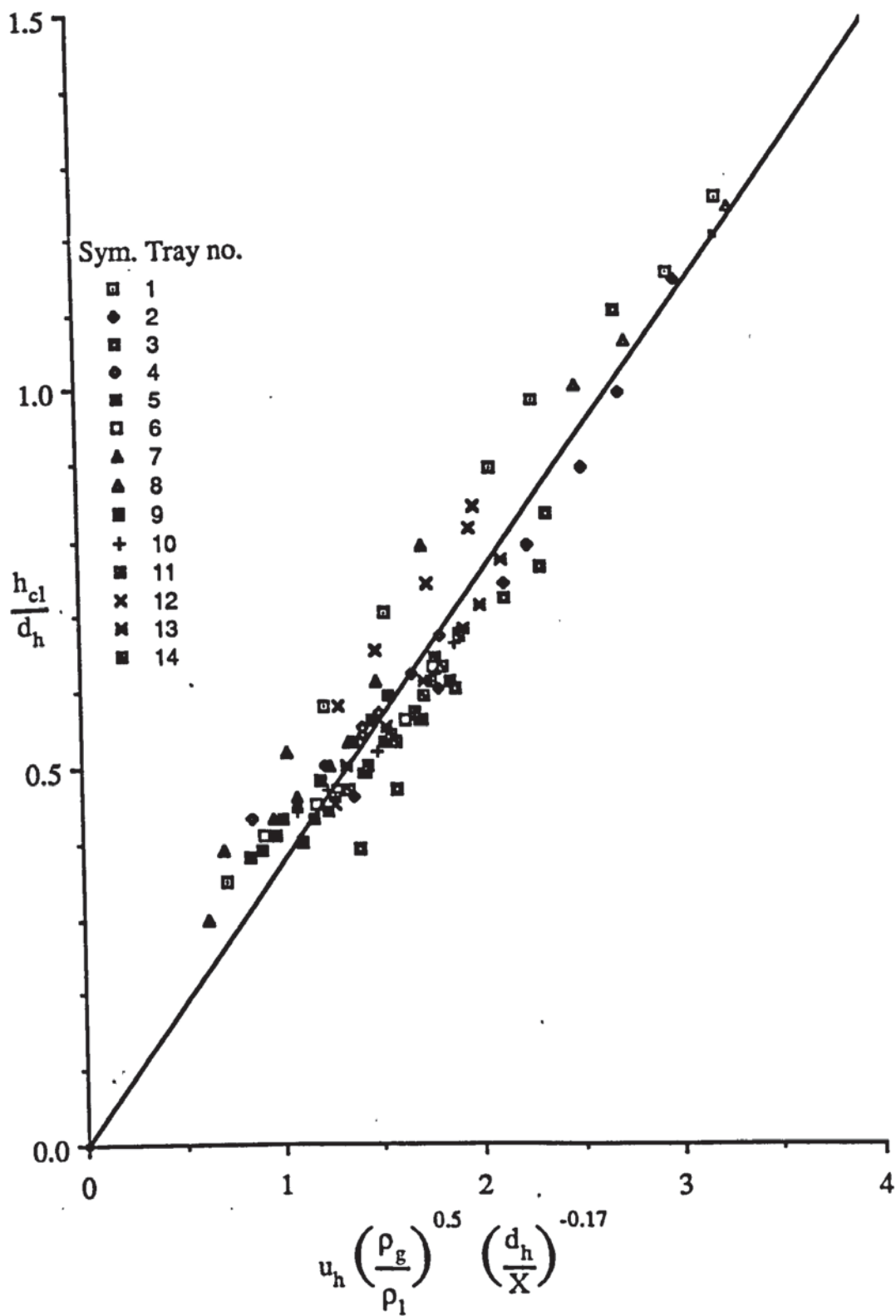


Figure 7.18. Proposed new correlation for spray to bubbly transition. Water fixed system.

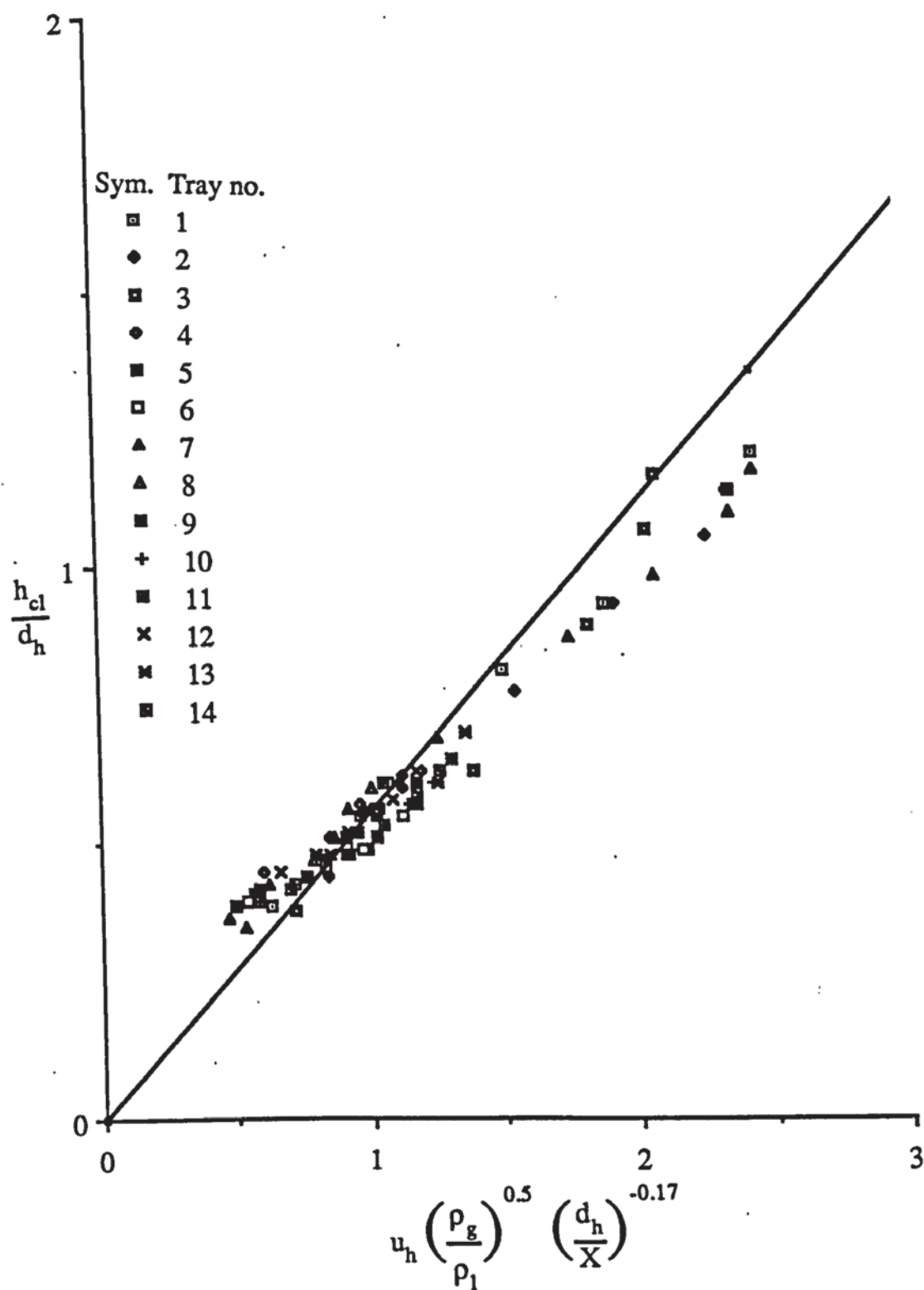


Figure 7.18.1. Proposed new correlation for spray to bubbly transition. Kerosene fixed.

CHAPTER 8

ELIMINATION OF FOAMS

8.1 Introduction

The design of distillation columns is still essentially empirical, but for most mixtures there are reasons why correlations of past experience provide a sound basis for the design (97). However in some circumstances, it is known that the empirical methods breakdown and columns flood at throughputs significantly less than the expected capacity. It is known from previous experience that columns have not achieved their rated throughput. In practice, these columns are derated by means of a 'foaming factor' which require the column cross sectional area to be increased by as much as 100%, although there is very little evidence to suggest foaming has actually occurred in the column. Such columns which are derated are columns in which both single and two liquid phases may occur. It has already been shown [section 5.5.2] that foaming occurred in a column which has a single liquid phase in one part of the column and two liquid phases in another section of the column. Foaming was observed over a number of trays at those concentrations where the liquid changed from one phase to two phase or vice versa.

In recent years, several workers have modelled the distillation of highly non-ideal mixtures that form two liquid phases (5-14). An essential element of all this work is an algorithm for testing the stability of the liquid phase on each tray. Methods have been proposed for determining whether phase splitting will occur and the subsequent equilibrium composition. None of these methods have indicated the type of flow regime in the column and the subsequent effect on the column capacity and no study has been undertaken on ways to avoid or eliminate the problem of foaming which may be caused by two liquid phases.

It is thought that foam may be avoided or controlled by designing a sieve plate to work in the spray regime (45,152), i.e. by the proper choice of the tray design to produce jetting rather than bubbling at the perforations. It is believed that foaming does not occur in the spray regime due to the inertia affects associated with the high gas momentum. The high gas momentum completely opposes the usual mechanisms which help to maintain the liquid film associated with foaming.

Depending on gas and liquid loadings it is known that small hole diameter trays operate most frequently in the bubbly regime, whilst larger hole diameter trays may operate in either the bubbly or the spray regime. Therefore, higher percentage free area trays and larger hole diameter trays appear to operate with higher velocities than low free area trays. However, it should be recognised that this observation is in part an outcome of the operating range of gas velocities of the respective trays studied. High hole diameter trays

could not be operated stably at low gas loadings because of weeping, and the stable operating range in the froth regime decreases as the hole diameter and hole areas are increased; both because of weeping and also because large hole diameter trays have a tendency to go into the spray regime before their small hole counterparts.

8.2 Objective of the Work

The objectives of this part of the work are:

- i. To eliminate the Ross type foam that was observed in the Oldershaw column experiments.
- ii. To see if the column capacity is reduced because of Ross foaming or the reduction is due to any other mechanism.

8.3 Methods of Foam Elimination

The following methods will be considered in the elimination of the Ross type foam.

- i. Use of alternative equipment - packed column.
- ii. Process design - use of additives.
- iii. Hardware design - tray designed to operate in the spray regime.

8.4 Packed Column

A 5.08 cm i.d. packed column, containing 70 cm of 6 mm Berl saddles, with a steam heated reboiler was used for foam elimination experiments. The column was operated at total reflux and atmospheric pressure. The column is shown in figure 8.1.

8.4.1 Experimental Procedure

A single phase mixture of n-hexane - water - propan-1-ol was charged to the reboiler. The cooling water to the condenser and the steam to the reboiler were turned on. The mixture was allowed to boil and observations were made to see if a build up of a foam occurred in the packing.

The composition was then changed to organic rich by adding n-hexane so that the effect of ratio of n-hexane/water could be noted.

8.4.2 Observations

It was noted that foam did not build up in the packing. However, in the case of the organic rich mixture the foam built up on top of the packing but there was no foam in the packed bed itself. This is because the packed bed did not have sufficiently large voids for the foam to develop. Thus, within the normal operating range of a packed column, foam did not form in the packing.

It was also observed that if the ratio of n-hexane/water was greater than 3.0, then foam builds up on top of the packing.

8.5 Use of Additives

The sintered plate column and the 50 plate Oldershaw column were used to test the effectiveness of additives. The solid compounds to be tested as eliminating additives were used only in the sintered plate column.

The compounds used in the sintered plate column and in the Oldershaw column are shown in table 8.1 and table 8.2 respectively.

Table 8.1. Additives used in sintered plate column

Compound	Phase
i. Silica gel	solid
ii. Ethyl silicate	solid
iii. Octyl alcohol	solid
iv. Ethyl amine	solid
v. Sodium silicate	solid
vi. Trimethyl amine	liquid
vii. Salicyl amide	liquid
viii. Trimethyl ortho phosphate	liquid
ix. Triphenyl ortho phosphate	liquid
x. Aluminium sodium silicate	liquid
xi. Kerosene	liquid

Table 8.2. Additives used in Oldershaw column

Compound	phase
i. Octyl alcohol	liquid
ii. Ethyl silicate	liquid
iii. Trimethyl amine	liquid
iv. Kerosene.	liquid

8.5.1 Experimental procedure - Sintered plate column.

Three ternary systems were studied:

- i. kerosene - water - acetone
- ii. n-hexane - water - propan-1-ol
- iii. cumene - water - propan-1-ol.

Equal volumes of water and organic were titrated with the solvent to get a single phase mixture and the mixture was poured onto the sintered plate. 12 litres/min of air was bubbled through the single phase mixture. The additives, listed in table 8.1 were added as the mixture was expanding to form a foam.

After completion of each run, the column was cleaned thoroughly to remove traces of the additives. Successive expansion of the foam in the column showed that there were no traces of the additive remaining from the previous experiment.

8.5.1.1 Observations

Initially the single phase mixture expanded due to a jet of air passing through it. After the addition of a very small quantity (0.5 g) of additive, the foam was destroyed immediately leading to a frothy solution cloudy in colour. All the additives listed in table 8.1 were observed to behave in this manner. The appearance of the final solution in both cases was similar to that observed when the foam collapsed without the use of additives.

8.5.2 Experimental Procedure - Oldershaw Column

The system studied was n-hexane - water - propan-1-ol. The procedure used has been outlined in section 5.5.1. However, once the foam was stabilised in the middle of the column, the additives, listed in table 8.2, were added dropwise from a vessel connected above the top plate.

The column was cleaned with acetone and subsequent experiments showed that all the additive had been removed.

8.5.2.1 Observations

i. **Octyl alcohol.**

The addition of a small quantity (100 ml) led to an increase in the number of plates which foamed in the middle section of the column. As observed before, two liquid phases were present in the top section of the column and a single liquid phase was present on the bottom plates of the column.

ii. **Ethyl silicate.**

After adding a small amount of ethyl silicate, foaming was observed in the separate region of the column (i.e. two liquid phases were present on the top few trays followed by a region containing foam on the trays; then a further region contained two liquid phases and finally another region of foam occurred on the bottom trays. The top foaming section had discrete circulating bubbles around the column wall, while the bottom foaming section bubbles contained in the form of a cellular foam. A large amount of ethyl silicate could not be added because the top plates walls were being coated with silicate.

iii. **Trimethyl amine [TMA].**

Initially two phases were present on the bottom section of the column and foam was present on the remainder of the plates. After about 250 cm³ of TMA had been added the foaming section was reduced to five plates in the bottom section of the column. By a reduction of heat in the reboiler the foam was completely eliminated and all trays were operating in the two liquid phase region.

iv. **Kerosene.**

On the addition of a small quantity of kerosene, the foam was restricted to the bottom twelve trays. Further addition of kerosene led to the elimination of foam and it was observed that all trays were operating in two phase region. By increasing or decreasing the heat input to the reboiler the foam did not reappear.

8.6 Perspex Simulator

It is known that in some circumstances, foam may be controlled by designing a sieve plate to operate in the spray regime. The perspex simulator, already described in section 4.3, was used to test the concept that foaming could be eliminated by operating in the spray regime. Air was blown through a dispersion on a commercial size and design of plate. The sieve plates used in the experiment are listed in table 8.3.

Table 8.3. Details of sieve plates used in experiment

Tray no.	Hole size d_h (mm)	Plate thickness X (mm)	No of holes	% free area	Triangular pitch (mm)	Ratio (d_h/X)
1	12.7	2.38	149	9.29	3.81	5.34
2	3.18	2.38	2613	10.18	0.95	1.33
3	3.18	2.38	155	1.0	1.82	1.33

8.6.1 Experimental procedure

Equal volumes of cumene and water were poured into a stirred tank and propan-1-ol added to make the solution into single phase. The solution was then pumped into the calibrated liquid reservoirs. The liquid was fed by gravity through independent feed lines onto the centre of the plate. The actual amount of liquid introduced onto the sieve plate could be calculated from the change in liquid levels of the reservoirs. Large quantities of the ternary single phase mixture could be added quickly through the three feed points on a tray.

An entrainment separator was fitted to the top of the column to prevent any liquid from being carried out of the apparatus with the air. The exhaust from the simulator was then passed through a scrubber to remove any propan-1-ol from the exhaust air. The scrubber used was 0.6 m square internally and had a packing height of 1.20 m, the packing used was 50 mm Raschig rings. The water to the scrubber was metered through a flow meter and six spray nozzles were used to spray the water onto the packed bed.

The water supply to the scrubber was turned on, the exhaust fan and the blower were started, the air flow rate was adjusted to such that air velocity would be above the weeping point and the single phase liquid mixture was allowed to flow onto the plate by gravity. The quantity of liquid mixture put on the plate was enough to form a fully developed spray regime or bubbly regime on the plate. Once the tray was operating in the desired regime the liquid flow onto the plate was stopped and then observations were made.

The details of experimental conditions used are listed in table 8.4.

Table 8.4. Experimental Conditions for air-water simulator

		Tray number		
		1	2	3
		Gas superficial velocity (m/s)		
Run no.	1	1.29	0.45	0.21
	2	-	1.10	0.21

8.6.2 Observations

Initial observations showed that when the liquid was added slowly onto the plate all the liquid was entrained very quickly. The plates were then modified to have three feed points located in the centre of the plate so that large amounts of liquid could be added quickly.

It was observed that the trays produced spray for all flow rates. The large hole tray with a free area of over 9% [a typical commercial value] produced spray even when operated at a velocity just above that required to prevent weeping. Very severe entrainment of liquid was observed with this tray.

The small hole diameter tray (3 mm) with a free area of over 10% produced spray at a velocity (0.45 m/s) [just above weeping point] and severe entrainment was again observed. The entrainment was again very severe with higher gas velocities (1.10 m/s).

Finally a tray was fabricated with 3 mm diameter holes and only 1% free area so that the gas superficial velocity could be reduced to avoid weeping. Again liquid entrainment was severe. In all cases the liquid on the tray entrained and eventually the tray became 'dry'.

For tray numbers 2 & 3 when operated in bubbly regime, a clear mist was seen rising above the bubbly dispersion to about three quarter way up the column. After about 10 minutes, some droplets were seen rising on top of bubbly dispersion. After further few minutes the size and height of droplets increased and the bubbly dispersion became frothy in appearance, eventually the tray operating regime switched to the spray regime. After short period of time the tray became 'dry' again. This sequence of tray switching from bubbly regime to spray regime is shown in figure 8.2 for tray number 3.

In all cases the unusual high rates of entrainment were observed for the one phase liquid as it approached the two phase boundary. The appearance of the two phases was detected by the appearance of cloudy liquid streaks flowing down the column wall and the remaining solution changing in colour from clear to 'milky' on the plate.

It was observed that the dispersion did not produce a foam of the type observed in the Oldershaw column and the sintered disc column, but produced a fine spray under conditions where 'normal' liquids produced a bubbly dispersion.

The spray to bubbly transition experiments were repeated for tray number 3. It was seen that about 2 litres of water and about 3 litres of cumene were required to reach the transition whilst about 6 litres of ternary single phase were required for the transition.

8.7 Sintered Disc Column Experiments

Further experiments were carried out in the small glass column using the cumene - propan-1-ol - water system to clarify the phenomena observed in the perspex simulator. The tray used had 1 mm diameter holes with approximately 1% and 10% free area.

8.7.1 Experimental Procedure

A single phase mixture was made and charged to the overhead storage vessel. The air was turned on and adjusted to 10 litre/min. The mixture was then added very slowly via the side opening and observations made.

8.7.2 Observations

With a 1% free area tray and following the addition of a small volume (about 2 cm³) of mixture, a spray was observed and the dispersion was being entrained severely. A further 15 cm³ of the mixture were added onto the plate. It was observed that after a period of time the mixture started foaming and the foam rose to a maximum height and then almost immediately the foam started decaying. It was found that after an hour some of the mixture was still present on the tray.

The same process was repeated for the 10% free area tray. However, it was observed that much more liquid was added to break the spray into a foaming solution. Eventually, as observed with the sintered disc, the foam expanded and once two liquid phases were formed the foam started to decay.

8.8 Discussion

The Ross type foam observed on a single sintered plate and in the Oldershaw column did not occur or build up on sieve trays operating in the spray or bubbly regime when mass transfer experiments were carried out with propan-1-ol being stripped from a cumene - water - propan-1-ol mixture. This was an unexpected result, because it was thought that with a tray operating in the bubbly regime and when the transition from a single

liquid phase to two liquid phases occurred, a Ross type foam was expected to build up in the column. Instead, it was observed that when the transition from a single liquid phase to two liquid phase happened, severe entrainment occurred.

A mechanism has already been proposed (section 7.11), which relates foaming to the spray/bubbly transition with two immiscible liquid phases. It was concluded that surface force ($\sigma_i/d_{\text{bubble}}$) is smaller for a kerosene fixed system in which the transition to the bubbly regime occurs at a much lower liquid holdup than in the corresponding water fixed system. In addition, measurements of surface tension in a ternary system (section 5.8) show that surface tension reduces to a low value near the single/two liquid phase boundary. This results in severe entrainment in the perspex simulator when this boundary is approached. Surface tension was also measured for various compositions near this phase boundary [section 5.8] where it was observed that surface tension values are low. It was also observed in section 5.7.2 that the change in concentration of the components was very small across the foam. Therefore, very little mass transfer occurs in the foam and so the diffusion coefficient is almost zero; this leads to severe entrainment near the single to two liquid phase boundary. Therefore, the existence of foaming and entrainment may be connected with lower surface tension near the single/two liquid phase boundary.

These observations may provide an explanation for the reduced capacity of distillation columns where changes from one liquid phase to two liquid phases occur. The reduction in capacity may be due to unusually high entrainment rather than foaming as was observed in the Oldershaw column.

8.9 Wind Tunnel Experiments

The wind tunnel experiments with single droplets were carried out to determine whether the different size of droplets seen above the bubbly dispersion in the perspex simulator were the result of droplets bursting or some other process. The details of equipment are listed else where (153) but a brief explanation of the operating procedure is outlined below.

8.9.1 Experimental Details

The fan was switched on and the apparatus was left running for about 1.5 hours to reach a steady state i.e. air was recirculated and hence the tunnel was at constant temperature.

When steady state had been reached the appropriate solution was placed in the nozzle and a few drops were purged from the nozzle to remove any air bubbles in the nozzle. The 5.2 cm working section was uncovered, the nozzle slid into the working

section, and the drop was released. The nozzle was withdrawn and the 5.2 cm hole covered.

Observation of the drop was maintained in order to ensure that no air bubble were trapped in the drop.

8.9.2 Measurement of Droplet Size

A video camera was focussed on the position where a drop would be contained in the wind tunnel. The stop watch was started on the camera, the drop was injected in the working section and filming of the drop commenced. After completion of the experiment the video tape was replayed and the diameter of the drop measured. The results are given in appendix 10.

8.9.3 Discussion of Results

It was observed that both the pure component drop and mixture drop did not split into smaller size drops. The evaporation time required for the drops to be blown out of the working section was greater for pure water [three times as much] and similar for cumene, propan-1-ol and the mixture. This is due to the high latent heat of vaporisation of water compared with other the components [figure 8.3].

8.10 Conclusions

- i. The foam observed in an Oldershaw column in the presence of single/two liquid phases can be eliminated by the use of additives but there is the disadvantage that additives are expensive and contamination of the product is possible.
- ii. A packed column or a packed section can be used to eliminate foam.
- iii. Foam did not form on the sieve trays in the perspex simulator when a single liquid phase changed to a two liquid phase under mass transfer conditions and also conditions where the bubbly regime would be expected. Instead severe entrainment occurred which can lead to the additional problem of flooding especially with large diameter hole trays and close tray spacing.
- iv. The amount of liquid containing the three component single phase mixture required to reach the spray to bubbly transition point is much greater than the quantity containing a pure component liquid required to reach the transition point.
- v. The foam observed in Oldershaw column and sintered plate column caused by interfacial problems was not observed in perspex simulator. Therefore, distillation columns may be flooding as a result of severe entrainment.

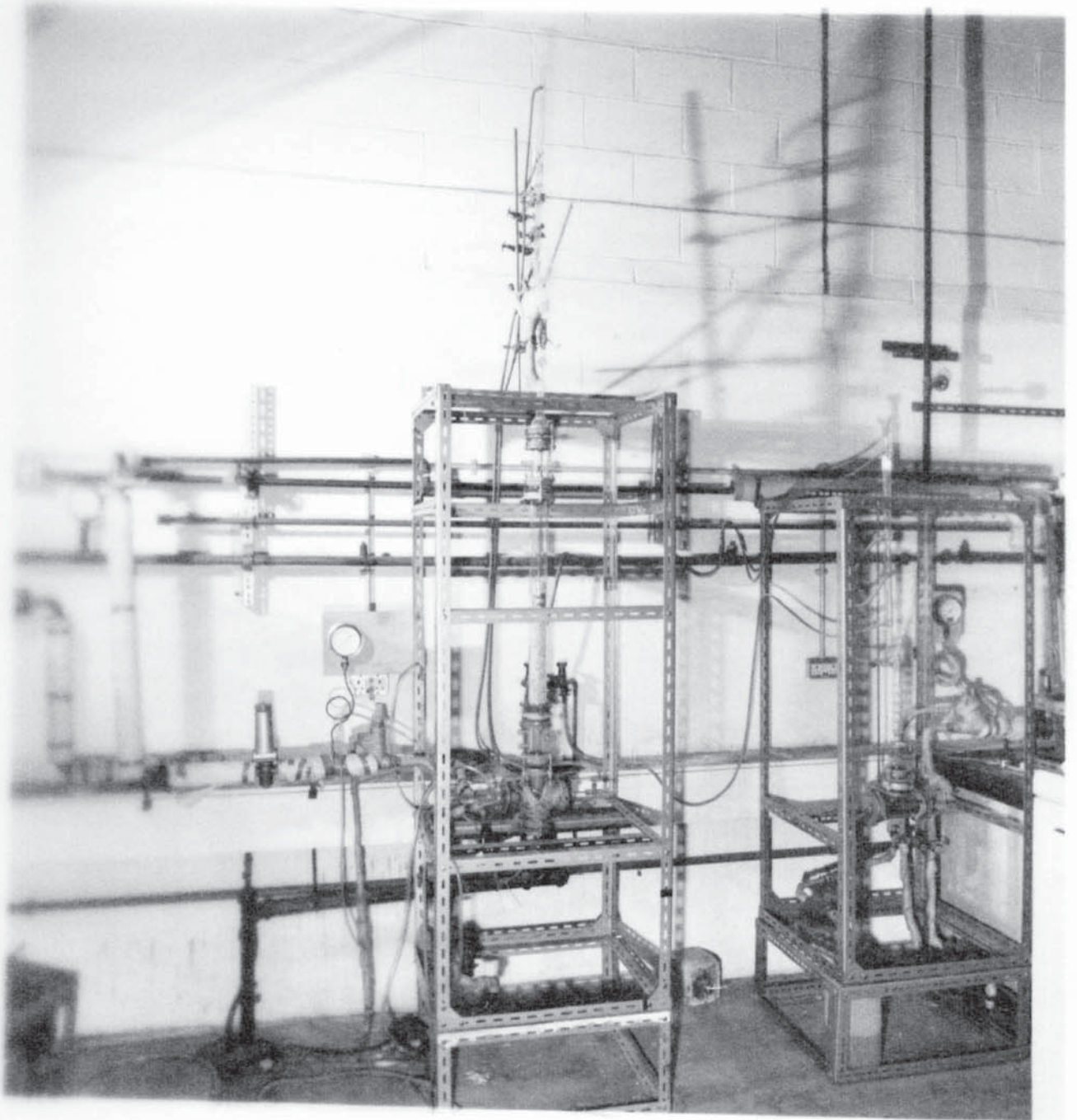
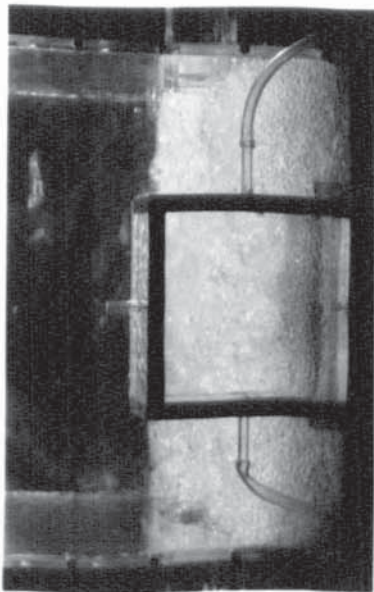
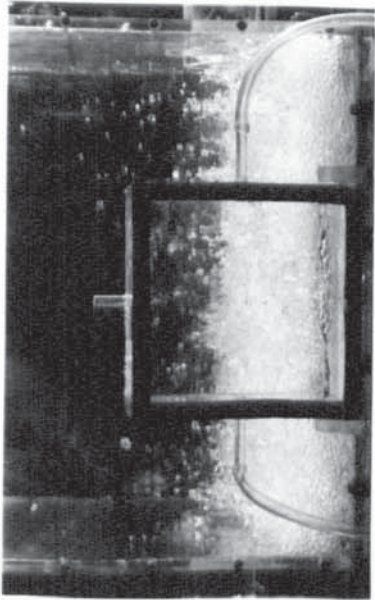


Figure 8.1. Packed column.

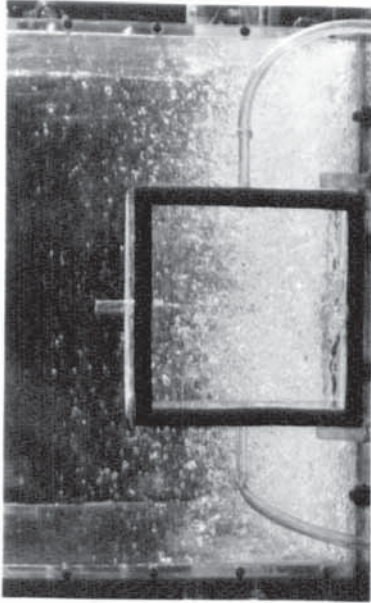
Figure 8.2. cumene - water - propan-1-ol system in perspex simulator.



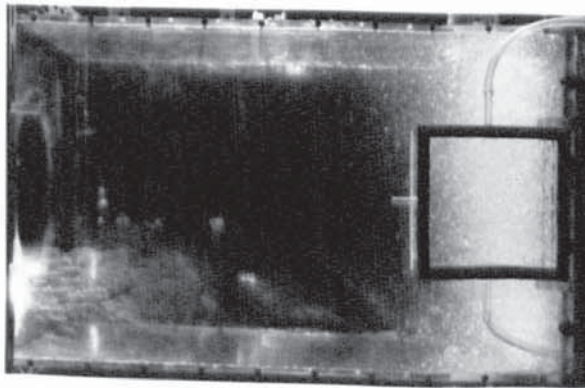
a. Tray operating in froth regime.



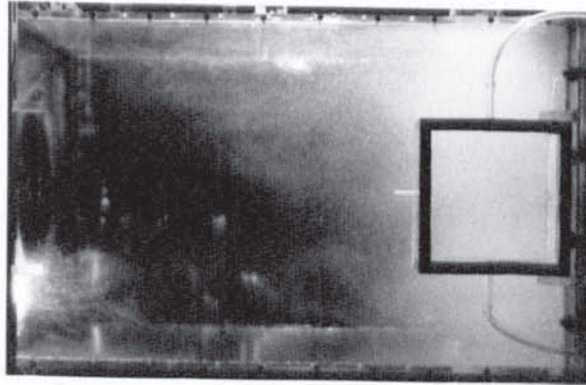
b. Droplets beginning to form on the froth surface.



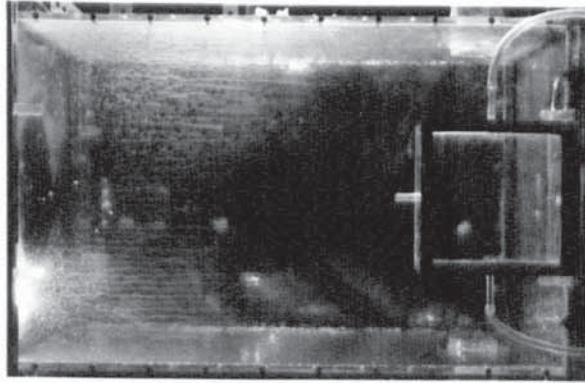
c. The intensity of droplets is increasing.



d. The intensity of droplets is increased further.

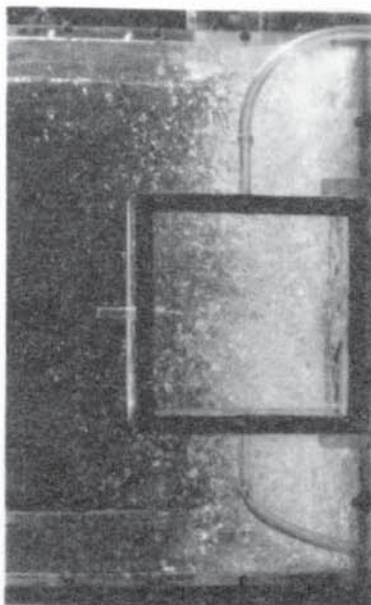
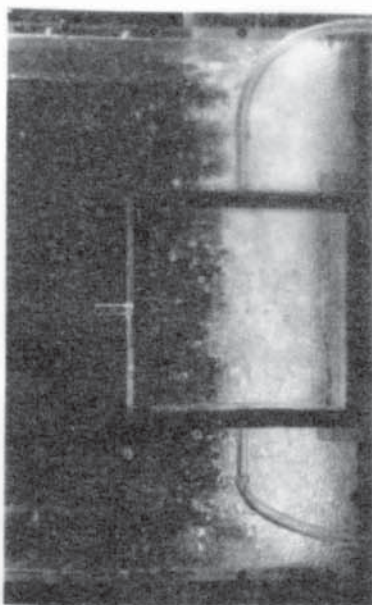
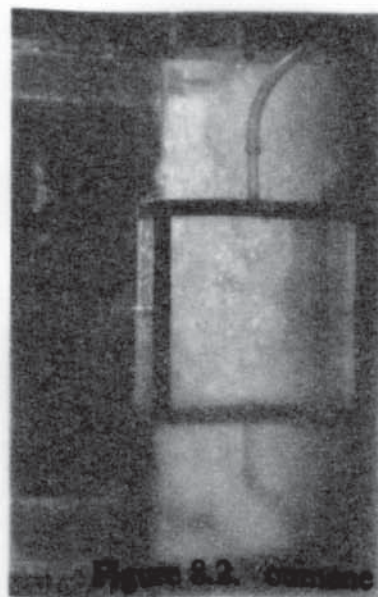


e. The tray is operating in spray regime.



f. All the liquid has entrained. The tray is 'dry'.

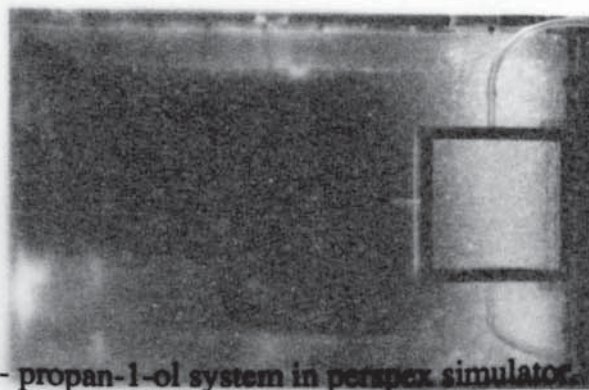
Cumene - Water - Propan-1-ol system in perspex simulator.



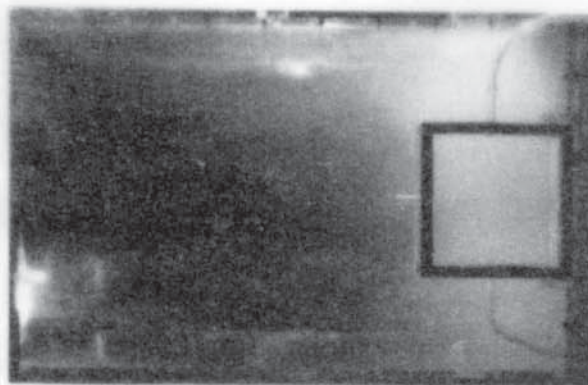
a. Initial state.

b. Droplets beginning to form on the fresh surface.

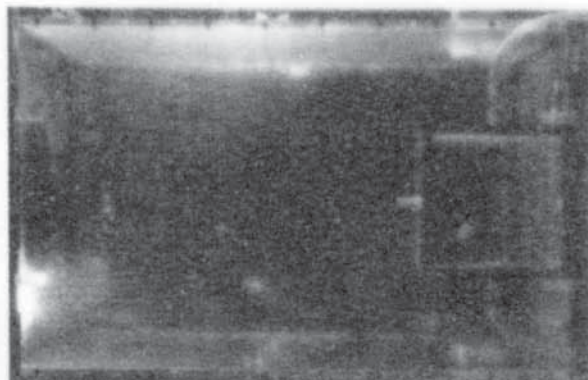
c. The intensity of droplets is increasing.



d. The intensity of droplets is increased further.



e. The tray is operating in spray regime.



f. All the liquid has entrained. The tray is dry.

Figure 8.2. Cumene - water - propan-1-ol system in perspex simulator.

Cumene - Water - Propan-1-ol system in perspex simulator.

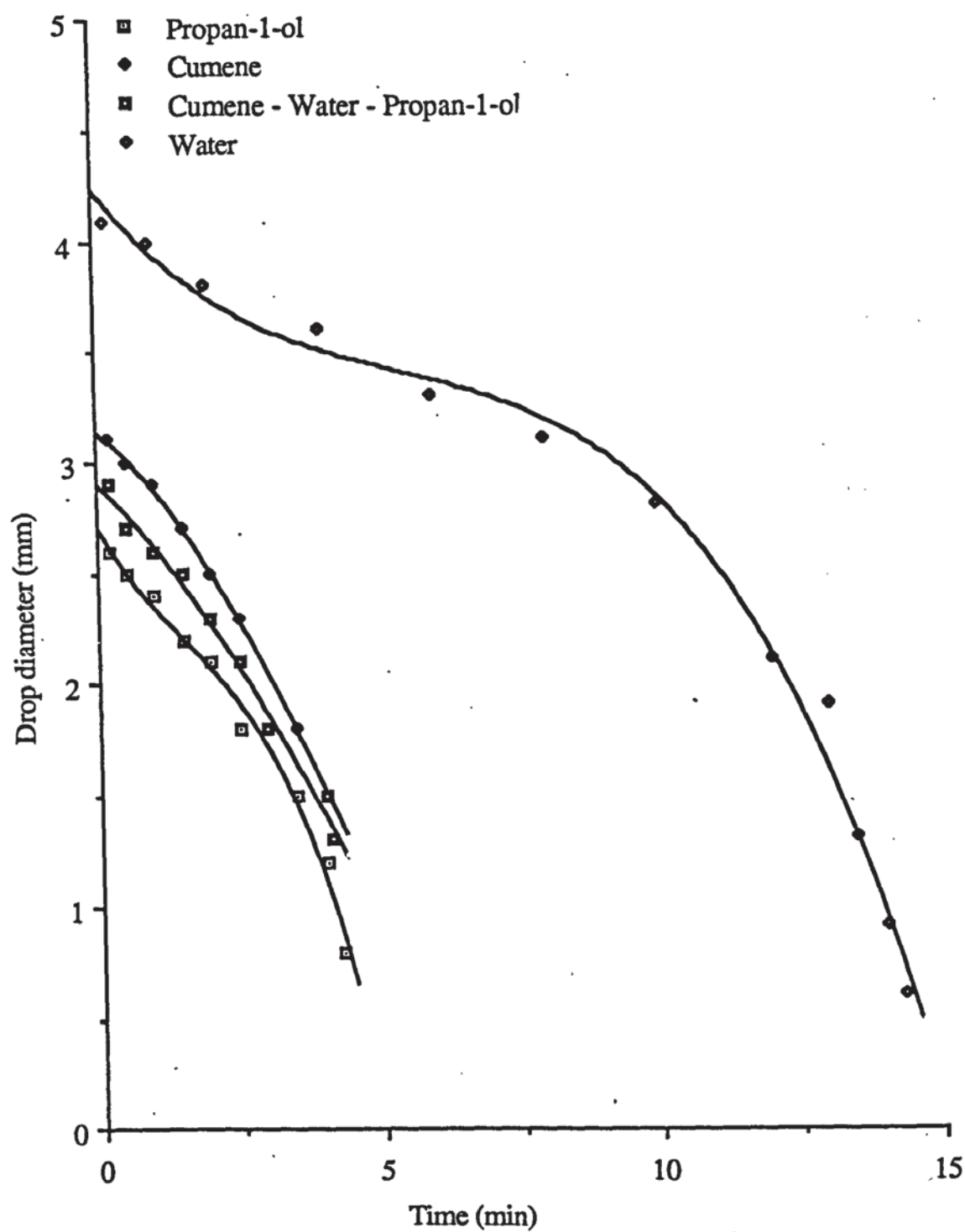


Figure 8.3. Changes in droplet diameter with time in wind tunnel.

CHAPTER 9

CONCLUSIONS

The following conclusions may be drawn from this research:

- i. Foaming was observed to occur when one liquid phase to two liquid phase mixtures were distilled in an Oldershaw column. This behaviour was similar to the foaming observed by Ross in a 'simple' one plate column.
- ii. The Oldershaw column distillation foams are similar to those produced by the gas-liquid test system on a sintered plate.
- iii. It is possible that the foaming and entrainment associated with the single/two liquid phase change may be connected with the very low surface tension of the liquid near the one phase/two phase boundary and the large changes of surface tension with composition over this range. However, surface tension has been measured and shown to change with composition and this may permit process design adjustments to minimise foaming.
- iv. The spray to bubbly transition for single and two liquid phase mixtures has been determined on a sieve plate apparatus. For single liquids the results compare well with Porter & Wong (17).
- v. The plate thickness and the ratio of hole diameter to tray thickness have an effect on the transition. This may explain discrepancies in the existing results and correlations.
- vi. A new correlation is proposed, based on the experimental results obtained in this study, which takes into consideration the effect of ratio of hole diameter to plate thickness.
- vii. Two liquid phase systems do have a spray to bubbly transition.
- viii. The spray to bubbly results for two liquid phases show that there are two distinct curves depending on how the transition is approached. In each case the transition curves lie below the pure liquid transition curves.
- ix. Correlations are proposed for the two different curves for two liquid phases.
- x. An air liquid test system has been developed for investigating Ross foaming effects in the column, using air-liquid perspex simulator columns to investigate equipment effect.
- xi. Ross systems were tested in the perspex simulator using commercial designs of sieve tray. Such systems did not produce foam but severe entrainment of the liquid into the gas stream occurred and the capacity of the tray was limited. The resulting increased entrainment of fine drops could only be reduced by working at a very

- low air velocity [i.e. the capacity of the tray is reduced, by more than 50%].
- xii. The two liquid phase spray to bubbly transition curves show the tray operating in the bubbly regime, while Ross type mixture show spray regime operation.
 - xiii. Ross systems produce spray entrainment at gas velocity and liquid holdups where normal liquids produce a bubbly mixture.
 - xiv. Packings can be used to eliminate foams.
 - xv. Additives can be used in the process design to eliminate foams.

CHAPTER 10

RECOMMENDATIONS FOR FUTURE WORK

All the experiments carried out in the air-water simulator were on a tray without a downcomer. Thus it may be that if the mixture is processed in a countercurrent column fitted with down-comers, limitations in the following areas may be noted: (a) bubbling area capacity limited by entrainment and (b) separation in the downcomer reduced by foaming. This provides a powerful tool for investigating further foaming problems in general and one/two phase mixtures in particular for the recommendations of improved design of columns processing foamy mixtures. However, the following recommendations are made:

- i. Further work is required concerning the transition from spray to bubbly regime for two liquid phases.
- ii. Further observation of foaming in the Oldershaw column which has been modified to permit samples to be taken from several plates. Studies of the effect of concentration on foaming to see if foaming can be reduced by process design. Also the effect of surface and interfacial tensions should be investigated further, since these phenomena are associated with low surface tensions. Hence, the effect of foam on plate efficiency needs further investigation.
- iii. Modification of the existing 0.45 m x 0.45 m air/liquid test rig to permit countercurrent flow and downcomer studies. Tests with the cumene-water-propan-1-ol system to include measurements of entrainment between trays and foam heights in the downcomer so as to establish the reason for reduced throughput. Then replacement of trays by packings.
- iv. The use of anti-foaming agents and additives to eliminate or control foam in process design needs further consideration i.e. their selection, economics, possible replacement for packing and other methods.
- v. Since different packings offer different surface area for gas-liquid contact, these should be investigated further to find suitable packing size, packing material and to correlate packed height with composition of the mixture.
- vi. No work is known in the open literature concerning entrainment from a one/two liquid phase system. Thus further work is required in this area.

REFERENCES

1. Ross, S., Nishioka, G., 1975, Int. Conf. on Foams, 8-10 Sept., Society of Chemical Industry (London), Brunel University.
2. Ross, S., Nishioka, G., 1975, J. Phys. Chem., 79, 1561.
3. Ross, S., 1969, Ind. Eng. Chem., Vol. 61, P. 49.
4. Ross, S., Nishioka, G., 1981, Chem. Ind., 47.
5. Riley, D. G., 1984, Ph.D. Thesis, University of Birmingham.
6. Ferraris, B. G., Morbidelli, M., 1981, A. I. Ch. E. J., 27 (1).
7. Kinoshita, M., Hashimoto, I., Takamatsu, T., 1983, J. Chem. Eng. Jpn., 16 (6).
8. Block, U., Hagner, B. A., 1976, A. I. Ch. E. J., 22 (3).
9. Bapat, P. M., Tavalatides, L. L., Smith, G. W., 1983, Chem. Eng. Sci., Vol. 38, No. 12.
10. Ross, S., Seider, W. D., 1980, Comp. & Chem. Eng., 5.
11. Boston, J. F., Shah, V. B., 1979, 86th National Meeting of A. I. Ch. E., April.
12. Ross, S., Seider, W. D., 1980, Comp. & Chem. Eng., 5, 7.
13. Prokopaski, G.J., Seider, W. D., 1980, Found. Comp. Chem. Proc. Des., Vol. 2. P. 239-272.
14. Prokopaski, G.J., Seider, W. D., 1983, A. I. Ch. E. J., 29, 49.
15. A. I. Ch. E. Research Meeting, 'Tray efficiencies in distillation columns', Final report, University of Delaware (1958).
16. A. I. Ch. E. Research Committee, 'Tray efficiencies in distillation columns', Final report, University of Michigan (1960).
17. Porter, K. E., Wong, P. F. Y., 1969, 2nd Int. Symp. on Distillation., Inst. Chem. Engrs., Brighton.
18. Fane, A. G., Sawistowski, H., 1968, Chem. Eng. Sci., 23, 943.
19. Burgess, R. G., Robinson, K., 1969, 2nd Int. Symp. on Distillation., Inst. Chem. Engrs., P. 2: 34, Brighton.
20. Andrew, S. P. S., 1969, 2nd Int. Symp. on Distillation., Inst. Chem. Engrs., Brighton.
21. Payne, J. G., Prince, R. G. H., 1977, Trans. Inst. Chem. Engrs., 55:266.
22. Pinczewski, W. V., Fell, C. J. D., 1972, Trans. Inst. Chem. Engrs., 51, 374.
23. Loon. R. E., Pinczewski, W. V., Fell, C. J. D., 1973, Trans. Inst. Chem. Engrs., 51, 374.
24. Pinczewski, W. V., Benke, N. D., Fell, C. J. D., 1975, A. I. Ch. E. J., 21 (6): 1210.

25. Pinczewski, W. V., 1973, Ph. D. Thesis, University of New South Wales.
26. Goederen, C. J. W., 1965, Chem. Eng. Sci., 20, 115.
27. Ho, G. E., Muller, R. L., Prince, R. G. H., 1969, 2nd Int. Symp. on Distillation., Inst. Chem. Engrs., Brighton.
28. Pinczewski, W. V., Fell, C. J. D., 1977, Trans. Inst. Chem. Engrs., 55, 46.
29. Pinczewski, W. V., Fell, C. J. D., 1974, Trans. Inst. Chem. Engrs., 55 (3), 224.
30. Fane, A. G., Lindsey, J. K., Sawistowski, H., 1973, Indian Chem. Engr., 15, 37.
31. Pinczewski, W. V., Fell, C. J. D., 1971, Can. J. Chem. Engng., 49, Aug, 548.
32. Calderbank, P. H., Rennie, J., 1962, Trans. Inst. Chem. Engrs., 40, 3.
33. Bikerman, J. J., 1973, 'Foams', Springer-Verlag, New York.
34. Ross, S., 1967, Chem. Eng. Prog., 63 (9), 41.
35. Ross, S., in Kirk-Othmer Encyclopedia of Chemical Technology, 1982, 3rd edn., Vol. 11, John Wiley & Sons.
36. Hart, D. J., Haselden, G. G., 1969, 2nd Int. Symp. on Distillation., Inst. Chem. Engrs., P. 1: 19, Brighton.
37. Lowery, R. P., Van Winkle, M., 1969, A. I. Ch. E. J., 15 (5), 665.
38. Hovestreydt, J., 1963, Chem. Eng. Sci., 18, 631.
39. Nakagaki, M., 1957, J. Phys. Chem., 61, P. 1266.
40. Van Ness, H. C., 1969, Ind. Eng. Chem. Fundam., 8, 464.
41. Lockett, M. J., 1986, 'Distillation Tray Fundamentals', Cambridge University Press.
42. Marangoni, C., 1871, Ann. Phys. Lpz., 143 (7), 337.
43. Zuiderweg, F. J., Harmens, A., 1958, Chem. Eng. Sci., 9, 89.
44. Bainbridge, G. S., Sawistowski, H., 1964, Chem. Eng. Sci., 19, 922.
45. Van der Meer, D., 1971, Vertakrenstechnische Gesellschaft in VDI/Insi. Chem. Engrs., Sept; Nuremberg, P. 99-108.
46. Van der Meer, D., Zuiderweg, F. J., Scheffer, H. J., 1971, Proc. Int. Solvent Extraction Conf., The Hague, Society of Chem. Ind. (London), Vol. 1, Paper 124, P. 350.
47. Glausser, W. E., 1964, Chem. Eng. Prog., 60 (10), 6-7.
48. Bolles, W. L., 1967, Chem. Eng. Sci., 63 (9), 48.
49. Sabia, A., 1966, Chem. Eng. Prog., 62 (5), 112.
50. Goldmann, T. B., 1966, World Petroleum, 37 9120 51.
51. Kerner, H. T., 1976, 'Foam Control Agents, Noyes Data Corp., New Jersey.
52. Robinson, J. V. R., Wood, W. W., 1948, J. Soc. Chem. Ind. (London),

67, 361.

53. Roberts, K., Axeberg, C., Osterlund, R., 1977, *J. Colloid Interface Sci.*, 62 (2).
54. Rennie, J., Smith, W., 1965, *Symp. on Transport Phenomena*, 67.
55. Rennie, J., Evans, F., 1962, *Brit. Chem. Engr.*, 7: 498.
56. Pozin, M. E., Mukhlenov, I. P., Tarat, E. Y., 1957, *J. Appl. Chem., USSR*, 30 (1), 43.
57. Hofhuis, P. A. M., Zuiderweg, F. J., 1979, *Inst. Chem. Engrs. Symp. Ser.*, No. 56, P. 2.2/1.
58. Muller, R. L., Prince, R. G. H., 1972, *Chem. Eng. Sci.*, Vol. 27, P. 1583.
59. Clift, R., Grace, J. R., Weber, M. E., 1978, 'Bubble Drops and Particles', Academic Press, London.
60. Kumar, R., Kuloor, N. R., in Drew, T. B., (ed)., 1970, 'Advances in Chemical Engineering', Vol. 8, Academic Press, London.
61. Calderbank, P. H., Moo-Young, M. B., 1960, *In. Symp. on Dist., Exeter*, 59.
62. Abdell-aal, H. K., Stites, G. B., Holland, C. D., 1966, *A. I. Ch. E. J.*, Vol. 12, No. 1, P. 174.
63. Pinczewski, W. V., 1981, *Chem. Eng. Sci.*, Vol. 36, P. 405.
64. Hill, J. H., Darton, R. C., 1976, *Trans. Inst. Chem. Engrs.*, Vol. 54.
65. Verschoor, H., 1950, *Trans. Inst. Chem. Engrs.*, Vol. 58, P. 52.
66. Orman, N. M., Foster, P. J., 1977, *Trans. Inst. Chem. Engrs.*, Vol. 55, P. 171.
67. Lockett, M. J., Kirk-Patrick, R. D., 1975, *Trans. Inst. Chem. Engrs.*, Vol. 53, P. 267.
68. Miyahra, T., Haga, N., Takahashi, T., 1982, *Int. Chem. Engng.*, Vol. 23, No. 3, P. 524.
69. Miyahra, T., Matsubi, Y., Yakahashi, T., 1983, *Int. Chem. Engng.*, Vol. 23, No. 3, P. 517.
70. Norbert, R., Vogelphol, A., 1982, *Ger. Chem.*, Vol. 5, P. 314.
71. Calderbank, P. H., 1975, *Trans. Inst. Chem. Engrs.*, 37, 173.
72. Calderbank, P. H., Evans, F., Rennie, J., 1960, *Int. Symp. on Dist.*, P. 51.
73. Davies, B. T., 1965, *Ph. D. Thesis*, University of Birmingham.
74. Wong, P. F. Y., 1969, *Ph. D. Thesis*, University of Birmingham.
75. Porter, K. E., Davies, B. T., Wong, P. F. Y., 1967, *Trans. Inst. Chem. Engrs.*, 45, T267.
76. Sargent, R. W. H., McMillan, W. P., 1974, *Trans. Inst. Chem. Engrs.*, Vol. 40, P. 91.
77. Hartland, S., Barber, A. D., 1974, *Trans. Inst. Chem. Engrs.*, Vol. 52, P. 43.
78. Steiner, L., Hunkeler, R., Hartland, S., 1977, *Trans. Inst. Chem. Engrs.*,

- Vol. 55, P. 153.
79. Calderbank, P. H., 1956, Trans. Inst. Chem. Engrs., Vol. 34, P. 79.
 80. Garner, F. H., Porter, K. E., 1960, Int. Symp. on Dist., P. 43.
 81. Burgess, J. M., Calderbank, P. H., 1975, Chem. Eng. Sci., Vol. 30, P. 1107.
 82. Lockett, M. J., Uddin, M. S., 1978, Trans. Inst. Chem. Engrs., Vol. 56, P. 194.
 83. Lockett, M. J., Kirk-Patrick, R. D., Uddin, M. S., 1979, Trans. Inst. Chem. Engrs., Vol. 57, P. 25.
 84. Spell, K. E., 1954, Trans. Inst. Chem. Engrs., Vol. 32, P. 168.
 85. Raper, J. A., Pinczewski, W. V., Fell, C. J. D., 1979, Inst. Chem. Engrs. Symp. Ser., No. 56, P. 2.2/57.
 86. Jeronimo, M. A., Sawistowski, H., 1973, Trans. Inst. Chem. Engrs., Vol. 51, P. 265.
 87. Yoshida, F., Nishibe, T., Nagai, S., 1965, Symp. on Transport Phenomena, P. 6: 34.
 88. Manning, E., 1964, Ind. Eng. Chem., 56, 5.
 89. Spell, K. E., Bakowski, S., 1973, Trans. Inst. Chem. Engrs., Vol. 51, P. 265.
 90. Payne, G. J., Prince, R. G. H., 1975, Trans. Inst. Chem. Engrs., Vol. 53, P. 209.
 91. Pinczewski, W. V., Yeo, H. K., Fell, C. J. D., 1973, Chem. Eng. Sci., 28, 226.
 92. Kutateladze, S. S., Styrikovick, M. A., 1958, Hydraulic Gas and Liquid Systems, Moscow.
 93. Akselrod, L. S., Yusova, G. M., 1957, J. Appl. Chem., USSR, 30.1, 739.
 94. Mukhlenov, I. J., 1958, J. Appl. Chem., 31, 40.
 95. Fane, A. G., Sawistowski, H., 1969, Int. Chem. Eng. Symp. Ser., No. 32, P. 1: 8.
 96. Prado, M., Johnson, M., Fair, J. R., 1987, Chem. Eng. Prog.,
 97. Loon. R. E., Pinczewski, W. V., Fell, C. J. D., 1972, Trans. Inst. Chem. Engrs., Vol. 50, P. 102.
 98. Lockett, M. J., Spiller, G. S., Porter, K. E., 1976, Trans. Inst. Chem. Engrs., Vol. 54, P. 302.
 99. Porter, K. E., Jenkins, J. D., 1979, Inst. Chem. Eng. Symp. Ser., No. 56, Vol. 3.
 100. Banerjee, J. S., Roy, N. K., Rao, M. N., 1969, Indian J. Tech., 7: 308.
 101. Lockett, M. J., 1981, Trans. Inst. Chem. Engrs., Vol. 59, P. 26.
 102. Prince, R. G. H., Jones, A. P., Panic, A. J., 1979, Inst. Chem. Eng. Symp. Ser., No. 56, P. 2.2: 27.
 103. Barber, A. D., Wijn, E. F., 1979, Inst. Chem. Eng. Symp. Ser., No. 56,

- P. 3.3: 15.
104. Ruff, K., 1974, *Chemie-Ing-Techn*, Nr. 18, 46 Jhrg, 769.
 105. Chen, J. J. J., Kwan, W. K., Wong, P. F. Y., *The Third Specific Congress*, Vol. 1, P.174.
 106. Wong, P. F. Y., Kwan, W. K., 1979, *Trans. Inst. Chem. Engrs.*, Vol. 57, P. 205.
 107. Eld, A. C., 1953, *Petrol Refiner*, 32, 5.
 108. Hunt, C. A., Hanson, D. N., Witke, K. E., 1955, *A. I. Ch. E. J.*, 441.
 109. Kister, H. Z., Pinczewski, W. V., Fell, C. J. D., 1981, *Ind. Eng. Chem. Proc. Des. Dev.*, 20 (3), 528.
 110. Kister, H. Z., Pinczewski, W. V., Fell, C. J. D., 1981, Paper Presented at the 90th National AIChE Meeting, Houston, April 1981.
 111. Thomas, W. J., Ogboga, O., 1978, *Ind. Eng. Chem. Proc. Des. Dev.*, 17 (4), 429.
 112. Fair, J. R., 1961, *Petro. Chem. Eng.* 33, Sept.
 113. Stichlmair, J., 1978, *Grundlagen Der Dimensionierung Des Gas/Flussig Keit-Kontak Apparatus-Boden Kolonne*, Verlag Chemie.
 114. Friend, L., Lemieux, E. J., Schreiner, W. C., 1960, *Chem. Engr*, 67, 151, Oct.
 115. Bain, J. L., Van Winkle, M., 1961, *A. I. Ch. E. J.*, 7, 363.
 116. Van Winkle, M., 1967, *'Distillation'*, Mc Graw Hill.
 117. Nutter, D. E., 1972, *Chem. Eng. Prog. Symp. Ser.*, No. 124, 68, 73.
 118. Raper, J. A., 1980, Ph. D. Thesis, University of New South Wales.
 119. Lemieux, E. J., Scotti, L. J., 1969, *Chem. Eng. Prog.*, 65 (3), 52.
 120. Fair, J. R., in R. H. Perry (ed), 1984, *Chem. Eng. Handbook*, 6th edn., McGraw Hill, NY.
 121. Zuiderweg, F. J., 1982, *Chem. Eng. Sci.*, Vol. 37, No. 10. P. 1441.
 122. Kister, H. Z., Hass, J. R., 1987, *Inst. Chem. Eng. Symp. Ser.*, No. 104, P. A483-A494.
 123. Newitt, D. M., Dombrowski, N., Knelmen, F. H., 1954, *Trans. Inst. Chem. Engrs.*, Vol. 32, P. 244.
 124. Davies, R. F., 1940, *Proc. Inst. Mech. Eng.*, 149, 198.
 125. Raleigh, Lord J. W. S., 1899, *Phil. Mag.*, P. 321.
 126. Lane, W. R., 1951, *Ind. Eng. Chem.*, 43, 1312.
 127. Dombrowski, N., Fraser, R. P., 1954, *Phil. Trans.*, 247A, 101.
 128. Teller, R. D., Rood, R. D., 1962, *A. I. Ch. E. J.*, 8, 369.
 129. Nielsen, R. D., Tek, M. R., York, J. L., 1965, *Proc. Symp. on Two Phase Flow*, Exeter.

130. Goeddle, E. F., Yuen, M. L., 1970, Fluid Mech., 40, 495.
131. Murphree, E. W., 1925, Ind. Eng. Chem., 17, 747.
132. Hausen, H., 1965, Chem. Eng. Tech., 25, 595.
133. Standart, G. L., 1965, Chem. Eng. Sci., 20, 611.
134. The Chemical Engineer, 1967, No. 206, CE 63.
135. Hartman, M., Griger, K., Standart, G. L., 1967, Chem. Proc. Eng., 48 (7), 63.
136. Hartman, M., Griger, K., Standart, G. L., 1967, Chem. Proc. Eng., 48 (8), 63.
137. Holland, C. D., 1963, 'Multicomponent Distillation', Prentice Hall.
138. Holland, C. D., Mc Mohan, K. S., 1970, Chem. Eng. Sci., 25, 431.
139. Holland, C. D., 1980, Chem. Eng. Sci., 35, 2235.
140. Standart, G., 1971, Chem. Eng. Sci., 26, 985.
141. Medina, A. G., Ashton, N. A., Mc Dermott, C., 1978, Chem. Eng. Sci., 33, 331.
142. Colburn, A. P., 1936, Ind. Eng. Chem., 17, 526.
143. Asquith, J. P., 1960, Int. Symp. on Distillation, p. 81.
144. Shakov, Yu. A., Noskov, A. A., Romankov, P. G., 1964, P. G. Zh. Prikl. Khim., Leningr., 37 (9): 2074.
145. Eduljee, H. E., 1958, Brit. Chem. Eng., 3, 14.
146. Foss, A. S., Gester, J. A., Pigford, R. L., 1958, A. I. Ch. E. J., 4, 231.
147. Wong, P. F. Y., Porter, K. E., 1967, Birmingham Chemical Engineer.
148. Zuiderweg, F. J., 1982, Chem. Eng. Sci., Vol. 37, No. 10, P. 1411.
149. Shinskey, F. G., 1977, 'Distillation Control', Mc Graw Hill, New York.
150. Bortolini, P., Brambilla, A., Nencetti, G. F., 1981, Proceedings Chempor '81, Porto, Portugal.
151. Zuiderweg, F. J., Verburg, H., Gilissen, F. H., 1960, Int. Symp. on Dist., P. 201.
152. Ashton, N. A., Arrowsmith, A., Yu, C. J., 1987, Inst. Chem. Eng. Symp. Ser., No. 104, P. B113-B126.
153. Cheung, W. W., 1983, Ph.D. Thesis, University of Aston in Birmingham.
154. Weast, R. C., (ed), 1987, HandBook of Chemistry and Physics (68th edition), CRC Press Inc.
155. Dean, J. J., (ed), 1972, Langes Handbook of Chemistry (13th edition), Mc Grawhill Book Company.

APPENDICES

APPENDIX 1 PHYSICAL PROPERTY DATA

Copound	Molecular Weight	Viscosity (Cp - @ 20°C)	Density kg/m ³	Surface tension dynes/cm (@ 20°C)	Boiling point (°C)	Melting point (°C)	Flash point (°C)
Acetone	50.08	0.326	789.9	32.7	56.24	95.35	-20.0
Benzene	78.11	0.652	876.5	30.22	80.10	5.53	-11.0
n-Butanol	74.12	2.948	809.8	20.7	117.7	-88.6	35.0
Cumene	120.19	2.18	861.8	-	152.4	-	-
Cyclohexane	84.16	0.68	778.5	25.5	80.7	6.5	-18.0
Ethanol	22.75	1.20	789.3	22.75	78.3	-114.0	8.0
Ethylene glycol	47.7	1.99	1 108.8	47.7	197.6	-13.0	110.0
n-Hexane	18.43	0.326	660.3	18.43	68.7	-95.4	-23.0
Kerosene	-	-	768.0	48.0	150-300	-	-
MEK	72.11	0.417	805.4	24.6	79.6	-	-
Methanol	32.61	0.597	791.4	22.61	64.7	-97.7	11.0
Propan-1-ol	72.88	1.13	803.5	23.4	97.2	126.2	15.0
Water	18.43	1.002	998.2	72.88	100.0	-	-

The data given in this table is from references (154,155).

APPENDIX 2

POLYNOMIAL COMPUTER PROGRAMME

```

C      PROGRAM TO FIT A POLYNOMIAL TO A SET OF DATA AND COMPUTE
C      THE COEFF. OF THE NORMAL EQUATION FOR LEAST SQUARE
C      PARAMETERS ARE
C          X,Y, ARRAY OF X,Y VALUES
C          N  NUMBER OF DATA PAIRS
C          MS,MF, THE RANGE OF DEGREE OF POLYNOMIALS
C      ARRAY OF COEFFS. OF LEAST SQUARE POLYNOMIALS
C
      DIMENSION X(500),Y(500),C(10),A(10,11),XN(500)
      DIMENSION XX(500),YY(500)
C
C      READ IN MS,MF,THE PROGRAM WILL FIND COEFFS FOR EACH DEGREE OF
C      POLYNOMIAL FROM MS TO MF
C      TO CHECK IF MAXIMUM DEGREE REQUESTED EXCEEDS N-1 IF REDUCE TO
C      N-1 AND PRINT MESSAGE
C
      READ(7,*)N
      MS=1
      MF=6
      DO 3 I=1,N
      READ(7,*)X X(I),YY(I)
3      CONTINUE
C
      DO 2 I=1,N
      X(I)=XX(I)
      Y(I)=YY(I)
2      CONTINUE
C
      IF(MF.LE.(N-1)) GOTO 5
      MF = N - 1
5      MFP1=MF+1
      MFP2=MF+2
C      PUT ONE IN TO A NEW ARRAY THIS WILL HOLD POWERS OF THE X VALUES
C      AS IT PROCEEDS

```



```

DO 10 I = 1,N
10  XN(I)=1
C    COMPUTE FIRST COLUMN AND N+1 ST COLUMN OF A,I MOVES DOWN THE
C    ROWS,J SUMS OVER THE N VALUES
      DO 30 I=1,MFP1
        A(I,1) = 0.0
        A(I,MFP2)=0.0
        DO 20 J = 1,N
          A(I,1) = A(I,1) + XN(J)
          A(I,MFP2)=A(I,MFP2)+Y(J)*XN(J)
20    XN(J)=XN(J)*X(J)
30    CONTINUE
C    COMPUTE THE LAST ROW OF A I MOVE DOWN THE ROWS, J SUM OVER THE
C    N VALUES
      DO 50 I=2,MFP1
        A(MFP1,I)=0.0
        DO 40 J = 1,N
          A(MFP1,I)=A(MFP1,I)+XN(J)
40    XN(J) = XN(J)*X(J)
50    CONTINUE
C    FILL THE REST OF THE MATRIX
      DO 70 J=2,MFP1
        DO 60 I=1,MF
          A(I,J)=A(I+1,J-1)
60    CONTINUE
70    CONTINUE
C    CALL SUBROUTINE TO SOLVE THE SYSTEM FOR DEGREE MS TO MF
C    GET THE LU DECOMPOSITION OF A
      CALL LUES(A,MFP1,10)
C    RESET THE R.HS INTO C
      MSP1 = MS + 1
      DO 95 I=MSP1,MFP1
        DO 90 J =1,I
90    C(J)= A(J,MFP2)
        CALL SSLE(A,C,I,10)
        IM1=I-1
C    WRITE OUT THE COEFF OF THE LEAST SQUARE
C    POLYNOMIAL
C    PRINT*,"COEFFICIENTS"

```

```

C      WRITE (*,202)IM1, (C(J), J=1,I)
202  FORMAT(3X,I5,4X,8(G16.7,2X))
C
      CALL EQUATION(C,I)
C
C      COMPUT AND PRINT VALUES OF BETA=SUM OF DEV SQUARED/(N-M-1)
      BETA =0.0
      DO 94 IPT = 1,N
      SUM=0.0
      DO 93 ICOEF = 2,I
      JCOEF=I-ICOEF+2
      SUM = (SUM + C(JCOEF))*X(IPT)
93    CONTINUE
      SUM=SUM+C(1)
      BETA=BETA+(Y(IPT)-SUM)**2
94    CONTINUE
      BETA = BETA/(N-I)
      WRITE (*,203) BETA
203  FORMAT(3X,F10.5)
95    CONTINUE
      STOP
      END

```

C

C*****

```

      SUBROUTINE EQUATION(C,I)
C
      DIMENSION C(10)
C
      M=I-1
      GOTO(10,20,30,40,50,60,70,80,90)M
10    WRITE(*,100) C(1),(C(J),J=1,J=2,I)
100   FORMAT(1X,'Y = ',F12.4,F12.4,'X**',I1)
      GOTO 999
20    WRITE(*,200) C(1),(C(J),J=1,J=2,I)
200   FORMAT(1X,'Y = ',F12.4,2(F12.4,'X**',I1))
      GOTO 999
30    WRITE(*,300) C(1),(C(J),J=1,J=2,I)
300   FORMAT(1X,'Y = ',F12.4,3(F12.4,'X**',I1))

```

```

      GOTO 999
40    WRITE(*,400) C(1),(C(J),J-1,J=2,I)
400   FORMAT(1X,'Y = ',F12.4,4(F12.4,'X**',I1))
      GOTO 999
50    WRITE(*,500) C(1),(C(J),J-1,J=2,I)
500   FORMAT(1X,'Y = ',F12.4,5(F12.4,'X**',I1))
60    WRITE(*,600) C(1),(C(J),J-1,J=2,I)
600   FORMAT(1X,'Y = ',F12.4,6(F12.4,'X**',I1))
      GOTO 999
70    WRITE(*,700) C(1),(C(J),J-1,J=2,I)
700   FORMAT(1X,'Y = ',F12.4,7(F12.4,'X**',I1))
      GOTO 999
80    WRITE(*,800) C(1),(C(J),J-1,J=2,I)
800   FORMAT(1X,'Y = ',F12.4,8(F12.4,'X**',I1))
      GOTO 999
90    WRITE(*,900) C(1),(C(J),J-1,J=2,I)
900   FORMAT(1X,'Y = ',F12.4,9(F12.4,'X**',I1))
C
999   RETURN
      END

C
C*****
      SUBROUTINE LUES(A,N,NDIM)
C
      DIMENSION A(NDIM,NDIM)
C      THIS ROUTINE FORMS LU EQUIVALENT OF SQUARE
C      THE VALUES ARE NOT INCLUDED IN THE RESULT
      DO 30 I = 1,N
        DO 30 J = 2,N
          SUM=0.0
          IF (J.GT.I)GOTO 15
          JM1=J-1
          DO 10 K=1,JM1
10         SUM=SUM+A(I,K)*A(K,J)
          A(I,J)=A(I,J)-SUM
          GO TO 30
15        IM1=I-1
          IF (IM1.EQ.0.0)GO TO 25

```



```

        DO 20 K=1,IM1
20      SUM = SUM +A(I,K)*A(K,J)
C      TEST FOR SMALL VALUE ON DIAGONAL
25      IF(ABS(A(I,I)).LT.1.E-10)GOTO 99
        A(I,I)=(A(I,I)-SUM)/A(I,I)
30      CONTINUE
        RETURN
99      WRITE (*,100) I
100     FORMAT(5X,I10.5,'REDUCTION NOT COMPLETED SMALL DIVISOR')
        RETURN
        END

C
C*****
SUBROUTINE SSLE (A,B,N,NDIM)
C
        DIMENSION A(NDIM,NDIM), B(NDIM)
C      THIS SUBROUTINE FINDS THE SOLUTION TO SET OF LINEAR EQUATIONS
C      DO THE REDUCTION STEP
        B(1)=B(1)/A(1,1)
        DO 20 I = 2,N
            IM1=I-1
2        CONTINUE
            SUM =0.0
            DO 10 K=1,IM1
10         SUM=SUM+A(I,K)*B(K)
20         B(I)=(B(I)-SUM)/A(I,I)
C      BACK SUBSTITUTION ELEMENT OF U ON DIAGONAL ARE ALL ONES
        DO 40 J = 2,N
            SUM=0.0
            DO 30 K = NMJP2,N
30         SUM=SUM+A(NMJP1,K)*B(K)
40         B(NMJP1)=B(NMJP1)-SUM
            RETURN
        END
EOF..

```

APPENDIX 3
LIQUID PROFILE IN OLDERSHAW COLUMN AT VARIOUS VOLUME
RATIOS OF WATER/n-HEXANE

Volume ratio of water/n-hexane	Plate no.	% n-Hexane	% Propan-1-ol	Temp.(°C)
2.0	1	15.192	60.402	-
	2	18.369	60.995	91.8
	7	31.406	48.340	91.5
	11	33.893	44.846	91.0
	12	55.375	25.602	91.0
	14	56.979	25.798	90.8
	16	56.023	24.071	89.5
	17	56.917	23.839	89.8
	19	58.034	23.839	89.5
	21	59.579	22.839	90.2
	27	61.121	22.389	90.2
	32	61.850	21.071	90.5
	34	62.765	20.642	60.7
	36	63.840	15.952	60.0
	37	74.314	15.340	60.2
	39	75.518	14.101	60.1
	41	77.481	13.455	59.5
	46	80.517	12.501	59.5
	51	83.964	11.367	56.5
	52	86.984	10.014	57.0

Volume ratio of water/n-hexane	Plate no.	% n-Hexane	% Propan-1-ol	Temp.(°C)
1.0	1	25.335	68.052	-
	2	22.091	59.492	89.0
	7	20.086	52.801	89.5
	11	18.383	50.487	89.0
	12	15.223	47.861	88.5
	14	14.367	44.151	88.5
	16	19.938	30.143	87.3
	17	18.858	30.390	87.5
	19	18.558	30.690	87.5
	21	19.203	30.063	88.8
	27	17.293	29.987	85.5
	32	17.738	29.052	59.8
	34	16.308	29.266	59.0
	36	11.638	22.122	59.5
	37	10.425	22.825	59.5
	39	10.887	21.147	58.6
	41	9.310	22.538	58.6
	46	9.930	21.395	58.6
	51	8.298	22.533	58.8
	52	8.939	20.369	60.0

Volume ratio of water/n-hexane	Plate no.	% n-Hexane	% Propan-1-ol	Temp.(°C)
0.5	1	6.171	75.035	-
	2	12.563	67.001	88.5
	7	22.226	58.853	89.0
	11	33.654	50.029	88.5
	12	34.087	47.891	88.5
	14	41.190	42.005	88.5
	16	56.750	29.105	87.3
	17	57.367	28.716	87.8
	19	55.971	28.339	88.0
	21	57.453	27.445	88.5
	27	57.885	27.149	60.5
	32	67.193	22.410	59.5
	34	68.685	21.887	58.7
	36	70.222	20.385	59.3
	37	71.844	20.503	59.2
	39	73.264	18.374	58.8
	41	75.731	15.701	58.8
	46	79.635	13.514	57.2
	51	82.812	11.362	56.5
	52	83.750	10.234	59.0

Volume ratio of water/n-hexane	Plate no.	% n-Hexane	% Propan-1-ol	Temp.(°C)
0.20	1	5.113	70.734	-
	2	16.130	63.738	89.5
	7	22.916	58.345	87.2
	11	29.582	50.734	60.5
	12	38.113	42.675	60.0
	14	50.338	30.573	59.8
	16	50.028	30.966	58.0
	17	52.188	28.136	58.7
	19	53.521	25.240	58.0
	21	77.721	18.857	59.5
	27	77.504	17.229	58.5
	32	78.210	15.651	57.2
	34	79.817	14.548	56.5
	36	79.461	14.695	56.8
	37	80.229	14.865	56.5
	39	80.809	13.222	55.8
	41	80.609	13.861	55.5
	46	81.399	12.350	52.5
	51	81.343	12.492	50.0
	52	81.279	12.858	39.5

APPENDIX 4

SURFACE TENSION RESULTS

Volume ratio of water/n-hexane	% n-Hexane	% Propan-1-ol	Surface tension (dynes/cm)
0.20	12.22	35.5	7.5
	10.6	41.7	8.1
	9.23	46.5	8.9
	8.33	50.0	9.5
	7.69	53.85	11.4
	7.15	57.14	13.5
	6.25	62.50	14.9
	5.0	70.0	16.8
	4.17	75.0	18.7
	3.57	78.57	19.8
	2.78	83.33	20.5
	2.28	86.36	20.9
	1.81	92.11	20.0
	0.83	95.04	19.1
	0.52	96.86	18.9
0.25	22.4	42.5	10.7
	21.12	46.8	11.8
	20.0	50.0	12.5
	18.18	54.55	13.4
	16.67	58.33	15.5
	13.33	66.67	18.6
	10.53	73.68	20.9
	8.0	80.0	22.1
	5.0	87.5	22.0
	3.33	91.67	20.7
	2.10	94.74	20.4

Volume ratio of water/n-hexane	% n-Hexane	% Propan-1-ol	Surface tension (dynes/cm)
0.50	26.55	42.5	15.4
	26.31	45.25	16.1
	23.25	52.24	17.2
	21.43	57.14	17.9
	20.0	60.0	18.9
	17.64	64.71	20.4
	15.75	68.42	21.6
	14.29	71.43	23.0
	11.54	76.92	23.8
	9.68	80.65	24.2
	6.52	86.96	23.9
	2.83	94.34	22.4
1.0	32.16	44.27	18.4
	30.55	48.15	19.8
	28.99	51.26	20.6
	27.27	54.55	22.0
	25.0	58.33	24.5
	21.42	64.29	25.9
	18.75	68.75	27.3
	16.67	72.22	28.0
	12.0	80.0	27.4
	7.5	87.50	25.8
	5.45	90.91	25.1

Volume ratio of water/n-hexane	% n-hexane	% Propan-1-ol	Surface tension (dynes/cm)
1.5	37.52	45.19	23.4
	34.29	48.13	25.2
	31.59	51.80	27.9
	28.66	57.62	30.3
	26.67	60.0	30.9
	25.0	62.5	31.5
	23.54	64.7	32.8
	19.05	71.43	32.5
	15.39	76.92	31.2
	11.11	83.33	30.1
	7.14	89.29	29.0
	3.79	94.34	28.5
	2.57	96.15	28.0
2.0	44.62	45.31	26.6
	42.50	48.5	30.1
	40.52	51.24	32.7
	34.55	58.12	34.6
	31.25	58.41	35.1
	29.41	62.5	37.5
	27.77	64.71	37.6
	23.81	66.67	38.4
	19.23	71.43	38.7
	16.12	76.92	36.8
	10.87	80.65	34.5
	6.58	86.96	32.0
	5.57	92.10	31.6
	3.79	96.15	30.4

APPENDIX 5 **SPRAY TO BUBBLY TRANSITION RESULTS**

Tray number 1

Run no.	ρ_g [kg/m ³]	ρ_l [kg/m ³]	u_s [m/s]	u_h [m/s]	h_{cl} [cm]	vol_w [m ³]	vol_k [m ³]
Water							
1	1.1845	998.232	0.45	8.180	0.20		
2			0.65	11.82	0.30		
3			0.86	15.64	0.40		
4			1.15	20.91	0.60		
5			1.25	22.73	0.68		
6			1.44	26.18	0.88		
7			1.70	30.91	1.03		
Kerosene							
1	1.1885	768.960	0.40	7.270	0.24		
2			0.60	10.91	0.33		
3			0.73	13.27	0.40		
4			0.97	17.64	0.58		
5			1.07	19.45	0.69		
6			1.30	23.64	0.90		
7			1.57	28.55	1.12		
Water fixed							
1	1.2088	917.9868	0.47	8.550	0.23	304.02	163.500
2		856.0834	0.75	13.64	0.39		488.720
3		840.2600	0.90	16.36	0.49		691.980
4		821.6929	1.14	20.73	0.66		1037.50
5		814.8144	1.24	22.55	0.73		1179.82
6		805.6435	1.46	26.36	0.95		1627.00
7		803.3508	1.56	28.63	1.03		1789.62
Kerosene fixed							
1		826.4600	0.50	9.090	0.20	102.510	304.02
2		897.3523	0.82	14.91	0.34	387.080	
3		927.1577	1.10	20.00	0.48	671.660	
4		940.9140	1.27	23.09	0.60	915.570	
5		952.3776	1.55	28.18	0.75	1220.47	
6		954.6703	1.65	30.00	0.78	1281.45	

Tray number 2

Run no.	ρ_g [kg/m ³]	ρ_l [kg/m ³]	u_s [m/s]	u_h [m/s]	h_{cl} [cm]	vol_w [m ³]	vol_k [m ³]
Water							
1	1.1925	998.433	0.60	11.28	0.56		
2			0.74	13.91	0.70		
3			0.90	16.92	0.85		
4			1.06	19.92	1.12		
5			1.30	24.44	1.20		
6			1.40	26.32	1.27		
7			1.42	26.69	1.27		
8			1.66	31.20	1.40		
Kerosene							
1	1.1925	768.960	0.50	9.400	0.59		
2			0.70	13.16	0.83		
3			0.80	15.04	0.95		
4			0.85	15.98	1.01		
5			1.05	19.74	1.17		
6			1.27	23.87	1.36		
7			1.45	27.26	1.48		
Water fixed							
1	1.1925	847.0454	0.62	11.65	0.65	445.90	875.330
2		828.6724	0.80	15.04	0.86		1302.90
3		819.4859	0.98	18.42	1.02		1627.41
4		814.8926	1.04	19.55	1.08		1749.37
5		810.2993	1.18	22.18	1.21		2013.62
6		808.0027	1.30	24.44	1.30		2196.55
7		803.4095	1.51	28.38	1.44		2481.13
Kerosene fixed							
1		872.6000	0.60	11.28	0.40	367.16	445.90
2		904.8435	0.84	15.79	0.54	651.73	
3		930.1778	1.08	20.30	0.74	1058.27	
4		943.9964	1.32	24.81	0.92	1424.14	
5		953.2088	1.50	28.20	1.08	1749.37	
6		953.2088	1.62	30.45	1.12	1830.68	

Tray number 3

Run no.	ρ_g [kg/m ³]	ρ_l [kg/m ³]	u_s [m/s]	u_h [m/s]	h_{cl} [cm]	vol_w [m ³]	vol_k [m ³]
Water							
1	1.1885	998.623	0.48	9.860	0.70		
2			0.52	10.68	0.80		
3			0.70	14.37	1.01		
4			0.76	15.61	1.05		
5			0.90	18.48	1.30		
6			1.20	24.64	1.52		
7			1.40	28.75	1.66		
8			1.70	34.91	1.75		
Kerosene							
1	1.1925	1768.960	0.44	9.030	0.86		
2			0.60	12.32	1.12		
3			0.70	14.37	1.25		
4			0.98	20.12	1.54		
5			1.35	27.72	1.80		
6			1.35	28.75	1.82		
Water fixed							
1	1.2088	826.3283	0.50	10.27	0.89	445.90	1363.16
2		819.4441	0.60	12.32	1.01		1607.08
3		810.2651	0.76	15.61	1.20		1993.29
4		805.6757	0.90	18.48	1.36		2318.51
5		803.3810	0.95	19.51	1.48		2562.43
6		803.3810	1.00	21.36	1.50		2603.09
7		798.7915	1.38	28.34	1.73		3070.60
Kerosene fixed							
1	1.1845	888.3848	0.50	10.27	0.46	489.120	445.90
2		943.5039	0.86	17.66	0.88	1342.84	
3		954.9870	1.23	25.26	1.16	1911.98	
4		959.5803	1.47	30.18	1.30	2196.55	
5		961.8769	1.61	33.06	1.33	2257.53	

Tray number 4

Run no.	ρ_g [kg/m ³]	ρ_l [kg/m ³]	u_s [m/s]	u_h [m/s]	h_{cl} [cm]	vol_w [m ³]	vol_k [m ³]
Water							
1	1.2088	999.127	1.28	12.57	0.24		
2			1.42	13.95	0.31		
3			1.63	16.01	0.39		
4			1.71	16.80	0.42		
5			1.88	18.47	0.48		
6			1.95	19.16	0.50		
Kerosene							
1	1.2047	768.960	0.60	12.38	0.32		
2			0.67	13.75	0.42		
3			0.73	15.03	0.50		
4			0.77	15.72	0.54		
5			0.77	15.91	0.55		
6			0.84	17.19	0.59		
7			0.88	18.17	0.62		
Water fixed							
1	1.1885	895.5519	1.26	12.38	0.27	304.02	244.800
2			1.45	14.24	0.39		488.720
3			1.55	15.23	0.45		610.680
4			1.58	15.52	0.45		610.680
5			1.62	15.91	0.48		671.660
6			1.75	17.19	0.53		773.290
7			1.90	18.66	0.58		874.920
Kerosene fixed							
1	1.1845	817.3253	1.25	12.28	0.19	82.1800	304.02
2		872.6000	1.49	14.64	0.27	244.800	
3		888.7217	1.66	16.31	0.31	326.100	
4		902.5404	1.83	17.98	0.36	427.740	
5		909.4497	1.88	18.47	0.38	468.390	

Tray number 5

Run no.	ρ_g [kg/m ³]	ρ_l [kg/m ³]	u_s [m/s]	u_h [m/s]	h_{cl} [cm]	vol_w [m ³]	vol_k [m ³]
Water							
1	1.2088	999.271	1.27	11.44	0.38		
2			1.31	11.80	0.40		
3			1.46	13.15	0.43		
4			1.55	13.96	0.50		
5			1.64	14.77	0.55		
6			1.75	15.77	0.62		
7			1.89	17.03	0.70		
8			1.97	17.75	0.72		
Kerosene							
1	1.2088	768.760	1.25	11.26	0.41		
2			1.37	12.34	0.48		
3			1.45	13.06	0.50		
4			1.60	14.41	0.60		
5			1.70	15.32	0.63		
6			1.87	16.85	0.76		
7			1.91	17.21	0.78		
8			1.98	17.84	0.78		
Water fixed							
1	1.2047	894.9436	1.28	11.53	0.40	445.90	367.16
2		885.7811	1.33	11.98	0.43		428.14
3		878.9093	1.40	12.61	0.46		489.12
4		874.3281	1.45	13.06	0.48		529.78
5		856.0032	1.60	14.41	0.57		712.71
6		831.4615	1.74	15.68	0.65		875.33
7		839.9689	1.85	16.67	0.70		976.96
8		837.6783	1.94	17.48	0.74		1058.2
Kerosene fixed							
1	1.2088	789.5945	1.24	11.17	0.24	41.9400	304.02
2		812.5217	1.34	12.07	0.27	102.920	445.90
3		858.3761	1.45	13.06	0.36	285.860	
4		883.5960	1.62	14.59	0.44	448.470	
5		890.4742	1.65	14.86	0.47	509.450	
6		896.0596	1.74	15.68	0.49	550.100	
7		908.8159	1.95	17.57	0.56	692.390	

Tray number 6

Run no.	ρ_g [kg/m ³]	ρ_l [kg/m ³]	u_s [m/s]	u_h [m/s]	h_{cl} [cm]	vol_w [m ³]	vol_k [m ³]	
Water								
1	1.2006	999.970	1.26	12.74	0.50			
2			1.32	13.35	0.60			
3			1.37	13.85	0.66			
4			1.50	15.17	0.73			
5			1.58	15.98	0.80			
6			1.69	17.09	0.89			
7			1.86	18.81	0.94			
8			1.97	19.92	0.99			
Kerosene								
1	1.2047	768.960	1.25	12.64	0.61			
2			1.36	13.75	0.82			
3			1.47	14.86	0.94			
4			1.60	16.18	1.05			
5			1.61	16.28	1.05			
6			1.75	17.69	1.16			
7			1.88	19.01	1.20			
8			1.93	19.51	1.22			
Water fixed								
1	1.1925	856.2319	1.27	12.84	0.58	445.90	733.040	
2		835.5623	1.40	14.16	0.75		1078.59	
3		830.9690	1.45	14.66	0.82		1220.88	
4		824.0791	1.50	15.17	0.90		1383.49	
5		817.1892	1.72	17.39	1.04		1668.06	
6		812.5960	1.92	19.41	1.13		1851.00	
Kerosene fixed								
1	1.1925	849.3421	1.25	12.64	0.34	849.3421	445.90	
2		888.3848	1.38	13.95	0.46			489.120
3		904.4612	1.49	15.07	0.53			631.410
4		918.2410	1.60	16.18	0.62			814.350
5		922.8342	1.72	17.39	0.67			915.980
6		929.7241	1.80	18.20	0.72			1017.61
7		932.0207	1.95	19.72	0.75			1078.59

Tray number 7

Run no.	ρ_g [kg/m ³]	ρ_l [kg/m ³]	u_s [m/s]	u_h [m/s]	h_{cl} [cm]	vol_w [m ³]	vol_k [m ³]	
Water								
1	1.1925	998.433	1.29	13.90	1.05			
2		998.433	1.34	14.42	1.20			
3			1.45	15.61	1.40			
4			1.47	15.82	1.41			
5			1.64	17.65	1.69			
6			1.84	19.81	1.85			
7			1.93	20.78	1.89			
Kerosene								
1	1.1925	768.960	1.22	13.13	1.10			
2			1.30	13.99	1.29			
3			1.45	15.61	1.55			
4			1.51	16.25	1.69			
5			1.62	17.44	1.83			
6			1.65	17.76	1.86			
7			1.80	19.38	2.02			
8			1.90	20.45	2.06			
Water fixed								
1	1.2047	824.0335	1.25	13.46	0.90	445.90	1383.49	
2		810.2651	1.37	14.75	1.22		2033.94	
3		805.6757	1.45	15.61	1.37		2338.84	
4		805.6757	1.47	15.82	1.38		2359.17	
5		801.0862	1.60	17.22	1.59		2786.02	
6		798.7915	1.70	18.30	1.72		3050.27	
7		796.4968	1.91	20.56	1.90		3416.15	
Kerosene fixed								
1	1.2088	913.6477	1.27	13.67	0.60	773.690	445.90	
2		934.3174	1.46	15.72	0.79			1159.90
3		948.0971	1.64	17.65	1.00			1586.76
4		952.6904	1.77	19.05	1.10			1790.02
5		954.9870	1.93	20.78	1.17			1932.31

Tray number 8

Run no.	ρ_g [kg/m ³]	ρ_l [kg/m ³]	u_s [m/s]	u_h [m/s]	h_{cl} [cm]	vol_w [m ³]	vol_k [m ³]	
Water								
1	1.1885	998.62	0.47	8.550	0.19			
2			0.70	12.73	0.30			
3			0.85	15.45	0.38			
4			1.05	19.09	0.48			
5			1.31	23.82	0.69			
6			1.50	27.27	0.89			
7			1.82	33.09	1.05			
Kerosene								
1	1.2006	768.960	0.45	8.180	0.22			
2			0.64	11.64	0.29			
3			0.79	14.36	0.38			
4			0.96	17.45	0.48			
5			1.11	20.18	0.59			
6			1.32	24.00	0.80			
7			1.67	30.36	1.10			
Water fixed								
1	1.1845	941.0648	0.45	8.180	0.20	304.02	102.01	
2		872.2229	0.75	13.64	0.33		366.76	
3		830.9177	1.10	20.00	0.55		813.94	
4		812.5599	1.38	25.09	0.80		1322.1	
5		807.9704	1.46	26.55	0.88		1484.7	
6		801.0862	1.70	30.91	1.05		1830.2	
Kerosene fixed								
1	1.2006	819.4815	0.49	8.910	0.17	41.5300	304.02	
2		890.6708	0.86	15.64	0.32			346.430
3		913.6351	1.00	18.18	0.40			509.040
4		936.5994	1.28	23.27	0.56			834.270
5		945.2851	1.46	26.55	0.66			1037.53
6		952.6744	1.63	29.64	0.75			1220.47
7		954.9708	1.75	31.82	0.78			1281.45

Tray number 9

Run no.	ρ_g [kg/m ³]	ρ_l [kg/m ³]	u_s [m/s]	u_h [m/s]	h_{cl} [cm]	vol_w [m ³]	vol_k [m ³]	
Water								
1	1.1885	998.021	1.25	11.26	0.50			
2			1.33	11.98	0.53			
3			1.45	13.06	0.57			
4			1.52	13.69	0.63			
5			1.70	15.32	0.74			
6			1.79	16.13	0.78			
7			1.94	17.48	0.85			
Kerosene								
1	1.1845	768.960	1.23	11.08	0.58			
2			1.33	11.98	0.63			
3			1.45	13.06	0.72			
4			1.58	14.23	0.83			
5			1.58	14.23	0.85			
6			1.74	15.68	0.94			
7			1.81	16.31	0.94			
Water fixed								
1	1.2006	863.3875	1.24	11.17	0.53	445.90	631.410	
2		854.1751	1.35	12.16	0.59		753.370	
3		842.6595	1.49	13.42	0.68		936.310	
4		840.3564	1.59	14.32	0.73		1037.94	
5		831.1440	1.69	15.23	0.82		1220.88	
6		826.5378	1.83	16.49	0.89		1363.16	
Kerosene fixed								
1	1.2088	819.6284	1.26	11.35	0.28	123.24	445.90	
2		890.2823	1.45	13.06	0.39			346.84
3		886.4186	1.62	14.59	0.45			468.80
4		895.6311	1.70	15.32	0.49			550.10
5		909.4497	1.90	17.12	0.56			692.39

Tray number 10

Run no.	ρ_g [kg/m ³]	ρ_l [kg/m ³]	u_s [m/s]	u_h [m/s]	h_{cl} [cm]	vol_w [m ³]	vol_k [m ³]	
Water								
1	1.1885	998.433	1.24	12.54	0.62			
2			1.39	14.05	0.80			
3			1.52	15.37	0.89			
4			1.65	16.68	0.99			
5			1.76	17.80	1.05			
6			1.84	18.60	1.07			
7			1.94	19.60	1.13			
Kerosene								
1	1.2006	768.960	1.22	12.34	0.64			
2			1.42	14.36	1.00			
3			1.60	16.18	1.22			
4			1.68	16.99	1.25			
5			1.81	18.30	1.34			
6			1.90	19.21	1.35			
Water fixed								
1	1.2047	842.2595	1.24	12.54	0.69	445.90	956.630	
2		833.0971	1.32	13.35	0.79		1159.90	
3		821.6440	1.45	14.66	0.95		1485.12	
4		817.0628	1.57	15.87	1.07		1729.04	
5		812.4816	1.73	17.49	1.14		1871.33	
6		810.1910	1.83	18.50	1.20		1993.29	
7		810.1910	1.88	19.01	1.21		2013.62	
Kerosene fixed								
1	1.2006	885.8887	1.25	12.64	0.45	468.800	445.90	
2		913.4014	1.44	14.56	0.59			753.370
3		922.5722	1.56	15.77	0.67			915.980
4		929.4504	1.70	17.19	0.73			1037.94
5		934.0358	1.81	18.30	0.79			1159.90
6		938.6213	1.93	19.51	0.83			1241.21

Tray number 11

Run no.	ρ_g [kg/m ³]	ρ_l [kg/m ³]	u_s [m/s]	u_h [m/s]	h_{cl} [cm]	vol_w [m ³]	vol_k [m ³]
Water							
1	1.1925	998.623	1.25	13.46	1.38		
2			1.33	14.32	1.52		
3			1.46	15.72	1.74		
4			1.57	16.90	1.90		
5			1.67	17.98	1.99		
6			1.76	18.95	2.10		
7			1.89	20.34	2.20		
Kerosene							
1	1.1925	768.960	1.46	13.13	1.47		
2			1.61	14.53	1.70		
3			1.76	15.82	1.85		
4			1.90	17.12	2.17		
5			2.04	18.41	2.29		
6			2.21	19.91	2.41		
Water fixed							
1	1.1845	803.5067	1.26	13.56	1.48	445.90	2562.43
		801.2035	1.36	14.64	1.62		2847.00
3		796.5973	1.46	15.72	1.83		3273.86
4		794.2942	1.58	17.01	2.00		3619.41
5		791.9911	1.68	18.08	2.15		3924.31
6		791.9911	1.79	19.27	2.25		4127.58
7		791.9911	1.87	20.13	2.29		4208.89
Kerosene fixed							
1	1.2088	932.9771	1.25	13.46	0.75	1078.59	445.90
2		949.1478	1.49	16.04	1.02	1627.41	
3		956.0781	1.62	17.44	1.15	1891.66	
4		960.6983	1.80	19.38	1.32	2237.21	
5		963.0084	1.95	20.99	1.34	2277.86	

Tray number 12

Run no.	ρ_g [kg/m ³]	ρ_l [kg/m ³]	u_s [m/s]	u_h [m/s]	h_{cl} [cm]	vol_w [m ³]	vol_k [m ³]
Water							
1	1.2047	999.271	1.26	11.35	0.54		
2			1.35	12.16	0.61		
3			1.40	12.61	0.62		
4			1.55	13.96	0.70		
5			1.68	15.14	0.79		
6			1.81	16.31	0.87		
7			1.95	17.57	0.91		
8			1.98	17.84	0.92		
Kerosene							
1	1.1925	768.960	1.04	11.17	0.62		
2			1.16	12.52	0.75		
3			1.26	13.51	0.81		
4			1.35	14.50	0.91		
5			1.53	16.49	1.00		
6			1.58	17.03	1.01		
Water fixed							
1	1.1885	851.7031	1.27	11.44	0.61	445.90	794.020
2		849.4047	1.31	11.80	0.62		814.350
3		840.2110	1.45	13.06	0.70		997.290
4		828.7189	1.65	14.86	0.84		1261.53
5		821.8373	1.80	16.22	0.94		1464.80
6		821.8237	1.87	16.85	0.95		1485.34
Kerosene fixed							
1	1.1925	840.2110	1.26	11.35	0.32	204.55	445.90
2		865.4936	1.38	12.43	0.38	326.51	
3		883.8810	1.50	13.51	0.44	448.47	
4		890.7763	1.61	14.50	0.47	509.45	
5		902.2684	1.69	15.23	0.52	611.08	
6		909.1636	1.85	16.67	0.56	692.39	

Tray number 13

Run no.	ρ_g [kg/m ³]	ρ_l [kg/m ³]	u_s [m/s]	u_h [m/s]	h_{cl} [cm]	vol_w [m ³]	vol_k [m ³]	
Water								
1	1.1845	998.232	1.24	13.11	0.82			
2			1.39	14.69	0.96			
3			1.52	16.07	1.05			
4			1.65	17.44	1.12			
5			1.76	18.60	1.2			
6			1.84	19.45	1.27			
7			1.94	20.51	1.29			
Kerosene								
1	1.2006	768.960	1.21	12.79	0.90			
2			1.40	14.80	1.09			
3			1.48	5.64	1.16			
4			1.70	17.97	1.35			
5			1.90	20.08	1.41			
Water fixed								
1	1.2042	828.6230	1.23	13.00	0.85	445.90	1281.86	
2		819.4441	1.35	14.27	0.98		1546.10	
3		814.8546	1.50	15.86	1.10		1790.02	
4		810.2651	1.67	17.65	1.23		2054.27	
5		807.9704	1.75	18.50	1.29		2176.23	
6		805.6757	1.89	19.98	1.35		2298.19	
Kerosene fixed								
1	1.1885	905.2559	1.24	13.11	0.54	651.730	445.90	
2		916.8064	1.37	14.48	0.61			794.020
3		930.6670	1.50	15.86	0.74			1058.27
4		937.5973	1.62	17.12	0.80			1180.23
5		939.9074	1.73	18.29	0.83			1241.21
6		942.2175	1.87	19.77	0.87			1322.51

Tray number 14

Run no.	ρ_g [kg/m ³]	ρ_l [kg/m ³]	u_s [m/s]	u_h [m/s]	h_{cl} [cm]	vol_w [m ³]	vol_k [m ³]
Water							
1	1.1925	998.802	1.25	13.46	1.45		
2			1.34	14.43	1.61		
3			1.45	15.82	1.85		
4			1.59	17.12	2.04		
5			1.65	17.76	2.08		
6			1.80	19.38	2.25		
7			1.95	20.99	2.34		
Kerosene							
1	1.1925	768.960	1.19	12.84	1.58		
2			1.31	14.05	1.81		
3			1.42	15.27	2.04		
4			1.62	17.49	2.13		
5			1.73	18.60	2.47		
Water fixed							
1	1.2006	803.3192	1.23	12.44	1.48	445.90	2562.43
2		798.7379	1.35	13.65	1.72		3050.27
3		794.1567	1.53	15.47	2.02		3660.07
4		794.1567	1.70	17.19	2.22		3706.60
5		789.5755	1.80	18.20	2.32		4269.86
6		789.5755	1.92	19.41	2.43		4493.46
Kerosene fixed							
1	1.1845	940.9140	1.24	13.35	0.89	1363.16	445.90
2		954.6703	1.42	15.29	1.15	1891.66	
3		956.9630	1.63	17.55	1.36	2054.27	
4		963.8412	1.76	18.95	1.50	2603.09	
5		966.1339	1.89	20.34	1.57	2826.68	

APPENDIX 6 **COMPUTER PROGRAMME TO CALCULATE h_{cl} FROM DIFFERENT** **SPRAY/BUBBLY TRANSITION CORRELATIONS**

```

C      MAIN PROGRAM
C      IN THE PROGRAMME HCL IS THE EXPERIMENTAL VALUE OF LIQUID HOLDUP
C      AND ZCT IS VALUE OF LIQUID HOLDUP PREDICTED BY CORRELATIONS.
      DIMENSION UH(300),HCL(300),DG(300),DL(300),DH(300),DF(300),TH(300)
      DIMENSION A(300),B(300),C(300),D(300),E(300),F(300),G(300),X(300)
      DIMENSION Y(400),ZCT(400)
      COMMON/INOUT/NSCR,NIN,NOUT
C
      NSCR=0
      NOUT=6
      NIN=8
C
      WRITE(NOUT,10)
10     FORMAT(6X,"UH",6X,"HCL",7X,"ZCT",7X,"ZCT/DH"/)
      CALL INCOR
      STOP
      END
C
C*****
      SUBROUTINE INCOR
C
C      THIS SUBROUTINE ALLOWS THE USER TO SELECT A CORRELATION FOR
C      EVALUATION OF HCL AT SPRAY REGIME TO BUBBLY REGIME TRANSITION
C
      COMMON/ DATA/US,UH,HCL,DG,DL,DH,TH,PIT,VOLW,VOLK,DF
      COMMON/INOUT/NSCR,NIN,NOUT
      COMMON/BLOCK1/N
      COMMON/BLOCK2/XST,XND,XL,XH
      CHARACTER NAMES(8)*20
C
      DATA NAMES/'PORTER/WONG','PAYNE/PRINCE','HOFHIUS/ZUIDERWEG',
      *'BARBER/WIJN','WONG/KWAN','LOCKETT CORLTON','EXIT/'

```

```

C
280    CONTINUE
C
      WRITE(NSCR,(' GIVE NSET'))
      READ(NSCR,*) NSET
      WRITE(NSCR,*) NSET
2000   CONTINUE
      CALL OPEN(NIN)
2222   WRITE(NSCR,778)
      NS=0
10     NS=NS+1
      WRITE(NSCR,*) NS
      READ(NIN,20,END=280) ITITLE
20     FORMAT(A80)
      WRITE(NSCR,*,END=280) NPOINT
      READ(NIN,*) NPOINT
      WRITE(6,21) ITITLE
21     FORMAT(A80)
C
C      WRITE MESSAGE TO INFORM USER OF AVAILABLE CORRELATIONS
C
778    FORMAT(1X,"THE SPRAY REGIME TO BUBBLY REGIME CORRELATION ARE:")
      DO 777 I=1,7
1777   WRITE(NSCR,100) I,NAMES(I)
C
100    FORMAT(1X,I2,2X,A20)
      WRITE(NSCR,444)
444    FORMAT(/1X,"SELECT THE NUMBER")
      READ(NSCR,*) NN
      IF(NN.EQ.7) THEN
        WRITE(NSCR,*) XST,XND,XL,XH,NNN
        READ(NSCR,*) XST,XND,XL,XH,NNN
      END IF
      WRITE(NOUT,300) NAMES(NN)
      WRITE(NSCR,300) NAMES(NN)
300    FORMAT(1X,'THE CORRELATION USED IS:',1X,A22,/)
C
      NCOUNT=0

```



```

211      NCOUNT=NCOUNT+1
C
      READ(NIN,*)US,UH,HCL,DG,DL,DH,TH,PIT,VOLW,VOLK,DF
C
      GO TO(1,2,3,4,5,6,7)NN
1      CALL PORTER
      GO TO 5000
2      CALL PRINCE
      GO TO 5000
3      CALL HOFHIUS
      GO TO 5000
4      CALL BARBER
      GO TO 5000
5      CALL WONG
      GO TO 5000
6      CALL LOKCOR
      GO TO 5000
7      GO TO 9999
C
5000     CONTINUE
      IF (NCOUNT-NPOINT) 211,7000,7000
7000     IF (NS-NSET) 10,8000,8000
8000     WRITE(NSCR,555)
555      FORMAT(1X,"DO YOU WANT TO TRY ANOTHER DATA")
      WRITE(NSCR,556)
556      FORMAT(1X,"IF *YES* ENTER 1 AND *NO* ENTER 0 ")
      READ(NSCR,*)NYESNO
      IF(NYESNO.EQ.1)THEN
      GO TO 2000
      ELSE
      WRITE(NSCR,666)
666      FORMAT(1X,"DO YOU WANT TO TRY ANOTHER CORRELATION")
      WRITE(NSCR,665)
665      FORMAT(1X,"IF *YES* ENTER 2 AND *NO* ENTER 3")
      READ(NSCR,*)NYESNO
      IF(NYESNO.EQ.2)THEN
      REWIND(NIN)
      GO TO 2222

```

```

        ELSE
        GO TO 3000
        END IF
        END IF
        GO TO 2000

C
9999    CONTINUE
3000    RETURN
        END

C
C*****
C
        SUBROUTINE PORTER

C
        COMMON/INOUT/NSCR,NIN,NOUT
        COMMON/ DATA/US,UH,HCL,DG,DL,DH,TH,PIT,VOLW,VOLK,DF
        COMMON/BB/ZCT

C
        UT=1.04*((DL/DG)**0.5)
        DH1=DH*2.540*100.0
        ZCT=DH1*DF*(4.0+9.0*((UH-UT)/(UH-US)))

C
        CALL OUTPUT(UH,HCL,ZCT,X)
        RETURN
        END

C
C*****C
        SUBROUTINE HOFHIUS

C
        COMMON/INOUT/NSCR,NIN,NOUT
        COMMON/ DATA/US,UH,HCL,DG,DL,DH,TH,PIT,VOLW,VOLK,DF
        COMMON/BB/ZCT

C
        G=9.81

C
        ZCT=100.0*DH*1.07*(((DG/DL)**(0.33))*(UH**(0.66)))/((G*100.0*
+DH)**(0.33)))

C

```

```

CALL OUTPUT(UH,HCL,ZCT,X)
RETURN
END

C
C*****
C
C
SUBROUTINE BARBER

C
COMMON/INOUT/NSCR,NIN,NOUT
COMMON/ DATA/US,UH,HCL,DG,DL,DH,TH,PIT,VOLW,VOLK,DF
COMMON/BB/ZCT

C
G=9.81

C
DDIF=UH*((DG/(DL-DG))**0.5)
ZCT=DH*1.35*(((DIFF/((G*(DH/100.0))**0.5))**0.4)-0.59)
+*((PIT/DH)**(1/3)))

C
CALL OUTPUT(UH,HCL,ZCT,X)
RETURN
END

C
C*****
C
C
SUBROUTINE PRINCE

C
COMMON/INOUT/NSCR,NIN,NOUT
COMMON/ DATA/US,UH,HCL,DG,DL,DH,TH,PIT,VOLW,VOLK,DF
COMMON/BB/ZCT

C
G=9.81
ZCT=DH*1.5*DF*(((DG/(DF*DL))*(UH**2))/((G*(DH*10.0)
+)**0.5))**0.5)

C
CALL OUTPUT(UH,HCL,ZCT,X)
RETURN
END

C

```



```

C*****
C
      SUBROUTINE WONG
C
      COMMON/INOUT/NSCR,NIN,NOUT
      COMMON/AA/VOID
      COMMON/ DATA/US,UH,HCL,DG,DL,DH,TH,PIT,VOLW,VOLK,DF
      COMMON/BB/ZCT
C
      G=9.81
      ZCT=DH*DF*(2.06+30.05*UH*((DG/(DL-DG))**0.5)*(1/(G**0.5)))
C
      CALL OUTPUT(UH,HCL,ZCT,X,)
      RETURN
      END
C
C*****
C
      SUBROUTINE LOKCOR
C
      COMMON/INOUT/NSCR,NIN,NOUT
      COMMON/ DATA/US,UH,HCL,DG,DL,DH,TH,PIT,VOLW,VOLK,DF
      COMMON/BB/ZCT
C
      ZCT=DH*2.78*((DG/DL)**0.5)*UH
C
      CALL OUTPUT(UH,HCL,ZCT,X)
      RETURN
      END
C
C*****
C
      SUBROUTINE OUTPUT
C
      COMMON/INOUT/NSCR,NIN,NOUT
      COMMON/ DATA/US,UH,HCL,DG,DL,DH,TH,PIT,VOLW,VOLK,DF
      COMMON/BB/ZCT
C

```

```

C      PRINT RESULTS (UH,HCL,X,Y)
C
      NOUT=6
      X=ZCT/DH
      WRITE(NOUT,200)UH,HCL,ZCT,X
C
200    FORMAT(5X,F7.4,5X,F7.4,5X,F7.4,5X,F7.4)
      RETURN
      END
C
C*****
C
      SUBROUTINE OPEN(NFILE)
C
      CHARACTER*8 FILENAME
C
      NSCR=0
      WRITE(NSCR,10) NFILE
10     FORMAT(1X,' ENTER FILE NAME FOR CHANNEL ',I4,'**')
      READ(NSCR,20) FILENAME
20     FORMAT(A8)
      OPEN(UNIT=NFILE,FILE='      '//FILENAME)
      WRITE(NSCR,30) FILENAME,NFILE
30     FORMAT(' ** FILENAME ',A8,' OPENED TO CHANNEL ',I4/)
      RETURN
      END
EOF..
EOT..

```

APPENDIX 7
DETAILS OF SIEVE TRAYS USED BY PREVIOUS RESEARCHERS

Researchers	Tray no	d_h (mm)	Thickness X (mm)	% free area	$[d_h/X]$
Porter/Wong (17)	1	3.18	6.35	5.50	0.50
	2	3.18	6.35	3.20	0.50
	3	3.18	6.35	9.40	0.50
	4	4.76	6.35	6.35	0.75
	5	6.35	6.35	4.90	1.00
	6	12.7	6.35	4.80	2.00
Pinczewski/Fell (22)	1	6.35	1.65	11.0	3.85
	2	12.7	1.65	5.90	7.70
	3	12.7	1.65	10.7	7.70
	3	12.7	1.65	10.7	7.70
	3	12.7	1.65	10.7	7.70
	4	12.7	1.65	16.1	7.70
	5	19.1	1.65	10.3	11.6
Payne/Prince (21)	1	6.35	6.35	4.0	1.00
	2	4.76	6.35	4.0	0.75
	3	6.35	6.35	4.0	1.00
	4	4.76	6.35	9.0	0.75
Prince/Jones/Panic (102)	1	6.35	6.35	4.0	1.00
	2	4.76	6.35	4.0	0.75

APPENDIX 8

COMPUTER PROGRAMME TO EVALUATE 'a' IN LOCKETT'S MODEL

```

C      MAIN PROGRAM
C
C      THIS PROGRAMME CALCULATES FACTOR 'n' IN LOCKETT'S MODEL BY EQUATING
C      MODEL TO THE EXPERIMENTAL  $h_{cl}/d_h$  AND PREDICTED  $h_{cl}/d_h$ .
C
C      THE VALUE OF: N=1 USES BARBER/WIJN CORRELATION
C                      N=2 USES HOFHUIS/ZUIDERWEG CORRELATION
C                      N=4 USES PAYNE/PRINCE CORRELATION
C
C      DIMENSION UH(300),HCL(300),DG(300),DL(300),DH(300),DF(300),TH(300)
C      DIMENSION A(300),B(300),C(300),D(300),E(300),F(300),G(300),X(300)
C      DIMENSION Y(400),ZCT(400)
C      COMMON/INOUT/NSCR,NIN,NOUT
C
C      NSCR=0
C      NOUT=6
C      NIN=8
C
C      CALL INCOR
C      STOP
C      END
C
C*****
C      SUBROUTINE INCOR
C
C      THIS SUBROUTINE ALLOWS THE USER TO SELECT A CORRELATION FOR
C      EVALUATION OF HCL AT SPRAY REGIME TO BUBBLY REGIME TRANSITION
C
C      COMMON/ DATA/US,UH,HCL,DG,DL,DH,TH,PIT,VOLW,VOLK,DF
C      COMMON/INOUT/NSCR,NIN,NOUT
C      COMMON/BLOCK1/N,NYESNO
C      COMMON/BLOCK2/XST,XND,XL,XH
C      COMMON/BB/ZCT,NPOINT

```

```

COMMON/CC/Z

C
280  CONTINUE

C
      WRITE(NSCR,(' GIVE NSET'))
      READ(NSCR,*) NSET
      WRITE(NSCR,*) NSET
2000  CONTINUE
      CALL OPEN(NIN)
      NS=0
10    NS=NS+1
      WRITE(NSCR,*) NS
      READ(NIN,20,END=280) ITITLE
20    FORMAT(A80)
      READ(NIN,*) NPOINT
      WRITE(NSCR,*,END=280) NPOINT
      WRITE(6,21) ITITLE
21    FORMAT(A80)
C
      WRITE(3,112)
112   FORMAT(' INPUT XST=FIRST INITIAL GUESS AT THE ROOT'/

1     '   XND=SECOND INITAIL GUESS'/
1     '   XL =LOWER PERMISSIBLE BOUND FOR THE SOLUTION'/
1     '   XH = HIGHER PERMISSIBLE BOUND FOR THE SOLUTION')

      READ *,XST,XND,XL,XH
      WRITE(3,(' INPUT N'))
      READ *,N

C
      WRITE(NSCR,111)
111   FORMAT(1X,"DO YOU WANT TO CALCULATE 'a' FROM EXPERIMENTAL RESULTS")
      WRITE(NSCR,556)
556   FORMAT(1X,"IF *YES* ENTER 1 AND *NO* ENTER 0 ")
      READ(NSCR,*)NYESNO

C
      NCOUNT=0
      NCOUNT=NCOUNT+1

```

```

SUM=0.0
C
DO 2 I=1,NPOINT
READ(NIN,*)US,UH,HCL,DG,DL,DH,TH,PIT,VOLW,VOLK,DF
C
CALL LOKMOD
SUM=SUM+Z
2 CONTINUE
SUM=SUM/FLOAT(NPOINT)
WRITE(10,*) SUM
C
IF (NS-NSET) 10,8000,8000
8000 WRITE(NSCR,555)
555 FORMAT(1X,"DO YOU WANT TO TRY ANOTHER DATA")
WRITE(NSCR,556)
556 FORMAT(1X,"IF *YES* ENTER 2 AND *NO* ENTER 3 ")
READ(NSCR,*)NY
IF(NY.EQ.2)THEN
GO TO 2000
ELSE
GO TO 3000
END IF
C
3000 RETURN
END
C
C*****
C
C SUBROUTINE LOKMOD
C
C THE MODEL USED IS THE JET PENETRATION MODEL DERIVED BY LOCKETT
C WHICH GENERALISES NUMBER OF EXISTING CORRELATIONS.
C
COMMON/BLOCK1/N,NYESNO
COMMON/BLOCK2/XST,XND,XL,XH
COMMON/ DATA/US,UH,HCL,DG,DL,DH,TH,PIT,VOLW,VOLK,DF
COMMON/INOUT/NSCR,NIN,NOUT
COMMON/BB/ZCT,NPOINT

```



```

COMMON/CC/Z

C
C
CALL SECANT(Z)

C
RETURN
END

C
C*****C
SUBROUTINE SECANT(Z)

C
C SECANT METHOD OF FINDING REAL ROOTS OF A NON-LINEAR EQUATION
C FCT IS USER PROVIDED SUBROUTINE
C SET INITIAL GUESSES AND UPPER AND LOWER BOUNDS
C
COMMON/BLOCK1/N,NYESNO
COMMON/BLOCK2/XST,XND,XL,XH
COMMON/BB/ZCT,NPOINT
EXTERNAL FCT
C SET ERROR TOLERANCE
EPS = 0.001
C SET MAX ITERATION
IEND = 200
CALL SECT(Z,FCT,EPS,IEND,RES,IER)
PRINT 10,Z
10 FORMAT(1X,"RESULT, Z=A=",E12.4)
RETURN
END

C
C*****C
C
SUBROUTINE FCT(Z,RES)

C
COMMON/ DATA/US,UH,HCL,DG,DL,DH,TH,PIT,VOLW,VOLK,DF
COMMON/BLOCK2/XST,XND,XL,XH
COMMON/BLOCK1/N,NYESNO
COMMON/INOUT/NSCR,NIN,NOUT
D=FLOAT(N)

```

C

```
IF(NYESNO.EQ.1)THEN
ZCT=HCL
ELSE
CONTINUE
```

C

```
IF (N.EQ.1) THEN
ZCT=1.35*((DG/DL)**0.25)*(UH**0.4)/((9.81
1*0.01*DH)**0.2)*(PIT/DH)**0.33-0.59*(PIT/DH)**0.33
```

C

```
ELSE IF(N.EQ.2) THEN
ZCT=1.07*((DG/DL)**0.33)*(UH**0.66)/9.81
1*DH*0.01)**0.33)
```

C

```
ELSE IF (N.EQ.4) THEN
ZCT=1.5*((DG/DL)**0.5)*UH*((1-DF)**0.5)/((9.81
1*DH*0.01)**0.5)
```

C

```
END IF
```

C

```
X = ((4.0+D)/D)/((4.0/D)**(4.0/(4.0+D)))
Y = (DG/DL)**(D/(4.0+D))
A=UH**((2.0*D)/(4.0+D))
B=(1-DF)**(4.0/(4.0+D))
C=(9.81*0.01*DH)**(D/(4.0+D))
Z2=A*B/C
Z1 = (1-DF)
```

C

```
RES = ZCT - X*Y*Z2/(Z**(4.0/(4.0+D))) + Z1/Z
RETURN
END
```

C

C*****

C

```
SUBROUTINE SECT(Z,FCT,EPS,IEND,RES,IER)
```

C

```
DIMENSION R(2),X(2)
COMMON/BLOCK1/N,NYESNO
```

```

COMMON/BLOCK2/XST,XND,XL,XH
COMMON/BB/ZCT,NPOINT
C
C      IER RETURN CODE ERROR, =0 NO ERROR
      H=XST-XND
      K=0
5      Z=XND
      CALL FCT(Z,RES)
      R(2)=RES
      X(2)=Z
      X(1)=XST
      IT = 0
10     IT=IT+1
      IF (IEND-IT) 20,20,40
20     IER = 1
      GO TO 100
40     Z = X(1)
      CALL FCT(Z,RES)
      R(1)=RES
      Z=X(1)-R(1)*(X(1)-X(2))/(R(1)-R(2))
      IF (Z-XL) 50,50,60
50     IF (K-1) 70,80,80
80     IER = 2
      GO TO 100
70     XST=XH
      XND=XH+H
      K=1
      GO TO 5
60     IF (Z-XH) 85,90,90
90     IF (K-1) 95,80,80
95     XST = XL
      XND = XST+H
      K = 1
      GO TO 5
85     E=ABS((Z-X(1))/Z)
      IF (E-EPS) 97,97,96
97     IER = 0
      Z = X(1)

```



```

        RES = R(1)
        GO TO 110
96      X(2)=X(1)
        X(1)=Z
        R(2)=R(1)
        GO TO 10
100     PRINT 120
110     RETURN
120     FORMAT(/5X,"SECT NOT CONVERGED ")
        END
C
C*****C
        SUBROUTINE OPEN(NFILE)

        CHARACTER*8 FILENAME
C
        NSCR=0
        WRITE(NSCR,10) NFILE
10      FORMAT(1X,' ENTER FILE NAME FOR CHANNEL ',I4,'**')
        READ(NSCR,20) FILENAME
20      FORMAT(A8)
        OPEN(UNIT=NFILE,FILE='      '//FILENAME)
        WRITE(NSCR,30) FILENAME,NFILE
30      FORMAT(' ** FILENAME ',A8,' OPENED TO CHANNEL ',I4/)
        RETURN
        END

EOF..
EOT..

```

APPENDIX 9

COMPUTER PROGRAMME TO CORRELATE EXPERIMENTAL RESULTS

```

C      MAIN PROGRAM
C      THIS PROGRAMME IS USED TO CORRELATE THE EXPERIMENTAL RESULTS FOR
C      SINGLE AND TWO LIQUID PHASES.
C
      DIMENSION UH(300),HCL(300),RG(300),RL(300),WMU(300)
      DIMENSION DO(300),RF(300),TH(300),X(5,400),Y(400)
      DIMENSION A(300),B(300),C(300),D(300),W(300),K(300)
      DIMENSION E(300),F(300),YE(300)
      REAL K
C
      NSCR=0
      NIN=8
      NOUT=6
      DO 69 I=1,400
      DO 70 J=1,5
      X(J,I)=0
70    CONTINUE
69    CONTINUE
C
      WRITE(NSCR,120)
      READ(NSCR,*) NPOINT
      CALL OPEN(NIN)
      ITER=0.0
      DO 2 I=1,NPOINT
      READ(NIN,*) UH(I),HCL(I),RG(I),RL(I),DO(I),TH(I),W(I),K(I)
C
      A(I)=HCL(I)/DO(I)
      B(I)=((RG(I)/RL(I))**(1/2))
      C(I)=B(I)*UH(I)
      D(I)=LOG(C(I))
      E(I)=LOG(A(I))
      Y(I)=E(I)-D(I)
      ITER=ITER+1
      WRITE(NSCR,*)ITER

```

```

2      CONTINUE
120    FORMAT(1X,'GIVE NUMBER OF POINTS')
      CLOSE(UNIT=NIN)
C
      DO 10 I=1,NPOINT
      X(1,I)=LOG(DO(I)/TH(I))
10     CONTINUE
C
      CALL CALC(X,Y,NPOINT)
C
      STOP
      END
C
C*****
C      REGRESSION ANALYSIS METHOD FOR PROCESS IDENTIFICATION
C      EQUATION FORMULATED IN DISCRETE FORM INCORPORATING
C      ZERO ORDER HOLD ELEMENT.
C
      SUBROUTINE CALC(X,Y,NPOINT)
C
      DIMENSION A(6),B(5),VAR(10),H(15,15),AX(400,10),G(10)
      DIMENSION DX(10),FDX(400),X(5,400),FX(400),VARIN(10)
      DIMENSION Y(400)
      REAL M(400),MIN,MFIN,KP
      INTEGER ORDER,ERRNUM
C
      NSCR=0
      NIN=8
      NOUT=6
C
      NPAR=2
      DO 3 I=1,2
      A(I)=0.7
3     CONTINUE
      PERT=0.001
      NCOUNT=0
      EPSIL=0.000001
      ITER=0

```



```

1000  ITER=ITER+1
      CALL EQUATION(A,NPOINT,X, Y,FX, SUMERROR)
      IF(ITER.EQ.1) THEN
      SUMERRORP=SUMERROR
      ENDIF

C
      TOL=ABS(SUMERRORP)-ABS(SUMERROR)
      IF(ABS(TOL).LT.EPSIL.AND.ITER.GT.1) THEN
      NCOUNT=NCOUNT+1
      ELSE
      NCOUNT=0
      ENDIF
      IF(NCOUNT.GE.5.AND.ITER.GT.1) GOTO 1001

C
      DO 10 I = 1,NPAR
      XX=A(I)
      IF(ABS(A(I)).EQ.0.) THEN
      A(I)=0.0001
      IPP=0
      ELSE
      IPP=1
      END IF
      A(I) = XX+0.0001*A(I)
      CALL EQUATION(A,NPOINT,X,Y,FDX,SUMERROR)
      DO 20 J =1,NPOINT
      AX(J,I)=(FX(J)-FDX(J))/(XX-A(I))
20    CONTINUE
      IF (IPP.EQ.0) THEN
      A(I)=0.
      IPP=1
      ELSE

C
      A(I)=XX
      END IF
10    CONTINUE
C
C
      G(3) = 2*AXT*FX1
      DO 30 I=1,NPAR

```

```

SUM=0.
DO 40 J=1,NPOINT
SUM = SUM+AX(J,I)*FX(J)*2.0
40  CONTINUE
G(I)=SUM
30  CONTINUE
C   H(3,3) =2*AXT*A
DO 50 I=1,NPAR
DO 50 K=1,NPAR
SUM =0.0
DO 70 J=1,NPOINT
SUM = SUM + 2.0*AX(J,I)*AX(J,K)
70  CONTINUE
H(I,K) = SUM
50  CONTINUE
C
CALL SIMUL(NPAR,H,VAR,DETER)
DO 80 I= 1,NPAR
SUM=0.0
DO 90 J=1,NPAR
SUM = SUM + (-1)*H(I,J)*G(J)
90  CONTINUE
DX(I) = SUM
80  CONTINUE
C
DO 100 I=1,NPAR
A(I) = A(I)+DX(I)
PRINT*,A(I)
100 CONTINUE
C
SUMERRORP = SUMERROR
GOTO 1000
1001 RETURN
END
C

```

```

C*****
C
SUBROUTINE EQUATION(A,NPOINT,X,Y,FX,SUMERROR)
C
DIMENSION A(6),X(5,400), Y(400), FX(400)
C
SUMERROR=0.0
DO 10 I = 1, NPOINT
VALUE = A(1) + A(2)*X(1,I)
C VALUE = A(1) + X(1,I)**A(2)
C VALUE = A(1) + A(2)*X(1,I) + A(3)*X(2,I)
FX(I) = Y(I) - VALUE
SUMERROR = SUMERROR + FX(I)*FX(I)
10 CONTINUE
C
RETURN
END
C
C*****
C
SUBROUTINE SIMUL(N, A, X,DETER)
C
DIMENSION JCOL(10),X(10),JORD(10),Y(10),A(15,15)
INTEGER IROW(10)
C
DO 44 I=1,10
IROW(I)=0
JCOL(I)=0
JORD(I)=0
44 CONTINUE
MAX = N
INDIC=-1
EPS=1.0E-04
IF (INDIC.GE.0) MAX=N+1
C
IF (N.LE.10) GO TO 5
WRITE(6,2000)
DETER =0.

```



```

RETURN
5  DETER =1.0
    DO 18 K = 1,N
        KM1 = K-1
        PIVOT = 0.0
        DO 11 I = 1,N
            DO 11 J =1,N
                IF ( K.EQ.1) GO TO 9
                DO 8 ISCAN = 1, KM1
                    DO 8 JSCAN = 1, KM1
                        IF (I.EQ.IROW(ISCAN)) GO TO 11
8                 IF (J.EQ.JCOL(JSCAN)) GO TO 11
9                 IF (ABS(A(I,J)).LE.ABS(PIVOT)) GO TO 11
                    PIVOT = A(I,J)
                    IROW(K) = I
                    JCOL(K) = J
11                CONTINUE
C
                IF (ABS(PIVOT).LT.EPS)THEN
                    RETURN
                ENDIF

C
13             IROWK = IROW(K)
                JCOLK = JCOL(K)
                DETER = DETER*PIVOT

C
                DO 14 J = 1,MAX
14             A(IROWK,J) = A(IROWK,J)/PIVOT
C
                A(IROWK,JCOLK) = 1./PIVOT
                DO 18 I = 1,N
                    AIJCK = A(I,JCOLK)
                    IF (I.EQ.IROWK) GOTO 18
                    A(I,JCOLK) = -AIJCK/PIVOT
                    DO 17 J = 1,MAX
17             IF (J.NE.JCOLK) A(I,J) = A(I,J) - AIJCK*A(IROWK,J)
18             CONTINUE
C

```

```

DO 20 I = 1,N
IROWI = IROW(I)
C   JORD(IROWI) = JCOLI
20  CONTINUE
C
INTCH = 0
NM1 = N-1
DO 22 I = 1,NM1
IP1 = I+1
DO 22 J = IP1,N
IF ( JORD(J).GE.JORD(I)) GOTO 22
JTEMP = JORD(J)
JORD(J) = JORD(I)
JORD(I) = JTEMP
INTCH = INTCH+1
22  CONTINUE
IF (INTCH/2*2.NE.INTCH) DETER = -DETER
C
DO 28 J = 1,N
DO 27 I = 1,N
IROWI = IROW(I)
JCOLI = JCOL(I)
27  Y(JCOLI) = A(IROWI,J)
DO 28 I = 1,N
28  A(I,J) = Y(I)
C
DO 30 I = 1,N
DO 29 J = 1,N
IROWJ = IROW(J)
JCOLJ = JCOL(J)
29  Y(IROWJ) = A(I,JCOLJ)
DO 30 J = 1,N
30  A(I,J) = Y(J)
C
DETER = DETER
RETURN
2000 FORMAT( 10H0N TOO BIG )
END

```

```

C
C*****
C
C      SUBROUTINE OPEN FOR INPUT AND OUTPUT
C
C      SUBROUTINE OPEN(NFILE)
C
C      CHARACTER*8 FILENAME
C
C      NSCR=0
C      WRITE(NSCR,10) NFILE
10      FORMAT(1X,' ENTER FILE NAME FOR CHANNEL ',I4,'**')
C      READ(NSCR,20) FILENAME
20      FORMAT(A8)
C      OPEN(UNIT=NFILE,FILE='      '//FILENAME)
C      WRITE(NSCR,30) FILENAME,NFILE
30      FORMAT(' ** FILENAME ',A8,' OPENED TO CHANNEL ',I4/)
C      RETURN
C      END
C
EOF..
EOT..

```


APPENDIX 10
VARIAION OF DROPLET DIAMETER WITH TIME

Propan-1-ol		Cumene		Cumene/Water/Propan-1-ol		Water	
time	diameter	time	diameter	time	diameter	time	diameter
(min)	(mm)	(min)	(mm)	(min)	(mm)	(min)	(mm)
0.2	2.6	0.2	3.1	0.2	2.9	0.2	4.1
0.5	2.5	0.5	3.0	0.5	2.7	1.0	4.0
1.0	2.4	1.0	2.9	1.0	2.6	2.0	3.8
1.5	2.2	1.5	2.7	1.5	2.5	4.0	3.6
2.0	2.1	2.0	2.5	2.0	2.3	6.0	3.3
2.5	1.8	2.5	2.3	2.5	2.1	8.0	3.1
3.5	1.5	3.5	2.1	3.0	1.8	10.0	2.8
4.0	1.2	3.9	1.8	4.0	1.5	12.0	2.1
4.3	0.8			4.1	1.3	13.0	1.9
						13.5	1.3
						14.0	0.9
						14.3	0.6

Page removed for copyright restrictions.